Nuclear receptor co-repressor functions in prostate cancer; *in vitro*, *in vivo* and *in silico* approaches

UNIVERSITY OF BIRMINGHAM

By

Sebastiano Battaglia

A thesis presented to the School of Medicine,

University of Birmingham,

For the degree of Doctor of Philosophy.

School of Medicie
Institute for Biomedical Research
University of Birmingham
July 2009

SUMMARY

Nuclear Receptor CoRepressor-1 (NCOR1) controls the actions of multiple transcription factors including nuclear receptors (NR). The prostate malignant cell line PC-3, displays a significant differential expression of a cohort of corepressors (*NCOR1*, *RIP140*, *LCOR*, *SLIRP*) and subsequent loss of responsiveness to NR ligands, including those for PPAR and VDR, compared to the non-malignant cell line RWPE1 at a transcriptional and phenotypical level. NR insensitivity can be antagonized by using the histone deacetylase inhibitor SAHA in combination with the PPARα and -γ ligand bezafibrate. Microarray approaches revealed co-treatment restored PPAR transcriptional actions towards target genes (e.g. *CDKN1A*, *PTGS2*, *ALOX5*, *CDC2*, *TGFBRAP1*). NCOR1-knock down by shRNA restored partially the transcriptional abilities of PPARs upon treatment with bezafibrate, mimicking the effect of SAHA on the genes identified. Interestingly, shNCOR1-PC-3 were more sensitive towards the PPARα and PPARγ ligands, ETYA and EPA respectively, but were unresponsive to $1,25(OH)_2$-D_3 and T3. This was reflected at the transcriptional level where in bezafibrate-treated shNCOR1-PC-3 the expression of PPAR target genes (*TGFBRAP1*, *CDKN1A*, *ALOX5*, *CDC2*) was restored mirroring the activity of SAHA. To profile the transcriptome regulated by NCOR1 during the cell cycle a microfluidic gene card approach was undertaken. PC-3 cells were FACS sorted in G1, S and G2 phases and demonstrated that shNCOR1-PC-3 cells restored the basal levels of key regulators of cell viability such as histone modifiers, *CDKN1A*, *TP53* and *CDH1*. ChIP analysis in siNCOR1-PC-3 cells also revealed that NCOR1 controls the epigenetic modifications at the *CDKN1A* and *TGFBRAP1* TSS differentially modulating H3K9 acetylation upon bezafibrate treatment, reflecting mRNA accumulation data.

The contribution of NCOR1 and NCOR2/SMRT in prostate development is unknown. To identify these functions more accurately Ncor1, and Ncor2/Smrt, are being knocked out in mice in prostate-specific manner using a Cre/Lox-P strategy where the Cre enzyme is controlled by the modified prostate-specific rat probasin promoter, ARR2PB.

CDKN1A is an example of a gene differentially regulated by bezafibrate in shNCOR1-PC-3, non responsive to 1,25$(OH)_2$-D_3 in wild type PC-3 and significantly induced in non malignant RWPE1 cells. To understand this complex regulation, and predict the regulatory mechanism of CDKN1A transcription, we sought to create an ordinary differential equations (ODE) model of the initial transcriptional events on the TSS of the *CDKN1A* gene in RWPE1 cells. We fitted time course data hypothesizing that a poised phospho-RNA PolII bound at the promoter region could explain a quick and steep induction in mRNA production followed by an equal steep degradation mediated by the miRNA miR-106B. This model will be used to interrogate malignant cell responses to NR ligands.

This thesis is dedicated to my great parents and to my awesome sister!

…VAI TRA…

AKNOWLEDGMENTS

There is a long list of people that I should thank for the help, the support and the friendship that they gave me during these last three years. Without them I probably would not be where I am right now, personally and professionally; I will name these people following the chronological order in which I met them during my wandering around Europe, hopping between universities, PCRs and happy hours.

First off, a great thanks goes to my supervisors: Dr. Moray Campbell (also for teaching me how to be a “committed disinterested observer”) and Dr. Chris Bunce for the support, for the patience that they had, for the friendship that they offered and for the passion they shared with me! I want also to thank Dr. Chris McCabe for the supervision he offered me during my last period in Birmingham and for the great time playing guitar! I want to thank James Thorne for helping me during my very first days in Birmingham, inside and outside the lab; Asad Abedin for being the first person, with James, that taught me molecular biology techniques; Farhat Khanim for always being present when we had troubles in the lab and for always supporting me even when stuff was not working; Dr. Francesco Falciani for introducing me to the world of Bioinformatics and to the “Italian community”; Craig Doig and Pedro Velica for sharing great times in the lab and many pints in the pub; all the people at the IBR especially Caroline, Greg, Vicky, Sally, Rowan, Rachel, Jo Tucka, Olly, Ellen, Yin, Mark Sherlock, Phil, Kirren, Gareth (also for all the training sessions), Liz Rabbit, Ana, Matt, Clare, and all the other that share with me great moments. I definitely want to thank friends (and colleagues) like Giacomo, Fra Crea, Cristiano, Andrea (entrambi), Walter, Anna, Stefano Cogo, Vasillio & Angeliki, Eugenio,

Steph, Marco Falco and Alberto “limone” Sesa for the invaluable friendship and the memorable moments that we spent together! One thanks goes to my great ex-flatmates Ashley and Clare; to Bob Spour to open my eyes on Muay Thai and for writing one of my tattoos and thanks to Andy for the great time teaching Muay Thai at the University and for bringing me to Wales!

During about 11 months spent in Berlin at the Max Plank Institute I could have never achieved what I did without the great support of Dr. Heiner Schrewe, Pedro Rocha, Mia Mayer and Manuela Scholze. They not only helped me to develop the Ncor constructs but they were always ready to answer my questions and patiently explain to me what to do even if they were busy and my questions were silly! All the people at the Max Plank have been really open and friendly with me, I would like to thank Mark, Benny, Joanna, Markus, Philip, Ive, Arnold, Nathalie, Shini, Jurgen, Hermann and all those that I cannot member but I met at the MPI. Moreover, I was lucky enough to meet a unique group of people outside the lab that greatly supported me in pursuing my way as a scientist and as a better person, I will never forget Matteo that gave me a house when I didn’t have one and still is a great friend; Jens that shared with me unforgivable moments and was next to me when I needed and hope to meet him soon; Simon (you are the man) for always being a great scientist/person and friend; Lisa that helped me growing, she was the first one to teach me to look beyond the surface of myself and others and showed me a deeper way of living; my ex-flatmates Simon and Miriam for helping me to cheer up after a day of work; Dan, whom I spent a great time with; and Dinara for the insightful discussions that luckily we still have.

I spent about a month at the University of Luxembourg where I moved my first steps in systems biology. Here a great thanks goes to Prof. Carsten Calberg and his team that warmly welcomed me and helped me to settle down; thanks to Katjia and Aleksandra, fellow ESRs and friends, for the professional and personal support; and thanks to Prof. Thomas Sauter for the suggestions on my model and for the everyday cheerful chats.

I moved to the Roswell Park Cancer Institute for the last two months of my PhD. Here, apart from my supervisor Dr. Moray Campbell and Craig that are always great colleagues and friends, I want to thank Orla (that also worked in Birmngham), Laura and Michelle for being part the great team that cheers me up inside and outside the lab. Thanks to Silvia, Piergiorgio, Leigh, Lee, Prof. Roberto Pili, Jason, Sara and Connor for the friendship and the support! Thanks also my great room mate Kelly for the awesome help she gave me as soon as I arrived and for the many headaches on Saturday mornings; thanks to all the guys I met here and helped me feeling like home: Andy, George, Mike, Jet, Mary, Amy, Alex and Jessie.

Thanks to all the fella ESRs, every meeting/course/conference was fantastic and memorable also thanks to the environment that we all created.

Undoubtedly the biggest support ever came from my family, my mum Marina, my dad Marcello and my awesome sister Cristina. They never stopped believing in me and even if I was always far away they have always been really close!! Thanks!!

LIST OF ABBREVIATIONS

1α,25(OH)$_2$D$_3$	1alpha,25-dihydroxy-vitamin D$_3$
ABC	ATP-binding cassette
AF-1	activation function 1
AF-2	activation function 2
AIB1	amplified in breast cancer 1
ALOX5	arachidonate-5-lypoxigenase
AMACR	α-methylacyl-CoA racemase
AMP	adenosine monophosphate
AMV	avian myeloblastosis
ANOVA	analysis of variance
AP1/2	activator protein 1/2
APAF1	apoptotic protease-activating factor 1
APC	adenopolyposis coli
APL	acute promyelocytic leukaemia
Apo-NR	unliganded NR
AR	androgen receptor
ATP	adenosine triphosphate
ATRA	all *trans*-retinoic acid
bp	base pair
BMP	bone morphogenic proteins
BRCA1/2	breast cancer 1/2
CAR	constitutive androsterone receptor
CBP	cAMP-responsive element-binding protein-binding protein
CDA	chenodeoxycholic acid
CDC2	cell division cycle 2
CDK	cyclin-dependent kinase
CDKN1A	cyclin-dependent kinase inhibitor 1 a
cDNA	complementary deoxyribonucleic acid
C/EBP	CCAAT/enhancer binding protein
CGAP	Cancer Genome Anatomy Project
ChIP	chromatin immunoprecipitation
CMV	Cytomegalovirus
CNS	central nervous system

CoA	coactivator
CoR	corepressor
CoREST	RE1-silencing transcription factor corepressor
CSC	cancer stem cell
Ct	cycle threshold
CYP	cytochrome P450 enzyme
CYP24	cytochrome P450 enzyme, 24-hydroxylase
CYP27	cytochrome P450 enzyme, 25-hydroxylase
DAD	deacetylase interaction domain
DAX1	DSS-AHC critical region on the chromosome X 1
DBD	DNA binding domain
DMEM	Dulbecco's modified eagles medium
DNA	deoxyribonucleic acid
DNMT	DNA methyltransferase
dNTP	deoxynucleotide triphosphate
DR3/4	direct repeat 3/4
DRIP	vitamin D receptor-interacting protein
EC_{50}	half maximal effective concentration
ECL	enhanced chemiluminescence
ECM	extracellular matrix
ED	estimated dose
EDTA	sodium ethylene tetraacetate
EGF	epidermal growth factor
EGFP	Enhanced Green Fluorescent Proteins
EGFR	epidermal growth factor receptor
EPA	eicosapentanoic acid
ESC	embryonic stem cell
ERα/β	oestrogen receptor alpha/beta
ERR	oestrogen related receptor
ETYA	eicosatetraynoic acid
EZH2	enhancer of Zeste homolog 2
FACS	fluorescence activated cell sorting
FCS	fetal calf serum
FDA	US Food and Drug Administration
FGF	fibroblast growth factor
FSH	follicle-stimulating hormone

FXR	farnesoid X-activated receptor
GADD45α	growth arrest and DNA damage-inducible gene α
GH	growth hormone
GR	glucocorticoid receptor
H1/2/3/4	histone 1/2/3/4
HAT	histone acetyltransferase
HDAC	histone deacetyltransferase
HDL	high-density lipoprotein
Holo-NR	ligand-bound NR
HPN	hepsin
HOX	homeobox proteins
IFNγ	interferon γ
IgG	immunoglobulin G
IGF	insulin-like growth factor
IGFR	insulin-like growth factor receptor
hr	hours
IC_{50}	half maximal inhibitory concentration
ID	interaction domain
IL2/6	interleukin 2/6
K	lysine
kb	kilo base
kDa	kilo Dalton
LBD	ligand binding domain
LCOR	ligand-dependent corepressor
LDL	low-density lipoprotein
LH	luteinising hormone
LXR	liver X receptor
MAP kinase	mitogen-activated protein kinase
MBD	methylated DNA-binding protein
MMLV	moloney murine leukemia virus
min	minute
mRNA	messenger ribonucleic acid
NaB	sodium butyrate
NAD	nicotinamide adenine dinucleotide
NCOR1	nuclear receptor corepressor-1
NR	nuclear receptor

N-terminal	amino-terminal
NuRD	nucleosomal remodelling and deacetylation
OD	optical density
p	probability value
PBS	phosphate buffered saline
PCa	prostate cancer
P/CAF	p300/CREB-binding protein-associated factor
PCR	polymerase chain reaction
PG	prostaglandin
PIA	proliferative inflammatory atrophy
PIN	prostatic intra-epithelial neoplasia
PPAR	peroxisome proliferator-activated receptor
PR	progesterone receptor
pRb	retinoblastoma protein
PSA	prostate specific antigen
PSC	prostate stem cells
PTCH	patched receptor
PTH	parathyroid hormone
PXR	pregnane X receptor
RAR	retinoic acid receptor
RD	repression domain
RE	response element
RIP140	nuclear receptor interacting protein 1 (NRIP1)
RNA	ribonucleic acid
RT-PCR	reverse-transcriptase polymerase chain reaction
RXR	retinoid X receptor
SAGE	serial analysis of gene expression
SAHA	suberoylanilide hydroxamic acid / Vorinostat
SANT	SWI3, ADA2, NCOR1 and TFIIIB B domain
SDS	sodium dodecyl sulphate
sec	second
S.E.M.	standard error of the mean
SHH	sonic hedgehog
SHP	small heterodimer partner
shRNA	short hairpin RNA
Sir2	silent information regulator 2

siRNA	short interfering ribonucleic acid
SIRT	sirtuin
SMAD	sma- and mad-related proteins
SMRT	silencing mediator of the retinoid and thyroid receptors
SRC	steroid receptor coactivator
SNC	NCOR2/SMRTe and NCOR1 conserved domain
STAT	signal transducers and activators of transcription
T_3	throid hormone T_3
TAFII250	TBP-associated factor, RNA polymerase II, 250 kD
TBE	Tris borate EDTA buffer
TBP	TATA box binding protein
TE	Tris-EDTA buffer
TFIIB	transcription factor IIB
TFIIIC	transcription factor IIIC
TGFα/β	transforming growth factor α/β
TGFBRAP1	transforming growth factor-β receptor associated protein-1
TIF2	transcription intermediary factor 2
TNF	tumour necrosis factor
TRα/β/γ	thyroid receptor alpha/beta/gamma
TR2/4	testicular orphan receptor 2/4
TRAMP	transgenic adenocarcinoma of the mouse prostate
TRIP15	thyroid-receptor interacting protein 15
TRAP	thyroid receptor-associated protein
TSA	trichostatin A
TSH	thyroid-stimulating hormone
TSS	transcription start site
UGE	urogenital sinus-epithelium
UGM	urogenital mesenchyme
UGS	urogenital sinus
UV	ultra-violet
VDR	vitamin D receptor
VDRE	vitamin D response element
WSTF	Williams syndrome transcription factor
YY1	yin yang 1

LIST OF FIGURES

LIST OF TABLES

PREFACE AND BACKGROUND EXPERIENCE

In March 2006 I started my PhD as a member the Marie Curie Research Training Network entitled "NucSys"(Systems Biology of Nuclear Receptors). This consortium was developed by Prof. Carsten Calberg (University of Luxembourg, Luxembourg) and Dr. Moray Campbell (University of Birmingham, UK / Roswell Park Cancer Institute, Buffalo, NY, USA) and in total included 14 teams from academia and industry based on 7 EU countries. The aim of this training network was to educate 18 ESRs (Early Stage Researchers) over a period of three years in different interdisciplinary fields; this was undertaken through short term and long term experiences in different labs to acquire new skills and approach new and multi-disciplinary environments.

My project started at the University of Birmingham (Birmingham, UK) under the supervision of Dr. Moray Campbell and Dr. Chris Bunce. Here I profiled the function of NCOR1 in prostate malignant PC-3 cells creating, and analysing, a stable NCOR1 knock down-PC-3 cell line. When Dr. Moray Campbell re-located to the USA, Dr. Chris McCabe also contributed to supervision.

The second step was to define Ncor1 and Ncor2/Smrt function in mouse prostate development; this was done at the Max Planck Institute for Molecular Genetics (Berlin, Germany) under the supervision of Dr. Heiner Schrewe. Here I generated targeting constructs for Ncor1 and Ncor2 and prepared floxed ES cells that are currently being used for blastocyst injection. These mice are being bred at Roswell Park Cancer Institute (Buffalo, NY, USA).

The last project aimed to model with a Systems Biology approach the transcriptional activation of the CDKN1A gene upon 1,25(OH)$_2$D$_3$ treatment. This was made at the University of Luxembourg (Luxembourg, Luxembourg) under the supervision of Prof. Carsten Calberg and Dr. Frank Bruggeman (Free University of Amsterdam, Amsterdam, The Netherlands) with the collaboration of a fellow ESR Katja Rybakova. Here, based on experimental data, I used an ordinary differential equation model (ODE) to profile the initial mRNA events within the first hour of transcriptional activation aiming to describe the mechanistic events that led to the accumulation and steep degradation.

1 – INTRODUCTION

1.1 - The Prostate Gland

The prostate is a tubuloalveolar exocrine gland that is found only in male mammals and surrounds the urethra at the base of the bladder. The main function of the prostate is to store and secrete a clear and slightly alkaline (pH 7.29) fluid that constitutes 10-30% of the volume of the seminal fluid. This, together with spermatozoa forms the semen. The composition of prostatic secretions varies among the species; other than being alkaline, they are generally composed of simple sugars and less than 1% of proteins, containing photolytic enzymes, acid phosphatase and Prostate Specific Antigen (PSA). The alkalinity of the seminal fluid helps to neutralize the acidity of the vaginal tract, prolonging the lifespan of the sperms. A healthy human prostate is slightly larger than a walnut.

The prostate can be divided in to four lobes (**Fig 1.1)**:

- the Anterior lobe is the portion of the gland that lies in front of the urethra. It is devoid of glandular tissue being formed completely of fibromuscolar tissue;
- the Medial lobe is a coned shaped portion of the gland situated between the ejaculatory ducts and the urethra;
- the Lateral lobes (right and left) form the main mass of the gland, they are continuous posteriorly and separated by the prostatic urethra;
- the Posterior lobe is used to describe the postero-medial part of the lateral lobes that can be palpated through the rectum during digital rectal exam (DRE).

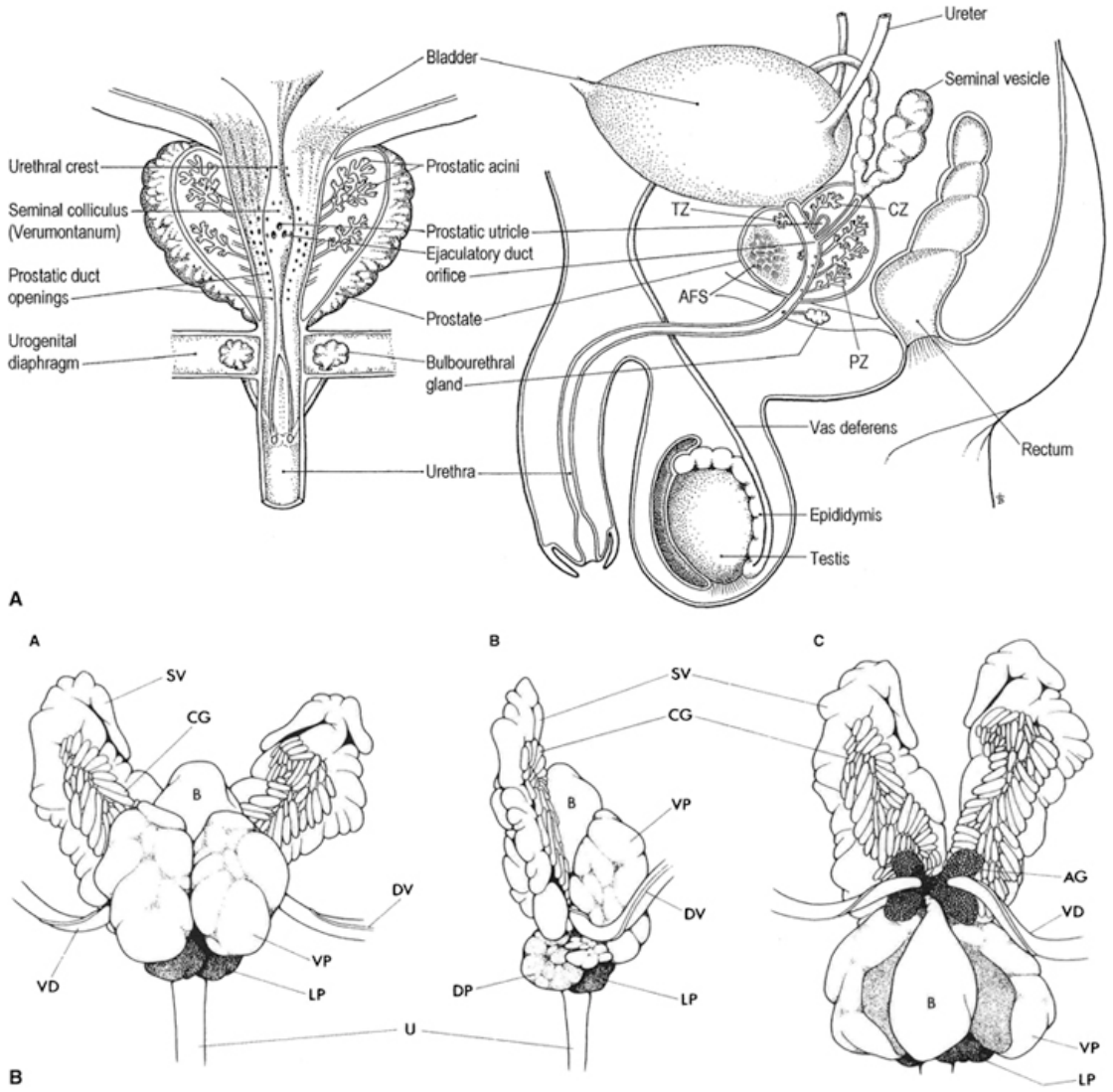

Fig 1.1 – *Diagrams of frontal and sagittal sections of the male urogenital complex illustrationg the anatomical position of the adult prostate and associated structures. The prostatic zones described by McNeal in 1983 [1] are indicated: central zone (CZ), peripheral zone (PZ), anterior fibromuscular stroma (AFS), and transition zone (TZ). (B) Male accessory sex organs of the adult male rat. A, anterior view; B, lateral view; C, anterior view with the bladder deflected caudally. Ampullary gland of the vas deferens (AG); bladder (B); coagulating gland (CG); dorsal prostate (DP); lateral prostate (LP); seminal vesicle (SV); ventral prostate (VP); vas deferens (VD); deferential vein (DV). Image taken from [2]*

The prostate also contains a high concentration of smooth muscle that leads to the expulsion of products made in the branched secretory acini through a branched

ductal system and thence the urethra. The anterior or ventral aspect of the gland is almost entirely fibromuscular, while the glandular region occupies the posterior part of the tissue and surrounds the ejaculatory ducts as they enter the urethra on each side of the verumontanum.

1.2 – Normal Prostate Gland Development

1.2.1 – Morphological aspect of prostate development

The formation of the prostate occurs relatively late in gestation when compared to the genesis of most organs. In humans, the prostate starts to form between 9-12 weeks of gestation; in mice prostatic development begins at E16.5 and in rats at E17.5. The enlargement of the human prostate is a consequence of sequential prior events, including production of testosterone by the fetal testis at around 8 weeks. Final growth and maturation occur at puberty when circulating androgens levels rise sharply. The initial event in prostate morphogenesis is the outgrowth of solid epithelial buds from the urogenital sinus (UGS) into the surrounding urogenital mesenchyme (UGM) in response to the binding of 5α-dihydrotestosterone to the androgen receptor (AR) localized in the surrounding mesenchymal tissue [3-5]. Epithelial cells of the developing prostate buds are characterized by the coexpression of cytokeratins 5, 8, 14 and 18 and p63 [6]. Notably AR is not present in epithelia during organ induction but is expressed in the mesenchyme suggesting that essential components for bud induction are found within the mesenchyme. Indeed, certain androgenic effects are elicited via paracrine influences from the AR-positive mesenchyme and do not require epithelial AR, whereas the expression of

androgen-dependent secretory proteins requires direct androgenic stimulation of the epithelium via epithelial AR. While mesenchymal effects on epithelial development form the basis of organogenesis during fetal and neonatal periods, analogous stromal-epithelial interactions continue throughout life and, in adulthood, presumably have a homeostatic role [7]. In the rat and mouse, as the solid epithelial buds canalize, the epithelium reorganizes in to two distinct cell populations: basal epithelial cells localize in the basal membrane to from a discontinuous layer of cells expressing cytokeratins 5 and 14 and p63 while tall luminar cells, expressing cytokeratins 8 and 18, form the ductal lumina.

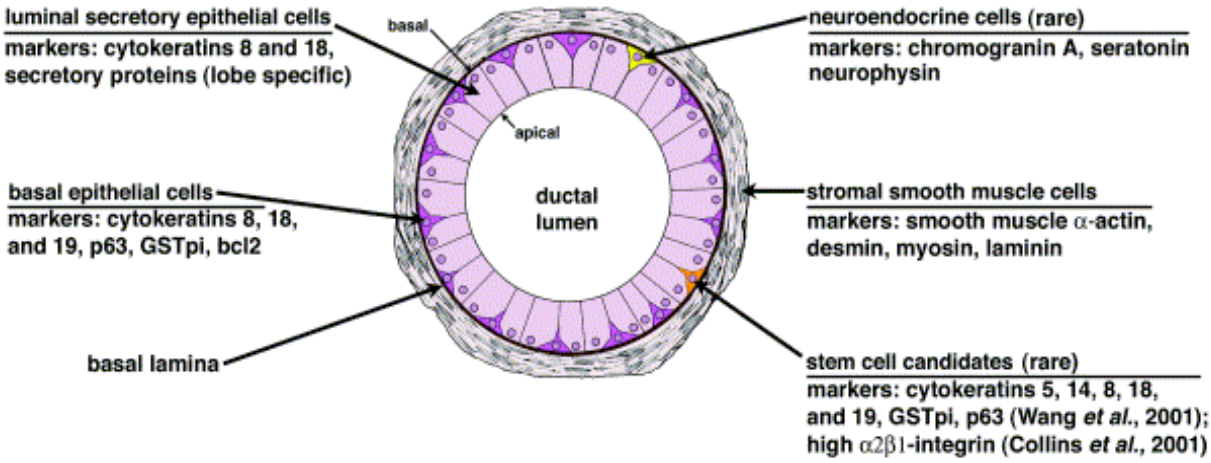

Fig 1.2 – *A diagram of the prostate ductal-cross section is shown with labels indicating cell types that are present in prostatic ducts including luminal secretory epithelial cells, basal epithelial cells, neuroendocrine cells, stromal smooth muscle cells, and stem cell candidates. Beneath the label for each cell type is a list of differentiation markers commonly used to distinguish these cell types. In the case of stem cell candidates, two studies have associated expression of either a set of markers including cytokeratins 5, 14, 8, 18, and 19, GSTpi, and p63 or high expression of α2β1-integrin with rare basal cells proposed as prostatic epithelial stem cell candidates. Image taken from [8].*

At the same time as the previous events happen, the prostate mesenchyme/stroma differentiates into a layer of smooth muscles that surrounds the prostatic buds. Both epithelial and mesenchymal cell differentiation is coordinated with branching morphogenesis and occurs in the proximal-to-distal direction [9, 10]. Notably mesenchyme-epithelial cell-cell interactions are initiated in fetal periods, in which an undifferentiated connective tissue (mesenchyme) induces epithelial development. It can also be considered as a reciprocal stimulation that, for many internal organs, means that epithelium induces smooth muscle differentiation. This indicates that the microenvironment that surrounds the adult prostate epithelium comprises mainly smooth muscle cells as well as extracellular matrix (ECM) [7], in fact about 22% of the stroma is made of smooth muscle androgen receptor-positive cells. Other less common cell types are neuroendocrine cells, present within the epithelial layer of both developing and adult human prostate, as well as rare basal epithelial cells with unique marker expression profiles similar to epithelial stem cells [6, 11]. Those cells are generally characterized by the lack of the AR or PSA expression; because of this and because circulating androgens do not influence their regulatory functions they can be considered androgen-independent. Similarly, basal cells express the AR mRNA and low levels of the AR protein but do not secrete PSA [12]. On the other hand secretory cells are androgen-dependent because they require circulating androgens for their continuous maintenance and undergo apoptosis when androgens are withdrawn [13].

Development of the prostate is spatially restricted by the availability of a few domains in the mesenchyme of the male urogenital tract that can produce prostate-

inducing paracrine signals. On the other hand the potential of the endothelium to respond to these signals is restricted to the endodermal epithelia with similar embryonic origins to the prostate [8]. Although the morphology of the prostate changes from species to species, the signals coming from the UGM are highly conserved [2].

1.2.2 – Signalling pathways in prostate development

Stroma-epithelial interactions lead to cell differentiation and branching morphogenesis through involvement of several key molecules, like the Fibroblast Growth Factors (FGFs), the Sonic HedgeHog (SHH) proteins, the Bone Morphogenic Proteins (BMPs, belong to the TGF-β superfamily) and the Homeobox proteins HOXA13 and HOXD13, in addition to a few others including the cell-surface glycoprotein CD44 and follistatin. CD44 is expressed in both epithelial and mesenchymal cells while its ligand, hyaluronan, is a polysaccharide present in the stromal matrix. Gakunga et al demonstrated the importance in prostate morphogenesis of CD44/hyaluronan interactions by antagonizing them, which inhibited androgen-stimulated ductal branching and prostate morphogenesis in serum-free organ culture of mouse anterior prostate [14]. Signaling includes FGF7 (KGF) and the similar FGF10 that from the mesenchyme bind to FGFR2 on the prostatic epithelium leading to the maintenance of Shh expression [8, 15]. This positive regulation is limited by the negative-feedback loop of downregulation of Fgf expression by SHH signalling. Mice lacking Shh fail to express Nkx3.1 [16], a putative prostate tumor suppressor that is expressed in a largely prostate-specific and

androgen-regulated manner and involved in epithelial homeostasis, have impaired prostate development.

The mesenchymal homeobox genes Hoxa13 and Hoxd13 promote further growth of the prostatic ducts. Knockouts of either Hoxa13 or Hoxd13 lead to small prostates and reduced branching morphogenesis, with total absence of the anterior prostate in Hoxd13$^{-/-}$ mice. Most of these ducts remain unbranched until birth in rodents but, subsequently, epithelial–mesenchymal interactions result in further elongation and branching morphogenesis. Part of the fine control is exerted by the mesenchymal signalling factors BMP4 and BMP7 that inhibit ductal branching and budding (reviewed in [17]), and stimulated by antagonist of Bmps like Fgf10 that, for example, represses Bmp4 expression in opposition to the stimulation by Shh (reviewed in [8]).

Notch1 is another key player in prostate development. Notch1 expression is down-regulated in mature prostates but becomes up-regulated in certain primary and metastatic tumor cells for example in the TRAMP (transgenic adenocarcinoma of the mouse prostate) model [18] suggesting a possible role for Notch1 signaling during prostatic development and tumorigenesis. This was further confirmed by the ablation of Notch1-expressing cells that profoundly prevented epithelial ductal outgrowth in the developing prostate and impaired prostatic re-growth in adult mice [19]. In addition, Notch1 expression is elevated following castration but returned to normal levels after androgen replacement suggesting an inverse correlation between levels of ciculating androgens and Notch1 levels.

The WNT genes encode a large and highly conserved family of secreted glycoproteins and its signalling network plays a crucial morphogenic role in most organs. β-catenin is activated by Wnts and constitutive expression of stable β-catenin in prostate epithelium of transgenic mice resulted in epithelial hyperplasia and squamous metaplasias by 8 weeks of age [20]. These findings suggest that the transdifferentiation of prostate epithelium into squamous metaplasias is an early response of endoderm-derived cells to β-catenin, and that the development of intra-acinous hyperplasia or neoplastic foci is a later event. Both UGM and UGE display strong expression of numerous Wnt genes during early development, several Wnt family members demonstrated characteristic spatial and temporal patterns of expression during prostate development suggesting that the canonical Wnt pathway plays an important regulatory role on epithelial cell proliferation during prostate development [17].

Finally, in a proximal to distal direction, the epithelial cell types differentiate under the control of different transcription factors such as the p53 family member p63, and forkhead family members such as FOXA1, promoting smooth muscle differentiation and localization around the epithelium and the ductal lumen. P63, along with p73, is a homologue of the p53 tumor suppressor gene [21], both human and mouse prostate basal cells express p63 protein and it can be used as a prostate differentiation marker to identify prostate stem cells [22]. Foxa1 is expressed throughout prostate development and maturation in all the lobes but specifically in AR expressing cells, whereas Foxa2 is present only during prostate budding and in cytokeratin 14-expressing basal epithelial cells [17].

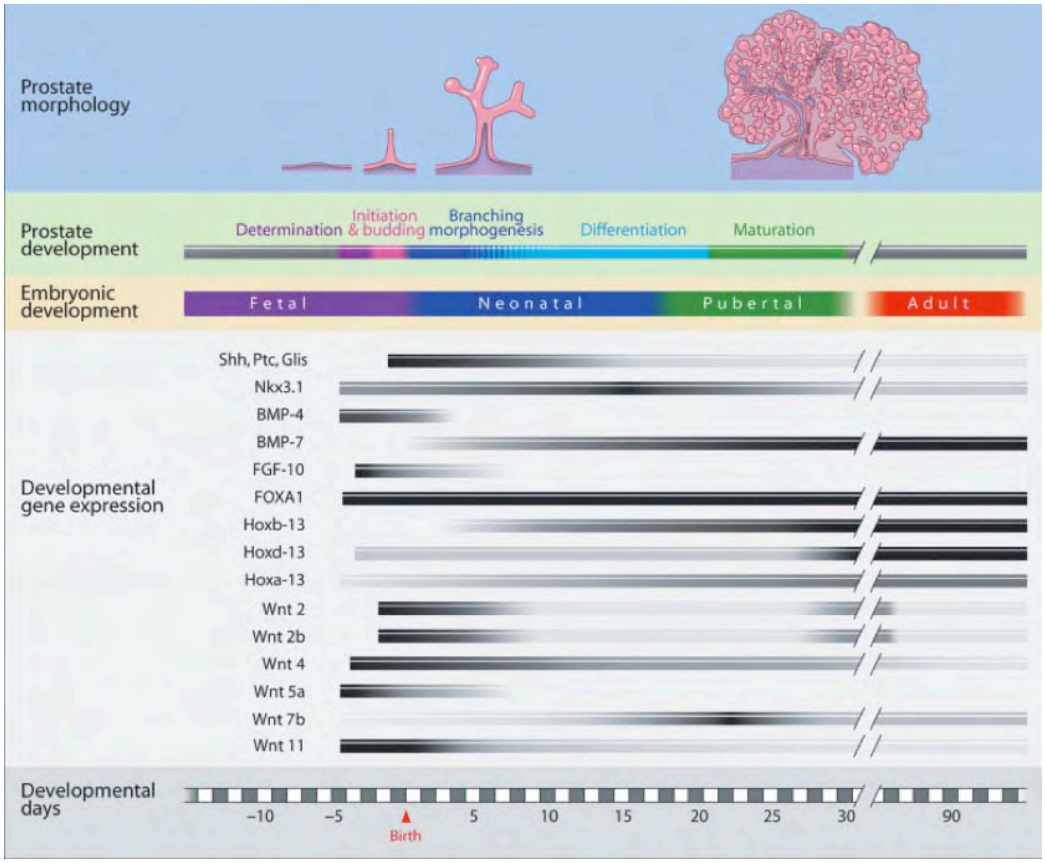

Fig 1.3 – *Rat prostate developmental stages, timeline and morphoregulatory gene expression. The days of fetal and postnatal life are shown at the bottom. Ventral prostate morphology and developmental stages (top) are sequentially aligned to the corresponding days that they appear. Note that cellular differentiation occurs during the later days of branching morphogenesis as indicated by blue-striped lines. Temporal patterns of morphoregulatory genes expression are shown in black-gray-white bars representing relative levels of gene expression as determined by quantitative real-time reverse-transcriptase polymerase chain reaction. Image taken from [17].*

This intricate network of paracrine signalling interactions finely promotes and regulates prostatic bud induction and subsequent branching morphogenesis. These processes are androgen-dependent and the lack of functional AR due to mutations in humans and mice leads to the absence of prostate [23, 24]; interestingly, development of the prostate gland was also observed in female urogenital sinuses after exposure to androgens [25]. During the postnatal period, under the influence

of androgens, the ducts form a patent lumen, and the epithelium lining the acini differentiate and synthesize a variety of secretory products.

1.2.3 – Androgen and other hormonal aspects of prostate organogenesis

NRs are ligand-inducible transcription factors activated by lipophilic molecules whose activity is finely controlled by several hetero-complexes. With few exceptions, co-repressors suppress NRs activity, enhancing their silencing effect in opposition to co-activators that instead enhance NRs action. 48 human nuclear receptors has been described and they can be divided into three groups based on their affinity to their ligands: 1) endocrine receptors (e.g. ERs, AR, VDR, RARs, TRs…), that bind their ligands with high affinity (K_d 0.1-1 nM); 2) adopted orphan receptors (e.g. RXRs, PPARs, LXRs, PXR…), that bind endogenous ligands with low affinity (K_d 1-1000uM) and 3) orphan receptors (e.g. DAX-1, SF-1, SHP, ROR…) for whom a ligand still hasn't been discovered. Upon ligand binding nuclear receptors undergo conformational changes that lower affinity for co-repressor complexes promoting the interaction with co-activator complexes that possesses histone acetyl transferase activity, which allows for transcriptional activation [26]; this leads to the assembly of a pre-initiation complex formed by p300/CPB (CREB binding protein), various TFs (e.g. TBP, TFIIB, TFIID) and Pol-II [26]. On the other hand, in absence of ligand, NRs seem to be bound to a ~2MDa repression complex that includes NCOR2/SMRT (Silencing Mediator of Retinoid and Thyroid hormone receptor [27]), NCOR1 (Nuclear Corepressor), HDAC3, TBL1 and TBLR1 [26]. This

complex leads to silencing of positively regulated target genes repressing transcription initiation.

Androgen action is mediated through the interaction with the AR, and the determination and initiation of prostate organogenesis in both human and rodent fetus is entirely dependent upon androgens produced by the fetal testes. Surgical castration or administration of anti-androgen drugs to rodents during fetal life results in inhibition of prostate development. In the '70s, it was determined by Wilson and Gloyna that the primary androgen responsible for prostatic development is dihydrotestosterone (DHT), the reduced metabolite of testosterone [28]. DHT is formed intracellularly in the prostate epithelium by 5α-reductase and has been shown to have even higher affinity for the AR than testosterone [29]. The fundamental role of AR in prostate development comes from the observation of prostatic absence in mice or humans with complete dysfunctional AR [30, 31]. AR is highly expressed in the UGS mesenchyme and responsible for prostate morphogenesis, whereas epithelial AR expression is induced after budding and branching morphogenesis has begun and is required for expression of secretory proteins in mouse and rat prostate [9].

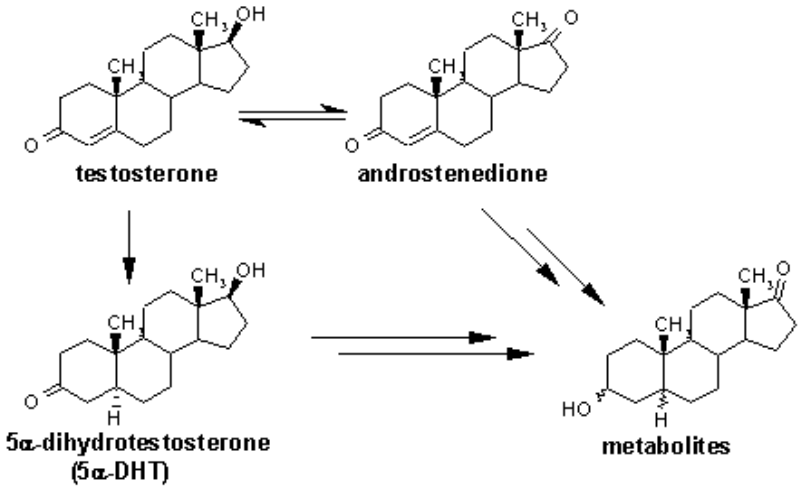

Fig 1.4 – *Schematic representation of testosterone metabolites. The 5α-reductases enzyme catalyzes the conversion of testosterone to 5α-dihydrotestosterone (DHT); the β-hydroxysteroid dehydrogenase converts testosterone into androstenedione; the aromatase enzymes can convert further the androstenedione into estrogen.*

AR induction in prostate epithelium begins as early as postnatal days 1–2 (before cytodifferentiation of the epithelium and mesenchyme) [9]. Therefore it is possible that androgen-driven epithelial signals contribute to morphogenesis of the prostate by affecting the differentiation of adjacent mesenchymal cells. Non-androgen stimulation is also possible due to the differential gene expression pattern along the proximal-distal axis of the prostate while AR expression does not vary [9]. The first known response to androgens by the murine urogenital sinus is the expression of the homeobox gene Nkx3.1 in patches of UGE at 15.5 dpc, which is two days before the appearance of prostatic buds [8]. Although expression of this gene in prostatic epithelium precedes AR expression, subsequent increased Nkx3.1 expression is dependent upon androgen signalling [2]. From this moment onwards the presence of testosterone and DHT are fundamental to achieve complete organ growth with full branching and complete cytodifferentiation. However ductal lumen formation

does not occur and luminal epithelial cells fail to differentiate with a marked decrease in prostatic organ size relative to glands grown with testosterone [32].

To capture the dynamics of AR signalling *in vivo* Hsieh and colleagues carried out a remarkable study creating a transgenic mouse where the sPSA (supra Prostate Specific Antigen) promoter drove the expression of the luciferase enzyme. They then monitored the luciferase activity during development in castrated and non-castrated animals; the results confirmed the importance of DHT in prostate development due to the absence of luciferase activity in castrated mice. There was also a minor detection of signal in legs and bones of a few animals [33] that could interestingly correlate with the fact that some prostate cancers can metastasize in the bone.

Estrogens also play an important role in prostate development; male ER knock out mice are infertile and have fewer epididymal sperm than heterozygous and wild type males [34]. Disruption of spermatogenesis and degeneration of the seminiferous tubules progresses from caudal to cranial pole after 10 weeks of gestation; however prostate, seminal vesicles and epididymis appeared morphologically normal [35]. Neonatal estrogens directly suppress Fgf10 and FgfR2iiib expression both *in vivo* and *in vitro* in the lateral and dorsal prostate, but not the ventral prostate (VP). Furthermore, organ culture studies show that Fgf10 replacement can rescue LP growth and branching inhibition as a result of estradiol administration [36]. Another study unexpectedly showed that male embryos grown between two female embryos (relative to a male that develops between two males) have higher serum estradiol, lower testosterone, increased expression of Ar in the

prostate and larger prostate in adulthood; this means that a small supplement of estrogen from adjacent female fetuses enhances androgen-dependent accessory organ development [37]. This is also confirmed by the finding that male rat fetuses exposed to very low environmental levels of estrogens (bisphenol A) show prostatic enlargement. On the other hand male embryos exposed to high concentrations of estrogens have reduced prostatic growth and compromised structural architecture in rats [38].

It has been suggested that retinoids can mediate the estrogenic effects on prostate development. Vitamin A has a pronounced role in epithelial growth and differentiation; in mice, vitamin A deficiency-induced keratinization of the vaginal epithelium and is similar to that seen with estrus and with neonatal estrogenization of the female reproductive tract, suggesting that retinoids may be mediating the action of estrogen [39]. In support of this theory, neonatal estrogen induction of proliferation and cornification of the vaginal epithelium can be suppressed by coadministration of retinyl acetate [40]. An RT-PCR screen of the rat anterior prostate (coagulating gland) revealed the presence of RARβ and -γ on day 0, whereas RARγ and the RXR isomers were undetectable [41]. As the prostatic cell population changes upon glandular development, the RAR levels shift accordingly, with an overall decrease in total RAR levels in the adult prostate. The normal adult prostate gland is less sensitive to retinoids than the immature developing prostate, which coincides with the known function of retinoids as regulators of tissue morphogenesis and differentiation. Similarly, the normal maturational decline in prostatic RARα mRNA levels did not occur in the estrogenized prostates, resulting in

continued high expression into adulthood and permanent imprint of the expression pattern [42].

In the prostate gland, androgens, estrogens, and retinoids act as upstream regulators of several of the critical developmental genes and timely expression of their cognate receptors is critical for normal morphogenesis. Transient and permanent disturbances in the expression of these transcription factors, as occurs after neonatal estrogen exposure, may consequently lead to abnormal or untimely expression of the prostatic master regulatory genes during the developmental critical windows. As development is an mono-directional, that, in turn, leads to permanent disturbances in the structure and differentiation of this organ [42].

These data together indicate that during prostate development the hormonal environment modulates gene expression temporally and spatially that, in turn, promotes ductal branching form the urogenital sinus and morphogenesis of the growing gland. The list of genes analyzed so far [8] could turn out to be even longer and will include further levels of regulation orchestrated by micro RNAs and epigenetic mechanisms that still need to be unveiled fully. Also, the role of NR such as VDR, PPARs, FXR and GR is still unclear.

1.3.3 – Prostate stem cells and prostate cancer stem cells

Organ stem cells are long-lived and, during the process of aging, they can acquire epigenetic modifications and genetic mutations though exposure to insults such as oxidative stress and DNA damage, resulting in the disregulation of normal cells processes. Prostate Stem Cells (PSCs) represent approximately 1% of the whole

population; a common method used to isolate them is FACS (Fluorescence Activated Cell Sorting), based on the expression of stem cells surface markers like CD133. The existence of prostate stem cells comes from an experiment of androgen cycling in the rodent. The prostate gland undergoes involution after castration but can completely regenerate if androgen levels are restored. As this cycle of involution-castration can be repeated many times, a population of long-lived, androgen-independent but responsive stem cells, responsible for the regeneration of the gland must exist [43]. In the prostate approximately 1% of basal cells express $CD133^{+}/\alpha2\beta1^{hi}$ [44, 45] and it has been shown that prostate cells expressing $CD133^{+}$ exhibited characteristics of stem cells including prostasphere formation and the development of prostatic-like acini when transplanted into immuno-compromised male mice [46].

Molecular profiling of $CD133^{+}/\alpha2\beta1^{hi}$ and $CD133^{-}$ cells isolated from benign prostatic hyperplasia specimens revealed that $CD133^{+}/\alpha2\beta1^{hi}$ cells exhibited an expression profile associated with embryonic stem cells and embryonic development along with other groups representing ion homeostasis, response to chemical and biotic stimuli, cell communication and cell proliferation. In contrast, $CD133^{-}$ cells expressed a profile resembling transit amplifying cells, with genes involved in cell cycle progression, RNA transcription and protein biosynthesis; key regulators of self-renewal and differentiation such as TGF-β, BMP, WNT, SHH and Notch pathways were also differentially regulated by $CD133^{+}/\alpha2\beta1^{hi}$ and $CD133^{-}$ cells [47]. Another study isolating cancer stem cells from human PCa tissues determined that CD44 is expressed in normal PSCs (prostate stem cells) as well as in

prostate CSCs (cancer stem cells); approximately 0.1% of cells in a tumor expressed $CD44^{+}/CD133^{+}/\alpha2\beta1^{hi}$ and they could re-express AR under the appropriate microenvironment, implying that the stem cell niche was crucial in regulating CSCs phenotype and function [48].

1.3 – Prostate neoplastic transformation and tumor progression

1.3.1 – Introduction

Various workers have suggested that the phenotypic characteristics of the cancer are determined by the stem or progenitor cell-of-origin [44]. This has potentially very significant therapeutic implications in terms of understanding disease progression and relapse. An epigenetic progenitor model [44] is a multi-step process in which epigenetic disruption of stem/progenitor cells is mediated by tumor progenitor genes. Subsequently, genetic mutations in gatekeeper genes are acquired along with genetic and epigenetic plasticity. This process could explain the late onset of prostate cancer and other adult cancers, tumor heterogeneity, latent cancers, the consequence of environmental effects, progression to recurrent disease, the genetics of cancer risk [49] and it indicates how the tumor characteristics could be determined by the stage at which these genetic alterations occurred [44].

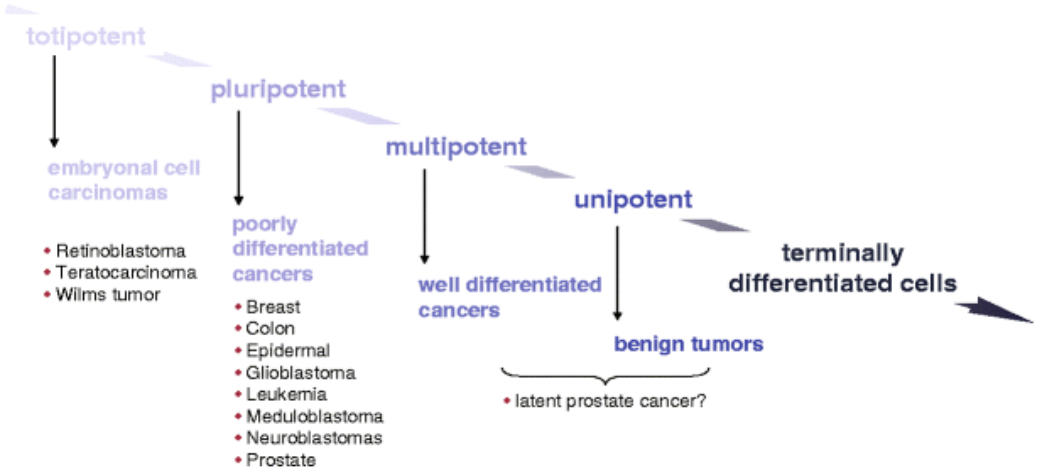

Fig 1.5 *– The progenitor origin of cancer. Epithelial or neuroendocrine cells may acquire epigenetic modifications and genetic mutations through DNA damage, oxidative stress, etc. during the process of differentiation. The phenotypic characteristics of the cancer would therefore be determined by the stem or progenitor cell-of-origin. From left to right (undifferentiated to differentiated cells) is shown how the initial onset of stem cells can differentiate into specific malignancies. Figure taken from [44].*

As shown in **Fig 1.5** mutations in embryonic stem cells would give rise to childhood tumors such as Wilms tumors and other embryonal tumors including teratocarcinomas and retinoblastoma [50]. Mutations in early progenitor cells would promote the development of poorly differentiated cancers including solid tumors such as prostate, breast, and colon cancer [50]. In contrast, well-differentiated cancers would arise from late progenitor cells and benign tumors from cells just prior to terminal differentiation [50].

The prostate cancer stem cell hypothesis has trigged new debates about the origins of PCas; whereas the roots of prostate cancer might be epigenetically written on certain stem cell lineages, the real origins of these aberrations remain unknown. The epigenetic lesions involved in cancer development are not fully understood because

there is no clear explanation of where originally these corruptions arise from. Clues come, for example, from the over expression of the histone methyltransferase EZH2 that, as a late event, is specifically overexpressed in metastatic and aggressive PCas. Although, the self-renewal ability of stem cells and the immortalization of cancer cells share a common role: the maintenance of a proliferative and undifferentiated status that, independently from androgen and cellular control, indefinitely persist in its growth. Exploiting cancer stem cells could be clinically interesting because it could help identify the mechanistic susceptibility to certain tumors, thus, creating either a more targeted therapy or a more efficient program for cancer prevention.

Prostate cancer (PCa) is a major problem at a worldwide level being a cause of death for more than 220.000 men annually worldwide [51]. This disease is highly heterogenic and a number of theories propose how environment, lifestyle, genetic and epigenetic factors can lead to neoplastic transformation [52]. Historically there is a higher incidence of prostate cancer in Western countries; this is mainly attributed to dietary and lifestyle factors, such an increased meat and dairy intake, in addition to reduce fruit and vegetable consumption and sedentary lifestyle, although this is a matter of some controversy.

Histologically, progression to carcinoma is somewhat reminiscent of other epithelial cancers. The first identifiable lesion involves an inflammatory response inside the prostate and is named Proliferative Inflammatory Atrophy (PIA), the next step leads to the development of Prostatic Intra-epithelial Neoplasia (PIN), characterized by nuclear and architectural changes in luminal epithelial cells with maintenance of the basal epithelium and basement membrane and it's a widely accepted precursor

lesion that can lead to adenocarcinoma [52]. The hypothesis of an inflammatory response is coherent with the Western diet that is low in protective antioxidants and exercise and high in potential carcinogens.

PCa is often multifocal and there can be several foci of PIA/PIN in a single prostate and each one of them can present different gene expression patterns and tissue organization. PCa is mostly graded by the Gleason score [53], where a low score mirrors the lesion's grade on the basis of the glandular architecture. Beside this, even two histologically similar tumors can turn out to be clinically different due to intra-tumoral and intra-personal variability, complicating a possible prognosis.

1.3.2 – Genetic aberrations and gene expression in PCa

Several investigators worldwide reported candidate genes and pathways possibly involved in PCa progression reflecting epidemiological and molecular features of prostate cancer and neoplastic lesions.

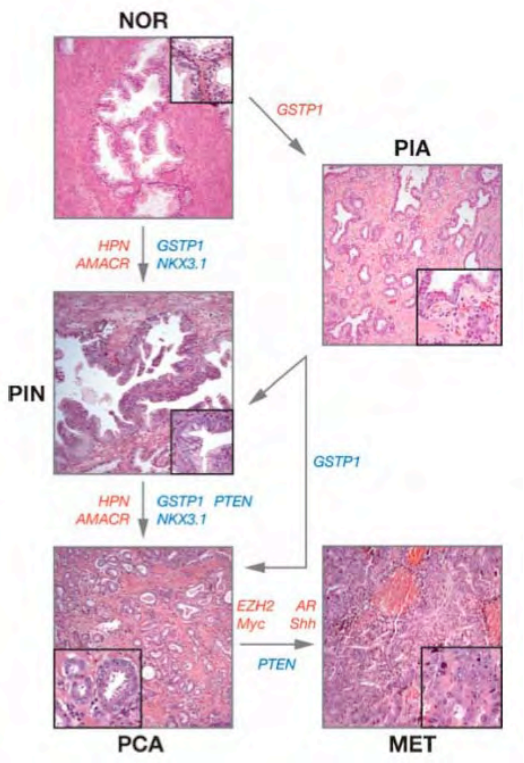

Fig 1.6 – *Genetics alterations during prostate cancer progression. Photomicrographs of hematoxylin and eosin-stained sections representative of the indicated tissue or lesion (10x original magnification, 40x inserts). Arrows indicate proposed routes of progression from normal (NOR) prostate glands to precursor lesions (PIN, PIA) to localized PCa to metastatic disease (MET). Pathway and candidate gene names in blue or red represent genes and pathways underexpressed or overexpressed, respectively, during the indicated transition. Figure taken from [52].*

The genes highlighted in **Fig 1.6** are the main players during the prostate tumorigenic processes; here they will be briefly described in the contest of histological progression to PCa.

1.3.2.1 – Glutathione S-Transferase Pi (GSTP1) in the protection against xenobiotic nutrients

Glutathione S-transferases are enzymes that protect against cancer development by catalyzing the conjugation of the chemical scavenger glutathione to reactive chemical species and they are silenced in most PCas by hypermethylation of the

CpG-island sequences in the GSTP1 promoter. The loss of GSTP1 in PIN is likely to increase the vulnerability to electrophilic or oxidant carcinogens such as 2-amino-1-methyl-6-phenylimidazol(4,5)pyridine (PhIP) often found in well-done or charred meat. These effects have been shown in different PCa cell lines including the androgen-dependent cell line LNCaP and they support the role of inflammation in PCa development (reviewed in [52]).

1.3.2.2 – Phosphate and Tensin Homolog (PTEN)

In 1997, PTEN was cloned and mapped to chromosome 10q27, a region undergoing frequent deletions in a variety of tumors, including prostate cancer [54, 55]. Loss of heterozygosity (LOH) is found up to 60% of the time whereas point mutations and deletions of the PTEN gene have also been reported in both PCa cell lines and xenograft models, as well as primary and metastatic tumors. Epigenetic inactivation of PTEN through promoter hypermethylation has been described in PCa xenografts, however the same phenomenon has not been yet identified in primary human tumors. The biological role of this protein is to suppress the PI3K/Akt signaling pathway that is often up-regulated in cancer promoting cell survival, replication and growth. The neutral endopeptidase (NEP) recruits PTEN to the plasma membrane, which increases the stability and phosphatase activity of PTEN, resulting in Akt inactivation. Pten null mice are die in embryo and $Pten^{-/-}$ ES cells formed aberrant embryoid bodies displaying an altered ability to differentiate into endodermal, ectodermal and mesodermal derivatives. Prostate-specific loss of Pten on both alleles results in completely penetrant high grade PIN and carcinoma with varying rates of metastatic disease [52].

1.3.2.3 – NK3 Transcription Factor Related, Locus 1 (NKX3.1)

The androgen-regulated NKX3.1 is an homeobox gene located in chromosome 8 in position p21 that is frequently a site of LOH in PCa (90%) as well as PIN (60%) (reviewed in [52]). NKX3.1 expression is largely dependent on androgen signalling, modulates PSA transcription (used as a marker for PCa) and acts as a transcriptional regulator [56]. NKX3.1 controls the rate at which proliferating, luminal epithelial cells exit the cell cycle and the deletion of one or both alleles extends the proliferative phase during prostate regeneration; this means that clusters of haploinsufficient and non-haploinsufficient target genes have been elegantly identified with different patterns of expression from gene to gene [57], indicating the different sensitivity of target genes to NKX3.1. Knockout mice display increasing prostatic epithelial hyperplasia and dysplasia with age; by one or two years of age, the mice show features similar to PIN but don't develop into carcinoma, however when $Nkx3.1^{-/-}$ mice are crossed with $Pten^{+/-}$ mice the offspring show high grade PIN with strong activation of Akt, and older mice show invasive carcinoma and easily develop metastasis [52]. These results together indicate the key role played by NKX3.1 alone or in association with other transcription factor in the early stages of prostate tumorigenesis.

1.3.2.3 – Nuclear receptors: AR, VDR, RARs, PPARs

- AR

As previously discussed, during prostate development cell survival is almost entirely dependent upon the AR. Most prostate tumors are initially responsive to androgen ablation, however almost all tumors eventually become androgen

independent and proliferate despite androgen ablation. It has been demonstrated by microarray analysis that the expression of androgen-dependent genes persisted after androgen ablation therapy [58], suggesting that those genes are likely to be involved in proliferation and survival of prostate cells. LNCaP cells, for example, can adapt to androgen deprivation by increasing their sensitivity to androgen by increasing AR expression [59]. Other groups also showed that the AR undergo mainly two kind of mutation; the first kind of mutation localized at specific regions of the receptor that can result in alterations of the androgen receptor function, whereas the second kind of mutations are distributed differently among the AR open reading frame and could cause androgen insensitivity or disruption of the AR signaling pathway [60]. In animal models xenografted with human prostate cancer cells that are AR-sensitive and non-sensitive, it has also been shown that the only gene expression change that was consistent with androgen independence was a two-to five-fold induction of the AR. This increase appeared necessary and sufficient for hormone-independent progression in mice; in fact cells with a modest increase in AR expression are also highly sensitive to androgens [52].

- *VDR*

VDR function in prostate cancer has been extensively investigated; although polymorphisms of the VDR gene significantly correlate with prostate cancer risk [61], epidemiological studies revealed a strong evidences linking sunlight exposure and development of prostate cancer, with males at higher latitudes being more affected than those in warmer countries. This is related to the production of the natural agonist $1,25(OH)_2D_3$ in the skin upon UV exposure; this exerts a protective

effect towards breast, colon and prostate cancer. However, in prostate cancer cells VDR signalling is skewed by epigenetic mechanisms, including altered corepressor expression, that can be partially rescued with the use of HDACs inhibitors [62]. *Vdr* deficient mice revealed the importance of this receptor in mammary gland development by regulating differentiation; also, the *vdr* ablated background have been crossed with tumourigenic models and support anti-tumour chemoprevention roles for VDR at least in breast cancer (reviewed in [63]). It remains to be seen to what extent this occurs in PCa.

- *RARs*

Richter et al. showed an antagonistic effect between the AR and RAR signalling in rat prostate carcinoma and non-carcinoma cell lines where testosterone effect was suppressed by treatment with retinoic acid (RA) [64]. The antiproliferative action of RA is mainly mediated by binding with RARβ whose promoter has been shown to be significantly hypermethylated in PCa specimens [65]; this was confirmed further by the lower mRNA levels of *RARβ* detected in prostate cancer tissues [66]. This epigenetic silencing of the RARβ gene can partially explain the loss of responsiveness towards RA in PC-3 cells that will be discussed in the Results chapter.

Ligand-activation of RARs is also modulated by the concentration of RA inside the cell; in fact, it has been shown that prostate carcinoma tissue contained five to eight times less retinoic acid than normal prostate or BPH.

- *PPARs*

Prostaglandins are readily secreted by the prostate and give rise to the H and D series prostaglandins and 15d-PGJ_2. Equally, the biology of the prostate is associated with the metabolism of fatty acids 15S-HETE. Therefore, the prostate seems to be a tissue where PPARγ may play a strong role in governing cell growth and differentiation. For example, signals derived from PGDS activity in the adjacent stroma, such as PGD2, activate PPARγ, and control epithelial proliferation. PPARγ actions in prostate cancer cell lines and primary cancer models include the induction of type II programmed cell death also known as autophagy. While *PPARα* levels are comparable between PCa and normal tissues, *PPARγ* expression was strongly upregulated [67]. These studies encouraged several groups to undertake clinical trials with PPARγ ligands and disease stabilization was reported (reviewed in [68]).

1.3.2.4 – Myc

c-Myc is located at chromosome 8q24, is a positive regulator of cell proliferation and the disregulation of the Myc family is one of the most common events in human cancer. Gains in chromosome 8 are one of the most common amplifications in human prostate tumors, even at the stage of PIN indicating that other genes in this region could be important for PCa progression [52]. In LNCaP cells it has been shown that Myc over-expressing cells can form colonies independently from the presence of androgens and Myc appears to be an important downstream effector of AR [69]. Mice over-expressing Myc in a prostate specific manner undergo PIN or carcinoma depending on the promoter used [52]; microarray analysis of murine

Myc-PCa interestingly identified a signature based on the overexpression of the protein kinases PIM-1, consistently with other findings of PIM-1 interacting with Myc, and PIM-1 predicts PSA recurrence in patients with localized PCa [52], and NKX3.1 downregulation.

1.3.2.5 – Hedgehog Pathway

The SHH pathway is known for its crucial role in prostate development as well as in the formation of prostate metastasis. Secreted SHH molecules bind to the patched receptor (PTCH), relieving PTCH-mediated inhibition of smoothened, a seven-transmembrane G protein coupled receptor. Smoothened signaling leads to activation of downstream target genes through glioma-associated oncogene homolog (GLI)-dependent transcription. PTCH is also a target of GLI, forming a negative feedback loop [70]. Several studies reported that the hedgehog pathway is activated in PCa in various frequency in benign prostate and localized or metastatic PCa. Subsequent treatment of xenografted cell lines with cyclospamide, a SHH pathway inhibitor, consistently inhibited growth, invasion and metastasis both *in vitro* and *in vivo* [52]. Several other groups published contrasting results regarding SHH expression in cancer cell lines [52] suggesting that the SHH signalling is highly contextual. These findings indicate that the SHH pathway is required for epithelial cell regeneration after androgen ablation, followed by androgen re-treatment, suggesting that PCa might develop from the trapping of normal prostate stem cells in a SHH pathway-dependent state of continuous renewal [71]. The involvement of prostate stem cells and the recent identification of cells with stem cell-like properties in other cancer has led to speculation that tissue-specific stem cells,

through the SHH pathway, may drive many cancers including PCa. This idea would be consistent with the role played by SHH in prostate development and in cancer progression in conjunction with its target gene NKX3.1 and the AR.

1.3.2.6 – Other candidate genes

Different groups used microarray technology to identify genes involved in prostate cancer development and, despite technical and manual variances, there are a few interesting candidates also validated by functional studies for their role in PCa. These are hepsin (HPN), α-methylacyl-CoA racemase (AMACR) and enhancer of Zeste homolog 2 (EZH2).

Hepsin (HPN)

Hepsin is a type II serine protease identified nearly in every microarray study profiling PCa [72]. *HPN* mRNA is upregulated in approximately 90% of prostate tumours, with expression confined to epithelial cells while its role in PCa progression is still unclear. At a protein level HPN is mainly expressed during the PIN stage and decreases in the transition to metastatic cancer. An interesting example of the role of HPN in prostate cancer is the over-expression of HPN in PC-3 cells (malignant, metastatic and androgen-independent prostate cell line) led to reduced cell proliferation and invasion [52], suggesting that an upregulation of this protein at later stages of PCa could be evolutionarily counter-productive. Mice with prostate-specific overexpression of HPN showed no obvious abnormalities in proliferation or apoptosis in the prostate, however a weakening of epithelial-

stromal adhesion and disorganization and disruption of the basal membrane was apparent [73].

α-methylacyl-CoA racemase (AMACR)

The enzyme AMACR, which is involved in peroxisomal β-oxidation of dietary branched-chain fatty acids, has also been identified as an important contributor to PCa. The functionally active protein is specifically overexpressed in PCa compared with benign epithelium and AMACR mRNA is also upregulated in PIN [reviewed in 52]. The major dietary source of branched-chain fatty acids, meat and dairy products, have been implicated in the increased incidence of PCa in Western countries; this is supported by higher levels of phytanic acid in PCa patients, which is caused primarily by dietary intake of dairy and red meat and requires AMACR for its metabolism. At the genetic level a single nucleotide polymorphisms (SNP) in the AMACR gene cosegregates with PCa in hereditary PCa families and knock down of this gene in androgen-dependent PCa cell lines has been shown to inhibit cell proliferation [52].

Enhancer of Zeste Homolog 2 (EZH2)

EZH2 is a member of the polycomb group family of transcriptional repressors and is specifically overexpressed in metastatic and aggressive localized PCas, the finding that it is overexpressed in other kinds of cancer and its ability of conferring proliferation advantages to normal cells may classify it as an oncogene [74]. EZH2 acts primarily as histone methyltransferase promoting gene silencing but it has been shown that its expression is controlled by the pRB/E2F pathway and it's

essential for proliferation in transformed and primary human cells, including PCa [74]. *EZ2F* is downregulated by p53, resulting in cell growth inhibition [52]. Even if its involvement in tumor survival has been proven, more experiments are necessary to elucidate EZ2F's role in prostate cancer pathogenesis more clearly.

Gene Fusion of TMPRSS2 and ETS Family Members

Many hematological malignancies display chromosomal aberrations, either as an inversion, like CBFb:MYH11 in leukemia, or translocation, like the 8;21 resulting in AML:ETO fusion transcript (reviewed in [52]). Tomlins and colleagues indentified the fusion product between the 5' region of the androgen regulated gene TMPRSS2 (belongs to the serine protease family, upregulated in androgen dependent PCa and downregulated in androgen-independent PCa) with ERG or ETV1 (both belong to the ETS transcription factors family) in PCas with aberrant expression of the ETS family members. Combining gene expression data with FISH then revealed that rearrangements in ERG or ETV1 loci occur in the majority of PCa cases [52].

1.4 – PEROXISOME PROLIFERATOR ACTIVATED RECEPTORS (PPARs)

The Peroxisome Proliferator Activated Receptors, or PPARs, are ligand inducible transcription factors that belong to the NR superfamily; they were identified in *Xenopus*, rodents and human in the early nineties being described as the receptors for compounds that induces peroxisome (organelles involved in β-oxidation of long chain FA and H_2O_2-based respiration) proliferation [75]. There are three different PPARs named as PPARα, PPARβ/δ and PPARγ respectively NR1C1, NR1C2 and NR1C3 [76] and they have emerged as important cellular sensors of levels of fatty

acids and fatty acid-derivatives mainly derived by the cyclooxigenase (COX) pathway. In fact, it was shown that polyunsaturated fatty acids bind the three PPAR isoforms with relative low affinity, whereas fatty acid derivatives show more selectivity [77, 78].

PPARs exhibit isotype-specific tissue expression patterns, with PPARα expressed at high level in organs with a significant catabolism of fatty acids, PPARβ/δ in all cell types analyzed with levels depending on the extent of the cell proliferation and differentiation and PPARγ found at high levels in the adipose tissues and lower levels in colon, immune cells and other tissues [79].

All the PPARs heterodimerize with RXR; interestingly synthetic agonists for RXR can activate the dimer exerting antidiabetic outcomes similar to those seen with PPAR ligands in mouse models of type 2 diabetes [80] suggesting that the PPARs are able to drive cellular responses despite the activating events.

1.4.1 - PPARα

Pparα was the first PPAR identified [81]. Human PPARα has been mapped to chromosome 22 adjacent to the region 22q12-q13.1 [82] whereas the mouse homolog maps on chromosome 15 [83]. The major function of PPARα is the regulation of energy homeostasis activating fatty acid catabolism, stimulating gluconeogenesis, ketone-body synthesis and lipoprotein assembly [80]. PPARα is activated by diverse class of compounds including saturated/unsaturated fatty acids (palmitic acid, oleic acid, linoleic acid and arachidonic acid) and hypolipidemic fibrates, that induce hepatic peroxisome proliferation, hepatomegaly and

hepatocarcinogenesis in rodents; this can occur through the production of reactive oxygen species as a by-product of β-oxidation reactions [84]. Pparα-null mice created were indeed resistant to the toxicity induced by treatment with the peroxisome proliferator clofibrate and to hepatocellular carcinomas but on the other hand they presented more extended inflammatory response than the wild type when exposed to the leukotriene B4, a potent chemotactic agent, sustaining anti-inflammatory role of Pparα. Interestingly fibrate compounds do not have the same toxic effect in humans. This is due to the reduced levels of PPARα, roughly 10 fold lower, in the human liver compared to the rodent liver; the PPREs (PPAR Responsive Elements) of genes involved in peroxisome proliferation, including acetyl CoA oxidase (ACO), also differ between rodents and humans and the human enhancer sequence of ACO cannot be activated by PPARα in transactivation experiments (reviewed in [80]).

The wide range of action of PPARα ligands has made this receptor a common therapeutic target for the treatment of dyslipidaemia, cardiovascular diseases and as anti-inflammatory agents.

1.4.2 - PPARγ

This receptor was initially cloned from a *Xenopus* cDNA library in 1992 and subsequently from several mammalians including humans [80]. Two PPARγ isoforms, γ1 and γ2, are expressed at the protein level in mouse and human; the γ2 form presents 30 additional amino acids at its N-terminus due to differential promoter usage within the same gene and subsequent alternative RNA processing.

Also, the localization of PPARγ2 is primarily in adipose tissue while PPARγ1 is widely expressed in heart, skeletal muscle, colon, small and large intestines, kidneys, pancreas and spleen [85].

In many cell types, PPARγ activation has anti-tumorigenic effects probably due to its anti-proliferative and pro-differentiation activities while other experiments showed that its activation could cause pro-carcinogenic effects. This contrast complicates any absolute assumption regarding the phenotypical effects due to PPARγ activation. In mouse models of colon cancer PPARγ expression is increased and administration of troglitazone in xenografted animals inhibit the development of tumors derived from colon cancer cells and the formation of colitis (also an inflammatory condition), a risk factor for further colorectal cancer development in humans. Colon cancer development can be driven by environmental factors such as diet and lifestyle; it has been proposed that the increased incidence of colon cancer in individuals with high fat diet could be due to the constant activation of PPARγ by fatty acids [80]. This contradictory result can be explained by the presence of an APC mutation in colon tissues; thus, an early treatment with PPARγ agonists can prevent the tumorigenic process while, as shown in APC^{min} mice, PPARγ activation after tumor initiation might be inefficient or deleterious [86]. APC^{min} mice have high levels of Pparγ in the colonic cells and are inappropriately sequestrated by β-catenin to a unique set of gene targets. Interestingly, PPARα ligands inhibit polyp formation in the APC^{min} model re-enforcing the concept that the Thiazolidinediones (TZD)-driven enhanced tumor formation in the APCmin mouse is a model artifact, or at least not general phenomena (reviewed in [68]).

PPARγ agonists like troglitazone have been successfully studied in breast cancer for the prevention of mammary carcinogenesis; *in vivo* studies showed that this ligand reduces the development of tumors derived from MCF-7 cell line in nude mice, while GW7845 prevents chemically induced breast carcinogenesis in rats[77]. PPARγ also inhibits proliferation of prostate cancer cell lines and decreases the expression of PSA and this effect is maintained *in vivo*, as troglitazone treatment stabilizes PSA levels in patients with advanced prostate cancer, in an androgen dependent manner. It has also been shown that mutated PPARγ can be present in prostate, thyroid and colon cancer (reviewed in [77]); all of these mutations lead to a decrease in PPARγ activity, which confirms its anti-carcinogenic effect. However, the frequency of these mutations is fairly low and the loss of both PPARγ alleles has never been described in any tumours so far, an observation that indicates that PPARγ might not be a true tumour suppressor.

PPARγ is a potent regulator of cellular energy homeostasis; it has been shown to increase expression of the mitochondrial uncoupling proteins, UPC-1, -2 and -3, *in vitro* and *in vivo*. On the other hand, it downregulates leptin expression, a secreted, adipocytes selective protein that inhibits feeding and augments catabolic lipid metabolism [80]. PPARγ agonists are also able to modulate insulin action through inhibition of TNFα. TNFα-induced insulin resistance in obese rodents and TNFα action in adipocytes in vitro (reviewed in [80]) suggesting a key metabolic role for this nuclear receptor.

The PPARγ pathway regulates the expression of β-catenin upon the presence of a functional APC-β-catenin pathway, sustaining the idea of a link between mutated

APC and PPARγ activation [86]; in pre-adipocytes and pituitary adenoma cells Pparγ activation negatively regulates the phosphorylation state of the Retinoblastoma Protein (Rb) inducing cell cycle arrest and S-phase entry most probably through decrease expression or increased degradation of cyclin D1 [77]. To confirm the control exerted by PPARγ on the cell cycle it has been shown that CDKN2C (cyclin-dependent kinase inhibitor 2C) and $p21^{waf1/cip1}$ expression are positively regulated in a ligand-dependent manner during adipogenesis and in breast cancer epithelial cell line [87]. The NF-κB pathway and the anti-apoptotic protein Bcl-2 were inhibited by 15-deoxy-PGJ2 treatment, leading HT-29 colon cancer cell line to apoptosis [88] suggesting a PPARγ/Bcl-2 feedback look that might contribute to life-death decision in colonic cells. Interestingly, in primary macrophages, breast and pancreatic, cancer cells treatment with the PPARγ agonist rosiglitazone stimulates expression of the tumour-suppressor gene PTEN, with subsequent decreases PI3K kinase activity, by binding of PPARγ to two responsive elements present in the PTEN promoter [89].

PPARγ ligands have been successfully used in clinical trials for the treatment of liposarcoma; however, some of the effects observed in cell culture can be different from those observed in clinic because of PPARγ-independent events. For example, using colon cancer cells as a model, PPARγ agonists have been shown to be potent anti-tumourigenic and anti-proliferative agents but most of them can be beneficial only in the early steps of oncogenesis due, for example, to the APC background of colon cancer cells.

1.4.3 - PPARβ/δ

The third PPAR isotype was called PPARβ when firstly isolated from *Xenopus* oocytes [75], but the mammalian Pparβ gene was not homologous to the *Xenopus* gene, so it was named Pparδ in mouse, Faar (fatty-acid activated receptor) in the rat and NUC1 in humans where it is located on the chromosome 6 in position p21.1-p21.2. Currently they are considered orthologues and are commonly named as PPARβ/δ [77].

As the other PPARs, PPARβ/δ can be activated by prostaglandins as COX-2 again plays a key role to catalyze the rate limiting step in the production of ligands, including the prostacyclin eicosanoid that appears to serve as the natural agonist for PPARβ/δ. PPARβ/δ is expressed in the implantation sites within the uterus and strongly upregulated during the decidualization process in a manner similar to COX-2 [90]. On the other hand Cox-2 null female mice display decreased fecundity, in part due to decreased blastocyte implantation, and, when Cox-2 null mice were treated with carboprostacyclin or the PPARβ/δ ligand L-165041, the implantation was restored [90]. PPARβ/δ is also expressed at high levels in the rat CNS at E18.5 [79] suggesting that it might play a critical role in regulating neurogenesis and neuronal differentiation suggesting a possible cross-talk with the RAR signalling.

PPARβ/δ is also passively regulated by the APC/β-catenin pathway in colorectal cancer cells where its levels are elevated; this repression occurs either through binding of the β-catenin/TCF4 complex on the PPARβ/δ promoter or through treatment with NSAID that disrupts the ability of the receptor to bind to its responsive elements [91]. These results confirm the involvement of COX-2 in

colorectal cancer where it can produce PPARβ/δ agonists like Prostaglandin I2 [91] whereas lowering cyclooxigenase activity via Non-Steroid Anti-Inflammatory Drugs (NSAID) leads to beneficial outcomes. In a PPARβ/δ-null colorectal cancer cell xenograft model tumorigenesis was decreased as well as polyp formation in Apc^{min}/Pparβ/δ-null mice [92] suggesting multiple links with the APC pathway on PPAR signalling in colon cancer tumour progression.

PPARβ/δ exerts its anti-apoptotic function through increased expression of *ILK* and *PDK1* to control cell adhesion, proliferation and survival; ILK and PDK1 in turn phosphorylate and activate the survival factor AKT1 [93]. Therefore it is likely that this PPARβ/δ promotes cell viability in other cell lines too.

1.5 – FIBRATES AND BEZAFIBRATE

Fibrates are a class of amphipathic carboxylic acids mainly used as hypolipidemic compounds; it is well established that treatment with fibrates results in substantial decreases in triglyceride levels associated with a moderate increase in high-density lipoprotein cholesterol (HDL-C) levels and usually a small reduction in low-density lipoprotein cholesterol (LDL-C) levels. Clinical trials demonstrated that fibrate therapy improves both insulin sensitivity as blood lipid profiles thereby significantly attenuating the risk of long term major cardiovascular events [94].

Bezafibrate was the first PPARα and -γ agonist clinically tested [95, 96] and it's the sole PPAR activator with more than a quarter of a century of a therapeutic experience with a good safety profile. The beneficial effects of bezafibrate treatment were confirmed in the BIP (Bezafibrate Infarction Prevention) study where 3090

patients treated with 400 mg/day of bezafibrate showed that, especially those with high triglycerides levels (>200 mg/dL), had a 40% reduction of coronary risk after five years of medication [97]. Patients in this trial treated with bezafibrate showed also a lower incidence of type 2 diabetes, moreover the mean time until onset of new diabetes was significantly delayed among the treated group with a significant 30% reduction risk of new diabetes development. As insulin resistance is considered to occur before the appearance of diabetes, it is important to know whether a drug can prevent it or not. With this purpose, *in vivo* experiments demonstrated that bezafibrate-treated overweight mice fed with a high-fat-sucrose diet had improved glucose tolerance and decreased body weight reducing adipocytes volume in most of the body [98]. The mechanism through which bezafibrate lowers triglycerides levels was shown to be mediated by PPARα activation and PPARα-independent downregulation of the transcription factor sterol regulatory element-binding protein (SREBP)-1c in mice, reducing sterols biosynthesis [99] and overall enhancing lipid metabolism.

As PPAR signalling pathway appears to be involved in either proliferation or survival of malignant cells, several studies have been undertaken to profile the anti-tumorigenic and preventive effect of fibrates on cancer cells. For example in glioblastoma cell lines bezafibrate, as well as ciglitazone and gemfibrozil, inhibited viability and induce cell cycle arrest throughout the re-expression of the cyclins $p27^{(Kip1)}$ and $p21^{(waf1/cip1)}$ [100]. In other studies bezafibrate has been successfully used in association with other drugs such as medroxyprogesterone acetate (MPA) in B-cell chronic lymphocytic leukemia (CLL) [101] and acute myeloid leukemia (AML)

[102] or with the NSAID nimesulide in colon cancer [103]. Ogawa et al instead used bezafibrate in combination with tamoxifen in breast-cancer patients to prevent non-alcoholic steatohepatitis (NASH) induced by tamoxifen treatment, preventing further liver damage [104].

1.6 – CO-REPRESSORS ACTIVITY IN PHYSIOLOGY AND DISEASE

Prostate development, as well as prostate tumourigenesis, is mediated by key genes (described above) whose transcription is regulated by a cohort of transcription factors and co-regulator complexes.

In the next section the key corepressors of the transcriptional machinery will be described to give an overview of their function in physiology and disease and illustrate some of the potential epigenetic mechanisms that may be important to cancer development.

1.6.1 - Co-repressor proteins limit transcription factor actions.

Transcription factors in gene regulation The principal co-repressor proteins were described for their capacity either to attenuate or suppress the transactivation function of transcription factors via epigenetic mechanisms. Among the transcription factors discovered, the superfamily of nuclear receptors (NRs) plays a key role in silencing or activating transcription of target genes involved in metabolism, development and reproduction [105].

1.6.2 - Co-repressors form a structurally diverse super-family of functionally related proteins

Different co-repressor complexes share the same common endpoint in silencing gene transcription. Three of these complexes, Sin3, Mi2/NuRD and CoREST, are highly conserved among *C. elegans, Drosophila melanogaster* and vertebrates, while the NCOR2/SMRT complex resembles the components found only in *Drosphila*; they commonly recruit class I and class II histone deacetylases [106] modifying the chromatin three-dimensional structure and its accessibility from transcription factors.

1.6.2.1 - NCOR and NCOR2/SMRT

Cloning and structure. NCOR1, (Nuclear Co-Repressor-1) can be considered a proto-typical co-repressor and was described in 1995 by Rosenfeld and co-workers. They used a yeast two-hybrid approach to identify a 270KDa protein (initially termed p270), which associates with DNA-bound TR/RXR heterodimers, in the absence of thyroid hormone, but not in its presence[107]. Subsequently human NCOR1 was located to the small arm of the chromosome 17 (17p11.2) [108]. Using a similar approach Chen *et al* isolated NCOR2/SMRT as a co-repressor in RAR-mediated repression of target genes [27]. Human NCOR2/SMRT similarly has a molecular mass of 273 KDa and is located on chromosome 12 in position q24.

NCOR2/SMRT also encodes a 2524-aa protein that is related to the C-terminal half of NCOR1 [109]. An N-terminal domain, named NCOR2/SMRTe and NCOR1 conserved

(SNC) domain, between amino acids 166 and 429 is strikingly conserved between NCOR2/SMRT and NCOR1 (86% identity and 91% similarity). At the N terminus of the SNC domain, lays an amphipathic helix containing five hydrophobic heptad repeats. The SNC domain is followed by two conserved repeats known as the SANT domains. The two SANT (SWI3, ADA2, NCOR1 and TFIIIB B) motifs are only marginally related to one another within the same protein (30% identity), whereas the individual motif is highly conserved between NCOR2/SMRT and NCOR1 in both the human and mouse origins (>75% identity) [109]. Two SANT DNA-binding domains are present between the residues 440-488 and 627-674 [110]; while the first SANT domain (SANT1) is dispensable, SANT2 is essential for interaction with HDAC3 [111]. Other groups described the importance of these domains in the interaction with HDAC1 [112, 113] and in CoREST-mediated neuronal gene regulation [113]. NCOR1 interacts with the otherwise inert HDAC3 via the deacetylase interaction domain (DAD) located between amino acids 313 and 1445 [111]; compared with the SANT domains this region has an additional N-terminal helix and a significant difference in the angle of helix 3 that results in the formation of a nonpolar cleft on the surface of the domain [114].

Also, both NCOR1 and NCOR2/SMRT contain three to four repression domains (RD1-3) [109, 115-117] at the N-terminal region; more precisely in NCOR1 RD1 and RD4 are involved in the interaction with TBL1 and TBLR1 [118], two very small and highly related proteins containing a WD-40 repeats region and present in the corepressor complex. TBL1 also interact through RD1 with SMRT and RD2 region is instead the bridge that connects HDAC3 to both corepressors [119]. Those two

regions share 45% of identity between NCOR1 and NCOR2/SMRT supporting the idea of a functional conservation [120], and further supporting the concept that these large proteins act as facilitative central hubs in order to recruit other components of the corepressor complexes.

Complexes and function. NCOR1 is able to form complexes with a very wide range of transcription factors and coregulator proteins, including Mad/Mxi, MyoD, BCL6/LAZ3, AML1-ETO, CBF, TFIIB and REST/NRSF (reviewed in [121]), generally repressing transcription of target gene. Once activated, the target transcription factor displaces the corepressor complex in favor of the coactivator complex. Interaction between NRs and NCOR1 involves remodeling of the trans-activation domain AF2 contained in the helix 12; this structure can be next to the ligand-binding domain (LBD) in the case of RAR-alpha, TR-beta, ER and PPAR-gamma, or far away in the case of RXR (reviewed in [121]). Binding of the co-repressor motif is further reinforced by antagonist binding, which blocks the AF2 helix from adopting the active position [122]; instead, when the AF2 helix is in ligand-bound conformation NCOR1 and NCOR2/SMRT do not interact with the LBD. It has been proposed that co-repressor/co-activator exchange upon ligand binding is caused by the difference in length of the interacting motifs that can be accommodated in the binding pocket in the apo- (unliganded) and holo- (ligand-bound) conformations [123]. Co-Activator interactions happen via the Leu-x-x-Leu-Leu motif, called “NR box” [121]. There are three different Interaction Domains (IDs) in NCOR1 (N1-3) and NCOR2/SMRT (S1-3), they contain similar motifs to the coactivators NR box and are named “CoRNR box”.

The spacing of the NR responsive elements in the heterodimer determines the interaction with the 1-box NCOR2/SMRT isoforms, this binds TRα/RXRβ DR-4, VDR/RXRβ DR-3 and RARα/RXRβ DR-5 complexes; the 2-box isoforms bind mostly TRα/RXRβ and TRβ/RXRα [124] heterocomplex; the 3-box isoforms bind NR-DNA complexes weakly, with two exceptions: the "all-exons" isoforms preferentially binds TRα/RXRβ and the Δ45b isoforms preferentially binds the VDR/RXRβ complex [125]. Disruption of any of the CoRNR boxes in both NCOR1 and NCOR2/SMRT does not abolish the interaction with TRα; in case of RARα instead, over that a higher affinity for NCOR2/SMRT, the disruption of any CoRNR box in either CoRs leads to a significantly reduced interaction with RARα, particularly in case of NCOR1 [126]. Within the three NCOR1 interaction domains (N1-3) it has been shown that N2 is important for the binding of the corepressor with TRβ1 but the specificity of this interaction is dictated by N3 *in vivo* [127]. This receptor has also been shown to bind NCOR1 through three interaction domains, where each ID motif contains a conserved hydrophobic core (I/LXXII) that resembles the hydrophobic core of NR boxes (LXXLL) that mediates p160 co-activator binding to the liganded state [128]. Hu *et al* established that these CoRNR (CoRepressor NR) boxes are required for NR interaction, and that CoRNR box peptides specifically block co-repressor interactions *in vitro* and repression *in vivo* [129].

An interesting example of NCOR1 mediated trans-repression of positively regulated genes is NCOR1 binding to PPAR-γ that involves a ligand-dependent sumoylation of the PPAR-γ ligand-binding domain, which targets PPARγ to NCOR1/HDAC3 complexes on promoters of genes target. This prevents recruitment of the

ubiquitylation/19S proteasome and NCOR1 clearing from the promoter region [130].

Epigenetic mechanisms of NCOR1-mediated gene silencing also involve interaction with the protein, Kaiso, a methylation dependent transcriptional repressor [131]. This protein was found in the immunopurified NCOR1 but not in NCOR2/SMRT complex and also doesn't bind other key components of the repression complex as TBL1/TBLR1 or HDAC3. Interaction between the POZ domain in Kaiso and the RD1 repression domain in NCOR1 allows this complex to interact with the methylated CpGs present in the promoter of target genes, silencing their transcription [132].

Due to the complex system involved in gene regulation, inhibition of transcription cannot be view as a static mechanism. An example of this dynamic machinery is the recruitment of corepressor complexes on the promoter region of inflammatory genes. After TNF-α treatment a time-dependent binding of NCOR1/HDAC3 and NCOR2/SMRT/HDAC1 complexes switch on the promoter region of IκBβ every 30-60 minutes, similar to the pattern registered for SRC-1 and -2 whereas SRC-3 recruitment oscillated between two peaks at 30 and 120 minutes [133, 134].

NCOR1 is subjected to several post-translational modifications; it has been reported that phosphorylated NCOR1 and NCOR2/SMRT can be translocated from the nucleus into the cytoplasm in colon cancer [135] .

Embryo development, as cell differentiation, require a precise network of regulatory elements, many of which appear to be modulated by NCOR1 and NCOR2/SMRT. In the case of adipocytes differentiation PPAR-γ has been shown to drive this process

upon ligand binding but its activity is dependent on NCOR1 expression; lowering levels of NCOR1 or NCOR2/SMRT leads to an increased expression of adipocyte-specific genes and proteins suggesting that NR corepressors modulate adipogenesis via effects on PPAR gamma activity [136].

Differentiation of neural stem cells into astrocytes is highly Ncor1-dependent; Hermanson *et al* demonstrated that Ncor1 is a principal regulator in neural stem cells. Ncor1-disrupted mice display impaired self-renewal and spontaneous differentiation in astroglia-like cells [137]. *In-vivo* experiments showed that Ncor1 also exerts critical roles at specific steps in erythroid, thymocyte, central nervous system (CNS) development and haematopoietic differentiation; knockout mice show severe anemia and secondary edema, embryos are generally smaller than wild type. $Ncor1^{-/-}$ mice generally die at day 15.5 of gestation with just a few occasionally surviving a couple of days longer [138].

Ncor2/Smrt knock-out is also lethal; $Ncor2/Smrt^{-/-}$ embryos generally die at ED 16.5 because of heart defects and present noticeable differences in CNS development. This is partially due to the activity of Jmjd3, a putative histone demethylase, responsible for demethylating H3K27me3 during neuronal stem cell differentiation; its expression is promoted by RA (Retinoic Acid) in neuronal stem cells and de-repressed by Ncor2/Smrt knock-out demonstrating a Ncor2/Smrt-dependent, RA-receptor-mediated regulation of this process [139]. Nonetheless Ncor2/Smrt regulates with Foxp1, a forkhead protein that acts as transcriptional repressor, a cohort of genes necessary for a proper myocardial development. In wild type hearts Ncor2/Smrt and Foxp1 are detected in the Cdkn1a promoter together

with H3K9me2 (mark associated with Cdkn1a repression [140, 141]) whether in both knockouts *p21* levels are elevated, leading to a block of proliferation and thinned myocardium [142].

An initial clue regarding NCOR1 role in prostate cancer was revealed by Ting et al. publishing that NCOR1 mediates VDR activation in different CWR22s prostate cancer cell line. The AR-NCOR1 interaction is key for the regulation of the androgen signaling, that is corrupted in prostate cancer. Hodgson et al. demonstrated that the AR-antagonist Mifepristone (currently used in prostate cancer treatment) efficiently enhances this interaction at nanomolar concentrations [143] while other demonstrated that this interaction is already present in prostate cancer cell lines [144].

Based on these results it is possible to assume that NCOR1 and NCOR2/SMRT are involved in several steps moving from totipotent stem cell towards differentiated organ with similarities among different tissues. Similarities are also present between cell differentiation and tumourigenesis processes and lies in the loss of gene regulation in malignancies.

1.6.2.2 - CoREST

Cloning and structure: REST/NRSF (RE1 silencing transcription factor/neural-restrictive silencing factor) functions to block expression of its target genes, primarily type II sodium channels [145]. These actions are mediated through interactions at the C-terminal with a 482-aa protein named CoREST, which contains

two 50-aa SANT domains separated by 191aa and it is present in a wide variety of both neural and non-neural cell types. Further, REST/NRSF is able to interact with a small C-terminal fragment containing a zinc finger motif that mediates repressor activity [110]. Most corepressors are found complexed with chromatin remodelling enzymes; in this case it has been shown that CoREST interacts with HDAC1 through an ELM2 domain [146].

Complexes and activity: CoREST is part of a multiprotein complex, termed BHC or BRAF-HDAC [147], together with HDAC1, -2, BHC80, BRAF35 and LSD1 (or BHC110), which is responsible for demethylating [148] mono- and di- methyl histone H3 lysine 4 (H3K4) or lysine 9 (H3K9) (thereby de-repressing AR target genes [149]). Together with LSD1, CoREST regulates transcriptional activity of Gfi-1 and Gfi-1b (Growth factor independence -1, -1b), zinc finger repressors critical for various developmental processes. Any interaction occurs through the repression SNAG domains located at their N-termini. It has also been shown that reduction of CoREST levels leads to increased expression of REST target genes and to a nearly fourfold increase of H3K4 methylation [150].

The CoREST complex is also involved in the neoplastic transformation controlling key players of cell proliferation and immortalization. A component of this corepressor complex is ZNF217; this gene codes for a Kuppel-like transcription factor and is a strong candidate oncogene found in breast cancer at the 20q13.2 amplicon [151]. The CoREST/ZNF217 complex has been found to sit on the promoter region of the $p15^{INK4b}$ gene [152]; this is a member of the INK4 family of CDKI that causes cell cycle arrest directly inhibiting CDK4 and -6 and its

loss/mutation has been reported in several cancers [153-155]. Downregulation via siRNA of ZNF217 and TGF-β treatment, that causes promoter release of ZNF217, mirror their effects with the upregulation of $p15^{INK4}$ [152] facilitating its transcriptional reactivation. CoREST contributes to the control of telomerase activity through repression of hTERT [156]. This suggests a role for CoREST as a bridge between HDACs and LSD1 in modulating histone modifications and gene repression in normal cells and contributing to the immortalization process in malignancies.

Another mechanism widely used to stably silence gene expression is DNA methylation at CpG islands; MeCP2 specifically recognise symmetrical methylated CpG pairs [157, 158]. Lack of MeCP2 leads to increased levels of CoREST and subsequent repression of the target genes such as the neurotrophic factor BDNF.

CoREST is involved in a so-called "reversible repression" where it participates in the recognition of methylated DNA and histone lysines in an active locus and, recruiting MeCP2, LSD1 and/or other histone modifiers, like HDACs, promotes a tight chromatin structure leading to an active repression [159].

1.6.2.4 - LCOR

Cloning and structure: LCOR was firstly isolated from a fetal brain c-DNA library in 2001 with a 1299bp open reading frame fragment (433 amino acids, 47.006 kDa) was named KIAA1795 [160]. The LCOR gene is located at the long arm of the chromosome 10 (10q24.1) covering 4.8 kb of cDNA sequence encompassing seven

exons and including four 5'UTR exons that contain several in-frame stop codons. Structurally LCOR presents a single NR box (LXXLL motif) that is essential for the interaction with NR such as ERα. It also contains a PRKKRGR motif at position 339 that is homologous to a nuclear localization signal (NLS) of the SV40 large T antigen-type and lies at the N-terminus of a putative helix-loop-helix domain. LCOR contains a consensus leptomycin B-sensitive nuclear export signal at position 149-164 suggesting that its access to transcription factors could be regulated by nuclear export under certain conditions [161] as demonstrated for NCOR1-NF-κB interaction [162].

Complexes and function: *LCOR* is mostly expressed in placenta, predominantly in the syncytiotrophoblasts, the layer where ER resides as well as progesterone (PR) and glucocorticoids (GR) receptors. This region represents a barrier between maternal and fetal circulation and a key site for hormone signalling, catabolism and biosynthesis [163]. LCOR could then act as a modulator of transcription factor signalling in a place where waves of endogenous hormones continuously stimulate NR. Consistent with this hypothesis, LCOR has been proven to associate with the LBD of a range of nuclear receptors including ERα, VDR, RARα, -ß and -γ and GR in a ligand-dependent manner. LCOR binds the AF-2 domain of ERα, and recognises the helix-3 where TIF-2 (or NCoA-2, Nuclear CoActivator-2) associates, suggesting a possible competition for that site.

LCOR could exert part of its repression activity through direct interaction with its C-terminal part and HDAC-3 and -6. Interestingly HDAC-3 is present in NCOR1

complexes and this could suggest a cross-talk or cooperation between these two corepressors. However, TSA treatment does not completely relieve VDR or PR LCOR-mediate repression and so other mechanisms might be involved.

1.6.2.6 - RIP140

Cloning and Structure: The receptor-interacting protein-140 (RIP140), located on 21q11 [164], was first identified by Cavailles *et al* in 1995 as a 1158 amino acid protein that binds in a ligand-dependent manner with the AF2 domain of ERα. In this system RIP140 can trans-activate estrogen receptor activity upon ligand binding while strongly trans-represses ER functions at higher concentrations [165]. Interestingly, the C-terminal domain of RIP140 was shown to contain a stronger repressor activity then either the whole length protein or the two other repressive regions at the N-termini [166]; indeed it contains four repressor domains (RD1-4) and two putative NLS. This protein also contains nine copies of the NR box, also found in SRC-1 and CBP, necessary and sufficient for the binding to liganded NRs [167]. Those motifs are spread on the whole protein with the addition on the C-terminus of a single LXXML motif where a leucine is substituted by a methionine [168].

Complexes and functions: The agonist-dependent silencing activity of RIP140 has been proven for a wide range of NR beside ERα. This list includes RARα/β, RXRα/β, TRα/β, GR, AR, VDR, PPARα/γ/δ, LXRα/β (reviewed in[169]). The main function of

RIP140 in these cases appears to be the limitation of the NR trans-activation although a ligand-dose dependent effect cannot be excluded.

RIP140 participates in epigenetic mechanisms of gene regulation influencing chromatin conformation by recruitment of histone remodelling enzymes; necessary for this function is the region between amino acids 78-303 that interacts with HDAC1 and HDAC3 [170] as well as HDAC2, -5 and -6, even if their function in RIP140-mediate repression resulted to be dispensable [166]. Another mechanism of repression involves the C-terminal Binding Proteins (CtBPs; -1 and -2). these highly conserved corepressors modulate NR activity, cell cycle and development [171] and have been shown to interact with RIP140 through different domains. This interaction, as well as those with HDACs, contributes to RIP140-mediated repression, but it's a component of a more complex mechanism that could explain the idea of RIP140 being a common interacting protein for diverse co-repressor complexes. This agonist-dependent repression, as for LCOR, appears important in order to avoid an over-activation of transcription factors, maintaining the physiological equilibrium requested for gene expression, metabolism and development.

1.6.2.9 - SLIRP

Cloning and Structure: SLIRP (SRA stem-loop interacting protein) has been recently identified by Hatchell *et al*. for its ability to bind STR7, a substructure of SRA (Steroid Receptor Activator), and modulate NR pathways.

Isolation of SRA binding protein through yeast three-hybrid screen of a primary human breast cancer cDNA revealed a predicted 109 amino acids sequence with a M_r of 12.7kDa. This mitochondrial protein is composed almost entirely of an N-terminal RNA recognition motif (RRM) containing RNP1 and RNP2 submotifs with considerably homologue to the SHARP (NCOR2/SMRT/HDAC1 associated repressor) [172] and nucleolin RRM motifs. The amino acid sequence is interestingly highly conserved between species underlying the importance that this protein could hinge.

Human SLIRP is located in the chromosome 14q24.3 just 1750 nt, adjacent to SKIP, a corepressor involved in NR signalling, indicating that those two transcripts could be coordinately regulated [173].

Complexes and Functions: Immunoprecipitating SLIRP revealed *in-vivo* association with STR7 with high specificity; however, SHARP also binds tightly to STR7 and it may compete with SLIRP for this interaction. SLIRP represses SRA coactivation in a dose-dependent manner also enhancing Tamoxifen antagonistic activities. Its range of interactions widens through different NR such as GR (Glucorticoid Receptor), AR (Androgen Receptor), TR (Thyroid Receptor), VDR (Vitamin-D Receptor) and PPAR-δ(Peroxisome Proliferator Activated Receptor) [173].

ChIP assays demonstrated that SLIRP is recruited on the E2-responsive pS2 promoter in the presence of SRA. Furthermore there is the possibility of a coordinative effect of SLIRP with NCOR1 or other co-repressors due to the

undetectable amount of NCOR1 in the promoter region when levels of SLIRP drop [173].

A wide variety of cell lines from different tissues express SLIRP and therefore it is possible that the role of this protein in physiological and pathological conditions could be crucial. Being a mitochondrial protein means that could be involved in the energy homeostasis pathway suggesting a role in other diseases.

1.7 - HISTONE DEACETYLASES AND HISTONE DEACETYLASES INHIBITORS

Around forty years ago, Vince Allfrey discovered the reversible acetylation of histone proteins and proposed that this post-translational modification could regulate gene expression [174]. The role of histone acetylation in transcriptional regulation remained controversial until 1996, when two papers reported the identification of the first acetyltransferases, GCN5 and the first histone deacetylase HDAC1 [175, 176]. Eighteen potential human histone deacetylases were identified and divided in three families: Class I HDACs (HDAC1, -2, -3 and -8) and Class II (HDAC4, -5, -6, -7, -9, -10 and -11), which are homologous to the yeast histone deacetylases Rpd3 and Hda1, respectively, and share some degree of sequence homology while Class III histone deacetylases (SIRT1-7) are homologous to the yeast protein Sir2 and use NAD as a cofactor.

1.7.1 – Biochemistry Of The HDAC Complexes

Histone deacetylases play a key role in the regulation of transcription by modifying the chromatin environment; in order to perform this function and achieve proper

modulation of their activity HDACs complex with other regulatory proteins, and in some cases, with themselves.

1.7.1.1 – Class I HDACs

Class I HDACs exhibit very weak activity in isolation and their multiple functions require interactions with specific factors that modulate the response to different stimuli. Complexes have been described for HDAC1, -2, -3, while little is known about the proteins interacting with HDAC8, -11. Class I deacetylases access specific regions of DNA but they lack DNA binding activity [177]. Access to specific chromosomal regions is facilitated through the large number of transcription and chromatin related factors like the corepressors SMRT and NCOR, YY1, RUNX2, RBP-1, SP-1, CTCF, the DNA methyltransferases DNMT1, the H3 histone methyltransferase Suv39H1 and the retinoblastoma protein, Rb that binds to HDAC1 (reviewed in [177]).

The corepressor Sin3 was shown to bind with a number of transcriptional regulators such as the helix-loop-helix heterodimers of the Mad family Mad/Max [178]. Moreover, Sin3 interacts with the 18 kDa protein Sap1830 and the 30 kDa protein Sap30 that was found to link the Sin3-HDAC complex to Swi/Snf. This complex appears to function as a switchboard that coordinates the interactions between HDACs and sequence-specific DNA binding proteins over than stabilizing the interaction between HDACs with NCOR1 and NCOR2/SMRT [179]. The human Sin3-HDAC complex was able to deacetylate all of the core histone when in isolation, but not when composing nucleosomes, suggesting that chromatin remodeling

precedes deacetylation in vivo [180]. HDAC1 and HDAC2 are part of the complexes with the Nucleosome Remodeling and Deacetylase (NuRD) complex together with the methyl-DNA binding protein MBD3, the corepressor Metastasis Associated Protein (MTA) 1, -2 and -3 and the ATP-dependent chromatin-remodeling protein Mi2. HDAC1 has also been found to interact with the CoREST/BHC complex through binding with the first SANT domain of the corepressor CoREST (reviewed in [177]). HDAC3 is another member of the Class I HDACs but, unlike HDAC1 and HDAC2, its function is less global and generally involved in the repression of target genes connected with the NR signalling. Most of the HDAC3-containing complexes are rather large (1-2 MDa) and most of them share several subunits; the most convincing studied complex appeared to contains HDAC3, NCOR/SMRT, Transduction β-Like protein (TBL1), Transducin β-Like Related protein (TBLR1) and the G-protein Pathway Suppressor-1 (GSP-1).

1.7.1.2 – Class II HDACs

- HDACs Class IIa

Class II HDACs consist of HDAC4, -5, -7, -9 and a splice variant of HDAC9 that contains only the N-terminus region of the protein named interacting transcription repressor (MITR); all of these enzymes contain binding sites for the myocyte enhancer factor 2 (MEF2) and CtBP [181]. The most striking feature of Class II HDACs is their ability to shuttle between the nucleus and the cytoplasm; this occurs through phosphorylation of one or two of the three N-terminal serines by calcium calmodulin-dependent protein kinase (CaMK), which is activated by Ca^{2+} release.

Once the HDAC reaches the cytoplasm and is thus phosphorylated, complex formation with 14-3-3 sequesters the enzyme in the cytoplasm, thwarting its ability to repress transcription [177].

Class II HDACs do not exhibit enzymatic activity in isolation but also only in conjunction with the NCOR1-NCOR2/SMRT corepressor complex [182]. However, given that this corepressor complex contains the Class I HDAC3, that is enzymatically active without Class II enzymes, the class II HDACs may be redundant, or, more likely, the enzymatic activity of the full complex (containing both HDACs) may target histone polypeptides as well as non-histone substrates [177].

- *HDACs Class IIb*

Class IIb consist of HDAC6 and -10; HDAC6 was found to be an α-tubulin deacetylase and able to binds polyubiquitin chains on mis-folded proteins. A link with Parkinson's disease was revealed when HDAC6 was found to interact with cytoplasmic dynein, a microtubule minus end-directed motor protein necessary for the transport of mis-folded proteins [183]. This evidence suggests that HDAC6 is an adapter protein that allows aggregated, mis-folded and polyubiquitinated proteins to come together with dynein, with subsequent transport to aggresomes [177]. Moreover, HDAC6 colocalizes with ubiquitin conjugated and α-synuclein in structures resembling neuronal inclusion bodies, Lewy bodies, a defining feature of Parkinson's disease [184].

1.7.1.3 – Class III HDACs

Class III HDACs are related to the yeast NAD+-dependent HDAC silent information regulator 2 (*Sir2p*), which is involved in gene silencing through the generation of heterochromatin-like compacted chromatin that is hypoacetylated in histone H3 and H4 tails [185]. Homologs of *Sir2p* are present in all higher organisms, including 7 homologs in human (SIRT1-7) [186].

SIRT1 in its native form is a homomultimer of about 400-500 kDa that most likely corresponds to a trimer although small amounts of the enzyme can be present in other complexes; it has a broad-spectrum catalytic activity targeting all core histones (preferring H4K16Ac, H3K9Ac and H1bK26Ac) as well as p53, TAFI68, BCL6, FOXO, Ku70 and NF-κB (RelA/p65) (reviewed in [177]).

SIRT2 is almost exclusively located in the cytoplasm and was shown to co-localize with tubulin and de deacetylate acetylated α-tubulin. Interestingly it was shown to immunoprecipitate with the known tubulin deacetylase HDAC6, suggesting a functional complex between those proteins [187]. Although SIRT3 was shown to be cleaved at the N-terminus it still hasn't been found in multiprotein complexes [177], leaving its role unclear.

It is clear that there is a strict cross-talk between NR signalling, co-repressors and HDACs activity that modulates the transcriptional landscape of prostate cells; this leads to dynamic responses of the system that influences cell viability and differentiation. This pathway can be modulated by endogenous and synthetic ligands either activating NRs or inhibiting HDACs in order to have an impact on the phenotype of normal and malignant prostate cells.

1.8 – SYSTEMS BIOLOGY

1.8.1 – Why do we model?

Most of the pathways present in textbooks and papers are the results of experimental observation that described for example the physical interaction between two proteins; in a linear system we can intuitively predict that if we reduce the concentration of a component upstream this will decrease the activity/concentration of a downstream product. The numerous pathways inside of a cell cross-talk between each other and there is little knowledge about what is the "weight" of each element in the network; knowing this, could 1) explain mechanistically how certain reactions occur, 2) allow researchers to precisely predict an outcome based on how the component interact with each other and 3) suggest further experiment to validate experimental data and, on another level, 4) help to predict patients sensitivity to treatments.

Prostate malignancies remain a complex disease where multiple component are simultaneously corrupted; within this system, nuclear receptors play a key role in prostate epithelium viability and survival, modulating the transcriptome in coordination with chromatin modifying enzymes that mark the epigenome landscape to uniquely activate or repress gene transcription. Systems biology offers the mathematical tools to understand the single components of these networks. In this way it is anticipated that biology will transition from being qualitative and descriptive to quantitative and predictive [188, 189].

1.8.2 – Concepts and Applications

Biological networks can be simply described as a number of interactions happening within a system to produce a genotypic, metabolic or phenotypic effect. The "system" could be a single cell, where thousands of proteins interact with each other or with nucleic acids, or it could also indicate an organ where not only intra-cellular reactions are taken in count, but also cell-to-cell interactions which contribute to the maintenance of the physiological functions of an organ. When, for any reason, the system get corrupted it's possible that the equilibrium of these reactions is lost with a resulting disease or neoplastic transformation.

All the components form networks that contain at least one hub that interacts with one, or more, single components or complexes. When one single component varies in concentration (i.e. because of up- or down-regulation of the mRNA) or activity (i.e. because of a mutation) the whole network, or system, is influenced. If this component is a key element of a hub the net result will be that part of the pathway, or pathways, will be heavily influenced by its physical or functional modification; on the other hand it's also possible that if a non-key component varies there are no noticeable functional changes in the pathway.

Systems Biology is a relatively new field that focuses on mathematical modeling of biological and biochemical networks in order to understand mechanistically and dynamically deep functions of the single components of a network. This can refer to DNA binding proteins, histone modifications, protein-protein interactions or biochemical reactions in normal or malignant cells, in physiology or disease.

There are two approaches to modeling: bottom-up and top-down. The first one refers to the integration of all the pieces of data collected to build up a reliable model of a relative big system while the second approach is the opposite, where a greater system is broken down into its smallest components. For the purposes of this thesis the bottom-up approach was undertaken, hence, mRNA and ChIP data were used as a starting point to model *CDKN1A* transcriptional initiation in prostate non-malignant cells RWPE-1.

1.8.3 – How to build up a model

Every reaction where two components (A, B) interact forming an intermediate complex (AB) can be described as a mass-balance equation as follow:

$$A + B \underset{k2}{\overset{k1}{\leftrightarrow}} AB \qquad (a$$

and the correct equation to describe the variations in concentration of A and B would be:

$$\frac{d[AB]}{dt} = k1[A] + k1[B] - k2[AB] \qquad (b$$

The term $\frac{d[AB]}{dt}$ indicates the changes in concentration of the complex AB in time that are given by $k1[A] + k1[B] - k2[AB]$, hence, by the initial concentration of A and B multiplied by the constant k1 (indicating the speed of the reaction) minus the concentration of the complex multiplied by the disassociation constant k2.

Ordinary differential equations (ODE) are a useful way to describe system's dynamic when the initial concentration, or number, of molecules is high because it does not take into account the probability in time that the interaction between two components happens. In the case of a single cell system where the focus is on describing the interaction of a protein with a response element (e.g. promoter region) there are just a few molecules to deal with and it is important understanding that there is a probability for a certain reaction to happen that diminishes in time. For the purposes of this thesis, and my first steps in modeling, ordinary differential equations were used to describe CDKN1A induction.

1.9 – Model development

1.9.1 – Software package

The software Mathematica 6 (Wolfram) was used. This software is command line based and this means that each operation is recalled with a specific command; vectors containing the desired options were generated and implemented in mathematical functions used for the simulation.

1.9.2 – Basic modeling scripts

As stated above the software Mathematica was used; at the beginning of each simulation it is possible to define the initial conditions of the system, the kinetics of the reactions and the differential equations used to describe those reactions.

For the simple system

$$x \xrightarrow{v1} y \xrightarrow{v2} a$$

where the specie ***x*** is transformed in the intermediate specie ***y***, at the rate *v1* to become then ***a***, at the rate *v2*, the initial conditions are the followings:

```
Var = {x[t], y[t], a[t]};
Balance = {x'[t] == -v1, y'[t] == v1 - v2, a'[t] == v2};
Rates = {v1 → k1 x[t], v2 → k2 y[t]};
Param = {k1 → 1, k2 → 0.1};
Init = {x[0] == 1, y[0] == 0, a[0] == 0};
```

where:

- **Var** indicates the variables of the reaction (e.g. **x**) that vary in the time **[t]**,
- **Balance** indicates the ODE (ordinary differential equation) that describes that reaction, indicated as first derivate (e.g. **x'**) of the variable
- **Rates** indicates the constants **ks** of each single reaction
- **Param** indicates the values of the previous constants
- **Init** indicates the initial conditions of the variables at the time **[0]**.

Once the initial constants are defined (for the purpose of this thesis the parameters were chosen in order to fit the biological data) they have to be implemented into equations as follow:

```
Rates /. Param
{v1 → x[t], v2 → 0.1 y[t]}
Balance /. Rates /. Param
{x'[t] == -x[t], y'[t] == x[t] - 0.1 y[t], a'[t] == 0.1 y[t]}
```

where:

- **Rates /. Param** unifies constants and their values

- **Balance /. Rates /. Param** implements the previous function in the ODEs

At this point it is necessary to run the simulation, this is made recalling an algorithm, already into the software package, that follows the specified parameters to find the coordinates of each variables at each time-point. This is made with the following scripts:

```
Sol = NDSolve[Join[Balance /. Rates /. Param, Init], Var, {t, 0, 10}]
```

where:

- **Sol = NDSolve** tells to the software to recall the algorithm **NDSolve** to solve the ODEs previously described. This command finds a numerical appriximation to a function that is equal to its first derivate at each point, hence obtaining the solution to the ordinary differential equations for the function described

- the parameters that the algorithm will take in consideration are described within the square brackets

- **{t, 0, 10}** indicates how long the simulation should run for.

Finally to visualize, graphically, the results from the simulation the graph is recalled with the following script:

```
Plot[{x[t] /. Sol, y[t] /. Sol, a[t] /. Sol}, {t, 0, 10}, PlotRange → {0, 1},
 PlotStyle → Thickness[0.005]]
```

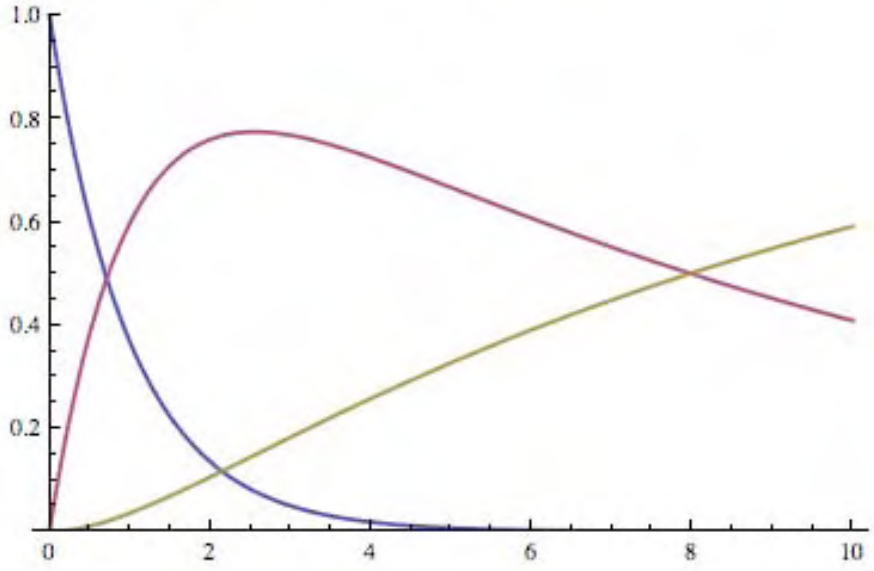

Fig 1.7 – *Results of the simulation with ODEs. The accumulation of three different species x (blue), y (violet) and a (yellow) based on the reaction x → y → a. Time is indicated in the x axes while the concentration of the species is on the y axes.*

where the software is told to **Plot** the variables in time **x[t]**, represented in blue, **y[t]**, represented in violet and **a[t]**, represented in yellow, from time zero to time 10, **{t, 0, 10}**, within the selected range of values **{0, 1}**.

1.9.3 – Advanced scripts

With Mathematica, after creating the initial conditions and a table to recall them, it is possible to implement into the same vector ODEs, using **If** functions (to create time constraints) and species specifications (to take in consideration only a certain number of species, e.g. only the first 30 mRNA molecules produced).

To explain this concept better, the next script indicates the differential equations, **InitODEN**, for **n** species of the variable polymerase **pol** at time **[0]** with initial

concentration equal to 1. An easier way to exemplify this command is to say that the formula takes into consideration a hypothetical Table with the list of **pol** from **i** to **n** and uses only the number of species specified in the equation:

```
InitODEN3[n_] := Join[{pol[0][0] == 1}, Table[pol[i][0] == 0, {i, n}]]
```

Subsequently construction of the algorithm occurs to describe the behavior of **pol** in the time **[t]**. For this example the operator **If** was used; this function creates constraints, such as time constraints, to investigate how the system behaves at specific time points in respect to certain conditions.

```
ODEN3[n_] :=
 Join[
  {pol[0]'[t] == If[500 < t < 900, -0.01 pol[0][t],
     If[1800 < t < 2600, 1 - 0.25 pol[0][t], If[2600 < t < 4000, -0.0005 pol[0][t],
       0.2 - 0.1 pol[0][t]]]]}, Table[pol[i]'[t] == 0.06 pol[i - 1][t] - 0.1 pol[i][t], {i, 1, n}]]

VarsODEN3[n_] := Table[pol[i][t], {i, 0, n}]

InitODEN3[5];

ODEN3[5];

VarsODEN3[5];
```

In this case the algorithm contains three different **If**s, with three different time constrains each, but the common formatting is:

If[*constrain happens***,** *condition 1 applies***,** *otherwise condition 2 applies***]**.

The remaining part of the script (**VarsODEN[n_]**, **InitODEN**, **ODEN**, **VarsODEN**) implements the initial conditions of the variables to the differential equations. The time constraint in this algorithm were chosen to verify how the system behaves in the initial 30 minutes.

It is then possible to run the model with the following script:

```
Sol3 = NDSolve[Join[ODEN3[100], InitODEN3[100]], VarsODEN3[100], {t, 0, 10000}];
```

which is similar to the one described above. The final graph can be visualized as follow:

```
Plot[Evaluate[Sum[pol[i][t], {i, 0, 0}] /. Sol3], {t, 0, 8000}, PlotRange → All,
 Frame → True, FrameLabel → {"time [sec]", "fold change"},
 PlotStyle → {Green, Thickness[0.005]}]
```

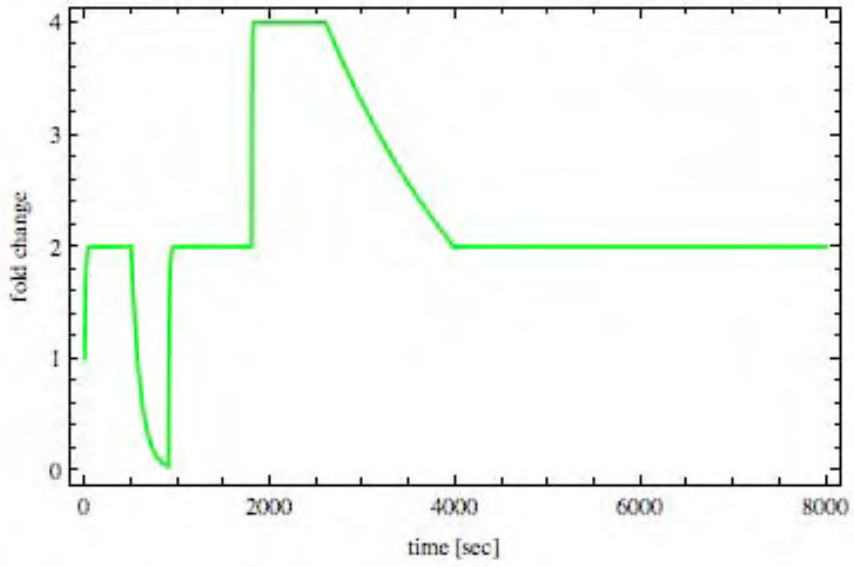

Fig 1.8 *– Results of the simulation of a hypothetical polymerase activity on the promoter of CDKN1A gene. Time and concentration of the polymerase are indicated on the x and y axes, respectively. Only the first 8000 seconds (133 min = ~ 2 hours) were taken in consideration as if the system goes into steady state after 4000 seconds.*

The final graph indicates the recruitment of the polymerase on a hypothetical promoter region; this simulation will be implemented in a larger model with miR-106B and CDKN1A transcription.

1.9.4 – Parameter Estimation

There are mainly three different ways to estimate the paramethers used in a model.

The first option is to infer those data from literature and implement them in the algorithm; the second option is to obtain those data from experimental data appositely

designed for the model analysed; the third option, used for this model, implies the use of an empirical approach, hence running the model changing the paramenters to evaluate those that better describe the model. A more detailed explanation of the parameter estimation stratey for the CDKN1A model will be presented in the results chapter.

PROJECT AIMS

- profile the responsiveness of PC-3 cells towards a broad panel of NR ligands (ETYA, EPA, bezafibrate, ATRA, D3)
- identify the role of the HDACi SAHA, either as a single ligand or in combination with NR ligands, in
    - cell proliferation
    - transcriptional regulation
    - epigenetic modification (H3K9Ac) of the promoter region of PPAR target genes
- evaluate the role of NCOR1 in PC-3 cells via shRNA approach
    - profile responsiveness of shNCOR1-PC-3 cells towards NR ligands
    - profile the transcriptional effect of bezafibrate in shNCOR1-PC-3 on PPAR target genes
    - identify the epigenetic modification (H3K9Ac) at the TSS region of PPAR target genes
- prepare Ncor1 and Ncor2/Smrt constructs for prostate-specific knock out of those genes
- prepare floxed ES cells
- prepare shRNA construct for Ncor1 and Ncor2/Smrt controlled by a prostate-specific promoter

- model integration of experimental data on CDKN1A transcriptional activation by a NR.

2 - GENERAL MATERIALS AND METHODS

2.1 Cell culture

The prostate cancer cell lines PC-3, DU 145, LNCaP and prostate non malignant cell line RWPE-1 were purchased from American Type Cell Culture Collection, ATCC, (http://www.lgcpromochem-atcc.com/); PC-3, DU 145 and LNCaP were maintained in RPMI1640 media (Sigma-Aldrich) supplemented with 10% Fetal Bovine Serum, FBS, (Gibco) and 2mM L-Glutamine. RWPE-1 cells were maintained in KSF media supplemented with Bovine Pituitary Extract and EGF (all from Gibco). To prevent infections, all media also contained 100 units/ml penicillin and 100 μg/ml streptomycin (Gibco). All cells were incubated at 37ºC in a humid atmosphere of 5% CO_2 in air. Confluent cells were passaged by trypsinising with Trypsin-EDTA (Sigma-Aldrich), briefly: media was aspirated, cells washed with 8 mls of chilled Phosphate Buffer Saline, PBS (Sigma-Aldrich) and incubated at 37ºC for 10 mins with 2mls of Trypsin-EDTA. Detached cells were then collected with 8mls of media and centrifuged 1400rpm for 5 mins; the supernatant was discarded and pellet resuspended in 10mls of fresh media. The dilution of cells seeded depends on the cell line which is summarised in **Tab 2.1**.

Cell line	Dilution of cells seeded into a fresh flask	No. of times per week cells were passaged
RWPE-1	1:4	1
LNCaP	1:7	1
DU 145	1:8	2
PC-3	1:8	2

Table 2.1 - *Rate of passage for the prostate cell lines*

2.2 Compounds

Bezafibrate, Eicosatetraynoic acid (ETYA), Eicosapentaenoic acid (EPA), Thyroid Hormone (T3), chenodeoxycholic acid (CDA), 1α,25,$(OH)_2D_3$ (Sigma) and All Trans Retinoic Acid (ATRA)(Sigma) were stored as 1mM solution in ethanol at 20ºC, 1α,25,$(OH)_2D_3$ and ATRA were also protected from light. SAHA was a kind gift Merck (USA). For experimental dilutions all the compounds were diluted in the corresponding diluent control.

2.3 Cell Proliferation Assay in Liquid Culture

2.3.1 Principle

The commercial kit Via Light Plus Cell Viability and Cytotoxicity BioAssay (Lonza, Switzerland) was used to quantify cell proliferation in liquid culture. This method exploits the bioluminescent measurement of ATP, present in metabolically active and viable cells; the enzyme luciferase catalyses the formation of light from ATP and luciferin:

$$\text{ATP} + \text{luciferin} + O_2 \xrightarrow{\text{luciferase}} \text{oxyluciferin} + \text{AMP} + \text{PPi} + CO_2 + \textit{LIGHT}$$

The intensity of the light emitted is then directly proportional to the amount of endogenous ATP, hence, to the number of proliferating cells.

2.3.2 Method

Exponentially growing PC-3 and RWPE-1 cells were plated at different densities due to their differential growth rates; PC-3 cells were seeded at 2000 cells/well and

RWPE-1 at 4000 cells/well into 80 µl of the respective media into each well of a 96-well, white walled, tissue culture treated plates (Costar). Cells were dosed with the appropriate compounds after 24 hours from initial seeding and then re-dosed after 48 hours, to resulting in a final volume of 100 µl. To harvest the total ATP in a well the manufacturer's instructions were followed. Briefly: 50 µl of cell lysis reagent were added in each well with the use of a multichannel pipette and left at room temperature for >10 mins; 100 µl of ATP monitoring reagent (containing luciferine and luciferase) were added in a dark environment and left >2 minutes. A microplate luminometer (Berthold Id Detection System, Fisher Scientific Ltd, UK) was used to measure light emission. ATP levels were recorded in Relative Luciferase Units (RLU) and inhibition of proliferation, when present, was expressed as a percentage relative to negative control, treated with diluent media only. All final results are the result of triplicate biological experiments.

2.4 Cell Sorting – Cell Cycle

2.4.1 Principle

Proliferating cells go through four different phases named G_1, S, G_2 and M. There is also a fifth phase called G_0 that includes quiescent cells before going into G_1. Each phase can be determined by detecting the relative amount of DNA in cells by using Hoescht (Roche) dye that binds nucleic acids. Cells that are in the G_1 phase have one copy of their DNA, while cells that are in G_2 phase and mitosis have two copies. Cells that are in S phase are actively copying their DNA and have a intermediate amount between G_1 and G_2/mitosis phases. The live cells are incubated with Hoechst dye

and then analyzed by Fluorescence-activated cell sorting (MoFlo, Beckman Coulter, USA); this technology for sorting a heterogeneous mixture of biological cells into two or more containers, one cell at a time, based upon the specific light scattering and fluorescent characteristics of each cell. The Hoechst dye is excited by ultraviolet light at around 350 nm, and emits blue/cyan fluorescence light around an emission maximum at 461 nm, this characteristic profile allows recognition of cells based upon their total amount of DNA: cells that are in G_2/mitosis have twice the amount of fluorescence than cells in G_1, while cells in S phase have an intermediate amount (**Fig 2.1**). This allows sorting of cells in different phases of the cell cycle and using them for further experiments.

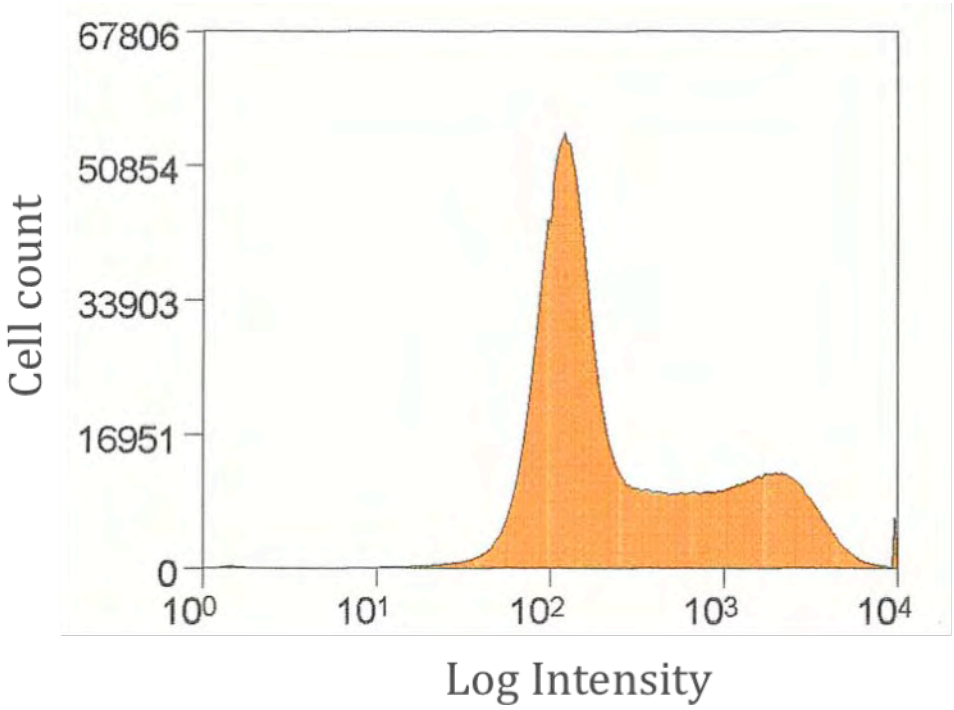

Fig 2.1 - *Representative cell cycle histogram. On the x axes the cell count and on the y axes the log intensity of the DNA content detected via Hoechst dye. The left side of the histogram indicates cells in G1 phase, the flat part at the centre indicates cells in S while G2 cells are on the far right of the histogram with the highest amount of DNA.*

2.4.2 - Method

Exponentially growing cells in T175 flasks were treated for four hours with 1α,25,$(OH)_2D_3$ at a final concentration of 100nM; cells were then trypsinized, resuspended in fresh media, centrifuged and resuspended with 5mls of media and 10uls of EDTA 100uM. This suspension was then used to cell-sort cells in G1, S and G2 with a Mo-Flow machine. Fractionated cells were then collected directly into TRI reagent (Ambion) and used for RNA extraction.

2.5 RNA Extraction, Reverse Transcription and Polymerase Chain Reaction (PCR)

Before performing a quantitative Reverse Transcriptase-Real Time PCR (Q-RT-PCR) there are other two steps: RNA extraction and cDNA synthesis by Reverse Transcription.

2.5.1 RNA Extraction

2.5.1.1 Principle

To extract RNA from adherent cells they were first collected by trypsinization and the resulting pellet was lysed with TRI reagent. This solution contains guanidine isothiocyanate (a strong denaturant) and phenol, which lyses and denatures endogenous RNases to avoid digestion of nucleic acids. The addition of 1-bromo-3-chloro-propane (Sigma) creates a second, organic, phase and centrifugation of this mixture results in the production of three phases: the dense, red organic phase containing proteins at the bottom; a white interphase containing DNA; an upper

aqueous phase containing RNA. The RNA layer is pipetted off and then the RNA is precipitated with isopropanol (Sigma) and contaminants such as salt are removed by washing the RNA pellet with 70 % ethanol; ethanol takes away the hydration shell around the DNA, adding a cation like Na+ or K+ and not only takes away the hydration shell, but also stabilizes the phosphate groups by making them interact with an opposing charge instead of water, allowing for futher resuspension of the RNA in nuclease free water.

2.5.1.2 - Method

Exponentially growing cells were trypsinized, pellet was collected into 10 ml tubes, resuspended in 1ml TRI reagent for approximately 5 million cells, transferred in a 1.5 ml eppendorf and incubated at room temperature for 10 mins: for each ml of TRI reagent, 100 µl of 1-bromo-3-chloro-propane was added and the solution was then vortexed for 15 seconds and incubated at room temperature for further 10 mins. The three phases were then separate centrifuging the samples at 12.000 rpm for 15 mins at 4ºC; the clear top phase containing RNA was immediately transferred to a new 1.5 ml eppendorf and resuspended with 500 ul of 2-propanol per each ml of TRI reagent. RNA was left to precipitate over night at 4ºC (or at least 20 min at RT). Tubes were then centrifuged at 12.000 rpm for 15 mins at 4ºC, pellet containing RNA was washed with 1 ml of ethanol 70% and centrifuged at 12.000 rpm for 10 mins at 4ºC. the supernatant was carefully removed and the pellet was left to air dry under a hood until any remaining ethanol had evaporated. The RNA was then resuspended in 30 ul of Nuclease Free Water (Promega) and stored at -80ºC.

2.5.1.3 - RNA quantification

A NanoDrop Machine (ND100, Labtech International , UK) was used to analyse the RNA extracted. Values obtained from reading 1 ul of sample were indicative of the quality of RNA, expressed from ratio λ260/λ280 (to indicate nucleic acid content vs non-nucleic acid content, good ratios are 1.8<x<2); the concentration calculated by the NanoDrop Machine was expressed in ng/ml.

2.5.2 Reverse Transcription

2.5.2.1 Principle

In order to measure the levels of extracted RNA in cells it's easier to convert the mRNA into DNA, which is more stable and can be easily amplified by PCR (Polymerase Chain Reaction). An RNA-dependent DNA polymerase (reverse transcriptase) , extracted from viruses such as avian myeloblastosis (AMV), synthesises complementary copies of DNA, also called, cDNA from mRNA template. Primers, short nucleic acid binding oligonucleotides, provide the starting point for reverse transcriptase. The primers are generally oligo dTs that bind the polyA tail of mRNA or random hexamers (random sequence of six nucleotides) that can bind to the corresponding sequence anywhere in the mRNA transcripts.

2.5.2.2 Method

1 ug of total RNA was initially heated at 70ºC for 10 minutes in a total volume of 10 ul with nuclease free water to denature any RNA secondary structure. The RNA was

then added to a 10 ul reaction mix containing 4 uls of 25mM $MgCl_2$, 2 uls of Random Primers (Promega – C1181) 0.6 ul of MMLV SuperScript™ II Reverse Transcriptase (Invitrogen – 18064-014), 2 uls of RT 10X buffer (50 mM Tris-HCl, pH 8.3, 50 mM KCl, 10 mM $MgCl_2$, 0.5 mM spermidine –helps preventing aspecific reactions– and 10 mM DTT –helps loosing the secondary structure of the RNA–), 20 units of RNase inhibitor (Invitrogen RNaseOUT - 10777019) and 2 uls, 2.5 mM each, of dNTPs (Invitrogen). Each reaction was then heated for 60 min at 42ºC and inactivated at 95ºC for 5 mins. Samples were stored at -20ºC for future experiments.

2.5.3 Quantitative TaqMan Real Time Polymerase Chain Reaction (Q-PCR)

2.5.3.1 General Principle of Q-PCR

Real Time PCR is a very sensitive technique able to generate quantitative gene expression data (used for SNPs assay or DNA analysis as well) allowing a high throughput of samples, which don't need any further processing afterwards. The first kind of Real Time PCR exploited a fluorescent dye such as ethidium bromide and SYBR Green that intercalates into, or binds to, the grooves of double-stranded DNA. This method is still commonly used along with the newer, more specific method called TaqMan Real Time PCR, that requires a fluorescent probe that anneals only to a specific part of the amplified target DNA sequence. The polymerase used in TaqMan possesses exonuclease activity to digest the probe while the new strand is synthesized, below the mechanism of action will be explained in details.

Real Time PCR machines are fluorescence-detecting thermocyclers, which simultaneously amplify NDA sequences and measure their concentration once per

cycle. This allows DNA quantification over the whole course of the PCR reaction. The accumulation of amplified product, and therefore the detectable fluorescence level from a highly expressed gene occurs at lower cycle number than a lowly expressed gene because the initial concentration of the cDNA is higher.

The given level of fluorescence is always fixed in the exponential phase of the PCR when the reaction is not limited. The number of PCR cycles necessary to achieve a set level of fluorescence is termed 'cycle threshold' (Ct). To normalise each cDNA sample, the Ct value of the housekeeping gene is subtracted from the Ct value of the target gene and this value is termed delta Ct (δCt). The δCt of an untreated control sample was then subtracted from a treated (e.g. $1\alpha,25(OH)_2D_3$) sample giving a value termed delta delta Ct (δδCt). Finally the relative fold-changes in mRNA levels were calculated using the equation: $2^{-\delta\delta Ct}$.

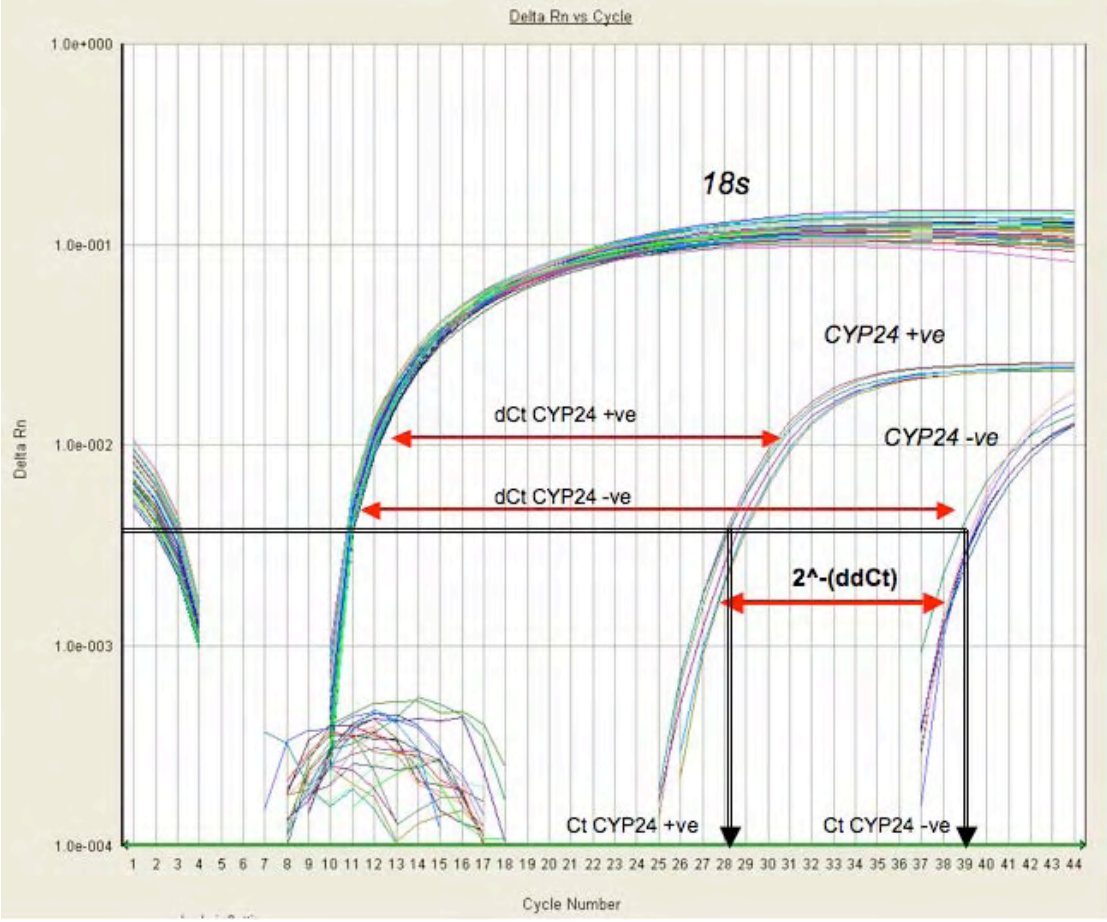

***Fig 2.2** – Theoretical example of the amplification curve of CYP24 in treated (+ve) vs untreated (-ve) PC-3 cells. Cycle thresholds (Cts) of the gene are related to 18s' Cts. Fold changes are calculated as explained above. In this case 1,25(OH)$_2$D$_3$ treatment effectively promotes accumulation of CYP24 mRNA as detected by the amplification curve shifted to the left if compared to the un-treated sample.*

2.5.3.2 Principles of TaqMan Real Time PCR

The main characteristic of a TaqMan is the presence of a third oligonucleotide in addition to the two primers. This probe anneals within the region to be amplified and, in order to prevent amplification of genomic DNA, is designed to cross the exon-exon boundary of the mRNA of interest. This oligonucleotide is chemically modified at its 5' end with a fluorescent reporter dye (generally FAM) and at its 3' with a quencher (generally TAMRA). While the probe is intact the dye is close

enough to the quencher that it prevents any fluorescence emission. During the extension phase of the PCR reaction, the taq polymerase has 5' to 3' exonuclease activity and digests any annealed probe. This causes the release and separation of the reporter dye and quencher enabling fluorescence to be detected.

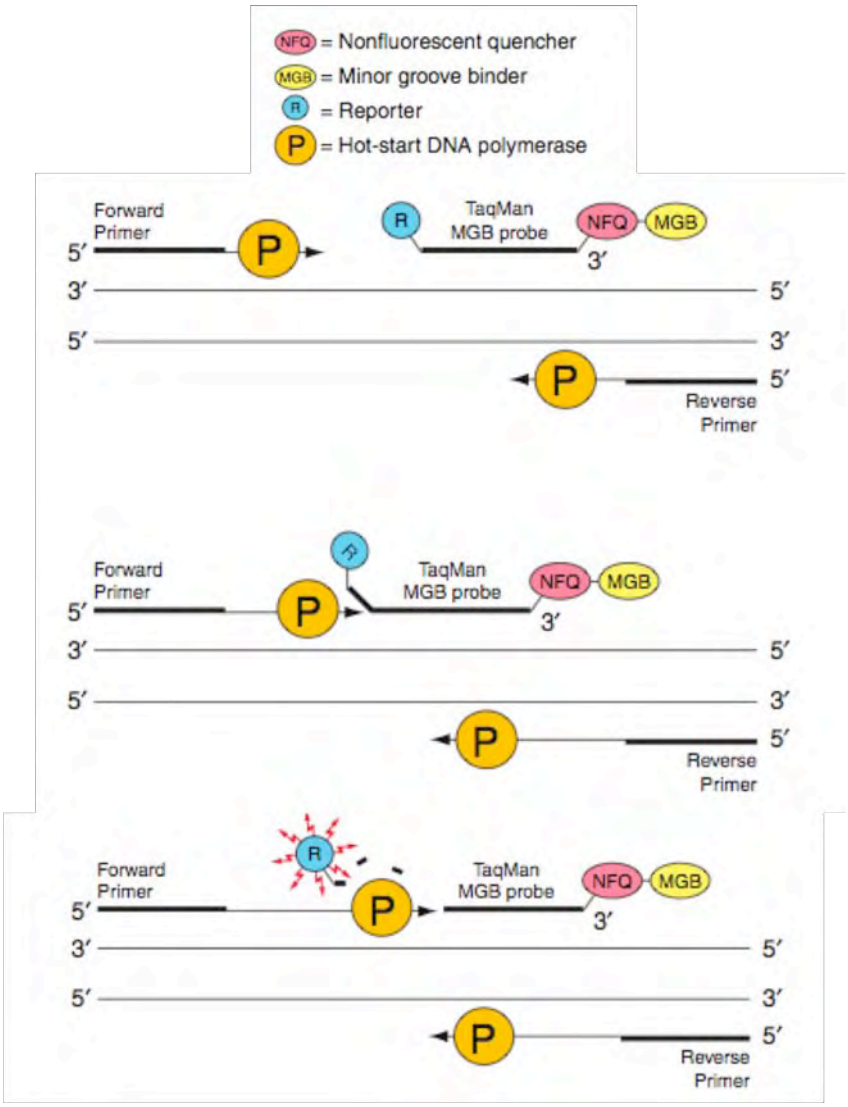

Fig 2.3 – *Description of the endonuclease activity of the taq polymerase. The more the probe is digested the more light is released by the report dye.*

One advantage of TaqMan PCR is that only the amplification of the DNA sequence of interest causes fluorescence, unlike a generic fluorescent dye that can also bind to

primer dimers or non-specific amplified DNA. Also, the TaqMan thermocycler that was used for this thesis (ABI Prism 7700, Applied Biosystems) can quantitate signals from different fluorescent dyes; therefore more than one DNA sequence can be amplified in the same reaction. Potential pipetting error was removed by amplifying the normalisation gene 18S in the same PCR reaction as the gene of interest.

2.5.3.3 Primers and Probes

The sequences used to design primers and probes for the mRNA of interest were obtained from published gene sequences [62, 190] and analysed with the Primer Express software (PE Applied Biosystem, UK). Primers were synthesised by Sigma-Genosis (Sigma-Aldrich). The 18S housekeeping gene and gene expression assay on demand primers and probes were also from Applied Biosystem.

Product Code	Gene Name
Hs00167536_m1	Alox5 – 5-lypoxigenase
Hs00226123_m1	FBXL6
Hs00364015_m1	SLIRP
Hs00936775_m1	CoREST
Hs00940781_m1	RIP140
Hs00974040_m1	LCoR
000442	miR106-B
001006	RNU48

Table 2.2 – *List of gene expression assay on demand primers and probes obtained by Applied Biosystem with relative product code.*

Gene bank accession no.	Primer	Sequence (5'-3')
NM_006311	NCoR1 Forward primer NCoR1 Reverse primer NCoR1 Probe	TGAAGGTCTTGGCCCAAAAG TTTGTCTTGATGTTCTCATGGTA CTGCCACTGTATAACCAGCCATCAGATACCA
NM_006312	SMRT Forward primer SMRT Reverse primer SMRT Probe	CACCCGGCAGTATCATGAGA CGAGCGTGATTCCTCCTCTT CTTCCGCATCGCCTGGTTTATT
AF_120268	TRIP15/Alien Forward TRIP15/Alien Reverse TRIP15/Alien Probe	CCTCATCCACTGATTATGGGAGT CATCATAATTCTTGAAGGCTTCA CCCTCAAGTGCATTTTACCACCACATTCTCT
NM_000782	CYP24 Forward primer CYP24 Reverse primer CYP24 Probe	CAAACCGTGGAAGGCCTATC ACTTCTTCCCCTTCCAGGATCA ACTACCGCAAAGAAGGCTACGGGCTG
NM_000389	CDKN1A Forward primer CDKN1A Reverse primer CDKN1A Probe	GCAGACCAGCATGACAGATTTC GGATTAGGGCTTCCTCTTGGA CCACTCCAAACGCCGGCTGATCTT
NM_001924	GADD45A Forward primer GADD45A Reverse primer GADD45A Probe	AAGACCGAAAGGATGGATAAGGT GTGATCGTGCGCTGACTCA TGCTGAGCACTTCCTCCAGGGCAT
NM_004257.	TGFBRAP1 Forward TGFBRAP1 Reverse TGFBRAP1 Probe	GCGGCTGTGTCCTTTCCATA GCGTCTGCTTCTGTTGCTGAT AGCGCTCGATGACGAATTCATCACAG
NM_001786.	CDC2 Forward CDC2 Reverse CDC2 Probe	CTAGCATCCCATGTCAAAAACTTG CAGTGCCATTTTGCCAGAAA TTTGCTCTCGAAAATGTTAATCTATGATCCAGC
NM_000963.	PTGS2 Forward PTGS2 Reverse PTGS2 Probe	GAATCATTCACCAGGCAAATTG TCTGTACTGCGGGTGGAACA TGGCAGGGTTGCTGGTGGTAGGA

Table 2.3 *– List of primers and probes used for this thesis with corresponding sequences. Primers and probes were designed with the software "Primer Express" (ABI) using the mRNA sequence of the gene of interest as input. Primers were ordered from Sigma Aldricht.*

2.5.3.4 Calibration and Optimization of Primers and Probes

Each set of primers and probes were calibrated to guarantee linearity of amplification. Primer efficiency experiments were carried out in order to ensure reliability on mRNA detection. This optimization step was undertaken to ensure a linear relationship between template concentration and Ct values when undertaking a multiplex reaction with both housekeeping genes and target genes. An optimum reaction yields Ct values which decrease for increasing cDNA concentrations in a linear manner.

2.5.3.5 Method

50 ng of cDNA were amplified in a 20 µl reaction containing 1x TaqMan PCR MasterMix (Sensimix dT - QT6T3, Quantace, UK), 125 nM FAM-TAMRA labelled probe and 1 uM of primers. All reactions were multiplexed with 1x VIC-TAMRA 18S (ABI). An ABI PRISM 7700 sequence detector machine (Applied Biosystems, Foster City, CA, USA) was used under the following cycle conditions: 50°C for 2 mins, 95°C for 10 mins, 40 cycles of 95°C for 15 secs, 60°C for 1 min and 72ºC for 30 secs. Final measurements were an average of a minimum of three independent experiments, in triplicate wells for each condition. Student's t-tests were performed to identify genes significantly expressed/regulated.

2.5.4 Microfluidic Gene Card

2.5.4.1 General Principle

Applied Biosystem developed a novel approach of analysing multiple gene expression profiles by using a custom array of gene-specific primer and probe sequences preloaded in a 384-well micro fluidic card. In each plate any set of genes is already pre-loaded into the well and present in duplicate copy arranged in 96 wells (96x2x2=384); this allows the researcher to analyse 96 genes in technical duplicate, for example running treated sample versus untreated in parallel on the same plate. The plate was run on a ABI 7900H thermocycler (Applied Biosystem) and analysed as a normal TaqMan reaction. A selection from the list of the selected genes can be seen in **Fig 2.4**.

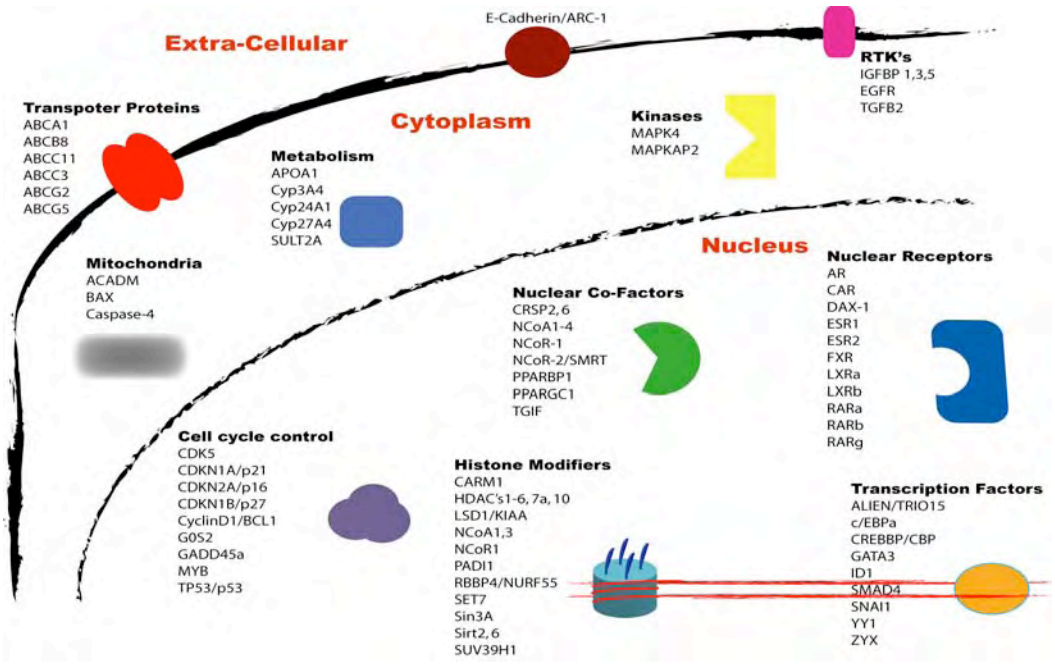

Fig 2.4 – *Visual representation of the genes preloaded into the microfluidic gene card. Indicated are the sub-cellular location and the main function (image from James Thorne, University of Birmingham, Birmingham, UK).*

2.5.4.2 Method

RNA concentration was set to be the lowest within the samples analysed. 200 µl of one-step reaction Master-Mix from Qiagen were added to the diluted RNA together with 4 µl of RT mix (Qiagen); 100 uls of the reaction mix were then dosed every two rows in the card. This was then centrifuged twice at 1000 rpm for 2 minutes to distribute homogeneously the sample into each well. Plate was then sealed and run on the ABI7900 machine under the following cycle conditions: 50ºC for 30 sec (reverse transcription), 95ºC for 15 min (activation enzyme), 94ºC for 45 sec (denaturation), 56ºC for 45 sec (annealing), 76ºC for 45 sec (elongation) for 40 cycles. Measurements were carried out on a minimum of three biological replicate for each condition (e.g. treated vs untreated).

2.5.4.3 Data Analysis

Due to the large volume of results obtained with this methodology, the use of an appropriate software able to manage high throughput data was compulsory; the choice was TMeV, a Java application freely available online (www.tm4.org/mev.html), that can be easily used to analyse microarray data. The statistical tests performed with this software are:

- *Student's t-test*: this analysis assesses wether the means of two groups (or genes) are statistically different from eachother. One sample t-test was

also used to determin if a group of genes was significanlty differentially expressed from an average value.

- *ANOVA (Analysis of Variance):* this analysis is an extension of the Student t-test to more than two experimental conditions. It identifies genes that have significant differences in means across three or more groups of samples
- *SAM (Significance Analysis of Microarray):* this analysis can be used to identify significant genes based on differential expression between sets of samples. Significance is evaluated via permutation of the samples (or genes) calculating the FDR (False Discovery Rate), which is the proportion of genes likely to have been identified by chance as being significant.

A heatmap, firstly used by Wishart in 1997 [191], represents visually the gene expression data collected, those generated for this thesis have in green and red bars down- and up-regulated genes, respectively. Heatmaps representing basal and treated PC-3 cells vs RWPE-1 cells were generated and hierarchical trees were built using Euclidean distance. This is a measurement of the geometric distance in the multidimensional space between two objects and it's the most used method for cluster analysis.

2.5.5 Protein Extraction and Western Immunoblotting

2.5.5.1 Western Immunoblotting – Introduction

Western Immunoblotting is a widespread technique used to measure specific target protein expression. The overall idea is to resolve the proteins by size and identify the one of interest on a membrane using a specific antibody (Ab). A general protocol includes a separation of the extracted proteins in a polyacrylamide gel in presence of Sodium Dodecyl Sulfate (SDS). SDS-PAGE (SDS polyacrylamide gel electrophoresis) maintains protein in a denatured state once they have been treated with strong reducing agents to remove secondary and tertiary structure (e.g. S-S disulfide bonds to SH and SH) and thus allows separation of proteins by their molecular weight. Sampled proteins become covered in the negatively charged SDS and move towards the positively charged electrode through the acrylamide mesh of the gel. Smaller proteins migrate faster through this mesh and the proteins are thus separated according to size (usually measured in kilo Daltons, kDa). The concentration of acrylamide determines the resolution of the gel - the greater the acrylamide concentration the better the resolution of lower molecular weight proteins. The lower the acrylamide concentration the better the resolution of higher molecular weight proteins. Proteins travel only in one dimension along the gel for most blots. Once the gel has been run the proteins are transferred onto a membrane, Polyvinylidene Fluoride (PVDF) or nitrocellulose. The membrane is then incubated with a solution at 5% milk in order to avoid non-specific binding of the antibody on

the membrane. Incubation with the primary Ab specifically recognizes the target protein; to obtain a stable signal from the bound antibody the use of a secondary antibody is compulsory. This is conjugated with a detection moiety such as an enzyme named Horse Radish Peroxidase (HRP) and will recognize the primary antibody; this reaction is species-specific, hence, the secondary antibody will recognise only primary antibodies that it was designed for. Using a chemoluminescent substrate to HRP (called ECL), containing Luminol and a Peroxide buffer, in combination with the HRP enzyme, it is possible to catalyze the oxidation of Luminol with creation of an excited state product called 3-aminophthalate*. This product decays to a lower energy state by releasing photons of light. Where this reaction happens is where the protein of interest is; this can be identified as a band impressed on a sheet of auto-radiographic film.

2.5.5.2 Protein Extraction

Exponentially growing cells were trypsinized and pelleted in a 10 ml falcon tube. Either whole protein extract or nuclear and cytosolic fractions were prepared.

2.5.5.2.1 Whole Protein Extract Preparation

Cells were lysed with buffer (containing 50 mM Tris-HCl pH 7.6-8, 150 mM NaCl, 1% NP-40, 1% sodium deoxycholate, 0.1% SDS in 250 ml of ddH_2O). For every ten million cells 200uls of RIPA buffer were used. The pellet was resuspended in the appropriate volume of buffer, gently homogenized and transferred in a 1.5 ml eppendorf. A protease inhibitor cocktail (Sigma) was added at the concentration of

one µl per each million cells. The vial was vortexed for 15 seconds at the highest settings and incubated at -20ºC for 20 minutes. This cycle was repeated 4 times. Finally the sample was centrifuged at 16000 rpm for 10 minutes; the supernatant containing protein was transferred in a clean 1.5 ml eppendorf and stored at -80ºC for future usage.

2.5.5.2.2 Nuclear and Cytosolic Extract Preparation

Separate nuclear from cytosolic fractions are important in case the aim is to analyze proteins expressed in a sub-cellular location. A commercial kit from BioVision, USA, called Nuclear/Cytosol Fractionation Kit (K266-100) was used. Instructions from the manufacturer were followed, briefly: cell pellet was resuspended in a lysis buffer, transferred into a 1.5 ml eppendorf, vortexed and incubated on ice. A Cytosolic Extraction Buffer was then added to the pellet; samples were incubated on ice and centrifuged to separate cytosolic protein from the nuclei. Supernatant, containing cytosolic proteins, was transferred into a clean 1.5 ml tube; the pellet was resuspended with a Nuclear Extraction Buffer, vortexed and incubated on ice for four cycles for a total of 40 minutes. Samples were centrifuged and the supernatant, containing nuclear proteins, was transferred into a clean 1.5 ml eppendorf. Tubes were stored at -80ºC for future usage.

2.5.5.3 Protein Quantification

The importance of knowing the concentration of the protein extracted is essential to load the same amount of protein for different samples in an SDS-PAGE gel.

For the purpose of this thesis the Bio-Rad DC Protein assay kit was used (Reagent A 500-0113, Reagent B 500-01114, Biorad). This assay is based on the observation that the absorbance maximum for an acidic solution of Coomassie Brilliant Blue G-250 shifts from 465 nm to 595 nm when binding to protein occurs. Both hydrophobic and ionic interactions stabilize the anionic form of the dye, causing a visible color change, thus, the higher the concentration of protein is, the bigger will be the color change.

2.5.5.3.1 Method

Standards were prepared at five different concentrations: 0 µg/µl, 0.625 µg/µl, 1.25 µg/µl, 2.5 µg/µl and 5 µl/µl diluting Bovine Serum Albumine (BSA) with ddH_2O. From each sample/standard 5 ul were loaded into a clear bottom 96 well/plate (Corning), 25 µls of Bradford reagent A and 200 µls of Bradford reagent B were added to each well, including two empty wells used to quantify the background noise. The plate was then incubated at room temperature for 10 minutes and read with the Victor^3 1420 Multilabel Counter (Perkim Elmer). Results were exported into a spreadsheet and analyzed with Excel. The correlation between standard concentrations and their absorbance ($x<1$) was analyzed with liner regression; $R^2 > 0.98$ was accepted. Once obtained the equation describing the linear correlation of that curve, concentration of the sample was derived as follows:

the equation $y = ax + b$ where:

y = absorbance

a = slope (curve inclination)

x = concentration of the sample

b = intercept (defines the elevation of the line)

was transformed in *x = (y-b)/a*

to determine the sample concentrations.

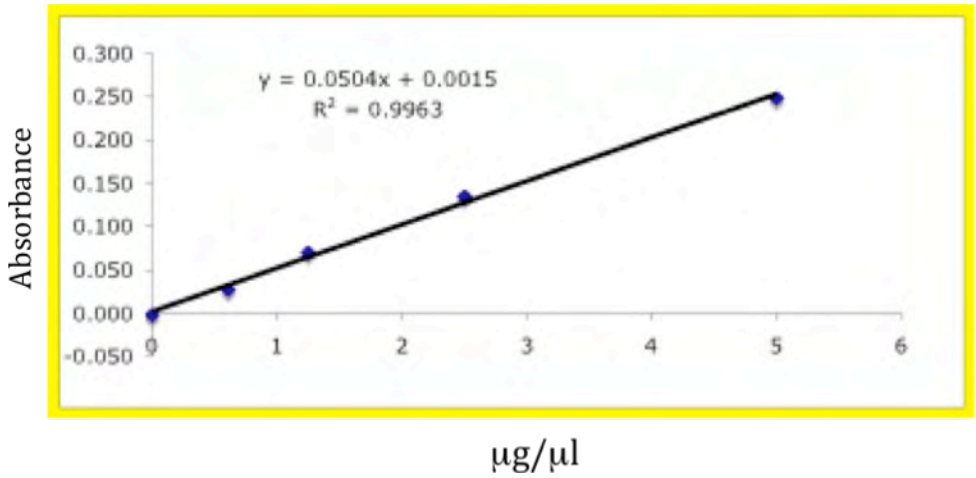

Fig 2.5 - *Example of linear regression curve obtained with standard BSA samples. The y axes indicates the absorbance that correlates with the concentration indicated on the x axes.*

2.5.5.4 General Method For Western Immunoblotting

For more detailed Western Immunoblotting protocols refer to **Table 2.5**.

2.5.5.4.1 Gel Preparation

Polyacrylamide gels were prepared at different concentrations due to the molecular weight of the protein of interest. Resolving gels were prepared as follow:

Compound	5%	8%	10%	12-1/2%
Amm-SO₄	Spatula tip	Spatula tip	Spatula tip	Spatula tip
dH₂O	6.7ml	4.8ml	3.5ml	1.9ml
Stock 2	10ml	10ml	10ml	10ml

Acrylamide	3.25ml	5.2ml	6.5ml	8.1ml
T-Med	6.2µl	6.2µl	6.2µl	6.2µl

STOCK2: (500ml) - 0.75M TRIS 45.5g, 0.2% SDS 1g, pH 8.8, made up with dH_2O

Stacking gels were prepared as follow:

Amm-SO₄	Spatula tip
dH₂O	3.7ml
Stock 1	5ml
Acrylamide	1.3ml
T-Med	3.4µl

STOCK1: (500ml) - 0.2 M TRIS 15.15 g, 0.2%SDS 1 g, pH 6.8, made up with dH_2O

Ammonium persulfate, T-MED (Tetramethylethylenediamine) were from Sigma and Acrylamide (Acrylamide/Bis-acrylamide 30%solutions 37.5:1) was from Gene Flow, UK.

Gels were prepared to be 1.5 mm thick by pouring them into the appropriate glassware (Biorad) and 10 wells combs (Biorad) were used.

While gels were polymerizing, the protein lysate (either whole cell lysate or nuclear and cytosolic extract) were prepared mixing 20 µg of protein with ddH_2O, up to 20 µl, and 6.7 µl of 4X SDS-Loading Buffer (for stock, 7.5 ml 4X: 1.5 ml 1 M Tris-HCl (pH 6.8), 3ml 1M DTT, 0.6g SDS powder, 0.03g Bromophenol blue, 3 ml (100% Glycerol)). Samples were boiled at 99ºC for 10 mins, quickly vortexed, placed on ice, centrifuged and then loaded into the appropriate wells. Gels were run at 120 Volts for 1 hour at room temperature in presence of 1X running buffer (1lt 10X: Glycine 141.1g, TRIS 30g, SDS 10g (all from Sigma), made up 1L dH_2O) until the dye front reached the bottom of the gel.

2.5.5.4.2 Protein Transfer

Proteins were transferred from the gel to an Immobilion P membrane (Millipore, USA); to do so the PVDF membrane was soaked in methanol for 15 sec (PVDF membrane is extremely hydrophobic and will not "wet" in aqueous solutions unless pre-expanded in methanol before it is used), placed in ultrapure water for 2 minutes and then equilibrated in 1X transfer buffer (1lt 10X: TRIS 30.28g, Glycine 144g, SDS 1g, made up 1L dH_2O – 1X: 100 ml 10X buffer, 700 ml dH_2O, 200 ml methanol) for 5 minutes.

To ensure a uniform contact between gel and membrane (thus an even transfer) the following sandwich was prepared:

Anode – Negative Pole
Sponge
Whatman Paper (X2)
Membrane
Gel
Whatman Paper (X2)
Sponge
Cathode – Positive Pole

These cassettes were places into appropriate boxes in presence of 1X transfer buffer and transfer was run for 1 hour at 80 Volt at room temperature; an icebox was added to the transfer tank to chill the transfer buffer.

2.5.5.4.3 Ponceau Staining

Once the transfer was finished membranes were stained with Ponceau Solution (Sigma) for 5 minutes. This allows the detection of proteins on the membrane, checking also the quality of the transfer. Membranes were then washed with dH_2O.

2.5.5.4.4 Membrane Block

To ensure that the primary antibody will bind only the desired protein the membrane was incubated for 1 hour at room temperature with a solution of 5% milk dissolved in TBS-T (1lt 10X: 50 ml 1M Tris-HCl pH 7.6, NaCl 20g, Tween-80 0.625ml, dH_2O 2449.4 ml). The proteins present in milk bind the membrane and prevent aspecific binding of the primary antibody.

2.5.5.4.5 Primary Antibody

The role of the primary antibody is to detect the protein of interest with the highest desirable specificity. The selected antibody was diluted at the indicated concentration (see table below) in TBS-T with 5% TBS-T/milk and the membrane was incubated over night at +4ºC. The only exceptions were beta-actin and Nucleolin that were incubated at room temperature for one hour.

After the incubation time, the membrane was washed three times for 5 min with TBS-T to remove the excess of antibody.

Ab name	Company - Product Code
NCoR1	Abcam – ab24552
NCoR2	Abcam – ab24551
PPAR-gamma	Santa Cruz – sc7273
PPAR-alpha	Santa Cruz - sc1985
VDR	Abcam - ab3548
COX2	Santa Cruz - sc19999
5-Lypoxigenase	Santa Cruz - sc8885
SLIRP	Abcam – ab51523
HDAC3	Santa Cruz - sc130319
SUMO-1	Cell Signaling - 4930
SENP6	Abcam – ab57239
β-actin	Abcam - ab6276
Nucleolin	Abcam – ab13541

Table 2.4 *- List of the primary antibody used for this thesis*

2.5.5.4.6 Secondary Antibody

The secondary antibody is generally HRP conjugated and permits recognition and detection od the primary antibody, hence proteins, on the membrane in presence of ECL. The origin of the primary antibody (mouse, rat, sheep) dictates the secondary chosen (anti-mouse, anti-rat, anti-sheep) and was diluted in TBS-T with 5% milk. The membrane was then incubated with this solution for one hour at room

temperature. Afterwards the membrane was washed three times for 5 min with TBS-T to remove the excess of antibody.

2.5.5.4.7 Chemoluminescent Detection of Protein Bands

The HRP catalyses the release of light from Luminol and Peroxide in presence of ECL substrate. For the aim of this thesis the Pierce SuperSignal West Pico Chemiluminescent Substrate (Pierce – 34078, USA) was used. One ml of reaction mix was spread on top of each membrane and incubated at room temperature for 5 min. The excess of ECL was removed by touching the corner of the membrane with a paper napkin; the membrane was then put between two layers of clinching film, exposed in the dark to the Amersham Hyperfilm ECL (28-9068-37) and ran into a developer machine (Kodak). Exposure time was then assessed based on the results of the first film.

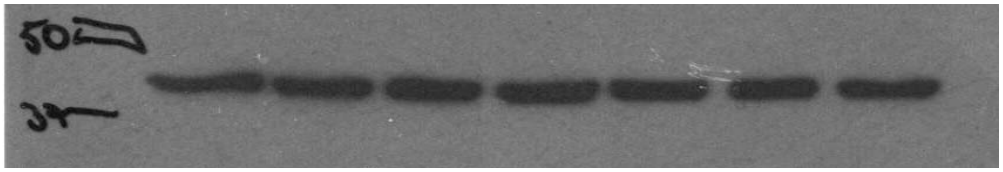

Fig 2.6 - *Example of evenly expressed beta-actin between different samples.*

2.5.5.5 Specific Methods For Western Blotting

Each antibody has a different efficiency and each protocol was optimized to obtain the most specific signal as possible with each analysis. In the table below are summarized the specifications for each different primary antibody.

Protein	% Gel - Run	Transfer	Blotto	I Ab	II Ab
NCOR- NCOR2/SMRT	4% - 3.20 hr -100 V	4 hr – 60 V	O/N	1:500	1:2000
PPAR-γ / α	10% - 1.15 hr -120 V	1.30 hr – 80 V	1.30 hr	1:1000	1:1000
SLIRP	12.5% - 1 hr – 120 V	1.15 hr – 80 V	1.15 hr	1:5000	1:5000
SUMO1	12.5% - 1 hr – 120 V	1.15 hr – 80 V	1.30 hr	1:1000	1:2000
COX2	10% - 1.20 hr – 120 V	1.30 hr – 80 V	1.30 hr	1:500	1:750
5-LO	10% - 1.20 hr – 120 V	1.30 hr – 80 V	1.30 hr	1:500	1:1000
HDAC3	10% - 1.20 hr – 120 V	1.30 hr – 80 V	1.30 hr	1:500	1:1000
SENP6	8% - 1.20 hr – 120 V	1.30 hr – 80 V	1.30 hr	1:1000	1:2000
β-actin	Any – 1hr – 120 V	1hr – 80V	1 hr	1:10000	1:5000
Nucleolin	10% - 1.15 hr – 120 V	1.15 hr – 80 V	1 hr	1:5000	1:2000

Tab 2.5 *– Specification for the Western Blot experiments done. Indicated, from the first column on the left to the last column on the right, are the name of the protein, how long the gel ran for, how long was it transferred for, how long was the blotto (5% milk in TBS-T), the dilution of the primary antibody (in 5% milk in TBS-T) and the dilution of the secondary antibody (5% milk in TBS-T).*

2.5.6 Knock-Down of NCOR1 using a short hairpins RNA strategy.

2.5.6.1 Short Hairpin RNA - Introduction

The use of short hairpin RNAs (shRNAs) is common for the generation of stably transfected knock-down cell lines. ShRNAs interfere with protein translation

binding RNA molecules; this leads either to their compartmentalization into sub-cellular compartments called P-bodies, or to their degradation. The biological endpoint is always an efficient block of the translation machinery and drastic reduction of the endogenous target protein. For the purpose of this thesis a specific shRNA to target the human NCOR1 was used.

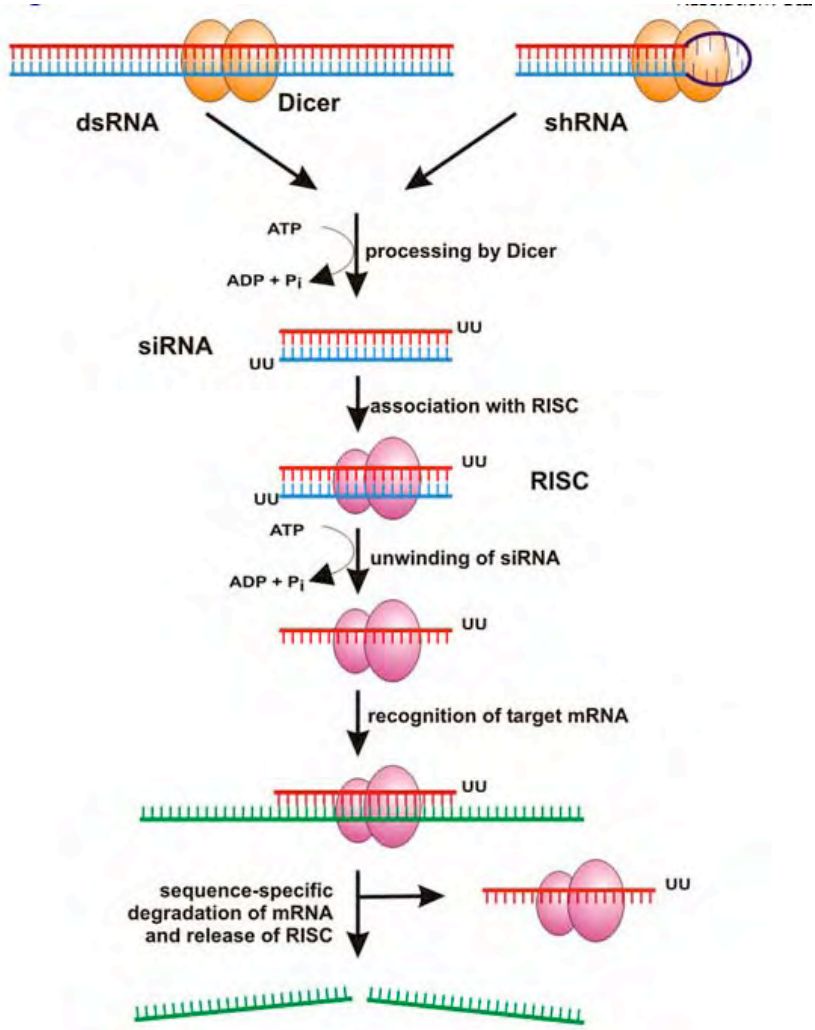

Fig 2.7 *– ShRNA pathway: the Dicer complex processes the shRNA before it's recognised by the RISC complex. This will lead the single stranded molecule to the target mRNA that will be degraded.*

2.5.6.2 Oligonucleotide Design

NCOR1 is a large protein: its transcript includes up to 46 exons with several splicing variants. To ensure the most-effective knock-down three different exons were targeted: exon 5, exon 38 and exon 44, plus a combination of all three of them. The oligos were designed to form a cassette that, once ligated into the vector, would have ensured shRNA transcription. (A scheme of the targeted exons is available in the Supplementary Images)

The NCOR1 mRNA sequence was taken from NCBI (NM_006311.2) and processed through the Qiagen siRNA design page (http://www.qiagen.com). A list of several possible oligos was screened and blasted to confirm which exon was targeted. The chosen sequences were then inserted into the cassette and ordered from Sigma-Genosis. The final sequences are the following:

Exon 5: AAGCTCCATCCTCTCCAATTT (700 - exon 5)

Fw:5'-GTACC-AA(GCTCCATCCTCTCCAATTT)-TTCAAGAGA-(AAATTGGAGAGGATGGAGC)TT-TTTTT-GGAAAT-3'

Rw:3'-G-TT(CGAGGTAGGAGAGGTTAAA)-AAGTTCTCT-(TTTAACCTCTCCTACCTCG)AA-AAAAA-CCTTT-AGATC-5'

Exon 38: AAGGCAAATCAAGCGGAAAAT (6231 - exon 38-39)

Fw:5'-GTACC -AA(GGCAAATCAAGCGGAAAAT)-TTCAAGAGA-(ATTTTCCGCTTGATTTGCC)TT-TTTTT-GGAAAT-3'

*Rw:*3'-G-TT(CCGTTTAGTTCGCCTTTTA)-AAGTTCTCT-(TAAAAGGCGAACTAAACGG)AA-AAAAA-CCTTT-AGATC-5'

Exon 44: AAGGCTCTCATGGGAAGCTTT (7044 - exon 44)

*Fw:*5'-GTACC-AA(GGCTCTCATGGGAAGCTTT)-TTCAAGAGA-(AAAGCTTCCCATGAGAGCC)TT-TTTTT-GGAAAT-3'

*Rw*3'-G-TT(CCGAGAGTACCCTTCGAAA)-AAGTTCTCT-(TTTCGAAGGGTACTCTCGG)AA-AAAAA-CCTTT-AGATC-5'

2.5.6.3 Short Hairpin RNA construct

To ensure an efficient production of the shRNA of interest the oligos containing the shRNA sequence were annealed and inserted into a pcDNA3.1 vector (Invitrogen). In this vector the original CMV promoter has been substituted with the human H1 promoter.

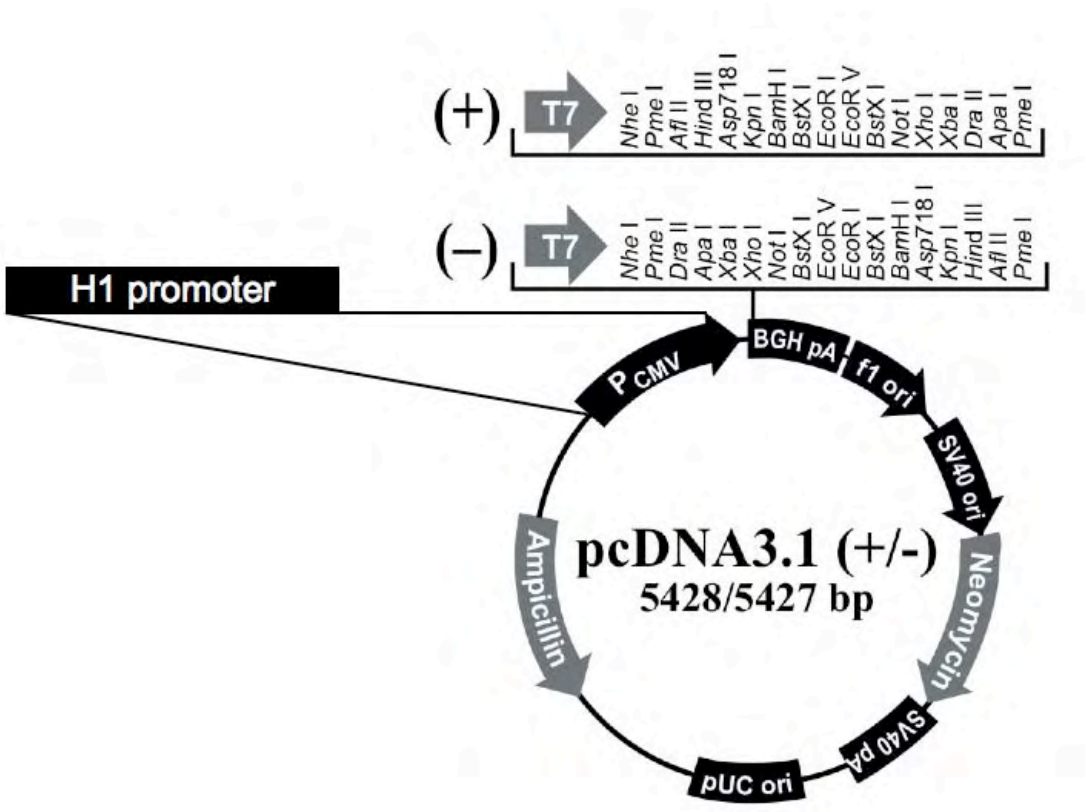

Fig 2.8 – *pcDNA 3.1 vector from Invitrogen. Human H1 promoter was inserted by Farhat Khanim (University of Birmingham, Birmingham, UK) to substitute the original CMV promoter.*

2.5.6.3.1 Annealing Method

Oligos were resuspended in TE buffer (10mM Tris, 1mM EDTA pH 7.4) at the concentration suggested by Sigma-Genosis (100 uM). Before ligation into the pcDNA3.1-H1 vector oligos were annealed: 2 uls of each strand (forward and reverse) were resuspended in 46 uls of TE buffer, heated at 80ºC for 10 mins and then cooled down at room temperature for about one hour. Samples were then stored at -20ºC.

2.5.6.3.2 Ligation Into pcDNA3.1-H1 Vector

T4 DNA Ligase, purified from E.Coli (Invitrogen SKU#15224-017), catalyzes the formation of phosphodiester bonds in the presence of ATP between double-stranded DNAs with 3´ hydroxyl and 5´ phosphate termini. For the ligation reaction: 2 uls of empty pcDNA3.1-H1 vector, 1 ul of ligated oligos, 10X Reaction Buffer (Promega), 1ul of T4 DNA ligase and 5 uls of nuclease free ddH_2O were incubated O/N at +4ºC.

2.5.6.3.3 Transformation of Competent Cells – Introduction

In microbiology, genetics, cell biology and molecular biology, competence is the ability of a cell to take up extracellular ("naked") DNA from its environment. Competence is distinguished into natural competence, a genetically specified ability of bacteria that is thought to occur under natural conditions as well as in the laboratory, and induced or artificial competence, arising when cells in laboratory cultures are treated to make them transiently permeable to DNA. Transformation,

instead, is the genetic alteration of a cell resulting from the uptake and expression of foreign genetic material (DNA), in this case a plasmid.

The idea behind transformation of artificially prepared competent cells is that chilling cells in the presence of divalent cations such as Ca^{2+} (in $CaCl_2$) prepares the cell walls to become permeable to plasmid DNA. Cells are incubated on ice with the DNA and then briefly heat shocked (eg 42 °C for 30–120 seconds), which causes the DNA to enter the cell. The last step is to select those cells containing the plasmid of interest, this can be done plating them in a Petri dish with an antibiotic; the plasmid contains an antibiotic resistance (Ampicillin in the case of the one used in this thesis), therefore only transformed cells are able to survive and grow in colonies that will be then selected.

2.5.6.3.4 Method

Competent cells from Invitrogen (12297-016) were stored at -80ºC and slowly thawed on ice. 100 uls were then resuspended with 4 uls of pcDNA3.1-H1 and incubated for 30 mins on ice. A brief heat shock was given bringing the reaction mix at 37ºC for 30 seconds, samples were then returned to ice for 2 mins. 250 uls of pre-warmed L-Broth (Sigma) were added to each sample and these were incubated at 37ºC shaking at 225 rpm for one hour. Tubes were briefly centrifuged at < 2000 rpm, most of the supernatant was poured off and the pellet was spread in Petri dishes containing L-Broth (Sigma) plus 100 µg/ml of L-Ampicillin. After an over-night incubation at 37ºC colonies were selected, picked up with a sterile tip and

resuspended in 5 mls L-Broth in a 50 ml falcon tube. This was then incubated at 37ºC over night shaking at 225 rpm and used for Minipreps.

2.5.6.3.5 Minipreps to isolate plasmid and Sample Digestion

Once the liquid cultures were ready, one ml of each sample was used to check whether plasmid DNA was inside the transformed competent cells. Wizard®PlusMinipreps DNA Purification System form Promega (A7100) was used and the manufacturer's instructions were followed. Briefly: cells were pelleted, resuspended and lysated; lysate was then filtered through a resin column and washed three times. The final eluted yields plasmid DNA that was resuspended in Nuclease Free Water, quantified and ran into a 1.5% Agarose (Sigma) gel to check purity. Samples were then stored at -20ºC.

To confirm the presence of the oligo in the site of insertion, vector was digested with Acc65 I and Xba I (both Promega) restriction enzymes: 10 µls of vector were resuspended with 1 µl Acc65 I, 1 µl XbaI, 2 uls of 10X Multicore Buffer (Promega) and 6 µls of dH_2O. The reaction mix was incubated at 37ºC for 2 hours. Afterwards the products were resolved on a 2% agarose gel to check the presence of the insert.

Once the presence of plasmid DNA was confirmed samples were sequenced to confirm that the insert was the sequence of interest.

2.5.6.3.7 Sequencing of the shNOR1 samples

Samples were prepared The reaction mix containing 0.4 µgs of DNA, 1 ul of reverse primer and nuclease free water up to 10 µls was brought to the Genomic Facilities in

the School of Biosciences (University of Birmingham, Birmingham, UK) where the sequencing experiments were undertaken.

Results were analyzed with 4Peaks for MacOSX, freely available online (http://mekentosj.com/4peaks). The different peaks refer to the probability of finding the nucleotide X in the position Y.

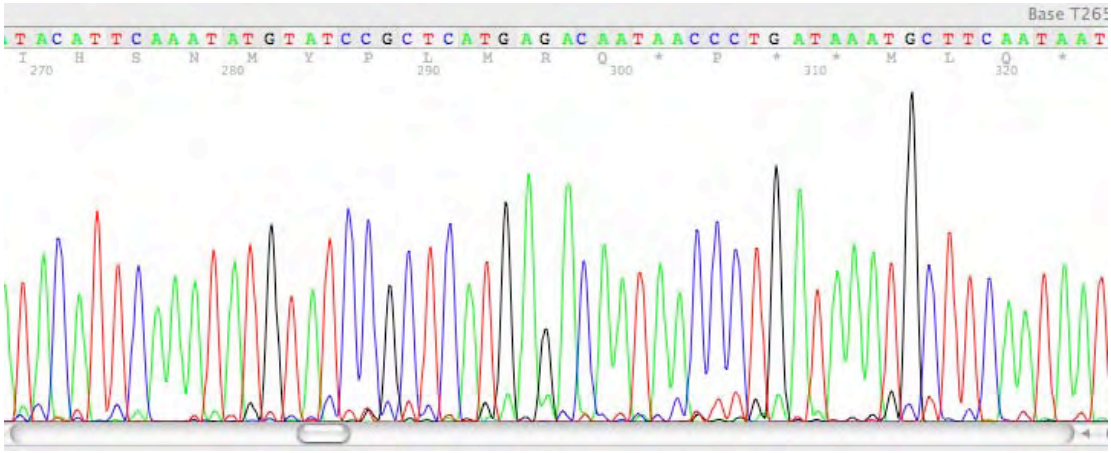

Fig 2.8 – *Layout from sequencing experiment. Each peak represents the probability of finding that specific nucleotide, its position is written below the sequence.*

Once the presence of the insert has been assessed another liquid culture in 500 mls of L-Broth was prepared and incubated over night at 37ºC shaking at 225 rpm.

2.5.6.3.6 Maxipreps to generate large quantity of plasmid DNA

A large scale purification kit from Qiagen was used to extract plasmid DNA from liquid cultures. DNA obtained from maxipreps in more pure than the one from minipreps and can be used for transfection experiments in mammalian cells. Manufacturer's instructions were followed, briefly: cells were pelleted, resuspended and lysed; lysate was then filtered though a resin column able to bind plasmid DNA.

This was then washed and finally eluted in Nuclease Free Water, quantified and stored at -20ºC.

2.5.6.4 Transfection of Prostate Cancer Cells

Transfection describes the introduction of foreign material into eukaryotic cells using a virus vector or other means of transfer. The term transfection for non-viral methods is most often used in reference to mammalian cells. For the purposes of this thesis FuGENE 6 (Roche Diagnostic) was used for the trasnfections.

2.5.6.4.1 Transfection Efficiency

PC-3 cells were transfected with different concentrations of FuGENE6/DNA in order to deliver as much plasmid as possible inside the cell. The concentrations tested were 0 nM, 25 nM, 50 nM, 100 nM, 150 nM. A Renilla reporter plasmid (AM4630, Invitrogen) was used and after 24, 48 and 96 hrs from initial transfection cells were checked under a fluorescence microscope, pictures were taken to identify the sample with the most efficient transfection. In this case 50 nM resulted to be the most efficient concentration.

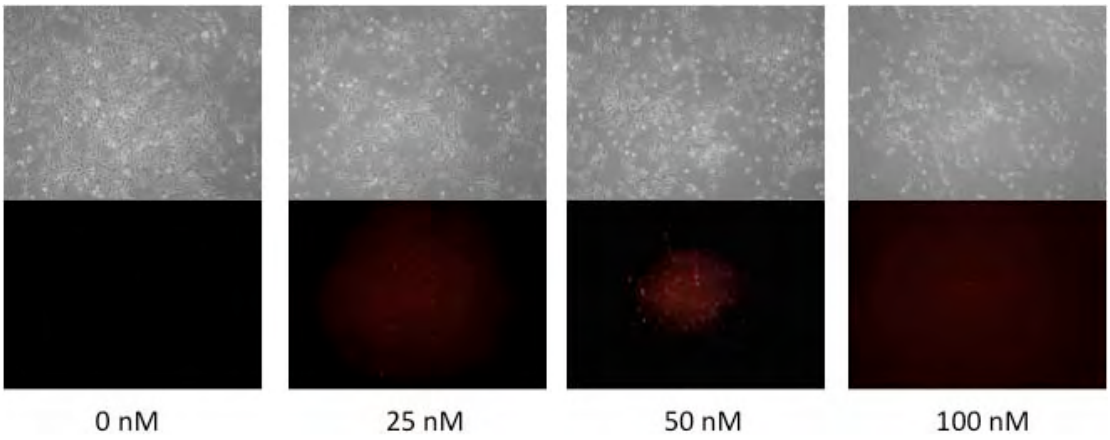

Fig 2.9 – *Transfection efficiency experiment. Method of transfection explained below, briefly, mid-exponential growing PC-3 cells were transfected with different concentrations of plasmid/FUGENE6 and analysed after 24, 48 and 96 hr under the microscope. Pictures indicate cells in the plate (TOP) while red cells indicate Renilla-trasnfected cells after 24 hr (BOTTOM).*

2.5.6.4.2 Method

Transfections were carried out in 6 well/plates, 3 wells/clone - shNCoR vs Vector Only. PC-3 cells were plated 10^5/well in 3 mls RPMI1640 (Sigma) (10% FBS (Gibco), 1% P/S (Invitrogen), 1% L-Glu (Invitrogen)) and seeded for about 36 hrs. For three wells 564 uls of serum free media and 36 uls of FuGENE 6 were left incubating for 5 mins at room temperature in a 1.5 ml eppendorf, 6 ugs of plasmid were added and left incubating for further 15 mins at room temperature. At this point 200 uls of each reaction mix were placed in each well and after 24 hrs media was substituted with selective media containing G418 1ug/ul (Sigma). After 48 hrs cells were plated in T25 and clones were selected after 96 hr. The presence of a specific NCOR1 knock-down was tested by qRT-PCR-TaqMan and Western Imunoblotting.

2.6 – Chromatin Immunoprecipitation Assay to Analyse H3K9 acetylation

2.6.1 – Background

Chromatin immunoprecipitation (ChIP) is a method used to determine the location of DNA binding sites on the genome for a particular protein of interest. This

technique gives a picture of the protein-DNA interactions that occur inside the nucleus of living cells or tissues. Histone modifications can also be recognised by specific antibodies; for the purposes of this thesis, the acetylation of Lysine 9 of the histone H3 (H3K9Ac) was analysed because this modification is a widely used marker for active promoter regions that positively regulate transcription .

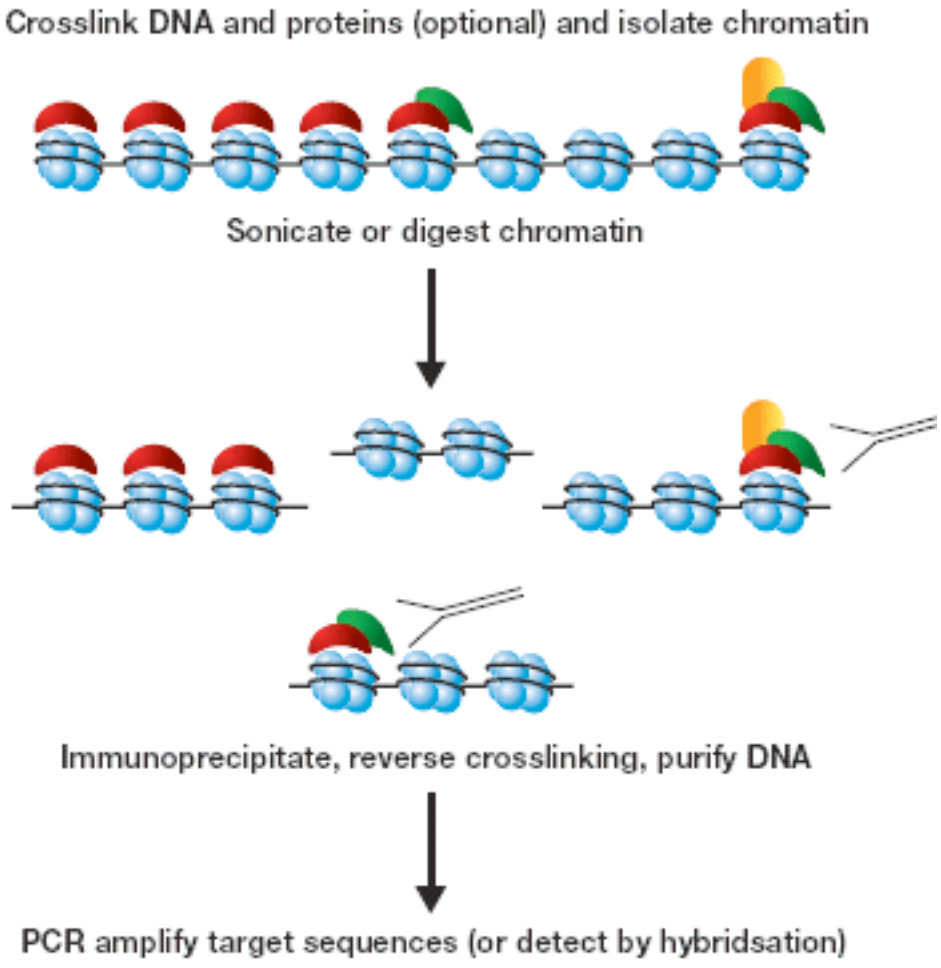

Fig 2.10 – *General workflow of an X-ChIP experiment. DNA is initially crosslinked to fix the proteins to the DNA, DNA is sonicated and the fragments incubated with a primary antibody directed against the selected epitope. The reverse crosslinking releases the antibody/proteins from the DNA; next, DNA is extracted and quantified by PCR analysis. Image taken from www.bbioo.com.*

2.6.2 – Method

Mid exponentially growing PC-3 cells were grown in 10 ml of RPMI 1640 media (previously described). Cells were first crosslinked adding 270 µl of 37% formaldehyde (PS2301, Sigma). To fix the protein to DNA and then incubated at 37ºC for 8 minutes; crosslinking was stopped adding 1.5 ml of 1M Glycine directly to the culture medium and incubated at RT for 5 minutes with gentle shacking. Medium was aspirated and cells washed with PBS containing 5 mM of NaB (303410, Sigma) (NaB prevents the deacetylation events to occur maintaining the acetylation status of H3K9); pellet was collected in ice cold PBS+NaB by scraping the flasks on ice, transferred in a 15 ml falcon tube and centrifuged at 700 g for 5 minutes at 4ºC. The cell pellet was resuspended in 1 ml of SDS-Lysis buffer (1% SDS, 10 mM EDTA and 50 mM Tris-HCl pH 8.1) and transferred into a new 1.5 ml eppendorf tube.

Samples were then sonicated at 4ºC for 5 minutes at medium intensity with 30 seconds pulses to obtain DNA fragments of ~500 bp. Debris were removed by centrifuging the samples at 16000 g for 5 minutes at 4ºC; the supernatant containing the chromatin fragments was divided in 4 x 200 µl aliquots: one sample for stock, one sample for H3K9Ac immunoprecipitation, one sample for IgG immunoprecipitation (control IP) and one INPUT (non-IP sample control). Aliquots were resuspended in further 300 µl of dilution buffer (0.01%SDS, 1.1% Triton X-100, 1.2 mM EDTA, 16.7 mM Tris-HCl pH 8.1 and 167 mM NaCl). IgG and H3K9Ac samples were incubated for at least 30 minutes on a rotating platform with 95 µl of Protein A Agarose 50% slurry (15918-014, Invitrogen) and 5 µl of Herring sperm DNA (15634-017, Invitrogen); this passage is a blocking step that reduces aspecific

binding of the antibody to the epitopes. Samples have to be briefly centrifuged at 170 g for 1 minute to remove the pellet before adding the antibody. For the IP step, 5 µl of the antibodies –H3K9Ac (rabbit, gift of Prof. Brian Turner and Dr. Laura O'Neill, University of Birmingham, Birmingham, UK) and IgG (rabbit, ab49697, Abcam)– were added to the samples and incubated over-night at 4ºC on a rotating platform.

Samples require a further step of purification to isolate the immunoprecipitated complexes; this was made with magnetic beads (Pure Proteome Prot A Magnetic beads, LSKMAGA10, Millipore).

Initially 50 µl of beads/sample were put in a 1.5 ml eppendorf tube, mixed with 500 µl of PBS with 0.1% Tween 20, placed on a magnetic rack, supernatant was taken off and beads were resuspended in further 100 µl of PBS/0.1% Tween 20. This was added to the samples and incubated at 4ºC for 1 hour on a rotating platform. The supernatant containing unbound DNA was discarded.

Samples were then washed with 500 µl of the following buffers at RT for 5 minutes on a rotating platform, respectively: 1X low salt immune complex washing buffer (0.1% SDS, 1%Triton X-100, 2 mM EDTA, 20 mM Tris-HCl pH 8.1 and 150 mM NaCl), 1X high salt immune complex washing buffer (0.1% SDS, 1%Triton X-100, 2 mM EDTA, 20 mM Tris-HCl pH 8.1 and 500 mM NaCl), 1X LiCl immune complex washing buffer (0.25 M LiCl, 1% NP40, 1% deoxycholate, 10 mM Tris-HCl pH 8.1 and 1 mM EDTA) and 2X TE buffer (10 mM Tris-HCl pH 8.0 and 1 mM EDTA). The use of different types of salts improves the effective removal of non-specific chromatin

interactions with the magnetic beads. LiCl is also soluble in buffers containing high amounts of SDS.

After the last wash samples were resuspended in 500 µl of elution buffer (0.1M $NaHCO_3$ and 1% SDS) and incubated at RT for 30 minutes on a rotating platform; this passage will release the DNA and the associated proteins from the immunocomplexes. The supernatant containing DNA was transferred into a new 1.5 ml eppendorf tube, 20 µl of 5 M NaCl were added to the samples and to the input (prepared in DAY 1); samples were then incubated over-night at 65ºC to reverse cross-link, hence, release the DNA from the proteins.

Subsequently, 20 µl of Tris-HCl pH 6.8, 10 µl of EDTA and 2 µl of Proteinase K (AM2546, Invitrogen) were added to the samples that were then incubated for 1 hour at 45ºC.

To isolate the DNA a phenol/chloroform extraction was performed. 50 µl of phenol/chloroform (P3803, Sigma) were added to each sample, vortexed and centrifuged at 13000 rpm for 5 minutes. The clear, organic top phase was transferred into another 1.5 ml eppendorf tube, 500 µl of chloroform (C2432, Sigma) were added, samples were vortexed and centrifuged at 13000 rpm for 5 minutes. The clear top phase, containing DNA was transferred into a new tube and mixed with 100 µl of 4 M LiCl, 0.5 µl of Glycogen (AM9510, Invitrogen) and 1 ml of ice-cold 100% EtOH; the samples were then incubated at -80ºC for 1 hour. This passage will precipitate the DNA. The tubes were centrifuged at 13000 rpm for 10 minutes at 4ºC, the supernatant was discarded and the pellet was washed with 100 µl 70% EtOH. The samples were centrifuged again at 13000 rpm for 5 minutes; the

supernatant was discarded, the pellet was left to air-dry for ~10 minutes and resuspended in 40 µl of Nuclease Free H_2O.

Finally, samples were quantified with the nanodrop (Thermo Scientific) and resuspended at the concentration of 20 ng/µl.

2.6.3 – PCR analysis of the extracted DNA

PCR analysis of the regions that were immunoprecipitated reveals whether the region of interest was enriched or depleted of the target protein/modification.

For the purposes of this thesis the regions analysed were for CDKN1A TSS and a putative PPARα binding region at +3733 nt from the TSS; for TGFBRAP1 a region at +261 bp from the TSS (this because the TSS was a GC rich region and no reliable primer sets were found) and a putative PPARα binding site at -929 from the TSS was analysed. Putative binding sites were identified via *in silico* screening by Merja Heinaniemi (University of Luxembourg, Luxembourg).

Primers used are:

Primer	Sequence (5'-3')
CDKN1A TSS Forward CDKN1A TSS Reverse	TATATCAGGGCCGCGCTG GGCTCCACAAGGAACTGACTTC
CDKN1A +3733 Forward CDKN1A +3733 Reverse	TTGAGGGCTCTGTCCACTGT TTAAAGGGCAGGAGATGGAA
TGFBRAP1 +261 Forward TGFBRAP1 +261 Reverse	TGTGCGACTTGGTAGCTGTC GCACACTTCATCCCACACAC
TGFBRAP1 -929 Forward TGFBRAP1 -929 Reverse	TTTTCCCAGGGATTTTCAGA GCCTTCAGGGTTGGGATAAT

Table 2.6 – *Sequences of the primers used in ChIP experiments in this thesis. Name of the gene and position relative to the TSS are indicated on the left side.*

40 ng of DNA were amplified in a 20 µl reaction containing 1x TaqMan PCR MasterMix and 1x SYBR Green (both form the kit Sensimix dT - QT6T3, Quantace, UK), with 1 µM of primers. An ABI PRISM 7300 sequence detector machine (Applied Biosystems, Foster City, CA, USA) was used under the following cycle conditions: 95°C for 10 min, 40 cycles of 95°C for 15 sec, 60°C for 1 min and 72ºC for 30 sec and lastly 95ºC for 15 sec, 60ºC for 1 min, 95ºC for 15 sec and 60ºC for 15 sec. The dissociation curve was checked for each sample after each experiment to confirm that the primers amplified only one region; samples with more than a single region amplified were excluded from the analysis. Final measurements were an average of a minimum of two independent experiments, in triplicate wells for each condition. Student's T-tests were performed to identify regions significantly enriched or depleted.

3 – EMBRYONIC STEM CELL CULTURE AND KNOCK-OUT, -DOWN METHODS

(Berlin - DE -, Max Planck Institute for Molecular Genetics, Dept. of Developmental Genetics)

3.1 – Preparation of feeder cells from mouse embryos

3.1.1 – Isolation of Mouse Embryonic Fibroblasts

13.5-14.5 dpc (day post coitum) mouse embryos were dissected from sacrificed mice and placed in PBS. Head and soft tissues (e.g lung, liver, heart and gut) were discarded and the carcasses were washed twice in PBS before being minced with scissors into small pieces of about 2-3 mm in diameter. These were then transferred into a 150-cm^2 flask with screw cap containing 30 ml of Trypsin-EDTA (Sigma) to digest the tissues, and a stir bar with molded pivot ring. The flask was then incubated at 37 ºC for 5 minutes. The supernatant was transferred to a 50 ml falcon tube containing 1.5 ml of Fetal Calf Serum (FCS) to inactivate the trypsin. The previous step was repeated twice to digest as much tissue as possible.

Digested cells were spin down for 5 min at 1000 rpm, resuspended in feeder cell medium (DMEM with 4.5 mg/ml glucose (Sigma), 10% FCS, 1% glutamine (Sigma, G7513), 1% penicillin/streptomycin (Sigma, P0906)) and incubated over night at 37 ºC. Cells at this stage were ready to be expanded and treated with mitomycin C in order to make them mitotically inactive.

3.1.2 – Mitomycin C Treatment

3.1.2.1 – Introduction

Mitomycin C is an aziridine-containing product isolated originally from *Streptomyces lavendulae*. It potently inhibits cell proliferation accomplishing this by reductive activation followed by two N-alkylations. Both alkylations are sequence specific for a guanine nucleoside in the sequence 5'-CpG-3'.

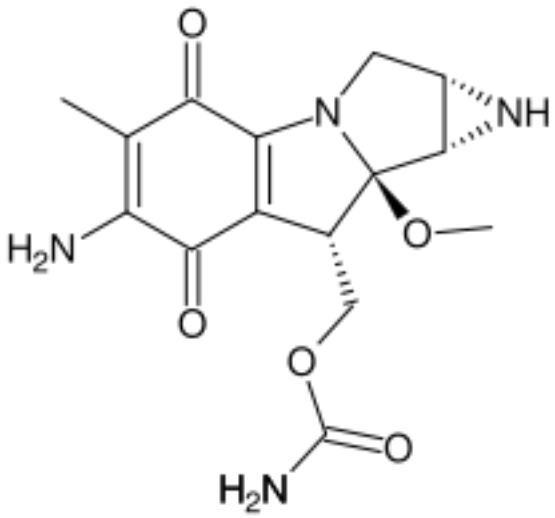

Fig 3.1 – *Mytomycin C chemical structure (from Wikipedia)*

3.1.2.2 – Method

Due to its toxicity gloves were always worn.

Once culture dishes were fully confluent, the media was aspirated and replaced with feeder media containing 0.01 mg/ml of mitomycin C (Sigma, M4287) and incubated for 2-3 hours at 37ºC. After that time media was carefully aspirated, plates were

washed three times with 20 ml of PBS, 10 ml of trypsin were added to each plate and incubated for 10 min at 37ºC. Cells were collected in a 50 ml falcon tube, spin down, resuspended in feeder media, counted and either plated for stem cells or frozen.

3.1.3 – Freezing/Thawing feeder cells

3.1.3.1 – Freezing method

- Feeder cells were trypsinized and counted with a haemocytometer; cells were frozen in vial of 2.5 or 5 x 10^6 cells. Cells were resuspended in 50% of the volume DMEM with 20% FCS, the remaining 50% of the volume consisted of 2X freezing media (for 100ml: 60 ml DMEM 4.5 mg/ml glucose w/o sodium pyruvate (Sigma, D9161), 20 ml FCS and 20 ml of Dimethylsulfoxide (DMSO) (Sigma, D2650)). Cryovials were transferred into freezing boxes (Nalgene) and cooled at -70 ºC overnight before being placed into liquid nitrogen.

3.1.3.2 – Thawing method

- Frozen feeder cells were thawed slowly in a 37 ºC bath, samples were resuspended in warm feeder cells media, centrifuged for 5 min at 1000 rpm and the pellet was resuspended again in feeder cells media.

3.1.4 – Plating feeder cells

Mitomycin C treated embryonic fibroblasts can be plated in feeder cell media at the density of of 3-4 x 10^4 cells/cm^2. After already two hours they will attach to the

bottom of the well/plate giving a monolayer that can be used for further experiments.

3.2 – Culture of Mouse Embryonic Stem Cells

3.2.1 – Preparation of gelatinized dishes for cell culture

Dishes used for embryonic stem cells (ESCs) cells had to be gelatinized in order to help ESCs to adhere optimal to the bottom of the dish.

Sterile 2% gelatin (Sigma, G1393) was diluted to 0.1% in Millipore water. Due to the diameter of the wells used from 100 µl to 3 ml of 0.1% gelatin were added and left 1 to 5 minutes at room temperature. The gelatin was then aspirated and the dish or plate, was left to air-dry under the hood.

3.2.2 – Media for ES cells

Embryonic Stem Cells media was prepared as follow for 500 ml:

- 400 ml DMEM KO (Gibco, 10829-018), optimized for growth of undifferentiated ES cells and its osmolarity was similar to that of mouse tissues;
- 75 ml FCS ES cell tested (Invitrogen, 10439-016), ES cell tested;
- 5 ml 100X glutamine, 200mM (Gibco, 25030);
- 5 ml 100X penicillin (5000 U/ml) / streptomycin (5000 µg/ml) (Gibco, 15070);
- 5 ml 100X non-essential amino acids (Gibco, 11140);

- 7 ml freshly prepared β-mercaptoethanol (2-ME): 7 µl of β-mercaptoethanol (Sigma, M7522) were resuspend in 10 ml of D-PBS (Gibco 14190), mixed well and 5 ml of the solution were filtered into the bottle of media. 2-ME was used to reduce the oxidative stress in ES cells;
- 5 ml 100X nucleosides;
- 50 µl LIF (Murine Leukemia Inhibitory Factor) ESGRO™ (Chemicon); LIF was used as undifferentiating agent.

3.2.3 – Passaging ES cells

3.2.3.1 – In dishes

The ES cell media was aspirated, dishes were washed with PBS and, for a 6 cm dishes, 1 ml of 1X Trypsin (0.5 g/l)-EDTA (0.2 g/l) (Sigma, 3924) was added. Cells were then incubated at 37 ºC for 10 min, resuspended in ES cell media, centrifuged, resuspended again in ES cell media and plated in new gelatinized dished containing a monolayer of feeder cells.

3.2.3.2 – In 96-well plates

ES cells media was aspirated, wells were washed twice with 100 µl of D-PBS and 70 µl of Trypsin-EDTA were added. Plates were incubated at 37 ºC for 10-15 minutes and in the meanwhile a new 96-well plate was prepared with 140 µl of ES cell media. Trypsinization was stopped adding 140 µl of ES cell media; cells were pipetted up and down and 70 µl were transferred into the new plate. Another 70 µl of ES cell media was added to the original plate and all plates were placed back into the incubator.

3.2.4 – Freezing/Thawing ES cells

3.2.4.1 – From dishes, freezing method

- ES cells were trypsinized and counted with a haemocytometer; 2.5 or 5 million cells were resuspended in 50% of the volume in 2X Bicarbonate free DMEM containing 10 mM Hepes and 20% FCS, the remaining 50% of the volume consisted of 2X ES freezing media (for 100ml: 60 ml Bicarbonate free DMEM containing 10 mM Hepes, 20 ml FCS and 20 ml Dimethylsulfoxide (DMSO) (Sigma D2650)). Cryovials were transferred into freezing boxes (Nalgene) and cooled at -70 ºC overnight before being placed into liquid nitrogen.

3.2.4.2 – From dishes, thawing method

- Frozen ES cells were thawed slowly in a 37 ºC bath, samples were resuspended in warm ES cells media, centrifuged for 5 min at 1000 rpm and pellet was resuspended again in ES media. The next morning media was changed to remove any dead cells. Media was changed daily.

3.2.4.3 – From 96-well plates, freezing method

- ES media was removed, cells were washed twice with 100 µl of D-PBS, 70 µl of Trypsin-EDTA were added and plates were incubated at 37ºC for 10-15 min. Trypsinization was blocked adding 140 µl of Bicarbonate-free DMEM/10 mM Hepes containing 20% FCS and pipetting up and down a few times using a multichannel pipette. While cells were in the incubator a U-bottomed 96-well plate was prepared containing 70 µl of 2X Bicarbonate-free ES cell freezing media, this plate will then be used for freezing ES cells. From the original plates 70 µl from each well were

transferred into the previously prepared plate, this was then sealed with Parafilm and placed at -80ºC; 70 µl of ES media were added to the original plate and this was placed in the incubator at 37ºC.

3.2.4.4 – From 96-well plates, thawing method

- Plates were taken out of the -80ºC freezer and placed in a 37 ºC incubator to allow cells to thaw. Pipet up and down with a multichannel pipette and transfer cells in a new plate containing ES cell media. Plates were incubated at 37ºC and media was changed daily.

3.2.5 – Electroporation of ES cells

Electroporation, or electropermeabilization, is a significant increase in the electrical conductivity and permeability of the cell plasma membrane caused by an externally applied electrical field. This process is able to create small breaks in the bacterial membrane that allows plasmid DNA to get into the host cell.

3.2.5.1 - Method

ES cells were trypsinized and cells were counted with an haemocytometer. 1 x 10^7 cells were transfered to a fresh tube, centrifuged, resuspended in 800 µl of PBS and transferred into an electroporation cuvette (Gene Pulser Cuvette, Bio-Rad, 1652088). At this point 25 µg of plasmid, linearized for homologous recombination, in sterile PBS were added to the cells. The cuvette were placed in the Gene Pulser machine (Biorad) and cells were electroporated under the following conditions:

- voltage: 240 V
- capacity: 500 µF

- resistance: ∞
- cuvette: 4 mm

Straight after, cells were plated in 6 cm dishes containing neo-resistant feeder cells EF/N.

The next morning media was changed to remove dead cells and after 36 hours media was replaced with selection media containing G418, FIAU or both depending on the plasmid used.

3.2.6 – Picking ES cell colonies

After cells went through selection single colonies were picked from the dishes and plated in a 96-well plate, one colony per plate.

Two 96-well plates containing 25 µl of Trypsin-EDTA per well were prepared, this allowed a better detachment of cells within the colony for a more homogeneous expansion inside the well. Using a pipette set up at 3 µl, with a 10 µl tip, colonies were picked scraping the bottom of the dish and aspirating the cells. They were then placed into the different wells. After the plate was full it was placed in the incubator at 37ºC for 5-10 minutes. Trypsinization was stopped by adding 100 µl of ES cell media and cells were transferred into a 96-well plate containing a fresh layer of feeder cells. Media was changed daily. Once cells reached confluence they were further split into other two plates: two for DNA extraction and one was frozen as master plate.

3.3 – Nucleic acid extraction

3.3.1 – DNA extraction

3.3.1.1 – From dishes

Cells were washed twice with PBS and 500 µl of Laird's buffer (200 mM NaCl, 100 mM Tris-HCl pH 8.3, 5 mM EDTA, 0.2% sodium dodecyl sulfate, pH 8,5) [192] containing 150 µg/ml of proteinase K were added. Samples incubated at 37 ºC over night. The following morning samples were transferred into an eppendorf 1.5 ml tube using tips with wider tip in order not to sheare the DNA, they were shaken at 37 ºC for one hour and centrifuged at RT for 20 minutes at full speed. Samples were then poured into eppendorf tubes containing 500 µl of 2-propanol and shaken to allow the DNA to precipitate. This precipitate was fished out with a tip and transfered into a new tube containing 200 µl of TE buffer (10 mM Tris, pH 7.5,1 mM EDTA pH 8.0). DNA was left resuspending for few hours.

3.3.1.2 – From 96-well plate

The original protocol is described in [193].

Before starting the lysis a scan of the plate was taken to keep record of the empty well.

Media was aspirated and wells washed twice with 150 µl of PBS, 50 µl of lysis buffer (for 500 ml: 5 ml 10 mM TrisHCl pH 7.5, 10 ml 10 mM EDTA pH 8.0, 1 ml 10 mM NaCl, 12.5 ml 0.5% sacrosyl); Proteinase K was added to final concentration of 1 mg/ml prior to use, pre-warmed at 60 ºC added to the wells and plates were

incubated over night at 60 ºC inside a humid chamber (prepared with a tupperware containing wet towels) to avoid evaporation.

The next day 100 µl of ice cold 100% EtOH containing 75 mM of NaCl were added to each well without mixing; plates were left at RT for 30 mins, at this time the DNA formed jelly-like transparent filaments at the bottom of the well. After this time the supernatant was discarded inverting the plates and wells were rinsed three times by adding 200 µl of 70% EtOH. This was discarded by inversion and DNA was left drying on the bench.

3.3.1.3 – Phenol Chloroform extraction

This procedure is used when there is the need of having high purity clean DNA.

Phase Lock Gel Heavy 1.5 ml vials (Eppendorf, 955154151) were used. These columns contain a semi-solid gel solution that acts as a barrier between the organic and aqueous phases, allowing the nucleic-acid-containing phase to be decanted or pipetted off.

Before use, tubes were firstly centrifuged at maximum speed for 30 seconds. After this, an equal volume of phenol and chloroform were well mixed and added to the DNA at a volume ratio 1:1. Samples were vortexed and immediately transferred to the Phase Lock columns, centrifuged for 5 minutes at full speed and supernatant (~100 µl) was transferred into a new 1.5 ml tube. 100 µl of H_2O were added followed by 20 µl of 3M NaAc pH 5.2 (In aqueous solution, sodium acetate breaks up into Na+ and [CH3COO]-; the positively charged sodium ions neutralize negatively charged backbone on the DNA, specifically the PO3- groups on the nucleic acids,

making the nucleic acid molecule far less hydrophilic, and therefore much less soluble in water.) and 660 µl of 100% cold EtOH (ethanol then makes much easier for Na+ to interact with the PO3-, shields their charge and makes the nucleic acid less hydrophilic, causing it to precipitate). Samples were well mixed and put at -20 ºC over night. The following day samples were centrifuged for 30 minutes at maximum speed at 4 ºC, supernatant was discarded and pellet washed twice with 70% EtOH. After EtOH evaporated DNA was dissolved in 50 µl of TE buffer.

3.3.1.5 – DNA precipitation after digestion

After that genomic DNA was digested with the appropriate restriction enzyme it had to be purified before being used in a Southern Blotting.

Samples were brought to a volume of 200 µl with H_2O, 20 µl of 3M NaAc pH 5.2 were added and samples mixed. After that 550 µl of 100% cold EtOH were added, samples were well mixed and incubated at -80 ºC for 30 minutes. Tubes were centrifuged at maximum speed for 30 minutes at 4 ºC. Pellet was washed twice with 100 µl of EtOH, left drying on the bench for 15 minutes and resuspended in 20 µl of TE buffer. To ensure that samples dissolved properly they were incubated at 37ºC for 20 minutes.

3.4 – Polymerase Chain Reactions

3.4.1 – Amplification and screening of the homology region

3.4.1.1 – Primers for the homology region

The primers tested and used are listed in the following *Table 1*:

NAME	SEQUENCE
Ncor1 Rev, I, II, III	tttcttcctcatgccattcc
Ncor1 For I	tttgcagcagagaagctttg
Ncor1 For II	ccccattccctccaaagtat
Ncor1 For III	gaaatccaagaggcatccaa
Ncor2/Smrt Rev	catacatgcaggtggagacg
Ncor2/Smrt For	ttgtgtgggccagagtagtg

Table 3.1 – *List of primers used for the amplification of the homology regions.*

After the first round of amplifications the fragments had to be modified inserting restriction enzyme sites at the extremities to allow better ligation to the vectors, this was done using the following primers:

NAME	SEQUENCE
Ncor1 XhoI Rev	cgtactcgagtttcttcctcatgccattcc
Ncor1 Sac1 For	gtcagagctcccccattccctccaaagtat
Ncor2 EcoRI Rev	gcgagaattccatacatgcaggtggagacg
Ncor2 EcoRI For	gcgagaattcttgtgtgggccagagtagtg

Table 3.2 *– List of primers used to insert sticky ends to the homology regions amplified.*

3.4.1.2 – Primers for LoxP sites

The insertion of LoxP sites in a target sequence of a gene is commonly used to conditionally knock out a gene, or part of it. The Cre enzyme catalyses the recombination within two LoxP sites exciding the sequence included within them.

Primers used were the following (the uppercase sequence indicates the LoxP site):

NAME	SEQUENCE
Ncor1 LoxP Rev	catggatccATAACTTCGTATAATGTATGCTATACGAAGTTATc
Ncor1 LoxP For	catggATAACTTCGTATAGCATACATTATACGAAGTTATggatc
Ncor2/Smrt LoxP Rev	cgATAACTTCGTATAGCATACATTATACGAAGTTATgaattcgat
Ncor2/Smrt LoxP For	cgaattcATAACTTCGTATAATGTATGCTATACGAAGTTATcgat

Table 3.3 – *Sequences of the oligonucleotides containing the LoxP sites, indicated in uppercase*

.

In order to ensure the insertion of the desired LoxP site in the right position a PCR screening was performed using primers flanking the LoxP sites. Primers are the following:

NAME	SEQUENCE
Ncor1 NcoI Rev	attttatgagttcagcctaatgtcc
Ncor1 NcoI For	tgcagaactggtggcaaata
Ncor2 PvuI Rev	tgagcaggtcacaccttcag
Ncor2 PvuI For	cacgggaggtgatcaagact

Table 3.4 – *Sequences of the primers used to validate the presence of the LoxP sites.*

3.4.1.3 – Primers for Neo selection cassette

A Neo-cassette was insert to confer neomycin resistance to positive clones. To check the integration of this fragment into our construct the following primers were used:

NAME	SEQUENCE
Ncor1 SnaBI Rev	ccaccacagatttgagcatc
Ncor2 ScaI For	tctccctttctttccgttca
Neo 5' Rev	atgtggaatgtgtgcgaggccag

Table 3.5 – *Sequences of the primers used to validate the presence of the Neo cassette*

The presence of two reverse primers for Ncor1 is explainable because the orientation of the Neo cassette in this construct is opposite of the one of Ncor2/SMRT.

3.4.1.4 – Primers for ES cells screening

After that ESCs clones were isolated we sought to do a first screening by PCR where the first LoxP site and the presence of Neo cassette, including ~2 kb outside of the homology region, were checked. Primers for the LoxP are listed above and those for the Neo cassette are the following

NAME	SEQUENCE
Ncor1 out Rev	cactggggaagaagagctagga
Ncor2 out Rev	ctccctaggcgcctttgtct
Neo poly-A For	tgggaagacaatagcaggcatgc
Ncor2 LoxP out FW	tagttcccaggcgtgtaacc
Ncor2 LoxP RW2	gccaaggtctcatccgatcgat

Table 3.6 – *Sequences of the primers used to screen the Neo cassette in electroporated ES cells*

3.4.1.5 – Handling of primers

Upon arrival all the primers were resuspended in TE buffer at the concentration of 100 μM (100 pm/μl); the working solution was prepared using 5 μl of each primer, forward and reverse, with 40 μl of ddH_2O for a final concentration of 10 μM.

3.4.2 – PCR amplification

Two different kits were successfully used to amplify the homology regions: Phusion High-Fidelity DNA Polymerase (Finnzymes, F530L) and TaKaRa LA Taq (Takara Bio Inc, RR002A). Two different BACs containing genomic fragments including Ncor1 (imaGenes, RPCIB731D07130Q) and Ncor2 (imaGenes, RPCIB731F11335Q) regions were also ordered.

Reaction mixes for the two different genes were prepared following the manufacturer's instructions, briefly:

PHUSION	*µl reagent (x1)*
H_20	36.5
5X GC Reaction Buffer	10
10 mM dNTPs	1
Primer Mix	1
TaqPol	0.5
DNA	1

The thermal profile for the Phusion kit was the following: 98 ºC for 30 sec, 35 cycles with 98 ºC for 20 sec, 65 ºC for 2 min and 72ºC for 10 min, 72 ºC for 10 min and 4 ºC for as long as it was needed.

TAKARA	*µl reagent (x1)*
H_20	19.5
10X LA PCR Buffer	5
25 mM $MgCl_2$	5
10 mM dNTPs	8
Primer Mix	1
TaKaRa LA Taq	0.5
DNA	1

The thermal profile for the Takara kit was the following: 98 ºC for 2 min, 35 cycles with 98 ºC for 10 sec, 60 ºC for 30 sec and 72 ºC for 10 min, 72 ºC for 10 min and 4 ºC for as long as it was needed.

For all the samples G4 ES cell DNA was used as negative control.

3.4.3 – Colony screening for DNA inserts and normal PCR

3.4.3.1 - Introduction

Once competent cells are transformed, it is possible to check for the presence of the desired insert picking up a certain number of colonies (generally from 30 to 50) and using as template for the PCR the bacteria that grew on the plate.

3.4.3.2 - Method

Before starting with the PCR a Petri dish containing L-broth agar and the desired antibiotic was prepared and a numbered grid drawn on the lid in order to precisely identify positive colonies after the screening.

Mastermix was prepared as follow, all reagents were from Invitrogen:

Reagent	*µl (x1)*
H_20	15.5
10X Buffer (Y02028)	2.5
50 mM $MgCl_2$ (Y02016)	0.75
100 mM dNTPs	0.5
Primer Mix	1
TaqPol (10342-055)	0.25

The reaction mix was dosed into ABI tubes (ABI, Micro Amp Tube Strips 0.2 ml, N8010580). Using a sterile tip single colonies were picked from the master plate

and quickly inoculated in the previously prepared dish, the same tip was then put into the tube to add template to the reaction.

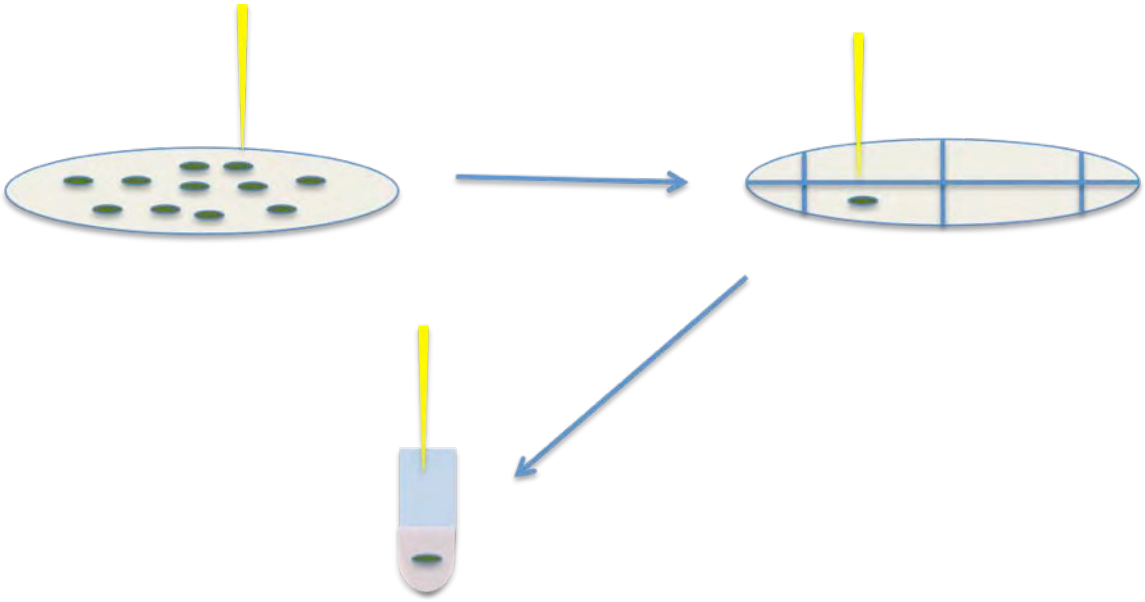

Fig 3.2 – *Scheme of how to pick colonies for PCR screening. The colonies were quickly touched with the tip, bacteria remained attached to the tip and were re-plated in a new Petri dish; the tip was then put into the tube with Mastermix and worked as a template for the reaction.*

The same reaction master mix was also prepared for PCRs when special kits weren't needed. The only differences were that 1 µl less of nuclease free H_2O was used and the template consisted of 1 µl of DNA.

The thermal profile for this kind of PCRs was the following: 94ºC for 3 min, 35 cycles at 94ºC for 30 sec, 55ºC for 30 sec (up to 3 min) and 72ºC for 30 sec, 72ºC for 10 min and 4ºC for as long as it was needed.

3.5 – DNA digestion

This procedure refers to an enzymatic reaction where the DNA is cleaved into smaller pieces by restriction enzymes that recognize precise sequences, catalyzing the digestion of that specific region.

3.5.1 – Enzymes and buffers

Each enzyme has its highest efficiency with its own buffer; all restriction enzymes were from Promega and are listed below, buffers were provided with the restriction enzyme:

NAME	BUFFER
BamHI (R6025)	E
EcoRI (R6017)	H
EcoRV (R6355)	D
NcoI (R6515)	D
NotI (R6435)	D
PvuI (R6325)	D
SacI (R6065)	J
ScaI (R6211)	K
SnaBI (R6795)	B
XhoI (R6165)	D
BamHi HC (R4027)	H
EcoRI HC (R4017)	H

Table 3.7 – *List of the restriction enzymes used in this thesis with the corresponding buffer.*

In case of double digestion the right buffer was chosen using the software EnzymeX (freely available at http://mekentosj.com/enzymex).

3.5.2 – Reactions

3.5.2.1 – Digestions for cloning and screening

Vectors, amplified fragments and DNA obtained from mini-, midi-preps were normally digested in a 20 µl reaction using 1 µl of enzyme, 2 µl of buffer, from 2 to 8 µl of DNA and H_2O until 20 µl. The tubes were incubated at 37ºC for 1 hour and samples analyzed in a 1% Agarose gel.

3.5.2.2 – Genomic DNA digestion for Southern Blotting

In case of genomic DNA digestion a higher concentration of restriction enzymes is required due to the high amount of target sequences that are present.

Each reaction was set up in 100 µl volume using 10 µl of buffer, 5 µl of high concentrated enzyme (HC), 50 µl of DNA, 1 µl of spermidine (Sigma, enhances enzymes' specificity diminishing non-specific cleavage of DNA), 1 µl of BSA (10 mg/ml) (Promega, R396D – BSA is needed by some enzymes to prevent their adhesion to reaction tubes or pipette surfaces and it also stabilizes some enzymes during incubation), 1 µl of RNase A (10 mg/ml) (Sigma – used to remove any remaining RNA from the template) and ddH_2O to a total volume of 100 µl.

Samples were incubated at 37 ºC over night and ran the following morning in an 0.6% agarose gel.

3.6 – Creating blunt ends products

3.6.1 - Klenow treatment

3.6.1.1 - Introduction

The DNA Polymerase I Large (Klenow) Fragment is a DNA-dependent DNA polymerase that lacks the 5′→3′ exonuclease activity of intact E. coli DNA Polymerase I but retains its 5′→3′ polymerase, 3′→5′ exonuclease and strand displacement activities. The enzyme is a 68 kDa C-terminal fragment of DNA Polymerase I. In case of fragments with 5' overhanging nucleotides, the 5′→3′ polymerase activity of Klenow Fragment can be used to fill in 5′-protruding ends with unlabeled or labeled dNTPs.

3.6.1.2 – Method

The reaction was setup as follow:

Reagent	*µl (x1)*
DNA Pol (M2201)	2
Buffer D	2
dNTPs (1 mM)	1
DNA	10
ddH_2O	5

Tubes were incubated for 15 minute at room temperature and 10 min at 75 ºC to inactivate the polymerase.

Samples were then stored at -20ºC.

3.6.2 - T4 polymerase treatment

3.6.2.1 – Introduction

T4 DNA Polymerase catalyzes the 5´→3´ synthesis of DNA from a primed single-stranded DNA template. Although possessing a potent 3´→5´ proofreading exonuclease, T4 DNA Polymerase contains no 5´→3´ exonuclease activity. In case of a fragment with 3' overhanging nucleotides, it can be used at low temperatures to create blunt end products exploiting the 3'→5' exonuclease activity.

3.6.2.2 – Method

The reaction was set up as follow:

Reagent	*µl (x1)*
T4 Pol (M4211)	2
dNTPs	0.5
DNA	10

Samples were incubated at 12ºC for 15 minutes before being stored at -20 ºC for further experiments.

3.8 – DNA ligation

DNA ligation is an ATP-dependent process that involves the formation of two covalent phosphodiester bonds between 3' hydroxyl ends of one nucleotide with the 5' phosphate end of another.

3.8.1 – Ligation of homology regions into vector

Two different vectors were used, pBluescriptSK (Stratagene) for Ncor1 and pCR BLUNT II TOPO (Invitrogen, Zero BLUNT TOPO PCR cloning kit, K2800-20) for Ncor2.

Fragments obtained from PCR amplification were ligated into their respective vectors using Promega reagents as follow:

Reagent	*µl (x1)*
T4 Ligase (M1794)	1
10X T4 Buffer (C126B)	10
Vector	0.5
Insert	8

Reaction mix was incubated for 15 minutes at room temperature and then put on ice for further experiments.

3.8.2 – Ligation of LoxP sites and Neo cassette into homology region

Vectors containing the homology region were previously digested with the appropriate enzyme, then the double strand (ds) DNA containing the LoxP site or the Neo-cassette were ligated into that region.

Reactions were setup as follow:

Reagent	*µl (x1)*
T4 Ligase (M1794)	1
10X T4 Buffer (C126B)	5
Digested vector	2
Oligos	2

Samples were incubated for 15 minutes at room temperature and then put on ice for further experiments.

3.8.2.1 – Drop dialysis of ligation reaction

Before transforming competent cells, the ligation reaction was placed on a small membrane in a dish containing ddH2O and incubated for 20 minutes at room temperature. For osmosis the water will move through the membrane into the samples, lowering the salt's concentration.

This process facilitates future ligase activity that could be otherwise affected by high salt concentration.

3.9 – Transformation of competent cells and plasmid DNA isolation

3.9.1 - Electroporation

Electrocompetent cells (Invitrogen, One Shot TOP10 E.Coli, C4040-52) were kept at -80 ºC and thawed on ice, 2 µl of DNA were added and reaction was transferred

immediately into a pre-chilled electroporation cuvette (Bio-Rad, 1652089). This was placed into the MicroPulser Electroporator (Bio-Rad) and voltage was set to 1.75 V. After electroporation 500 µl of S.O.C. media (Invitrogen, 46-0700) were added, reaction was pipetted into 1.5 ml tubes and left for one hour at 37ºC shaking.

3.9.2 – Chemical transformation

Home made DH5α or chemically competent cells (Invitrogen, One Shot TOP10 E. Coli , C4040-03) were kept at -80 ºC and thawed on ice, 2 µl of DNA were added and cells were incubated in ice for 5-15 minutes, heat-shocked at 42ºC for 45 seconds and placed in ice for 2 minutes. 500 µl of S.O.C. media (Invitrogen, 46-0700) were added, reaction was transferred into 1.5 ml tubes and incubated at 37 ºC shaking for one hour.

After transformation all bacteria were plated in Petri dishes containing LB plus the necessary antibiotic for selection.

3.9.3 – DNA mini- and midi-preps

After that single colonies were successfully isolated from the master plate, they were inoculate first in two ml of L-Broth for mini-preps and then into 50 ml of medium for midi-preps. The first step was fundamental to screen positive clones and with the second step clean plasmid DNA was isolated for further experiments.

3.9.3.1 – Mini-preps

The QIAprep Spin Miniprep Kit (Qiagen, 27106) was used and all buffers were provided with the kit. Plasmid DNA was extracted following the manufacturer's

instructions. Chosen colonies were left growing over night in 2 ml of media at 37ºC shaking, 1 ml was transferred into a 1.5 ml tube and centrifuged at maximum speed for 3 minutes. Pellet was kept and sequentially resuspended in P1 buffer, P2 buffer (lysis buffer) and P3 buffer (containing LyseBlue reagent colors the sample in case of correct lysis). Samples were then centrifuged at maximum speed, supernatant was kept and flowed throw the Qiagen column where DNA bound to the membrane. Columns were then centrifuged and washed twice with PE buffer (containing EtOH). With the final spin DNA was eluted in 50 µl of TE buffer and collected in 1.5 ml tubes for further usage.

3.9.3.2 – Midi-preps

QIAGEN Plasmid Midi Kit (Qiagen, 12145) was used and buffers were provided with the kit. Plasmid DNA was purified following the manufacturer's instructions.

Previously checked colonies were inoculated into 50 ml of media per sample and incubated overnight at 37ºC shaking. The day after whole volume was transferred in a 50 ml falcon tube and centrifuged at maximum speed for 5 minutes. Pellet was kept and resuspended as above for mini-preps. Lysate was then poured into a syringe and transferred into columns after equilibration with QBT buffer; the flow through was discarded and columns washed twice with QC buffer. Samples were eluted with QF buffer into 15 ml eppendorf tubes, 3.5 ml of isopropanol were added and tubes were centrifuged for 30 min at maximum speed at 4ºC to precipitate the DNA. Pellet was kept and washed with 2ml of 70% EtOH, air-dried and finally resuspended in 300 µl of TE buffer for further experiments.

3.10 – Southern Blotting

Southern blotting is a technique that allows the recognition of a specific DNA fragment bound to a membrane by a radiolabeled probe after that genomic DNA has been digested with the chosen restriction enzyme.

3.10.1 – General description

Genomic DNA was digested and run in a low percentage gel. After capillary transfer onto a nylon membrane it was hybridized overnight with the radiolabeled probe; the following day series of washes reduced the unspecific binding to the membrane. The signal was then detected with a phosphorimager and analyzed.

3.10.2 – Method

3.10.2.1 – Solutions and kits

- SSC/SSC+SDS: SSC is a abbreviation of Sodium chloride and Sodium Citrate solution, which is normally used to transfer nuclear acid from gel to membrane DNA is transferred more efficiently to nitrocellulose membranes as a sodium salt where 90% of the effective negative charge has been neutralized by sodium chloride/citrate. Also SSC and SDS determine the stringency of the washes; the lower the concentration of SSC the higher the stringency due to reduced salts concentration.

  20X SSC 1 liter: 800 ml H2O, 175.3 g NaCl, 88.2 g sodium citrate, pH 7.0 with NaOH, adjust to 1 lt.

- NaOH: 0.5M NaOH would separate double-stranded DNA into single-stranded DNA because only ssDNA can be transferred onto the membrane.
- HCl: 0.25M HCl was used to depurinate DNA. Fragments greater than 15 kb are hard to transfer onto the blotting membrane and depurination with HCl takes the purines out, cutting the DNA into smaller fragments and allowing a more efficient transfer.
- Blotting Paper Sheets (Munktell, 2.521.120140 G) and Whatman paper were used to set up the blot and facilitate the capillary transfer of DNA onto the nylon membrane (Zeta-Probe GT, Bio-Rad, 162-0196).
- Express Hyb (Clontech, 636831) as prehybridization solution was required before hybridization to block non-specific binding. It contains concentrated salt and SDS that excludes water molecules from the probe and target, allowing better hybridization. Also, the more water molecules that are excluded, the tighter the interaction between the probe and target becomes.
- Radioactive [^{32}P]-dCTP was provided by Hartman Analysis (SRP405).
- Amersham Rediprime II (GE Healthcare, RPN1633) was used to label probes with [^{32}P]-dCTP. The primer-template complex is a substrate for the Klenow fragment of DNA polymerase I. By replacing a non-radioactive nucleotide with the radiolabelled equivalent in the reaction mixture, newly synthesized DNA is made radioactive.
- Columns (NICK Columns with Sephadex G-50 DNA grade, GE Healthcare, 17-0855-02) to purify probes were used after labeling.

3.10.2.2 – Protocol

DNA was digested overnight at 37ºC as described in the previous section; DNA was precipitated as described in the *DNA extraction* paragraph, loaded into a 0.6% Agarose gel and ran until the bands of interest were clearly separated and under UV lights, using a tip, the gel ladder was marked in the points of interest. Before blotting onto the membrane, the DNA in the gel had to be chemically denaturated, to do this the gel was washed twice with 0.25 M of HCl for 10 minutes, once with H_2O for 5 minutes and once with 0.5 M NaOH for 40 minutes. The membrane was washed for 2 minutes in water and equilibrated for 5 minutes in 0.5 M NaOH before blotting.

The capillary transfer was setup as following and left overnight on the bench:

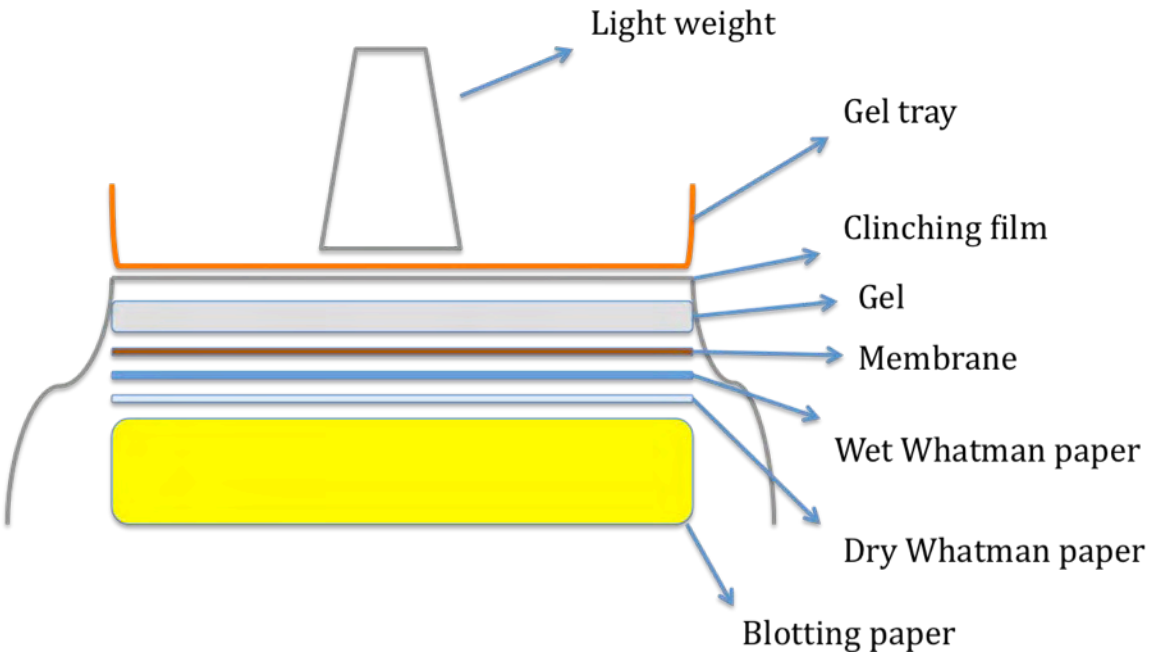

Fig 3.3 – *Schematic representation of the capillary transfer of DNA into membrane.*

The following day slots and ladder were marked on the membrane with a pencil cause graphite absorbs radioactivity and permits to easily identify samples and length of the fragments.

Membrane was then washed with 2X SSC for 10 min at room temperature, placed into clean bottles and incubated at 65ºC for 30 min rotating with pre-hybridization solution.

In the meanwhile probes were labeled as follow:

1 µl of probe (~30-50 ng) was diluted with 44 µl of TE buffer, denaturated at 95ºC for 3 minutes and incubated in ice for further 2 minutes. The 45 µl were transferred to the Rediprime II solution without mixing; 5 µl of ^{32}P-dCTP were added and gently mixed to turn the solution into violet. Samples were incubated at 37ºC for 10 min; meanwhile columns were rinsed with TE buffer and equilibrated with 3 ml of TE buffer till all the liquid flushed out. The radioactive samples were added to the columns, 400 µl of TE were carefully pipetted on top of it and the first flow trough was collected and discarded; other 400 µl of TE buffer were added to elute the probe, this was collected into new tubes, denaturated at 95ºC for 3 minutes and incubated on ice for 2 minutes.

The labeled probes were carefully pipetted into the bottles containing the membranes and incubated overnight at 65ºC slowly rotating.

The next day 2X SSC/1%SDS and 0.1X SSC/0.1% SDS solutions were warmed up at 65 ºC; the bottles were emptied and rinsed twice with 2X SSC, the first time the

liquid was carefully discarded and the second time was poured with the membrane into a pizza-box, this was then left shaking at room temperature for 10 minutes. Membranes were then washed with 2X SSC 1% SDS for 15-20 minutes at 65ºC, radioactivity was then checked and, if still hot, a further 15-20 minutes wash was required with 2X SSC 1% SDS (not stringent) or 0.1X SSC 0.1% SDS (stringent). The final wash was made in 2X SSC at room temperature for 5 minutes.

Membranes were then wrapped up in clinching film and exposed in a cassette overnight.

The phosphor screen was placed on the scanner and image analyzed with GIMP (freely available at www.gimp.org) .

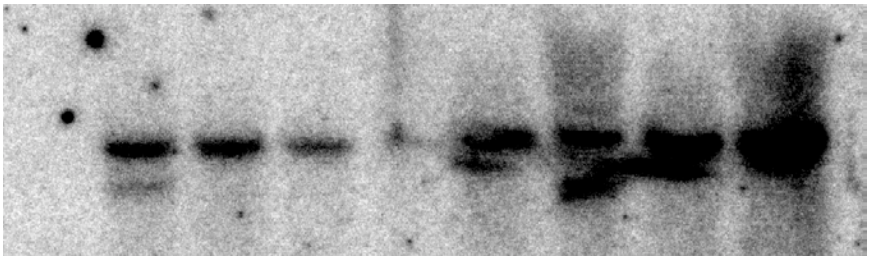

Fig 3.4 – *Example of a southern blotting image.*

3.11 – shRNAs synthesis and cloning

To clone the desired hairpins in order to perform an efficient knockdown the kit LOCK-iT PolII miR RNAi Expression Vector Kit (Invitrogen, 451102) was ordered; all buffers, vector and reagents were included in the kit.

3.11.1 – Oligonucleotides

Oligonucleotides targeting the desired regions of Ncor1 and Ncor2 were designed and ordered from the Invitrogen website (www.invitrogen.com). A schematic representation of the murine Ncor1 and Ncor2/Smrt with the targeted exons is available in the Supplementary Figures.

Sequences are the following:

Oligo Name	Target	Sequence
ex11_top	*NCoR1*	TGCTGAATGGTGGCTGAAAGACCAGCGTTTTGGCCACTGACTGACGCTGGTCTCAGCCACCATT
ex11_bottom	*NCoR1*	CCTGAATGGTGGCTGAGACCAGCGTCAGTCAGTGGCCAAAACGCTGGTCTTTCAGCCACCATTC
ex27_top	*NCoR1*	TGCTGATAACATGGCCCTTGGATGCAGTTTTGGCCACTGACTGACTGCATCCAGGCCATGTTAT
ex27_bottom	*NCoR1*	CCTGATAACATGGCCTGGATGCAGTCAGTCAGTGGCCAAAACTGCATCCAAGGGCCATGTTATC
ex37_top	*NCoR1*	TGCTGTAACCTGGCAGCTTCATGCTTGTTTTGGCCACTGACTGACAAGCATGACTGCCAGGTTA
ex37_bottom	*NCoR1*	CCTGTAACCTGGCAGTCATGCTTGTCAGTCAGTGGCCAAAACAAGCATGAAGCTGCCAGGTTAC
ex8_top	*NCoR2*	TGCTGTACAAGATCAGCTTCTTCCGCGTTTTGGCCACTGACTGACGCGGAAGACTGATCTTGTA
ex8_bottom	*NCoR2*	CCTGTACAAGATCAGTCTTCCGCGTCAGTCAGTGGCCAAAACGCGGAAGAAGCTGATCTTGTAC
ex32_top	*NCoR2*	TGCTGTGTAGATGTCAGCTTCCGGTCGTTTTGGCCACTGACTGACGACCGGAATGACATCTACA
ex32_bottom	*NCoR2*	CCTGTGTAGATGTCATTCCGGTCGTCAGTCAGTGGCCAAAACGACCGGAAGCTGACATCTACAC
ex42_top	*NCoR2*	TGCTGTATTCTGGCTCGTTCCGGTTGGTTTTGGCCACTGACTGACCAACCGGAGAGCCAGAATA
ex42_bottom	*NCoR2*	CCTGTATTCTGGCTCTCCGGTTGGTCAGTCAGTGGCCAAAACCAACCGGAACGAGCCAGAATAC

Table 3.8 – *Sequences of the hairpins used to target Ncor1 and Ncor2/Smrt. Indicated the exon number, the strand and the gene targeted.*

3.11.2 – Annealing oligos

Before being ligated into the vector all the pairs of oligos (top – bottom) had to be annealed. This was made following the manufacturer instructions, briefly:

Reagent	*µl (x1)*
Top strand oligo	5
Bottom strand oligo	5
10X Annealing buffer	2
DNase/RNase free H_2O	8

Samples were heated at 95ºC for 4 min and left cool down on the bench for 5-10 minutes, briefly centrifuged, diluted at the concentration of 10 nM from the initial 50 µM and stored for further experiments.

3.11.3 – Ligation reaction

Double strand oligos were ligated into pcDNA 6.2-GW/EmGFP-miR vector included in the kit as follow:

Reagent	*µl (x1)*
5X reaction buffer	4
Vector	2
ds oligos	4
T4 DNA ligase	1
DNase/RNase free H_2O	9

Samples were mixed pipetting up and down, incubated at room temperature for 5 minutes and placed on ice.

3.11.4 – Transformation of competent cells

One Shot TOP10 Competent E.Coli were provided with the kit and transformed as previously described.

3.11.5 – Selection of positive clones

Clones that grew on the selection plate were selected, inoculated in 2 ml of LB for minipreps, DNA extracted and the presence of the insert was assessed by restriction enzyme digestion. Positive clones were sent to sequencing to confirm that the correct ligation happened and then inoculated in midipreps to obtain high purity plasmid DNA for further experiments.

4 – RESULTS

4.1 – LIGAND RESPONSIVENESS IN PROSTATE MALIGNANCIES

Activation of NRs via lipophilic molecules has diverse transcriptional and phenotypical effects in prostate epithelial cells including activation of target genes that result is inhibition of proliferation. Different prostate cancer cell lines have different sensitivities to these molecules and this includes a significant loss of responsiveness.

The following studies aim to describe these events with the aim of understanding how to restore the physiological activity of NR *in vitro* and *in vivo*. Specifically, the studies are focused on the epigenetic corruption of NR signalling in prostate cancer addressing to what extent it can be restored using either histone deacetylase inhibitors (SAHA) or a more targeted and specific approach knocking by down NCOR1 via shRNA.

4.1.1 – Cell proliferation in RWPE1 vs PC-3

Cell lines are described in Materials and Methods.

The activity of NR agonists in PC-3 prostate cancer cells was compared to a parallel data set in non-malignant epithelial cells RWPE-1 (RWPE-1 cells data from James Thorne, University of Birmingham, Birmingham, UK) using a high throughput proliferation assay based on cellular ATP. A cohort of ligands was chosen in order to screen the antiproliferative effect: bezafibrate (peroxisome proliferator activated receptors – PPARα and PPARγ), $1,25(OH)_2D_3$ (vitamin D receptor – VDR), eicosapentaenoic acid (EPA, PPARα), eicosatetraynoic acid (ETYA, PPARγ),

chenodeoxycholic acid (CDA, farnesoid X receptor – FXR), litocholic acid (LCA, VDR and farnesoid X receptor – FXR), docosahexaenoic acid (DHA, FXR, PPARα and PPARγ) and all-trans retinoic acid (ATRA, retinoic acid receptor – RARs); cells were plated in 96 well plates and treated for 96 hours with the designed agonist with a re-dose after 48 hours, after that cell proliferation was quantified. All agonists but DHA efficiently inhibited RWPE-1 cells **(Fig 4.1)** while PC-3 cells demonstrated a consistent loss of sensitivity towards the ligands.

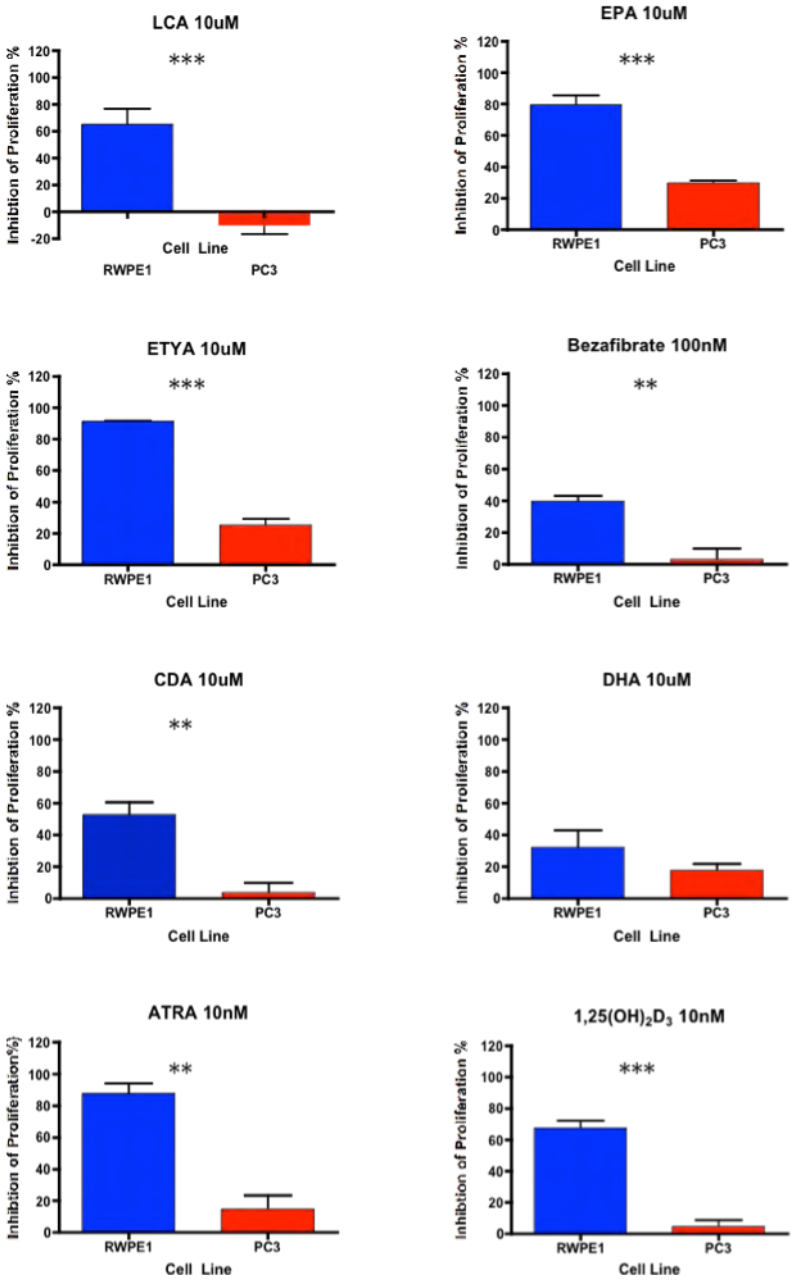

Fig 4.1 – *Antiproliferative effect of nuclear receptor ligands in non malignant prostate epithelial cells RWPE-1 (blue) and malignant PC-3 (red); 2x10^3 cells were plated in a 96 well/plate and treated for 96 hours with the indicated ligand, with a re-dose after 48 hours. Bar charts indicate inhibition of proliferation upon treatment with: 1 μM bezafibrate, 100 nM 1,25(OH)$_2$D$_3$, 10 μM EPA, 10 μM ETYA, 10 μM LCA, 10 μM DHA and 10 μM ATRA. Data shown are the mean of at least biological triplicates +/- S.E.M.. Student t-test was performed to establish that the difference in proliferation between PC-3 and RWPE-1 cells was significant; **=p<0.01, ***=p<0.001.*

These results demonstrated that PC-3 cells display suppressed anti-proliferative ability for PPARα, PPARγ, VDR, RAR and FXR. Identifying the mechanisms that contribute to the agonist-resistance in PC-3 cells has applications in translational research where androgen-independent prostate cancer still remains the most common cause of mortality for this cancer.

4.1.2 – Gene regulation

PC-3 cells remain phenotypically unaltered after treatment with nuclear receptor ligands. In the attempt to define the basis for this, the transcriptional responses in PC-3 cells were analysed. Previous studies in the group established in prostate cancer cells that elevated levels of NCOR2/SMRT act as one such mechanism to suppress VDR responsiveness [62, 194]; other workers have re-enforced these concepts [195, 196] Similarly, epigenetic mechanisms appear to disrupt the PPAR actions [197, 198]. Therefore the extent to which a similar mechanism was disrupting other NRs was investigated.

4.1.3 – Corepressor and nuclear receptor expression in prostate cells

In physiological conditions there is a balance between transactivation, mediated by activated transcriptional complexes that include co-activator proteins, and repression, mediated by non-activated transcription factors associated with co-repressor complexes. For example, an equilibrium is due to the ratio between the amount of nuclear receptor and regulatory complexes. Hypothetically, if levels of

nuclear receptors are unchanged while the regulatory complexes vary then there will be a loss of balance with higher activation or higher repression of target genes.

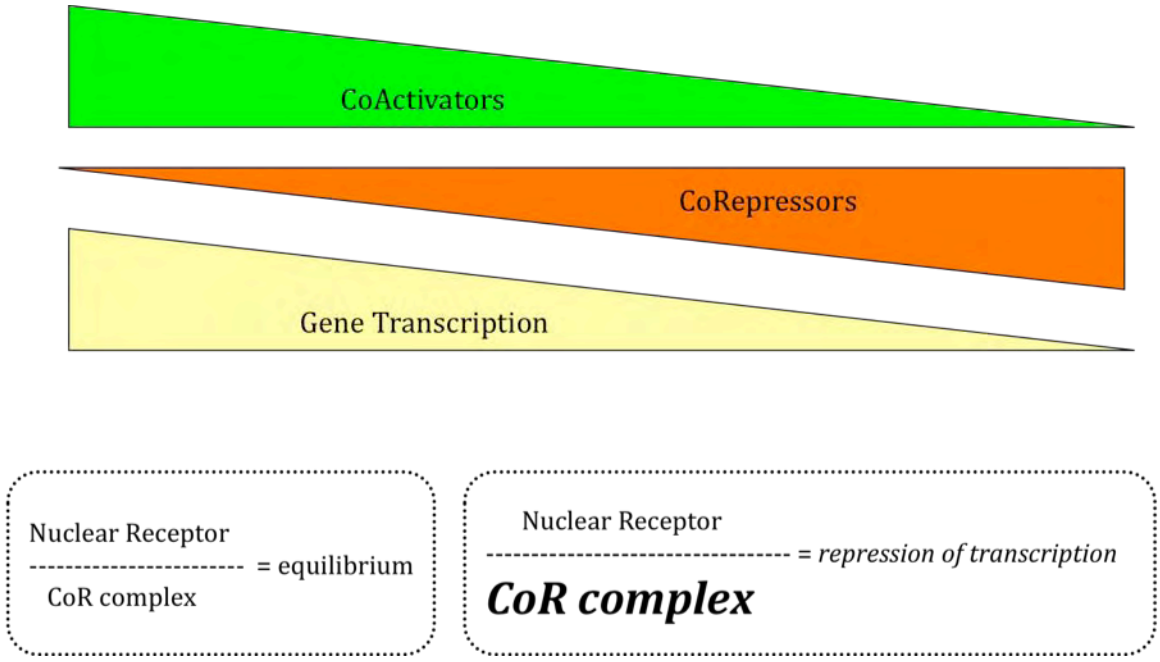

Fig 4.2 – *Representation of the physiological equilibrium between complexes that activate or repress transcription and nuclear receptors. Gene transcription (yellow triangle) is regulated by the amount of CoActivator complex (green triangle) and CoRepressors (orange triangle); when the concentration of corepressors rise and the amount of NR remain constants, or diminishes, then the balance of the equation is shifted towards repression and transcription is inhibited.*

The loss of responsiveness in prostate suggests that this balance is shifted towards transrepression. To investigate the basis for the loss of responsiveness, qRT-PCR was used to measure the mRNA levels of a cohort of co-repressor genes involved in transcriptional silencing; COPS2, CoREST, LCoR, NCOR1, NCOR2/SMRT, RIP140 and SLIRP (*described in the introduction)* . Total RNA from mid-exponentially proliferating RWPE-1, DU145 and PC-3 cells was extracted and reverse-transcribed prior qRT-PCR analysis.

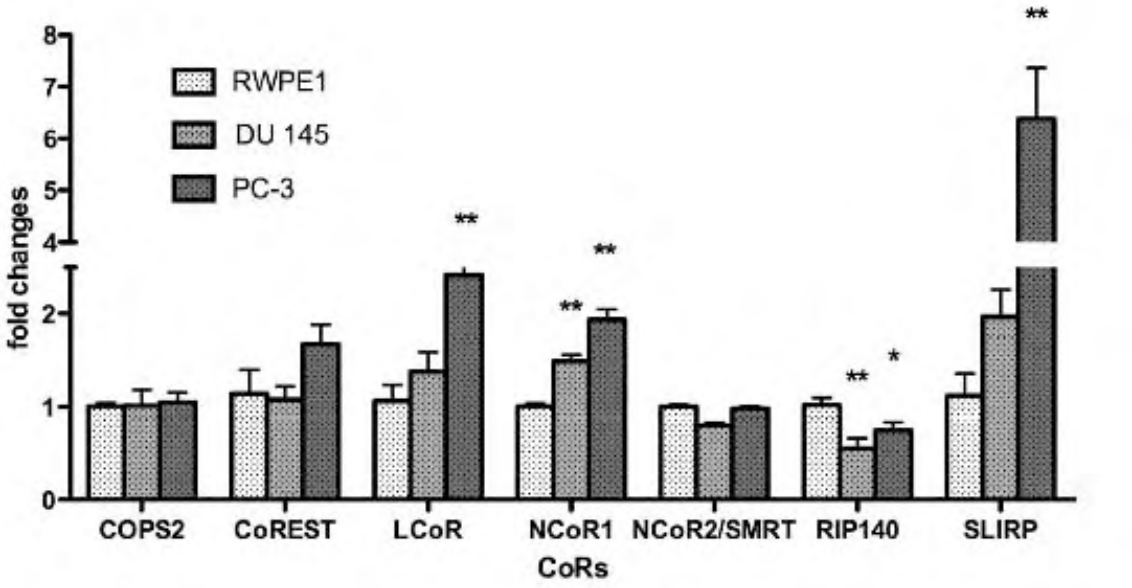

Fig 4.3 *– Basal mRNA levels of a selected cohort of corepressors in three different epithelial cell lines RWPE-1 (white), DU145 (light grey) and PC-3 (dark grey). The results are the average of at least biological triplicate experiments. Whole RNA was extracted, quantified and reverse transcribed prior qRT-PCR analysis. Student t-test was performed comparing DU145 and PC-3 to RWPE-1 cells (* = p<0.05, ** = p<0.01). The y axes indicates the fold changes relative to RWPE-1 cells.*

As shown in **Fig 4.3** basal mRNA levels of *NCOR1*, *LCoR* and *SLIRP* were significantly upregulated in PC-3 cells ($p<0.05$) and *RIP140* was significantly reduced ($p<0.05$); a similar patter was present in DU145 cells.

Protein levels for the major co-repressors, NCOR1, NCOR2/SMRT (Orla Maguire, Roswell Park Cancer Institute, Buffalo NY, USA) and SLIRP, were measured in mid-exponentially growing RWPE-1, LNCaP, DU145 and PC-3 cells. Both NCOR1 and NCOR2/SMRT complex with HDAC enzymes maintaining de-acetylated histone tails in order to repress transcription; HDAC3 is the best know HDAC that interacts allosterically with NCOR1 and NCOR2/SMRT present in co-repressor protein

complexes and Western immunoblot analysis demonstrated that this component too is elevated in PC-3 cells.

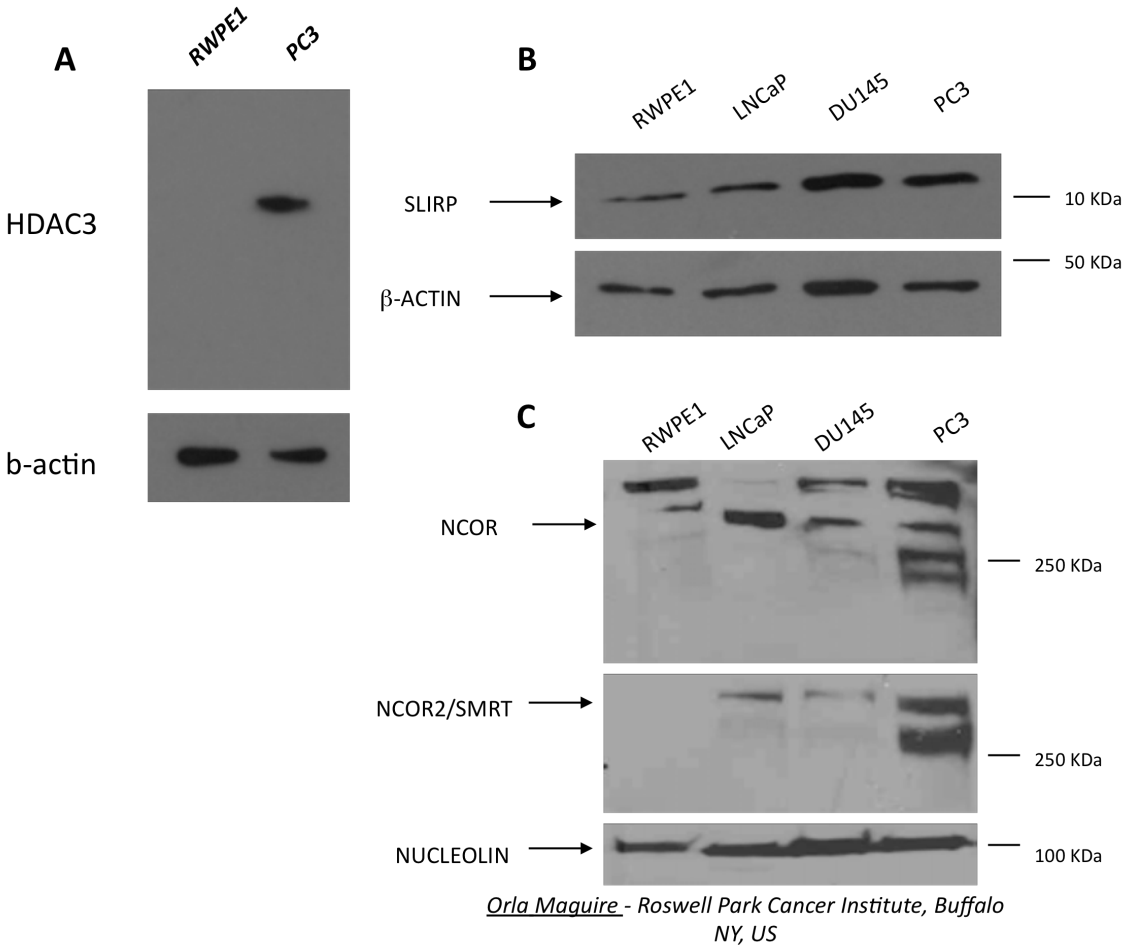

Fig 4.4 – *Western immunoblot for NCOR1 and NCOR2/SMRT in RWPE-1, LNCaP, DU145 and PC-3 cells (TOP) and HDAC3 in malignant PC-3 and non-malignant RWPE-1 cells. 60 μg of whole protein lysate was used were loaded into an SDS-page and analysed with the antibodies listed in Materials and Methods. Chemoluminescent detection of the proteins occurred through HRP-conjugated secondary antibody and ECL. The analysis was repeated in at least two biological replicates. Nucleolin was used a loading control for NCOR1 and NCOR2/SMRT and β-actin for SLIRP and HDAC3 western blotting because both proteins accurately reflect the total protein content independently from the cell background.*

Compared to RWPE-1 cells, NCOR1 levels are higher in all three cancer cell lines (PC-3, DU145 and LNCaP) while SLIRP levels also increase with malignancy. HDAC3 levels are undetectable in RWPE-1 cells and clearly higher in PC-3 cells.

These results suggested that co-repressors mRNA and protein expression is elevated in prostate cancer cell lines Levels of PPARα, PPARα and VDR were analysed in mid-exponentially growing RWPE-1, LNCaP, DU145 and PC-3 cells. PPARγ and VDR were expressed at comparable levels in all four cell lines whereas PPARα was absent in LNCaP cells.

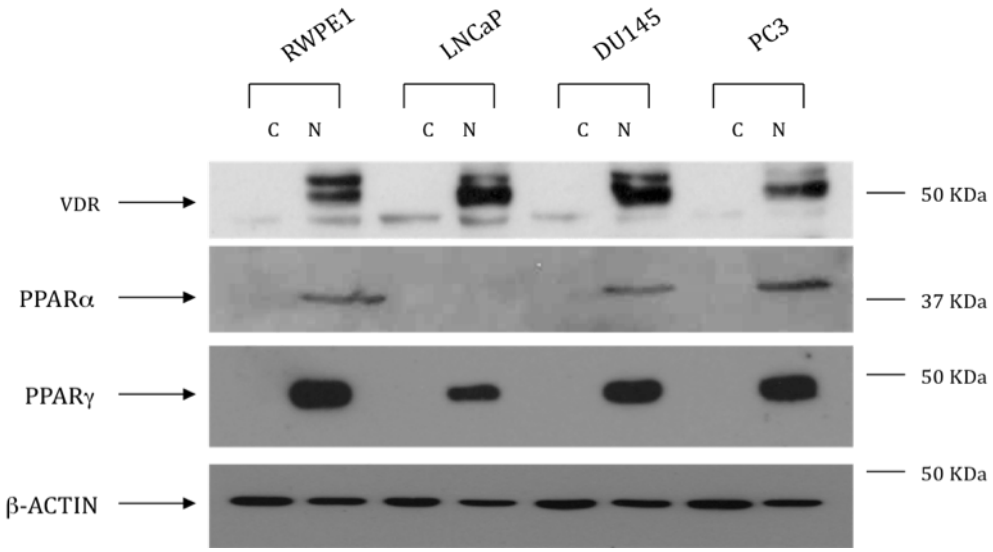

Fig 4.5 – *Basal nuclear receptor levels RWPE-1, LNCaP, DU145 and PC-3. 20 μg of cytoplasmic (C) and nuclear (N) lysates were obtained from mid-exponential growing cells, quantified and loaded in SDS-page gel for Western immunoblotting; nitrocellulose membranes were probed with anti-VDR, anti-PPARα or PPARγ antibodies. Chemoluminescent detection of the proteins occurred through HRP-conjugated secondary antibody and ECL. The analysis was repeated in at least two biological replicates. Equal loading was ensured by the detection of beta-actin; although this protein is mainly located in the cytoplasm, several papers [199-201] reported the presence of this protein in the nucleus.*

Key NR analysed were essentially evenly expressed across RWPE-1, DU145 and PC-3 cells, while LNCaP cells showed a lower expression of both PPARα and PPARγ.

These results supported the initial hypothesis that a key component in the loss of sensitivity towards NR agonists in prostate cancer cell lines is represented by the altered expression of co-repressor complexes together with an unchanged expression of the receptors resulting in an altered ratio. This can lead to a chromatin environment that inhibits transcription factors from binding to their responsive elements, thus, blocking transcription. This may allow for selective repression of the gene targets.

4.1.3 – Analysis of the nuclear receptor network using microfluidic Q-RT-PCR$_M$

To investigate relationships between the global loss of ligand responsiveness in PC-3 cells and the expression of the NR network microfluidic Q-RT-PCR, (qRT-PCR$_M$) was undertaken (gene list as in [202]). Initially the basal expression of the NR network was examined. 96 genes were examined that are involved in metabolism of NR ligands, transcriptional regulation by NR, cell cycle control, apoptosis and membrane transport of ligands.

The basal expression of all the genes across the three phases of the cell cycle was analysed to unveil the phase-specific differences between RWPE-1 and PC-3 cells. These expression patterns support the concept that loss of receptor responsiveness does not correlate fully with reduced receptor expression. To allow for cell population heterogeneity, differential proliferation rates and to reveal the impact of the cell cycle the NR network expression patterns was profiled by Q-RT-PCR$_M$ in

different cell cycle phases. 14 of 20 NRs expressed in normal prostate [203] had differential expression through the cell cycle in PC-3 cells compared to RWPE-1 cells, 9 were up-regulated, notably in G_1 and G_2/M (e.g. *PPARG*, *VDR*), 5 down-regulated in all phases (e.g. *THRB*) and the remaining receptors were undetected in either cell system (e.g. *RARB*). Also significantly up-regulated in G_1 and G_2/M cells were NR co-regulators (e.g. *NCOR2/SMRT, NCOA2, PPARGC1A*), histone modifying enzymes (e.g. *HDAC4, SIRT2*, and the demethylase *AOF2*/*LSD1*), the EMT regulator *SNAI1* and NF-kB activators (*IKBKB*, *IKBKG*). Expression of VDR and PPAR target genes displayed both elevation (e.g. *IGFBP1, G0S2, PTGS2* (encodes COX-2)) and repression (e.g. *CDH1, CDKN1A* (encodes $p21^{(waf1/cip1)}$) [204-209]) and other targets (e.g. *ALOX*-5 (encodes 5-LO)), were undetected in PC-3 cells and omitted. SAM analyses of these data identified gene expression patterns that were significantly altered between all phases of the cell cycle and further distinguished PC-3 from RWPE-1 cells, including *NCOR1* and *TRIP15/COPS2/Alien* uniquely down regulated in S phase and re-expressed in G_2/M (**Fig 4.6**). The findings suggest that ligand insensitivity correlates with a distorted NR network and this includes elevated co-repressor levels and a condensed chromatin conformation.

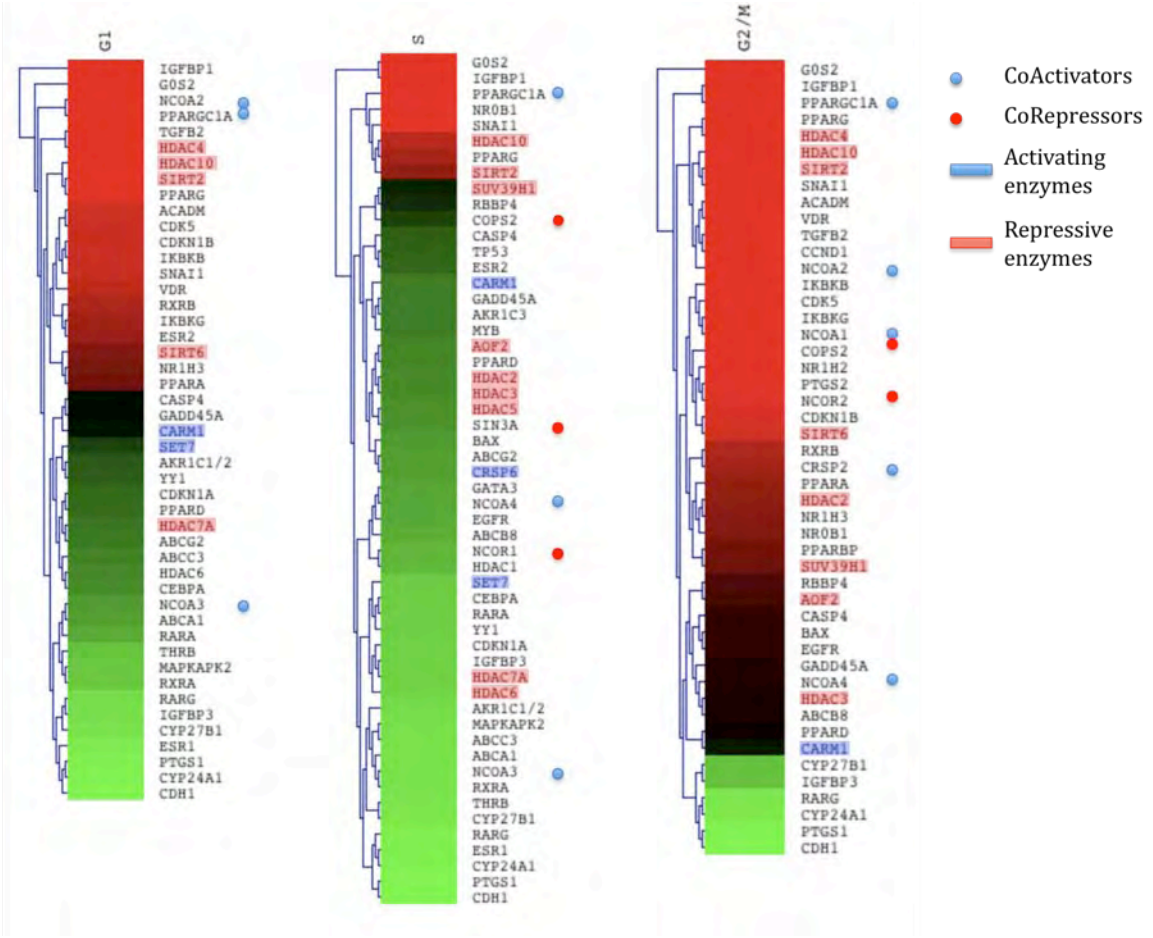

Fig 4.6 – *Heatmap representing the genes differentially expressed between RWPE-1 and PC-3 cells in each of the three phases of the cell cycle. One sample student t-test was made to establish the genes significantly differentially expressed between the two cell lines, p<0.01. Green boxes indicate downregulated genes and red boxes indicate upregulated genes. To better visually represent the data a hierarchical clustering was made using the Support Tree algorithm in TmeV, this function contstructs the tree resampling the gene values using iterations and the metric used was euclidean distance. Highlighted are corepressor and coactivator enzymes as well as histone modifiers linked with positive or repressive histone marks. Data are the mean of at least three biological replicate and technical quadruplicate from values obtained with Q-RT-PCR$_M$ analysis.*

These cell cycle phase-specific expression patterns suggest that the actions of the nuclear receptor network in PC-3 cells are skewed, rather than abrogated, with increased expression of receptors, and both positive and negative regulators of receptor activity, notably in G_1 and G_2/M. Reflecting this, target genes, for example

for VDR and PPARs, displayed both enhanced and diminished basal expression levels. Well-established target genes for VDR and PPARs [204-207] displayed significantly elevated levels in either all (*IGFBP1, G0S2)* or in G_1 and G_2/M (e.g. *ACADM*, *PPARα*, *PPARγ, GADD45A*) phases of the cell cycle in PC-3 cells. By contrast a cohort of targets were repressed in all phases (*IGFBP3* and *ABCA1)*, whereas others were omitted from the heatmap analyses, as they were undetected in either one or more cell cycle phases in PC-3 cells (*ALOX-5*, *CDKN1A*, *CDH1*, *CDKN2A*, *CYP24*, *PTGS1*, *CEBPA*).

Subsequently PC-3 cells were treated for 4 hours with $1,25(OH)_2D_3$ and again sorted in the different phases of the cell cycle to capture the transcriptional dynamicity during the G_1, S and G_2/M phases. As a positive control for VDR activation by $1,25(OH)_2D_3$, *CYP24* expression was analysed by single gene Q-RT-PCR using the RNA extracted from sorted PC-3 cells.

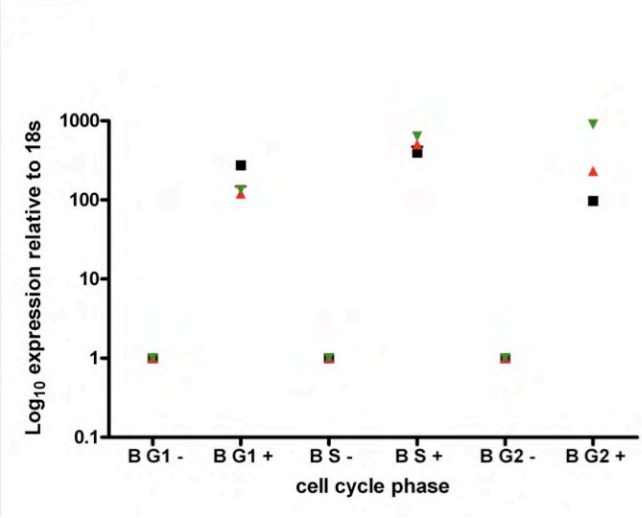

Fig 4.7 – *CYP24 mRNA accumulation in sorted PC-3 cells treated for four hours with 100 nM of 1,25(OH)$_2$D$_3$. RNA was extracted and reverse-transcribed prior qRT-PCR analysis. The results represent three biological replicates (black, green and red) and mRNA accumulation is shown as log$_{10}$ of the fold changes.*

By comparison to *CYP24*, treatment with 1,25(OH)$_2$D$_3$ did not influence strongly the transcriptome of PC-3 cells. RWPE-1 cells demonstrated a significant upregulation in G1 phase of many genes after treatment. ANOVA analysis revealed that in RWPE-1 cells approximately 60 genes were differentially expressed across the three phases (James Thorne, University of Birmingham, Birmingham, UK) while in PC-3 cells only two genes, apart from *CYP24* were highly induced across the phases. *CDKN1A* and *Cyclin E1* (necessary for G1/S transition), were significantly differentially expressed ($p<0.05$). From **Fig 4.7** is possible to see that a 4 hr treatment with 100 nM of 1,25(OH)$_2$D$_3$ did not upregulated genes in G1 as much as in RWPE-1 cells and induced a different expression pattern in PC-3 cells; only very

few genes were statistically significantly regulated probably due to the high variabillity across the replicates.

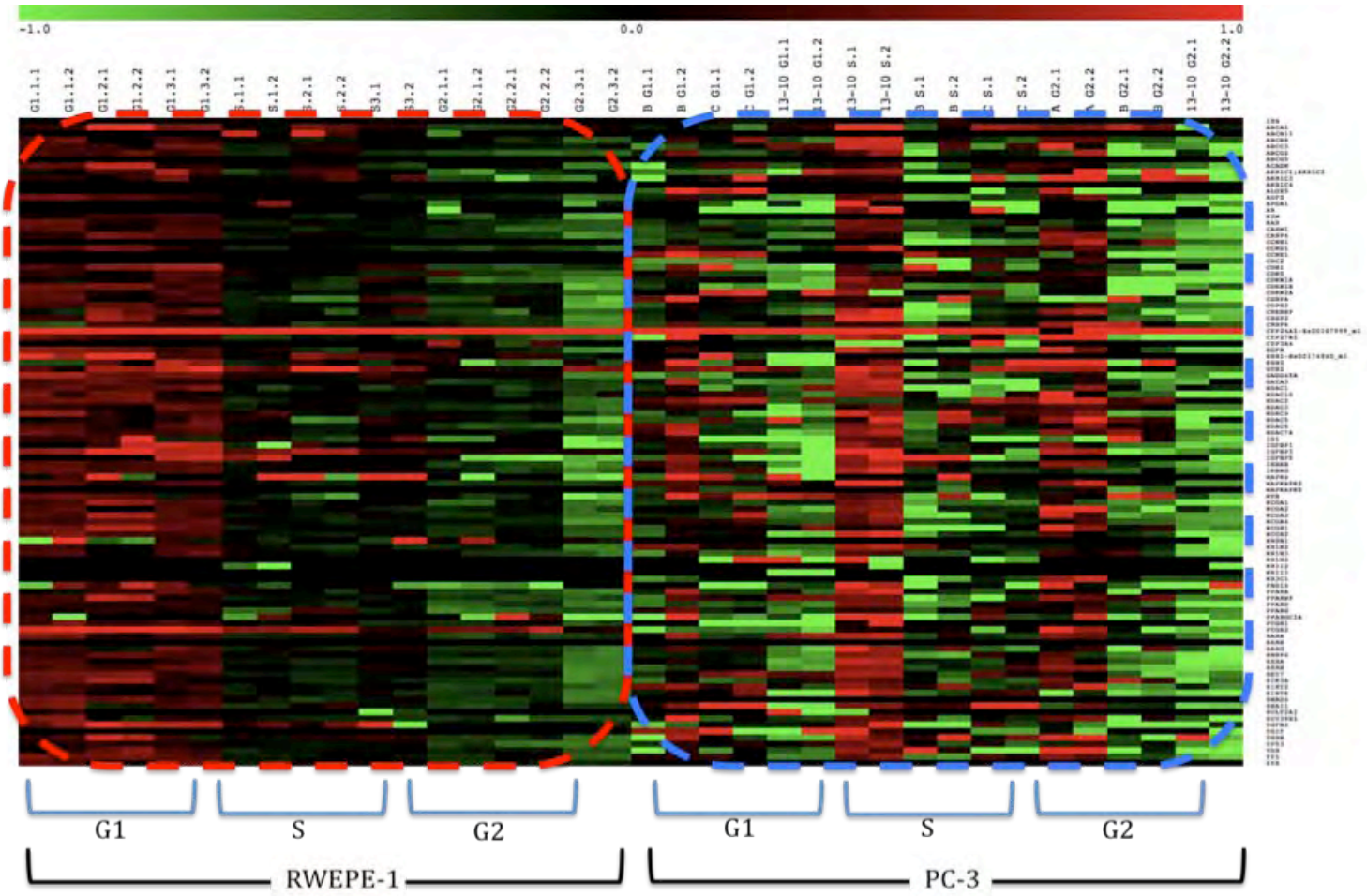

Fig 4.8 *– Heatmap representing mRNA accumulation of 96 genes in RWPE-1 and PC-3 cells treated for four hours with 100 nM of 1,25(OH)$_2$D$_3$. Red and green bars represent up- and down-regulated genes, respectively. The represented values are three biological replicate and two technical replicates measured via microfluidic Q-RT-PCR.. The right side of the heatmap contains the genes analysed and the top side indicates the sample names. Noticeable is the difference in the expression pattern between RWPE-1 and PC-3 cells being the first one constant across the phases (from G1 towards G2) and the second one scattered with different variability across the phases.*

These results suggest that, although PC-3 cells have a certain level of regulation mediated by ligand-induced VDR, they present several levels of corruption that

dynamically interact transforming a physiological NR system; understanding which hubs in this network are the most important would mean understanding which components rule and direct cancer cells through tumorigenic transformation. In turn these targets, or hubs, may be good candidate targets for therapy.

4.1.4 – The effect of the HDAC inhibitor, SAHA, effect on the nuclear receptor network in prostate epithelial cells

The use of histone deacetylases inhibitors reverts the acetylation status of histone lysine residues. This can promote NR transcription via de-stabilization of co-repressor complexes; this hypothesis was tested using SAHA (suberoylanilide hydroxamic acid or Vorinostat) alone or in combination with nuclear receptor ligands and analyzing transcriptional changes and levels of proliferation.

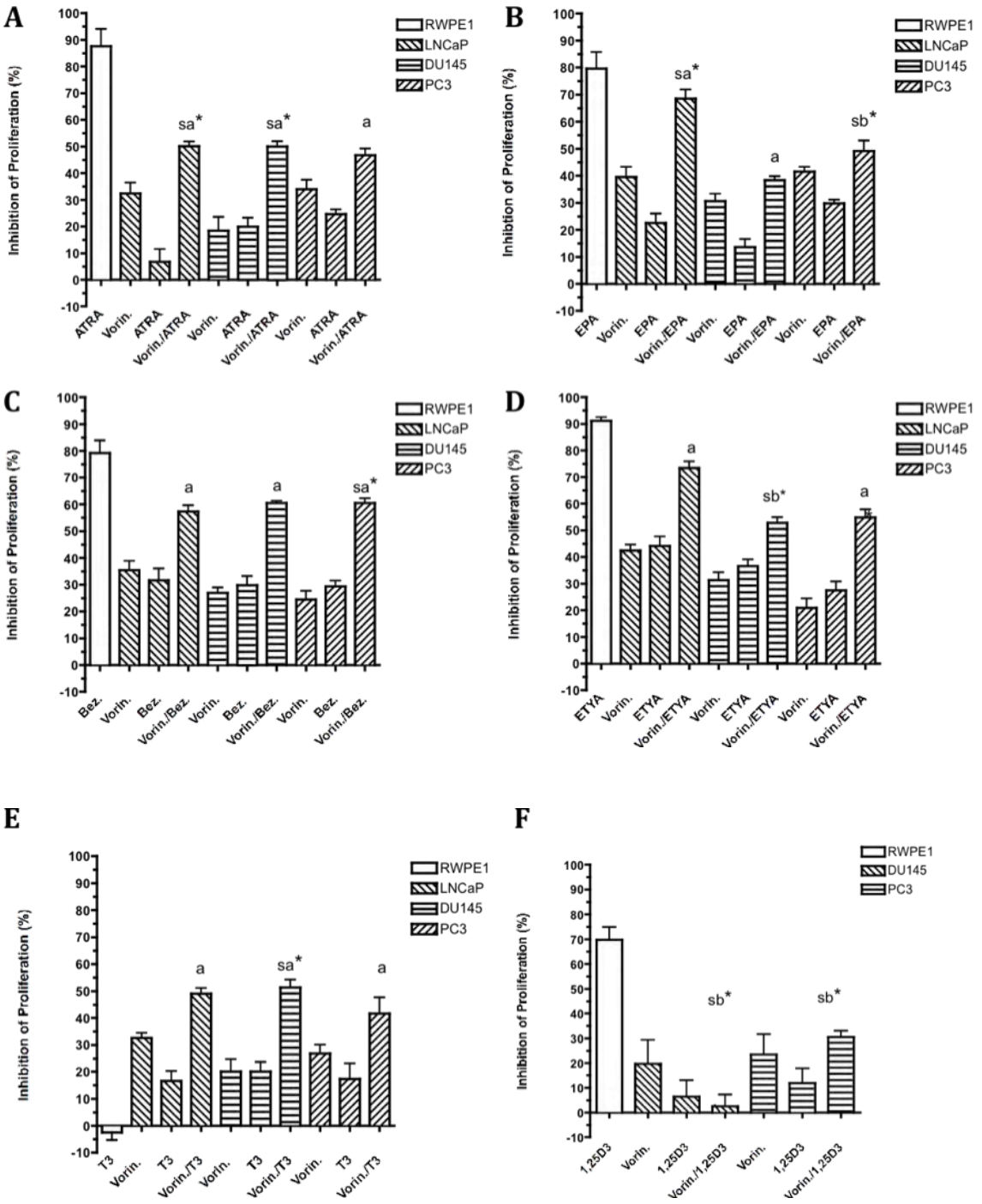

Fig 4.9 *– Additive effect of 0.5 μM of SAHA (Vorinostat) in combination with nuclear receptor ligands, this concentration was chosen for its low toxicity and minimal antiproliferative and was obtained from an initial optimization experiment that aimed to find the ED_{25} dose: (A) 10 nM ATRA (RAR), (B) 10 μM EPA (PPARα), (C) 10 μM ETYA (PPARγ), (D) 0.5 μM Bezafibrate (PPARα, -γ), (E) T3 (TR), (F) 100 nM $1,25(OH)_2D_3$, (VDR). Two thousand cells were plated in a 96 well/plate and treated with the ligand*

for 96 hours with a re-dose at 48 hours. Results were compared to the same ligand in RWPE-1 cells. Strong additive effects (sa) were those where the experimental value were significantly higher than the predicted value, additive (a) effects were those where the experimental value did not significantly differ from the predicted value, sub-additive (sb) effects were those where the experimental value was significantly less than the predicated value. Statistical significance was calculated using a one tailed Mann-Whitney test (p<0.05, ** p<0.01) [210]. Data represent the mean of biological triplicate undertaken in triplicate wells.*

The results suggest that SAHA has an antiproliferative effect irrespective of the cell background; in combination with PPARs and RAR, SAHA shows an additive, antiproliferative effect on prostate cancer epithelial cells whereas it does not enhance the antiproliferative effect of $1,25(OH)_2D_3$. This could be explained by a different cohort of HDACs recruited by the complex-bound VDR; as previously demonstrated, $1,25(OH)_2D_3$ shows additive effect with Trichostatin A (TSA) [62, 211]. However, this does not occur with SAHA suggesting that the combinatorial role of HDACs inhibitors and NR ligands is receptor-specific.

4.1.5 – Genome wide analysis of the combinatorial effect of SAHA and bezafibrate on PC-3 cells.

After assessing the phenotypical effect of SAHA in combination with NR ligands genome wide changes in gene expression mediated by the PPAR system were analysed, following 5 hours treatment with 0.5μM Bezafibrate (PPAR-α/γ ligand) and 0.5 μM SAHA, either separately or in combination. A 30k probe array prepared in collaboration with the Cancer Research UK, DNA Microarray Facility (Institute for Cancer Research, Sutton, UK), identified 62 genes modulated in an additive manner (28 and 34 elevated and repressed respectively). Gene ontology definition terms

identified functionally-related gene groups including transcriptional regulators, signal transduction components, lipid metabolism and protein stabilization. Comparing the expression patterns to those in prostate cancer libraries [203, 212] refined this list further. Screening through prostate cancer libraries (Cancer Genome Anatomy Project (CGAP) and the Oncomine) revealed that, within the 23 genes uniquely upregulated by SAHA and bezafibrate, 10 of them were normally downregulated in prostate cancer while 17 of the 35 uniquely downregulated genes were initially upregulated in prostate cancer.

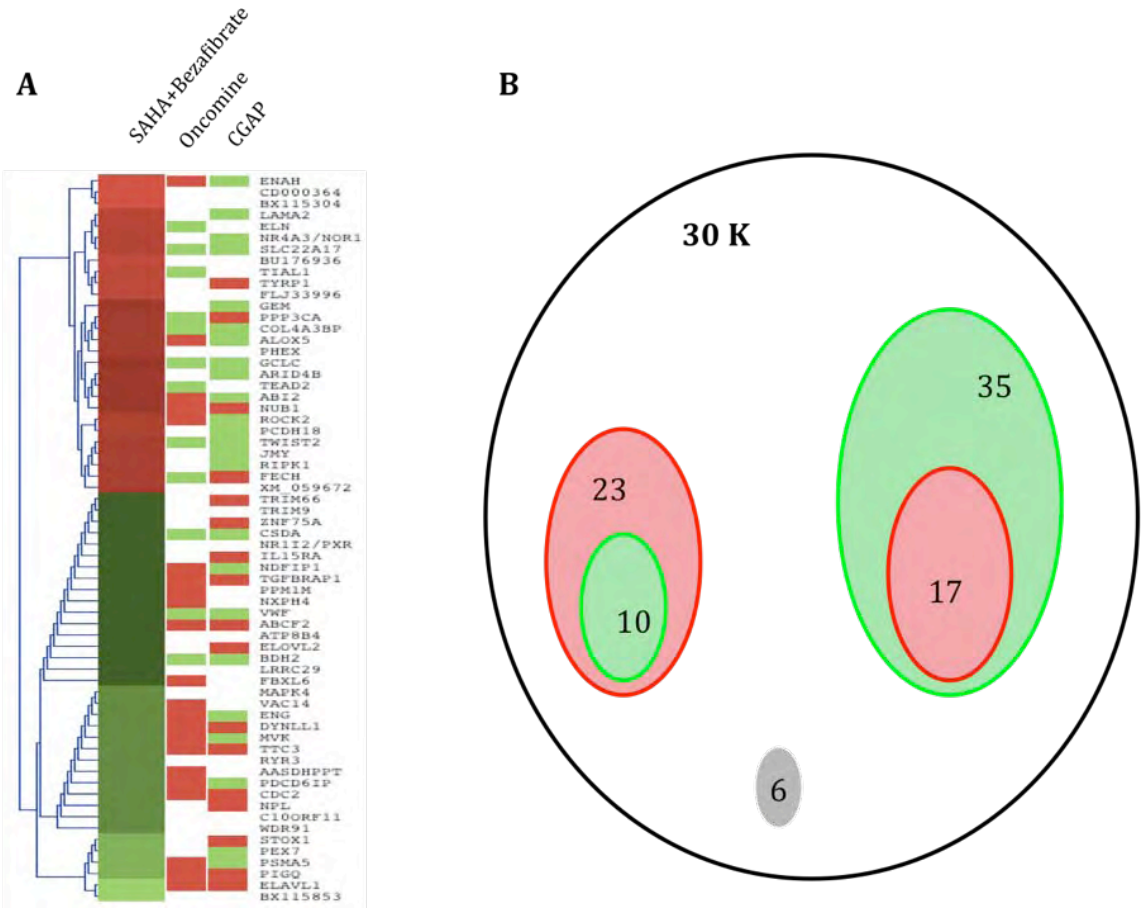

Fig 4.10 – *(A) Heatmap representing genes uniquely regulated by the double treatment with SAHA and bezafibrate, indicated is also the expression patter in cancer tissues retrieved by Oncomine and the Cancer Genome Anatomy Project. Green and red bars indicate down- and up-regulated genes, respectively. (B) Venn Diagram*

representing the previous data: 10 out of 23 upregulated gene were down-regulated in cancer and the expression of 17 out of 35 downregulated genes in cancer was restored by the combined treatment.

The initial list of more than 60 genes uniquely regulated was narrowed down by mining literature and online public databases such as SAGE Genie (http://cgap.nci.nih.gov/SAGE), Omim (http://www.ncbi.nlm.nih.gov/omim), Oncomine (http://www.oncomine.org) and Gene Cards (http://www.genecards.org/). This helped to focus mainly on genes involved in key cellular function like apoptosis, cell cycle, metabolism and NR signalling. A final list of genes for validation included 16 genes: 8 upregulated (JMY, ALOX5, ARID4B, TYRP1, TIAL1, TWIST2, TEAD2 and NR4A3) and 8 downregulated (IL15R, TGFBRAP1, ELAV1, CDC2, TRIM66, FBXL6, PDCD6IP and CSDA) – **Fig 4.11 A+B**.

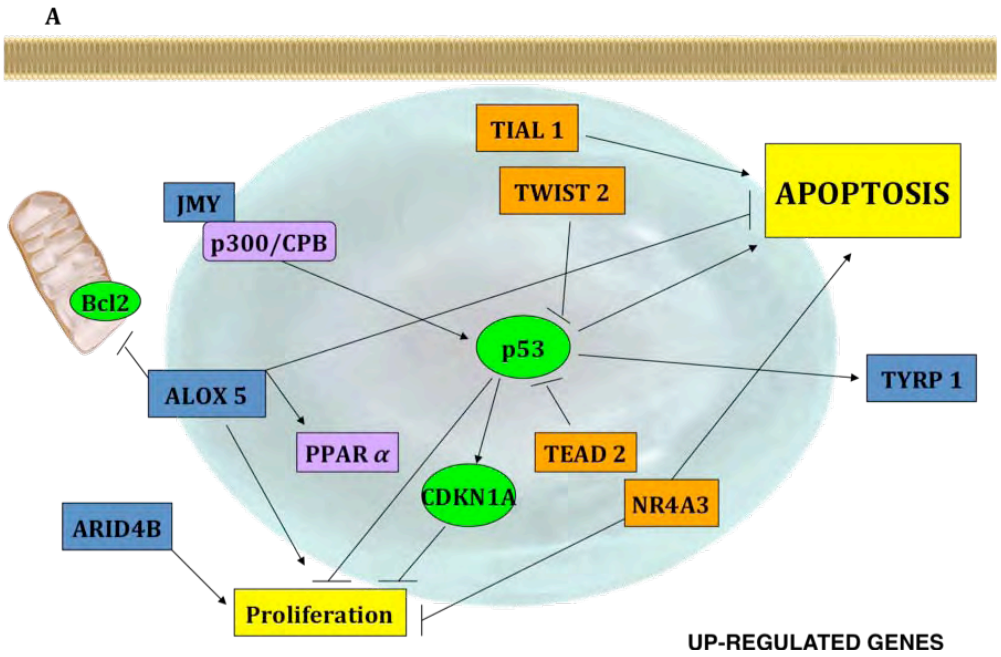

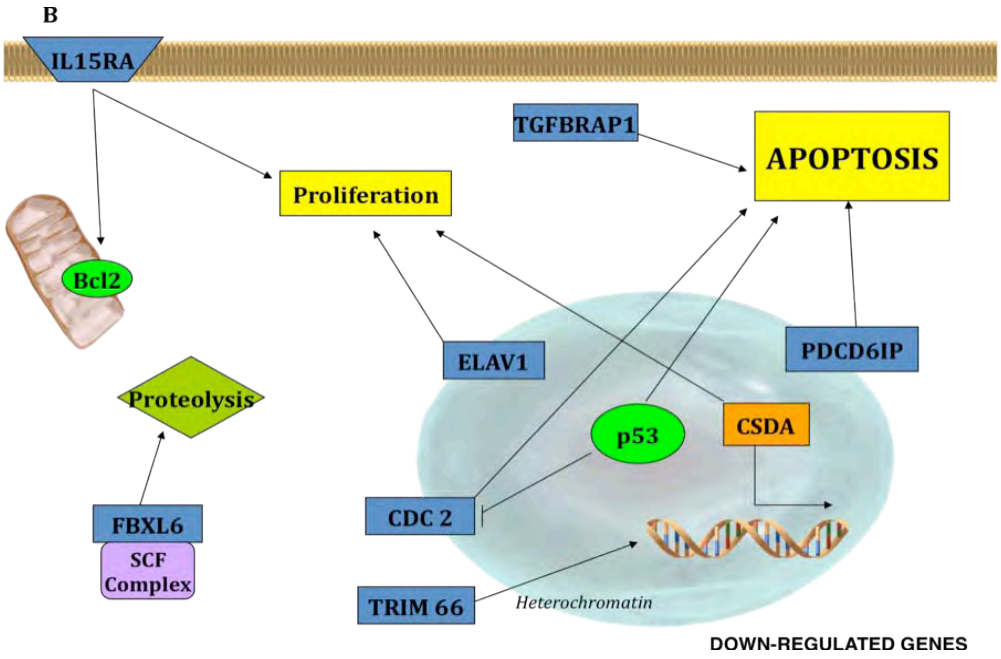

Fig 4.11 – *Schematic representation of genes found to be uniquely up-regulated (A) and down-regulated (B) by the double treatment with SAHA and bezafibrate. Blue and orange boxes indicate cytoplasmic and nuclear products, respectively. Yellow boxes indicate cellular functions; arrows indicate positive interaction between two genes and flat-ended lines indicate inhibitory interaction.*

4.1.6 – Microarray validation of candidate genes uniquely regulated by SAHA and bezafibrate

To confirm that the double treatment with SAHA and Bezafibrate uniquely regulate this cohort of 16 genes we performed time course experiments up to 24 hours with 0.5 μM of either SAHA or Bezafibrate or the two together in mid-exponentially growing PC-3 cells. Whole RNA was extracted and reverse transcribed before analyzing the candidate genes via Q-RT-PCR. The following screening criteria was undertaken to find those genes that were uniquely upregulated at either 6 or 12 hours with the double treatment of SAHA and Bezafibrate.

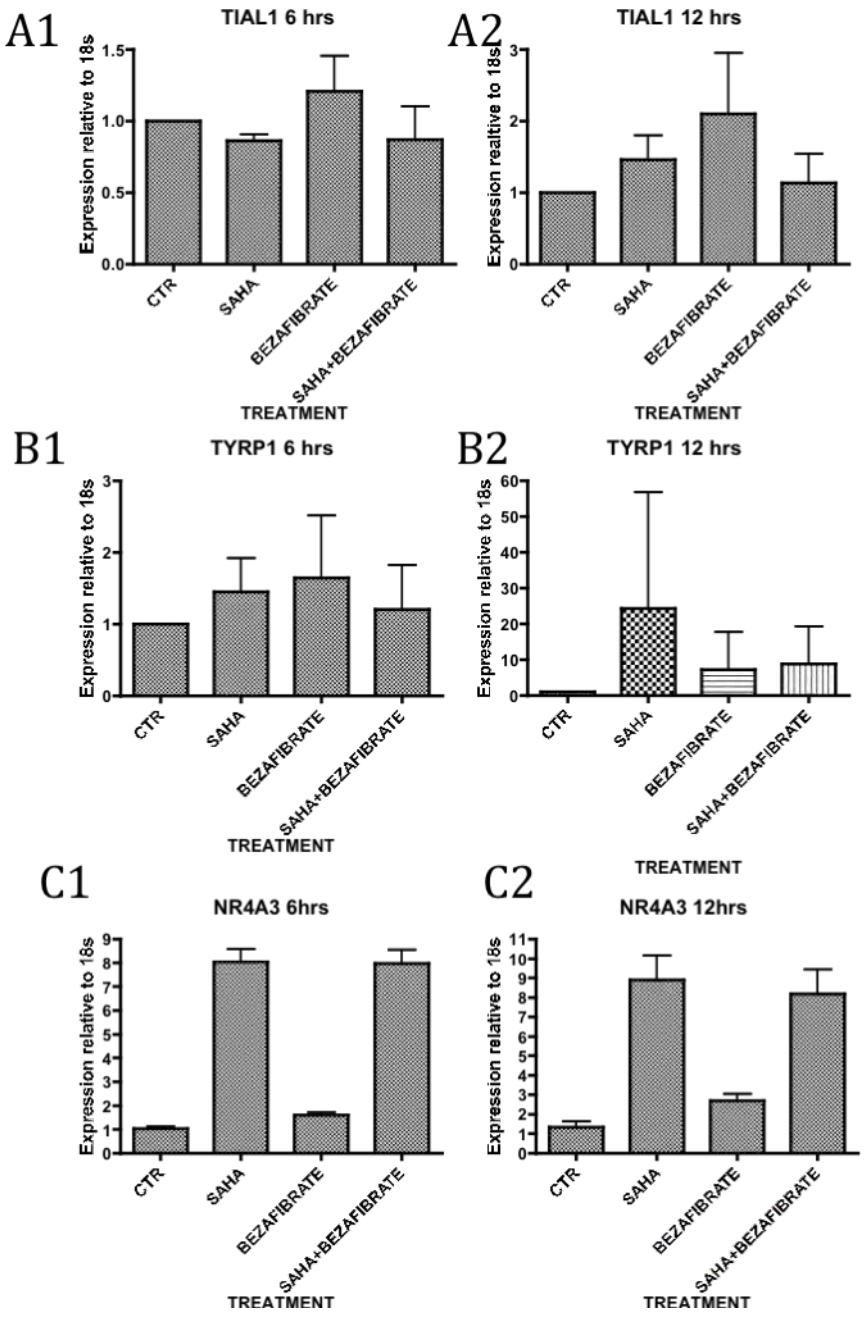
A1
TIAL1 6 hrs
Expression relative to 18s
1.5
1.0
0.5
0.0
CTR
SAHA
BEZAFIBRATE
SAHA+BEZAFIBRATE
TREATMENT
A2
TIAL1 12 hrs
Expression realtive to 18s
3
2
1
0
CTR
SAHA
BEZAFIBRATE
SAHA+BEZAFIBRATE
TREATMENT
B1
TYRP1 6 hrs
Expression relative to 18s
3
2
1
0
CTR
SAHA
BEZAFIBRATE
SAHA+BEZAFIBRATE
TREATMENT
B2
TYRP1 12 hrs
Expression relative to 18s
60
50
40
30
20
10
0
CTR
SAHA
BEZAFIBRATE
SAHA+BEZAFIBRATE
TREATMENT
C1
NR4A3 6hrs
Expression relative to 18s
9
8
7
6
5
4
3
2
1
0
CTR
SAHA
BEZAFIBRATE
SAHA+BEZAFIBRATE
TREATMENT
C2
NR4A3 12hrs
Expression relative to 18s
11
10
9
8
7
6
5
4
3
2
1
0
CTR
SAHA
BEZAFIBRATE
SAHA+BEZAFIBRATE
TREATMENT

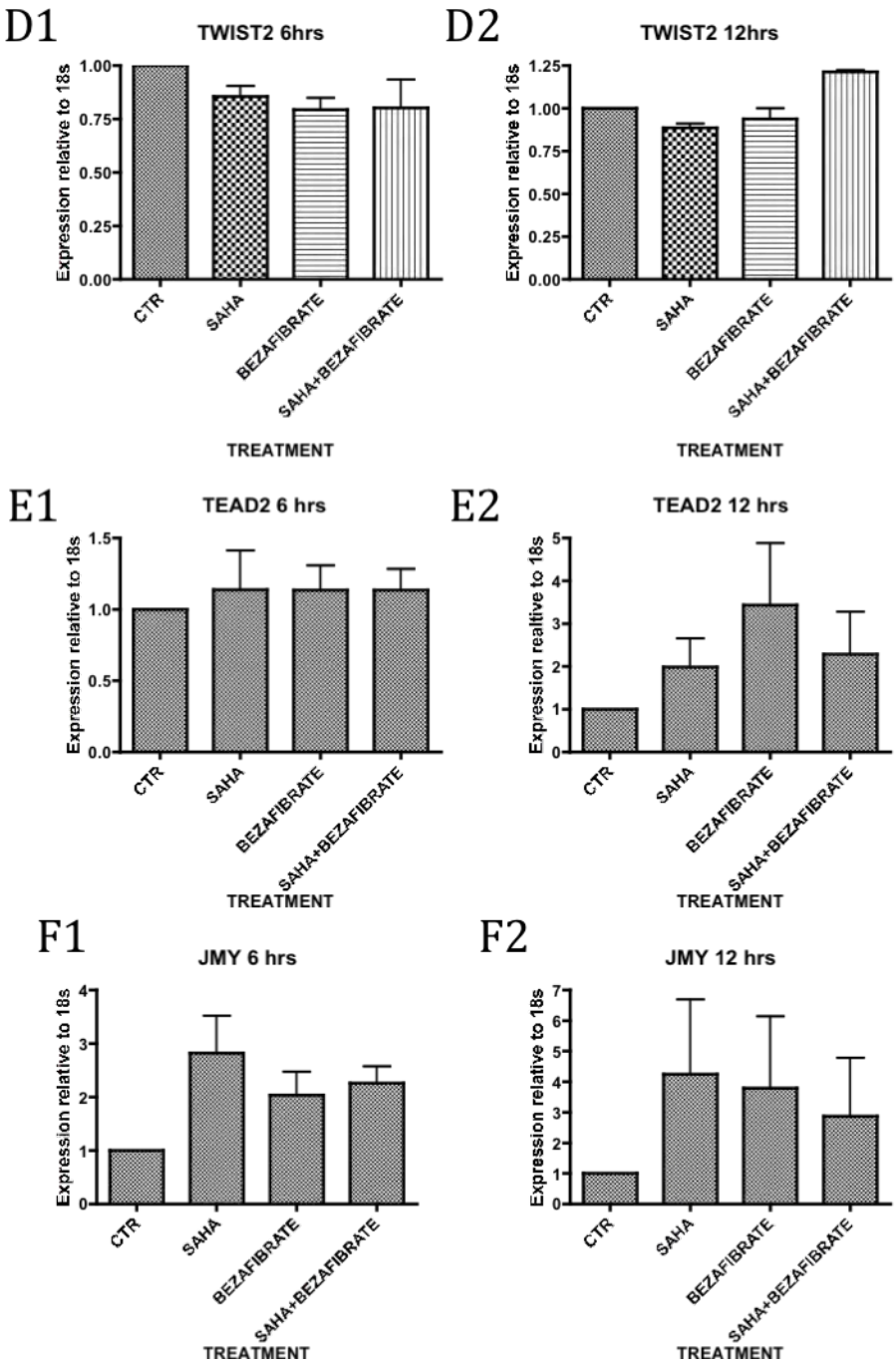
D1
TWIST2 6hrs
Expression relative to 18s
1.00
0.75
0.50
0.25
0.00
CTR
SAHA
BEZAFIBRATE
SAHA+BEZAFIBRATE
TREATMENT
D2
TWIST2 12hrs
Expression relative to 18s
1.25
1.00
0.75
0.50
0.25
0.00
CTR
SAHA
BEZAFIBRATE
SAHA+BEZAFIBRATE
TREATMENT
E1
TEAD2 6 hrs
Expression relative to 18s
1.5
1.0
0.5
0.0
CTR
SAHA
BEZAFIBRATE
SAHA+BEZAFIBRATE
TREATMENT
E2
TEAD2 12 hrs
Expression realtive to 18s
5
4
3
2
1
0
CTR
SAHA
BEZAFIBRATE
SAHA+BEZAFIBRATE
TREATMENT
F1
JMY 6 hrs
Expression relative to 18s
4
3
2
1
0
CTR
SAHA
BEZAFIBRATE
SAHA+BEZAFIBRATE
TREATMENT
F2
JMY 12 hrs
Expression relative to 18s
7
6
5
4
3
2
1
0
CTR
SAHA
BEZAFIBRATE
SAHA+BEZAFIBRATE
TREATMENT

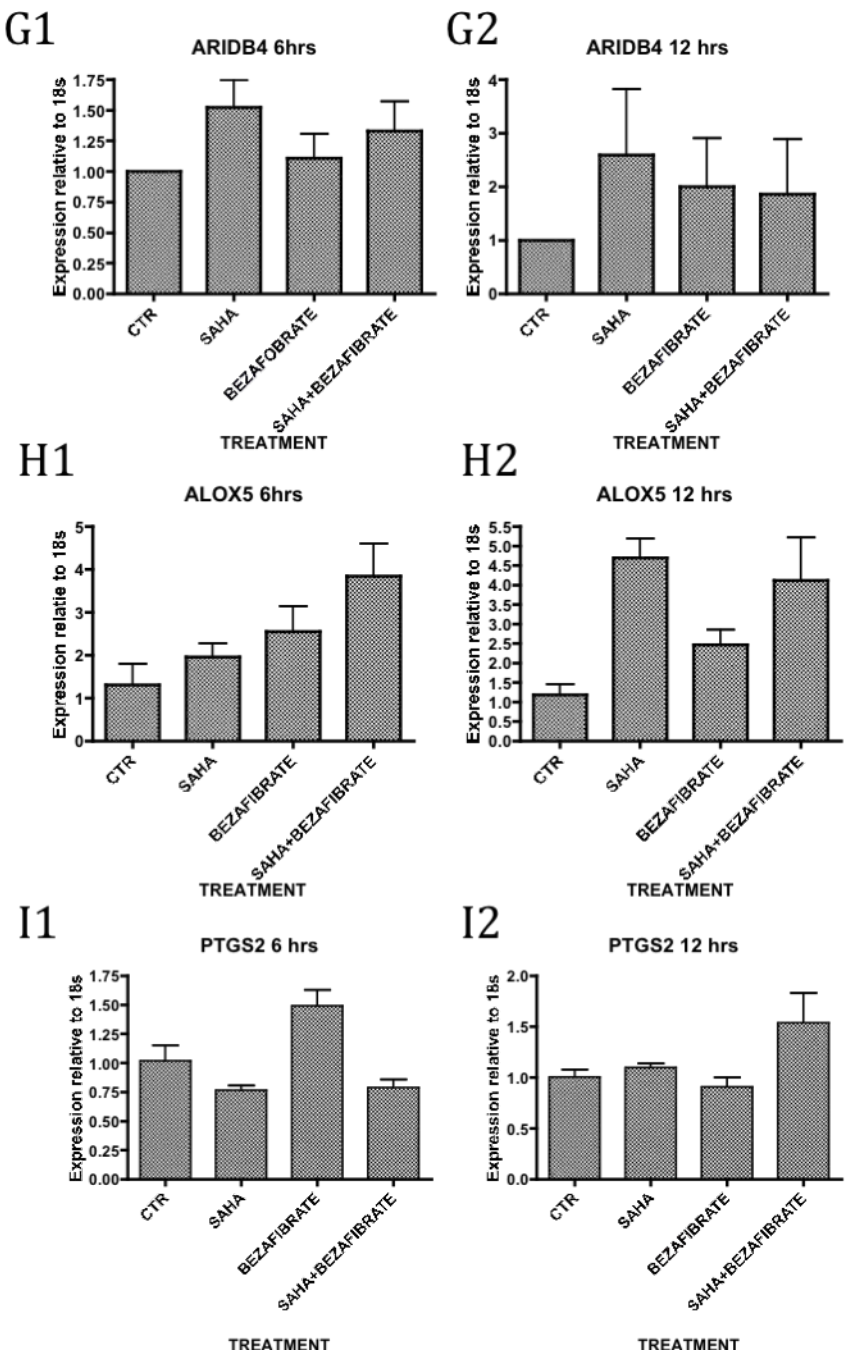
G1
ARIDB4 6hrs
Expression relative to 18s
CTR
SAHA
BEZAFOBRATE
SAHA+BEZAFIBRATE
TREATMENT
G2
ARIDB4 12 hrs
Expression relative to 18s
CTR
SAHA
BEZAFIBRATE
SAHA+BEZAFIBRATE
TREATMENT
H1
ALOX5 6hrs
Expression relatie to 18s
CTR
SAHA
BEZAFIBRATE
SAHA+BEZAFIBRATE
TREATMENT
H2
ALOX5 12 hrs
Expression relative to 18s
CTR
SAHA
BEZAFIBRATE
SAHA+BEZAFIBRATE
TREATMENT
I1
PTGS2 6 hrs
Expression relative to 18s
CTR
SAHA
BEZAFIBRATE
SAHA+BEZAFIBRATE
TREATMENT
I2
PTGS2 12 hrs
Expression relative to 18s
CTR
SAHA
BEZAFIBRATE
SAHA+BEZAFIBRATE
TREATMENT

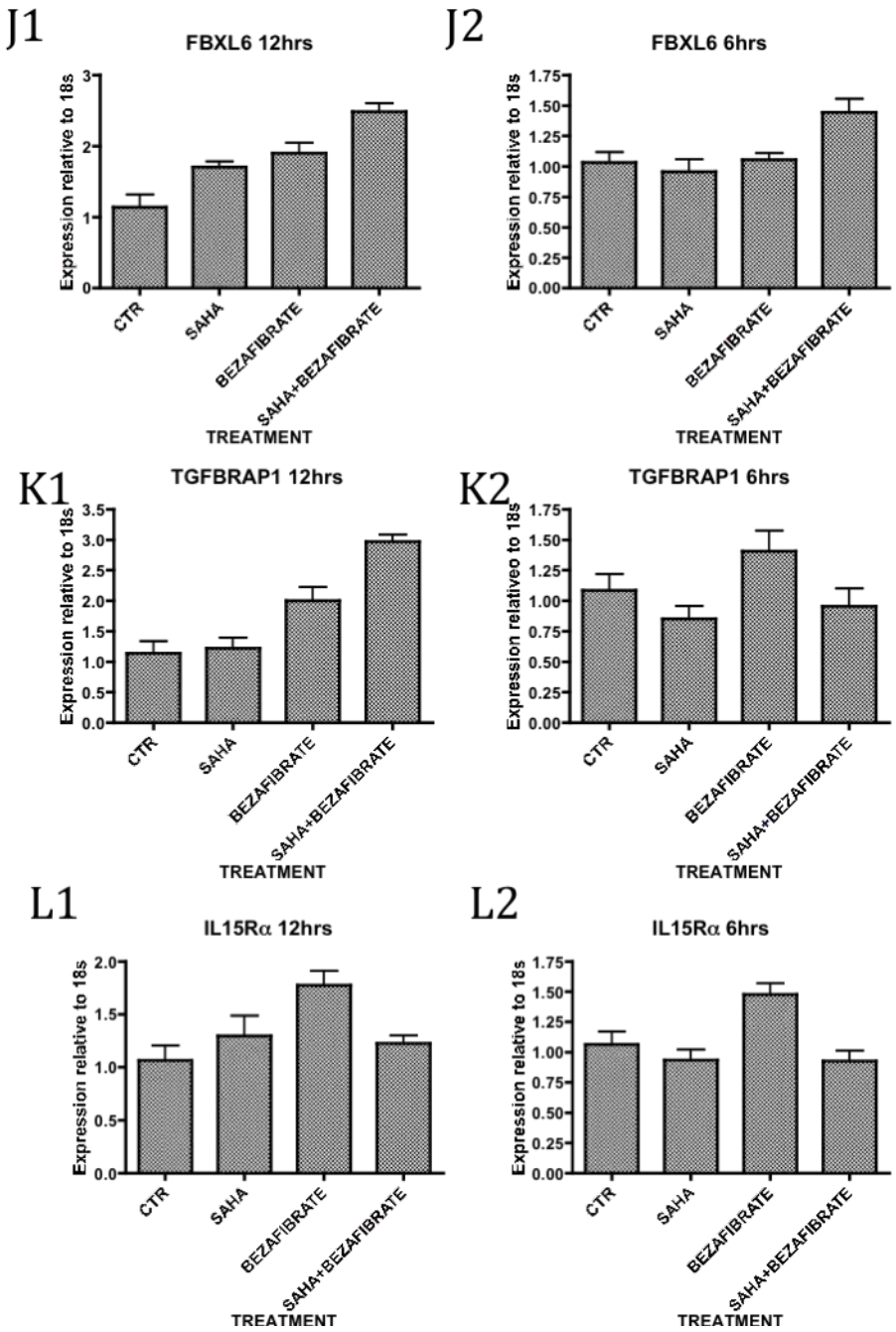
J1
FBXL6 12hrs
Expression relative to 18s
CTR
SAHA
BEZAFIBRATE
SAHA+BEZAFIBRATE
TREATMENT
J2
FBXL6 6hrs
Expression relative to 18s
CTR
SAHA
BEZAFIBRATE
SAHA+BEZAFIBRATE
TREATMENT
K1
TGFBRAP1 12hrs
Expression relative to 18s
CTR
SAHA
BEZAFIBRATE
SAHA+BEZAFIBRATE
TREATMENT
K2
TGFBRAP1 6hrs
Expression relativeo to 18s
CTR
SAHA
BEZAFIBRATE
SAHA+BEZAFIBRATE
TREATMENT
L1
IL15Rα 12hrs
Expression relative to 18s
CTR
SAHA
BEZAFIBRATE
SAHA+BEZAFIBRATE
TREATMENT
L2
IL15Rα 6hrs
Expression relative to 18s
CTR
SAHA
BEZAFIBRATE
SAHA+BEZAFIBRATE
TREATMENT

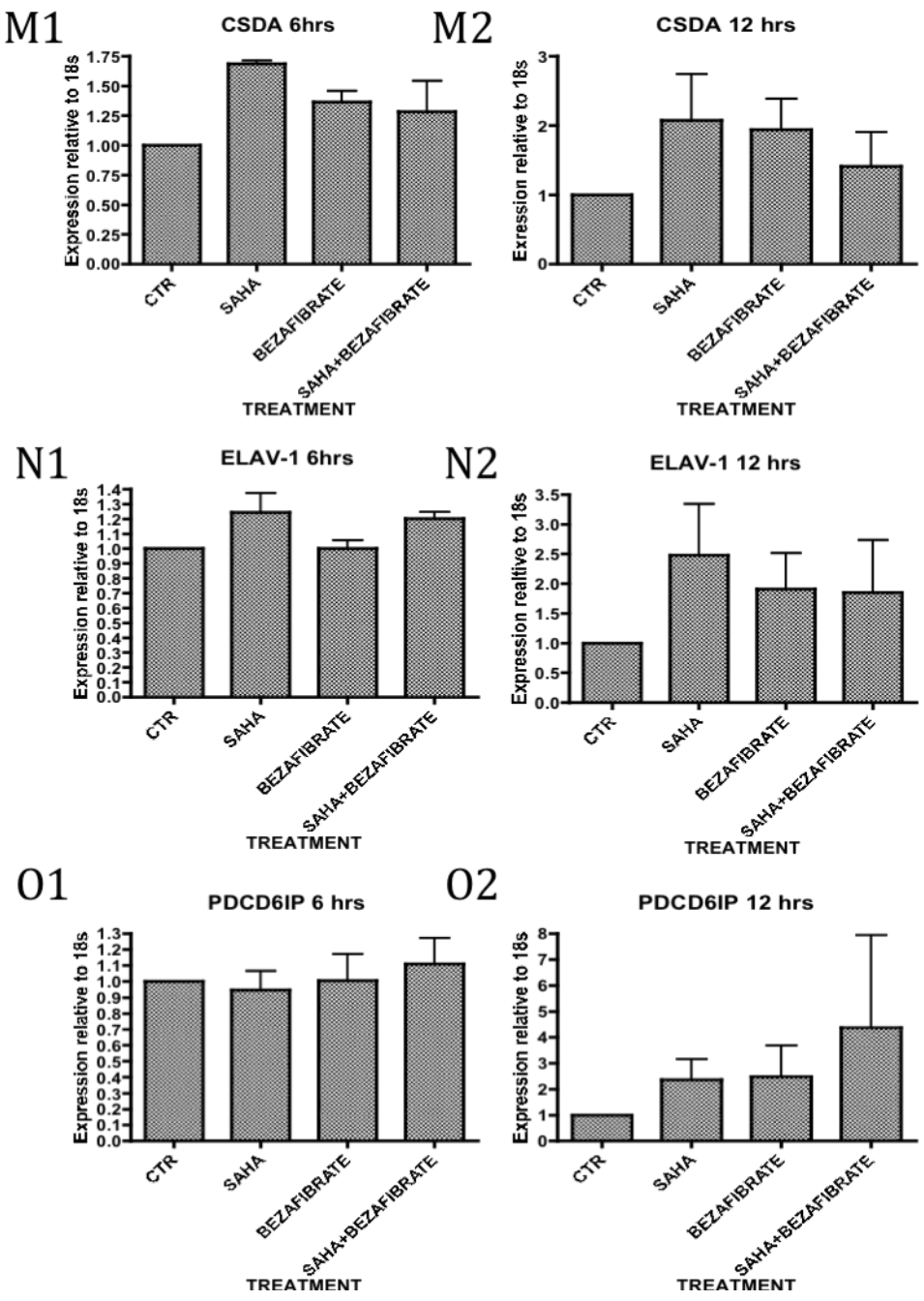
M1
CSDA 6hrs
Expression relative to 18s
CTR
SAHA
BEZAFIBRATE
SAHA+BEZAFIBRATE
TREATMENT
M2
CSDA 12 hrs
Exression relative to 18s
CTR
SAHA
BEZAFIBRATE
SAHA+BEZAFIBRATE
TREATMENT
N1
ELAV-1 6hrs
Expression relative to 18s
CTR
SAHA
BEZAFIBRATE
SAHA+BEZAFIBRATE
TREATMENT
N2
ELAV-1 12 hrs
Expression realtive to 18s
CTR
SAHA
BEZAFIBRATE
SAHA+BEZAFIBRATE
TREATMENT
O1
PDCD6IP 6 hrs
Expression relative to 18s
CTR
SAHA
BEZAFIBRATE
SAHA+BEZAFIBRATE
TREATMENT
O2
PDCD6IP 12 hrs
Expression relative to 18s
CTR
SAHA
BEZAFIBRATE
SAHA+BEZAFIBRATE
TREATMENT

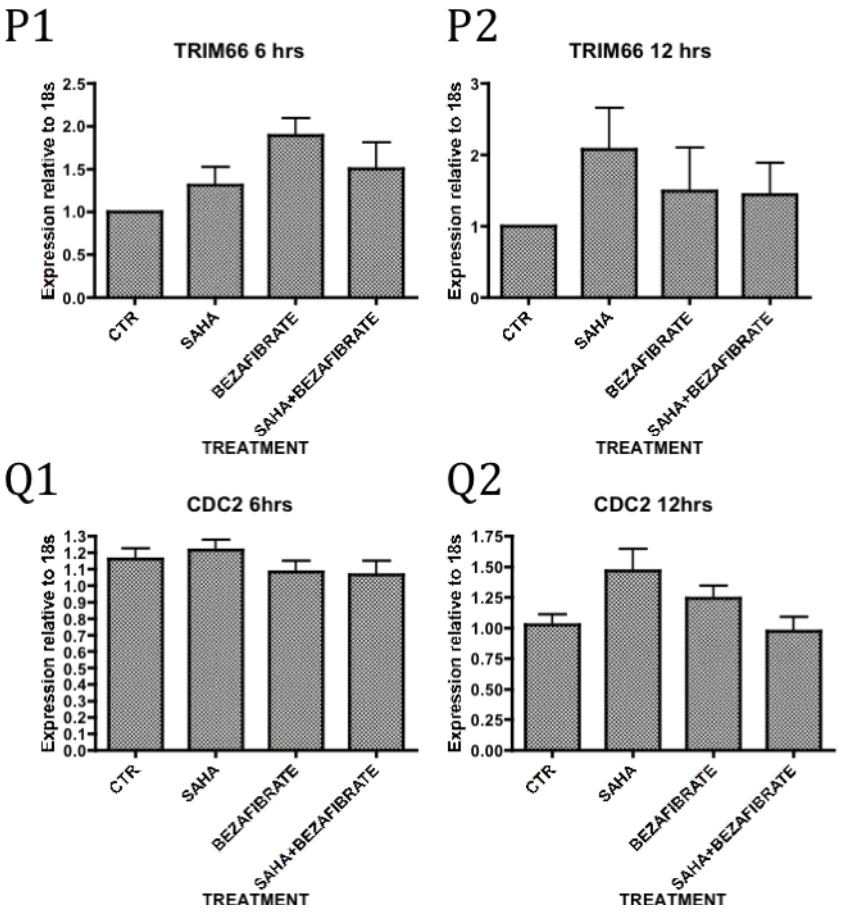

Fig 4.12 – *Q-RT-PCR screening for 16 candidate genes identified via microarray analysis for being uniquely regulated by the double treatment with 0.5 μM SAHA and 0.5 μM Bezafibrate. PTGS2 was identified via network analysis for being metabolically related to ALOX5. Shown are genes initially up-regulated (A1 to I2) and downregulated (F1 to Q2). 10^5 PC-3 cells were plated per each well in a 6 well/plate, seeded for at least 24 hours and treated with the ligand for either 6 or 12 hours; total RNA was extracted and reverse-transcribed prior Q-RT-PCR analysis. Assay on demand primers and probes were used as described in Materials and Methods. All the data are the mean value of at least biological triplicate datasets +/- S.E.M..*

After confirming which genes identified at the initial round of validation to be uniquely regulated by the double treatment, a cohort were profiled further with a detailed time course analysis over 24 hours (**Fig 4.13 A-D)**.

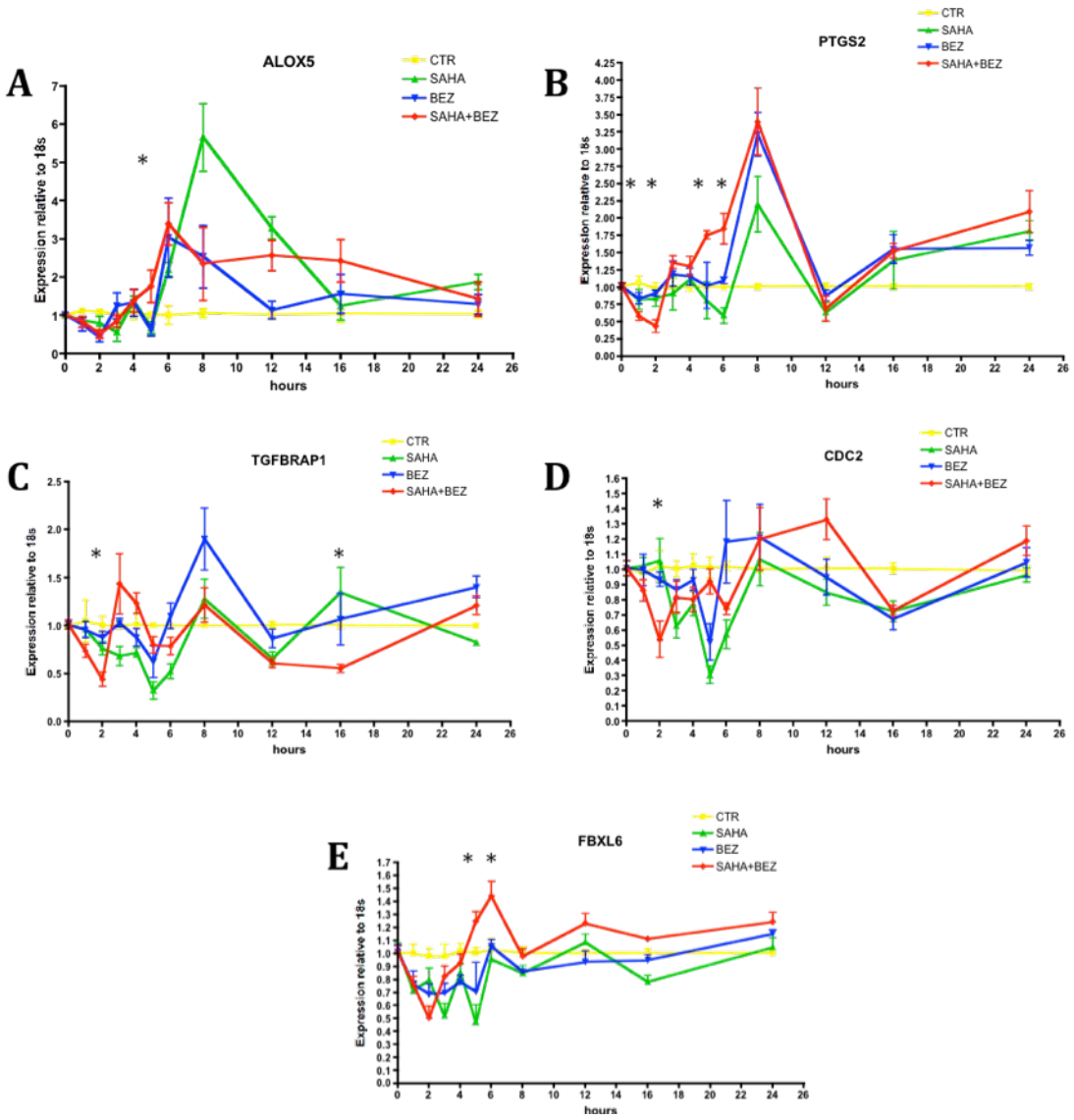

Fig 4.13 – *Time course experiments for five selected genes: ALOX5 (A), PTGS2 (B), TGFBRAP1 (C), CDC2 (D) and FBXL6 (E). RNA was extracted from mid-exponentially growing PC-3 cells and reverse transcribed prior Q-RT-PCR analysis. Custom designed primers and probes were validated and used for this experiment; the complete list can be found in Materials and Methods. Experiments performed with the single ligands or with the combination of the two revealed several time points where the mRNA was uniquely regulated by the combined action of 0.5 μM SAHA and 0.5 μM bezafibrate. Each time point is the mean value of at least three biological replicates +/- S.E.M.. One way ANOVA was used to discover statistical significance of the double treatment with SAHA and bezafibrate, *=p<0.05.*

Statistical analysis demonstrated that the following genes were significantly regulated by the double treatment with 0.5μM of both SAHA and bezafibrate: *ALOX5* (5 hr), *TGFBRAP1* (2 and 16 hr), *FBXL6* (5 and 6 hr), *PTGS2* (1, 2, 5 and 6 hr) and *CDC2* (2 hrs).

Time course experiments demonstrated that all the genes are dynamically and uniquely regulated by the combined treatment at different time points; this suggests that the transcriptome of PC-3 cells was subject to different levels of regulation including chromatin remodeling and mRNA degradation events that dynamically modulate gene transcription. Even further, the possibility of re-activating the PPAR signalling in prostate malignant cells using histone deacetylases inhibitors suggest that the NR network is squelched by a corrupted epigenome. Both SAHA and Bezafibrate are already used in clinical trials and have very good safety profile suggesting that they can be used in combination use for further trials.

4.1.7 – NCOR Knock down approach through shRNA in PC-3 cells

To investigate the hypothesis that a corrupted NR transcriptome occurs through elevated levels of NCOR1, a shRNA approach was undertaken to reduce NCOR1 levels in PC-3 cells. A schematic representation of the NCOR1 gene and the exons target by the shRNA approach is available in the Supplementary Figures.

The exons targeted were number 5, 38 and 44 (sequences available in Materials and Methods); the single stranded oligos were annealed and ligated into the empty pcDNA3.1-H1 vector (described in Materials and Methods); the ligation was checked

via restriction enzyme digestion (Acc65 and XbaI) **(Fig 4.14)** and sequencing **(Fig 4.15)**.

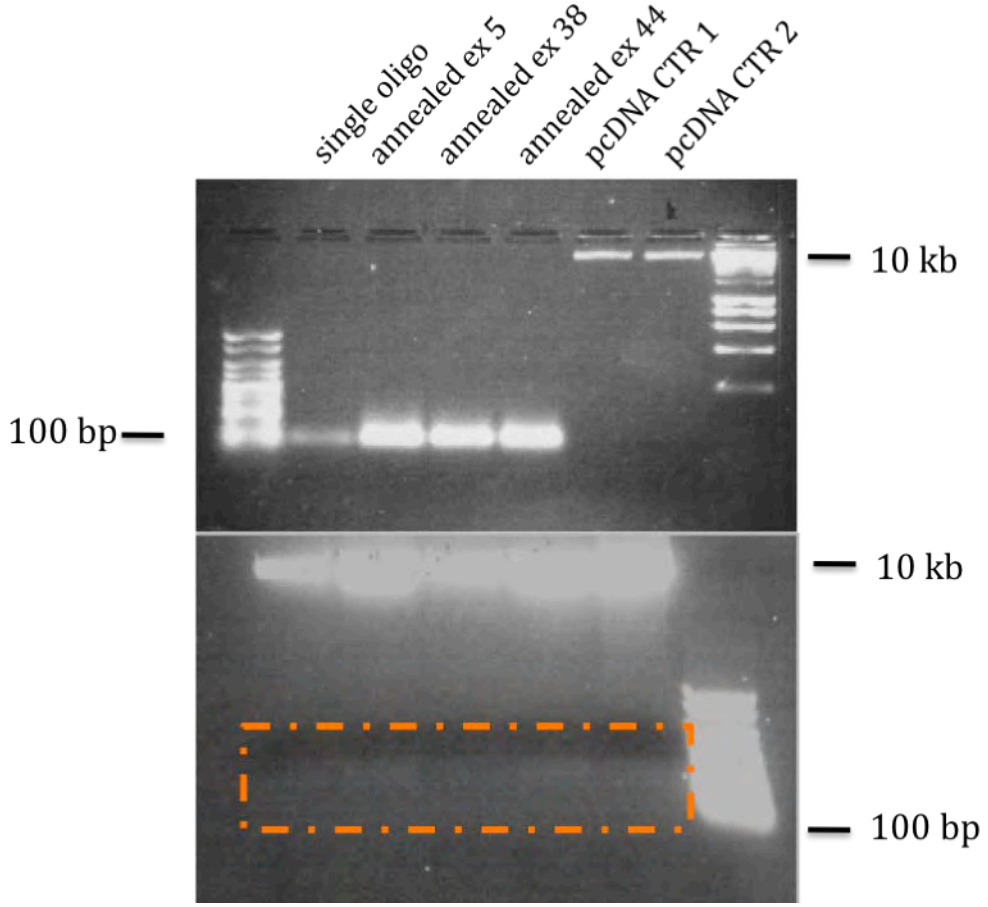

Fig 4.14 *– (TOP) annealed oligos for shNCOR1 and pcDNA3.1-H1 vectors loaded to ensure the ratio between vector/oligos in order to perform an efficient ligation. (BOTTOM) digestion with Acc65I and XbaI to show the presence of the inserted fragment (200 bp). The ladder is over-exposed due to the presence of a low concentration of digested product; however the samples were used successfully for sequencing as shown in Fig 4.15.*

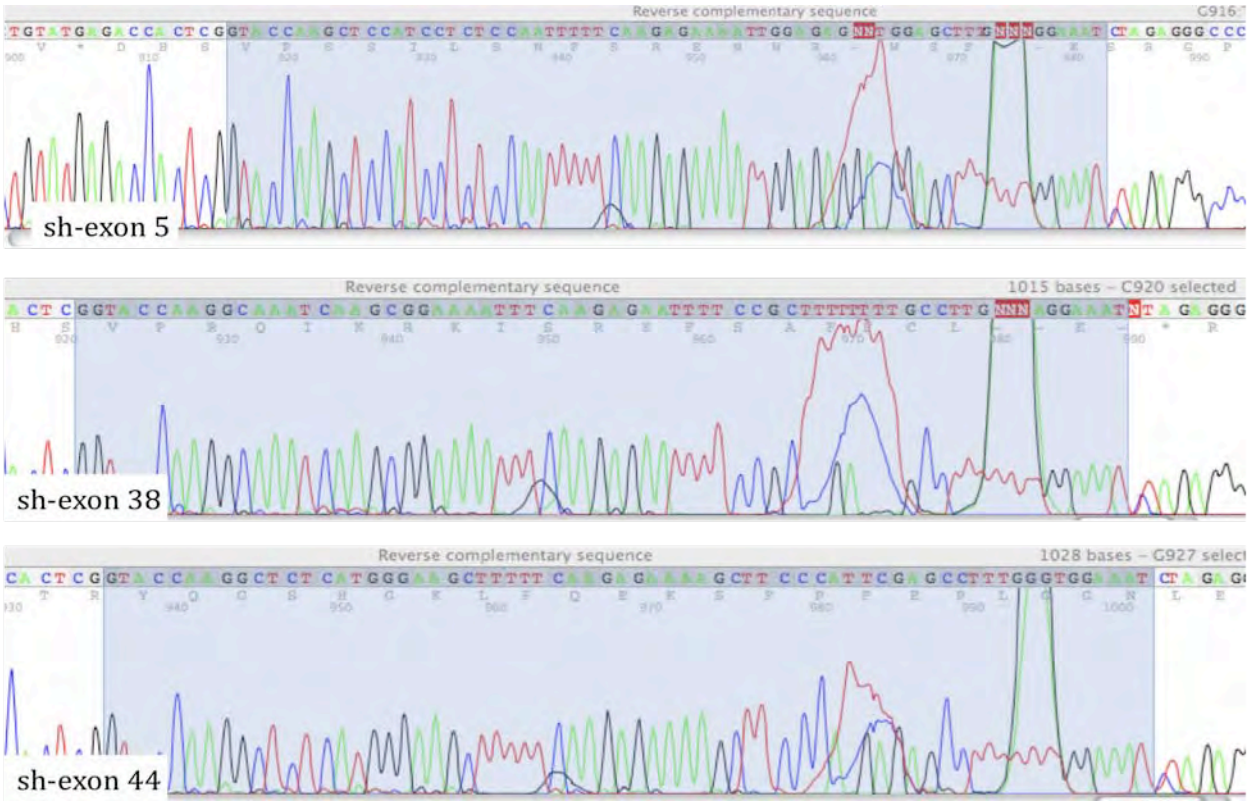

Fig 4.15 – *Sequencing results of the pcDNA3.1H1 clones containing the inserts directed against exon 5, 38 and 44. Highlighted in blue are the sequences containing the hairpins, full sequences are available in the Materials and Methods chapter. Sequencing was performed by the Genomic Facilities in the School of Biosciences at the University of Birmingham, Birmingham, UK.*

PC-3 cells were then transfected with the single vector or with a combination of all the three different targeting constructs using FUGENE6 (protocol in Materials and Methods); G418 at the optimized concentration of 1 mg/ml was used for positive selection of cells with the insert.

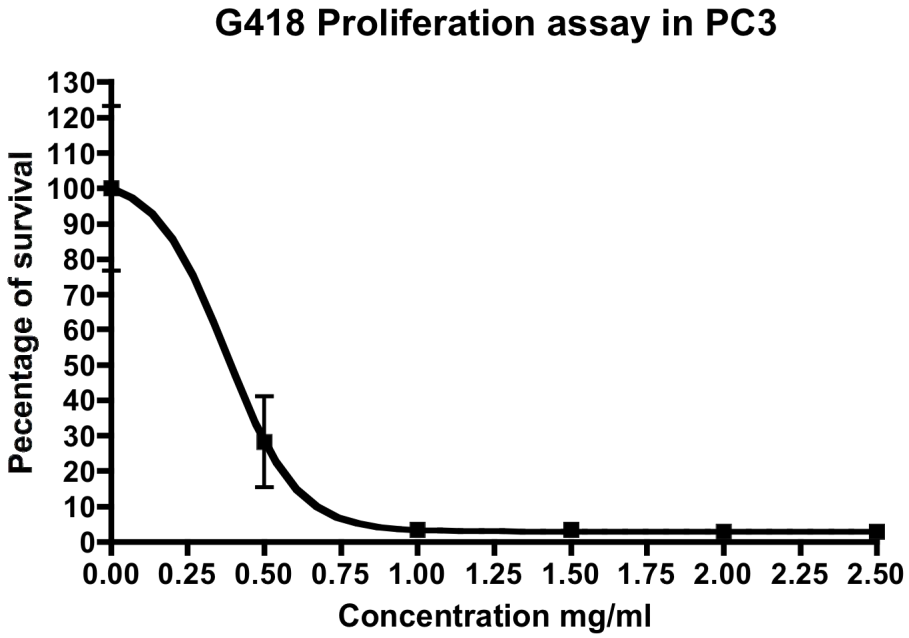

Fig 4.16 – *Dose response of G418 in PC-3 cells. This experiment was undertaken to find the concentration of G418 suitable to maintain PC-3- shNCOR1 resistant cells. two thousands cells were plated in flat white bottom a 96 well/plate, treated for 96 hours with the designed concentration of G418 and re-dosed after 48 hours. The percentage of proliferating cells was measured via ATP assay (described in Materials and Methods). Data shown are the average of a biological duplicate and technical triplicate (three wells per each sample per each replicate) +/- S.E.M..*

Serial dilutions were prepared in order to select single-clone colonies; these colonies were expanded further and screened to check the knockdown levels via qRT-PCR and Western blotting (**Fig 4.17**).

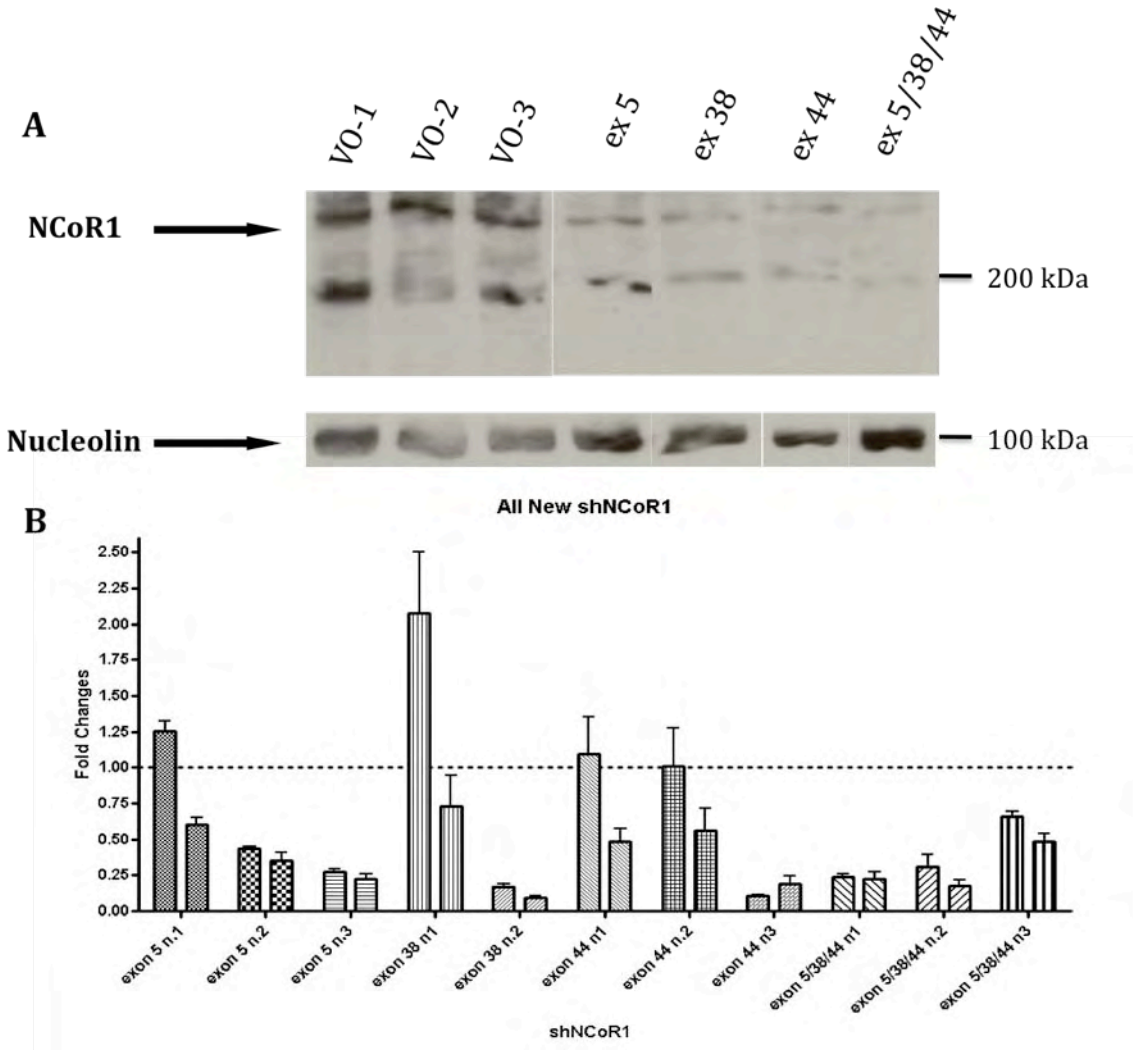

Fig 4.17 – *NCOR1 knock down via shRNA in PC-3 cells at the protein (A) and mRNA (B) level. Nuclear lysate from mid-exponential growing cells was used for Western immunoblotting analysis with the anti-NCOR1 antibody (listed in Materials and Methods). Total RNA was extracted from different clones and reverse transcribed prior qRT-PCR; mRNA levels were compared to two different VO clones and VO-2 was chosen. Data shown are the results of biological triplicate +/- S.E.M.. For further analysis the clone 38.2 was selected.*

The results demonstrated that the shNCOR1-PC-3 38-2 clone showed the greatest knockdown at both protein and mRNA levels and was selected for all the further experiments.

4.1.8 – Microfluidic Gene Card analysis (Q-RT-PCR$_M$) in shNCOR1-PC-3 and VO-PC-3 cells

A microfluidic Q-RT-PCR approach was used to investigate better the function of NCOR1 in PC-3 cells and understand its regulatory function in the NR network. Again, to capture the dynamics of the cell cycle, untreated mid-exponentially growing cells were FACS sorted in G1, S and G2 phases and collected into TRI reagent; RNA was extracted, diluted at the appropriate concentration and loaded with the Qiagen one-step Mastermix in the gene cards. Q-RT-PCR$_M$ analyses revealed that reducing NCOR1 expression significantly re-expressed genes across the cell cycle including *CDH1* (**Fig 4.18 A**). Subsequent SAM analyses identified a further cluster of genes significantly up-regulated in G2 phase, in response to lowered NCOR1, including *ALOX-5*, *CDKN1A, TP53* (**Fig 4.18 B**). CDH1 transcription leads to the translation of a transmembrane glycoprotein that controls intracellular adhesion and has been found to be down regulated in metastatic cancer [213-215]; the finding that NCOR1 control its expression, together with *CDKN1A* and *TP53*, highlights the partially key role that NCOR1 plays in the invasiveness of malignant cells.

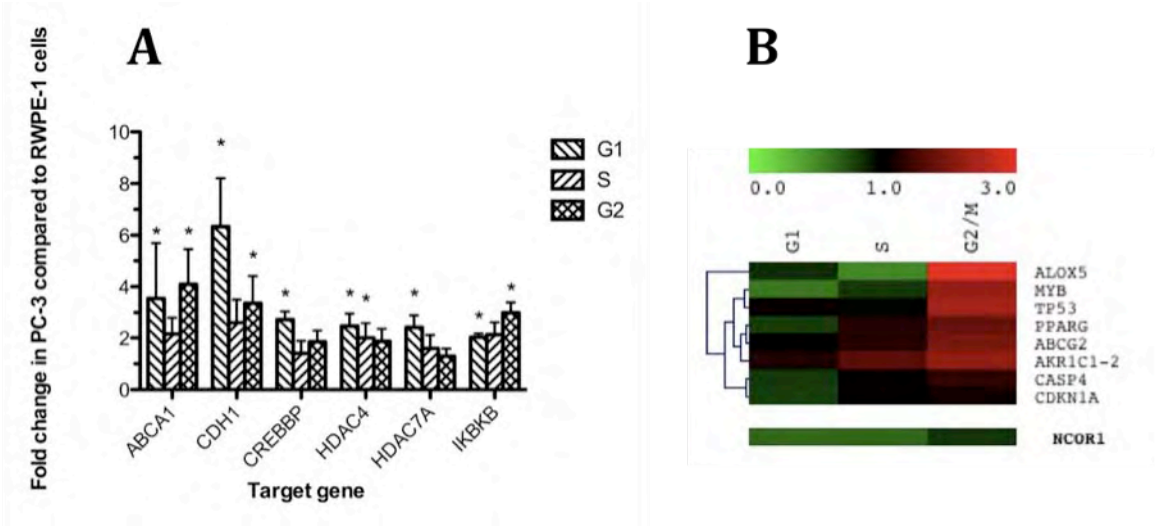

Fig 4.18 – *Gene expression in shNCOR1-PC-3 versus VO-PC-3. Data shown are the mean of at least biological duplicate and technical quadruplicate (tow set of probes were present in each well). (A) Genes significantly differentially expressed in at least one phase of the cell cycle between shNCOR1-PC-3 and VO-PC-3, *=p<0.05. Statistical significance was measured with a one-sample t-test comparing the obtained values against the mean of 1 (index of no changes). (B) Heatmap showing genes significantly differentially expressed across the three phases of the cell cycle. Significance was measured via Significance Analysis of Microarray (SAM) test and cluster analysis was performed using Euclidean distance. Up- and down-regulated genes are represented by red and green boxes, respectively. NCOR1 knock down levels are shown at the bottom of the image.*

4.1.9 – Enhanced anti-proliferative effect shNCOR1 on NR responsiveness

As first step the sensitivity of shNCOR1-PC-3 towards a broad panel of NR ligands was analysed to check whether reduced levels of NCOR1 altered the antiproliferative effect of NR ligands.

Two thousand cells were plated per well in a 96 well/plate and treated for 96 hours with the selected ligand; ATP concentration was then measured in both shNCOR1-PC-3 and VO-PC-3. At a phenotypical level, the antiproliferative effect of EPA (PPARα ligand), ETYA (PPARγ ligand) and ATRA (RAR ligand) were significantly enhanced by NCOR1 knockdown, shNCOR1-PC-3 were also slightly more sensitive

to Bezafibrate but interestingly they were not sensitized further to $1,25(OH)_2D_3$ and T_3 (**Fig 4.19**). VDR was shown by others to bind SMRT preferentially over NCOR1, and as already mentioned, $1,25(OH)_2D_3$ had additive effect only with TSA, while SAHA did not enhance its antiproliferative effect PC-3 cells [62, 211].

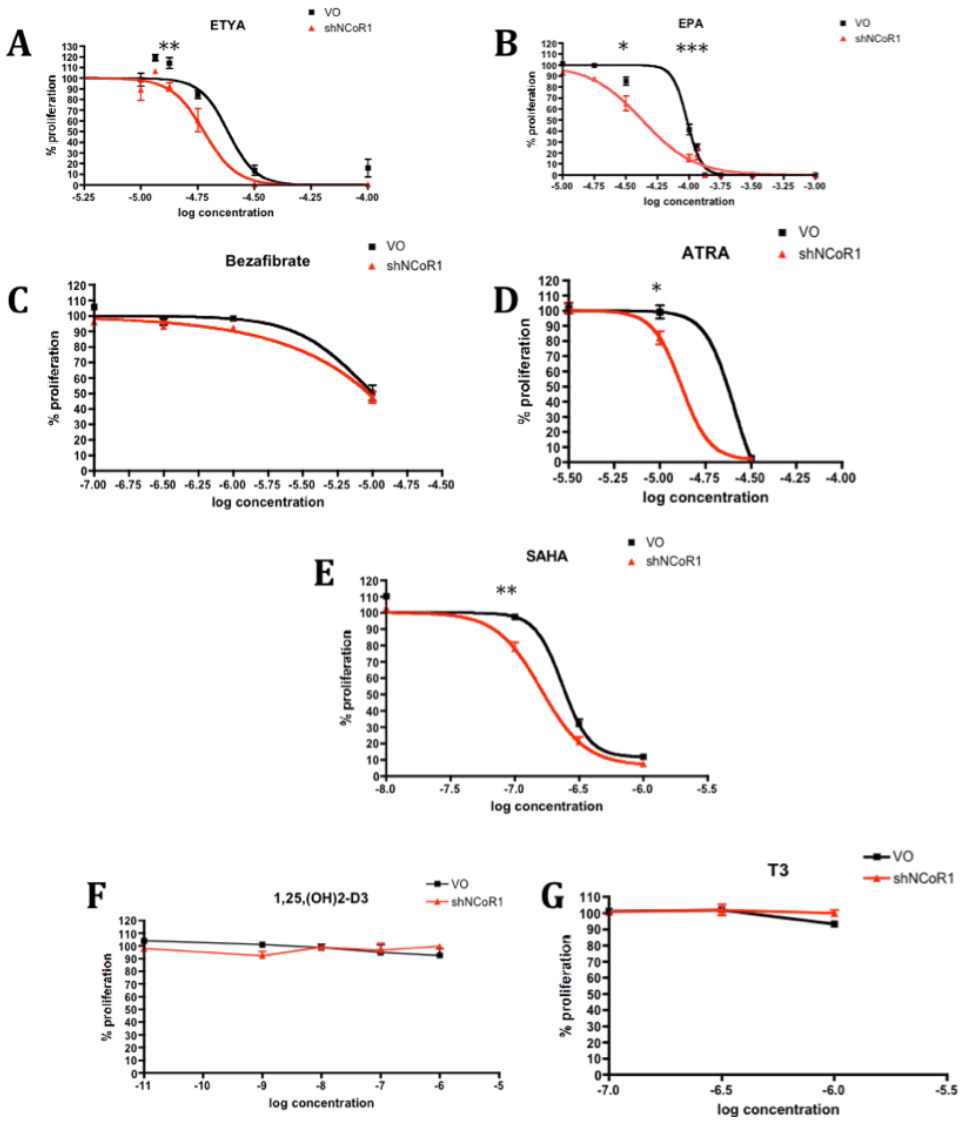

Fig 4.19 *– Smoothed dose response curves for a cohort of nuclear receptor ligands comparing VO-PC-3 (black) with shNCOR1-PC-3 (red). Two thousand cells were plated in a flat-bottom 96 well/plate and treated for 96 hours with the selected agonist with a re-dose at 48 hours. Proliferation was measured via ATP assay comparing ligand-treated cells versus diluent-treated cells. The results show that shNCOR1-PC-3 show a*

*consistent increased sensitivity towards the ligands, except 1,25(OH)$_2$D$_3$ and thyroid hormone T3. Each data point represents the mean value of three separate experiments each undertaken in triplicate wells +/- S.E.M.. Student t-test (Mann-Whitney test) was performed to reveal whether shNCOR-1-PC-3 cells were significantly more sensitive than VO-PC-3 cells to NR ligand; *=p<0.05, **=p<0.01, ***=p<0.001.*

The EC50s from the dose-response curves to all NR ligands were measured and, in average, they were 200 nM lower in shNCOR1-PC-3 than in VO-PC-3 cells.

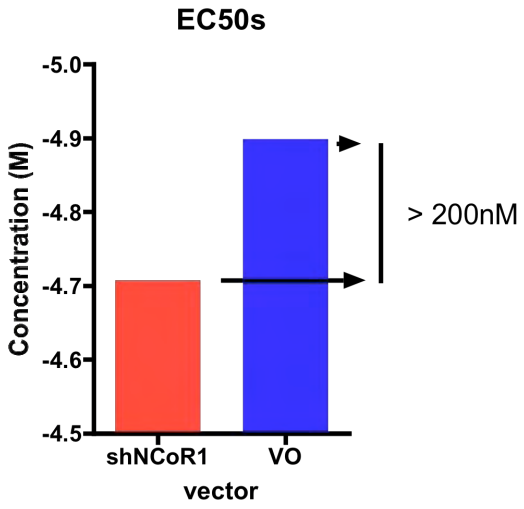

Fig 4.20 – *Bar chart indicating the average EC50s for EPA, ETYA, Bezafibrate, ATRA and SAHA the treatments in shNCOR1-PC-3 (red) and PC-3-VO (blue).*

Although shNCOR1-PC-3 cells were selectively more sensitive to NR ligands their proliferation rate and morphology did not differ from PC-3-VO (data not shown).

SAHA has a wide range of action affecting the acetylation state of histone and non-histone proteins. Knocking down NCOR1 using a shRNA approach created a more defined system that allowed the investigation of the activity of this gene in a cancer system. To demonstrate to what extent the effect of NCOR1 resembles the activity of SAHA in PC-3 cells the effect of 10nM ATRA, 10 μM EPA, 10 μM ETYA and 0.5 μM Bezafibrate either alone or in combination with 0.5 μM SAHA in LNCaP, DU145 and

wild type PC-3 cells (**Fig 4.9**) was compared with the antiproliferative effect of 10 μM ATRA, 30 μM EPA and 20 μM ETYA in PC-3VO and shNCOR1-PC-3 (**Fig 4.21**).

LIGAND	ADDITIVE TO SAHA	ENHANCED BY shNCOR1
ETYA	+	+
EPA	+	+
Bezafibrate	+	+/-
ATRA	+	+
SAHA	/	+
$1,25(OH)_2D_3$	-	-
T3	-	-

Fig 4.21 –*Summary table for the effect of NR ligands on PC-3 cells and their activity in combination with either SAHA or shNCOR1. From left to right the columns indicate the NR ligand, the effect in combination with SAHA and the enhanced effect by NCOR1 knock down in shNCOR1-PC-3 cells compared to VO-PC-3 cells.*

As shown by **Fig 4.19** and **Fig 4.21** the antiproliferative activity of NR ligands was enhanced by shNCOR1 only in a selected cluster of receptors. These NR are all phylogenetically related suggesting that conserved sequences can partially explain why knocking down NCOR1 does not globally enhance the antiproliferative effect of NR agonists.

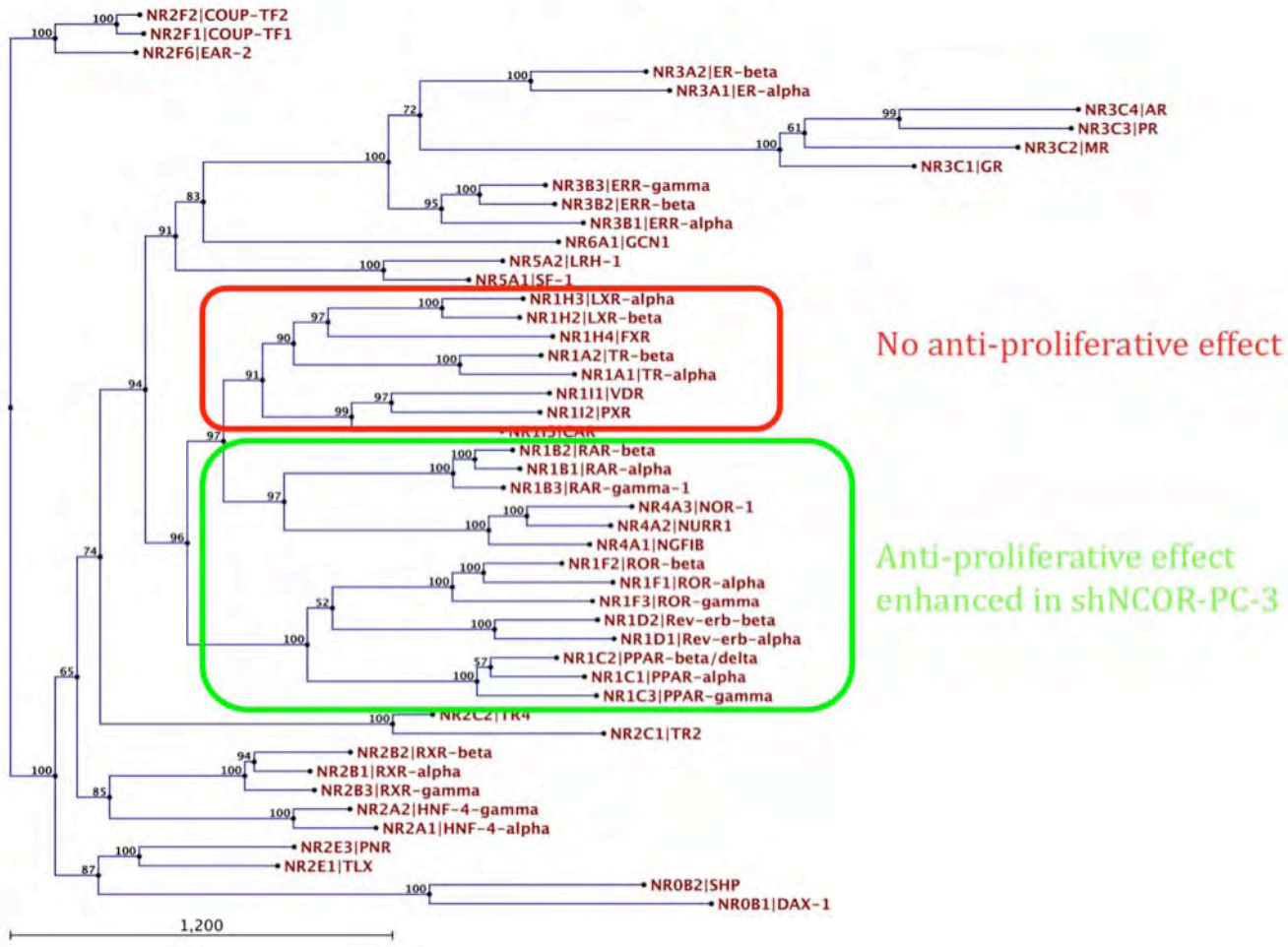

Fig 4.22 *– Nuclear Receptor phylogenetic tree. This image was downloaded from Wikipedia (www.wikipedia.org), was prepared using CLC Free Workbench Version 3.2.2 (http://www.clcbio.com) and the amino acid sequences was downloaded from the PubMed protein database (http://www.pubmed.gov). Highlighted in red are the NR that did not have an enhanced antiproliferative activity upon agonist treatment in shNCOR1-PC-3 cells; highlighted in green are the NR whose antiproliferative activity was enhanced upon agonist treatment in shNCOR1-PC-3 cells compared with VO-PC-3 cells.*

4.1.10 – Gene de-repression in shNCOR1-PC-3 cells

Cells treated with single nuclear receptor agonists in combination with SAHA showed an additive effect towards both cell proliferation and gene transcription. The next step was to demonstrate whether NCOR1 knockdown was able to regulate NR gene transcription in a manner that reflects SAHA co-treatment.

The first approach aimed to demonstrate that the genes uniquely expressed by the combination of SAHA and bezafibrate in the microarray (*CDC2*, *TGBRAP1*, *ALOX5*, *PTGS2* and *FBXL6*) could be similarly regulated by the combination of NCOR1 knock down and bezafibrate treatment. Mid-exponential growing shNCOR1-PC-3 and PC-3-VO were treated with single agents (0.5 μM Bezafibrate or 100 nM $1,25(OH)_2D_3$) for 3 and 8 hours, whole RNA was extracted and reverse-transcribed prior to Q-RT-PCR analysis. Interestingly, the results show that reduced levels of NCOR1 affect both positively and negatively the mRNA accumulation of target genes, suggesting a ligand-dependent mechanism of repression by NCOR1. The time points from the bezafibrate and SAHA time course experiments where the genes were uniquely and significantly regulated by the co-treatment were found to mirror broadly the pattern of mRNA accumulation in shNCOR1-PC-3 treated with bezafibrate alone.

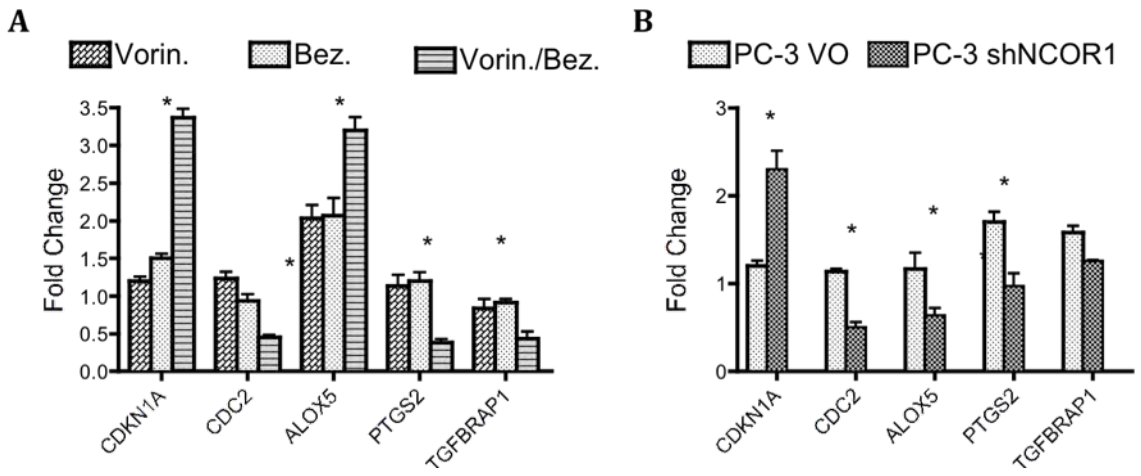

Fig 4.23 - *PC-3 cells were treated with bezafibrate (0.5 mM) plus vorinostat (0.5 mM), and VO-PC-3 and shNCOR1-PC-3 cells were treated with bezafibrate (0.5 mM) over a 16 hour time course, mRNA extracted and subjected to Q-RT-PCR. (A) mRNA levels at 4 hr (CDKN1A), 5 hr (ALOX-5), 2 hr (CDC2, PTGS2, TGFBRAP11). (B) mRNA levels at 3 hr (CDKN1A, CDC2, ALOX5, PTGS2) and 8 hr (TGFBRAP1) in PC-3 shNCOR1 cells and PC-3 VO cells. Each data point represents the mean of three separate experiments amplified in triplicate wells +/- S.E.M. Student t-test was used to measure statistical significance comparing knock down against vector only control samples (*p < 0.05).*

The upregulation of *CDKN1A* caused by the combined treatment of SAHA and bezafibrate was mirrored by the bezafibrate-alone treated shNCOR1-PC-3; *CDC2*, *PTGS2* and *TGFBRAP1* downregulation was found also in the knock down bezafibrate-treated cells while *ALOX5* pattern was interestingly opposite.

It was also checked whether reduced levels of NCOR1 could influence the expression of VDR target genes bearing in mind that NCOR1 knockdown did not change the sensitivity of PC-3 cells towards $1,25(OH)_2D_3$. Two classic VDR target genes were also taken in consideration: *CYP24* (involved in $1,25(OH)_2D_3$ catabolism), and *CDKN1A* (involved in cell cycle control). *CDKN1A* levels were not influenced by the knockdown while, interestingly, *CYP24* mRNA accumulation in shNCOR1-PC-3 was reduced at both 3 and 8 hours compared to PC-3-VO. However, these last results are not totally surprising because they show that the $1,25(OH)_2D_3$-dependent

upregulation of *CYP24* is not a mechanism driven uniquely by the vitamin D receptor and implies some secondary effects that loop in the system independently from NCOR1. Moreover, the *CYP24* data are consistent with previously published cyclohexamide data [62] where it has been shown that the combined treatment cyclohexamide and $1,25(OH)_2D_3$ led to a significant reduction in the induction of *CYP24* in PC-3 cells, supporting the concept that upregulation of this genes is not only a direct effect VDR-mediated.

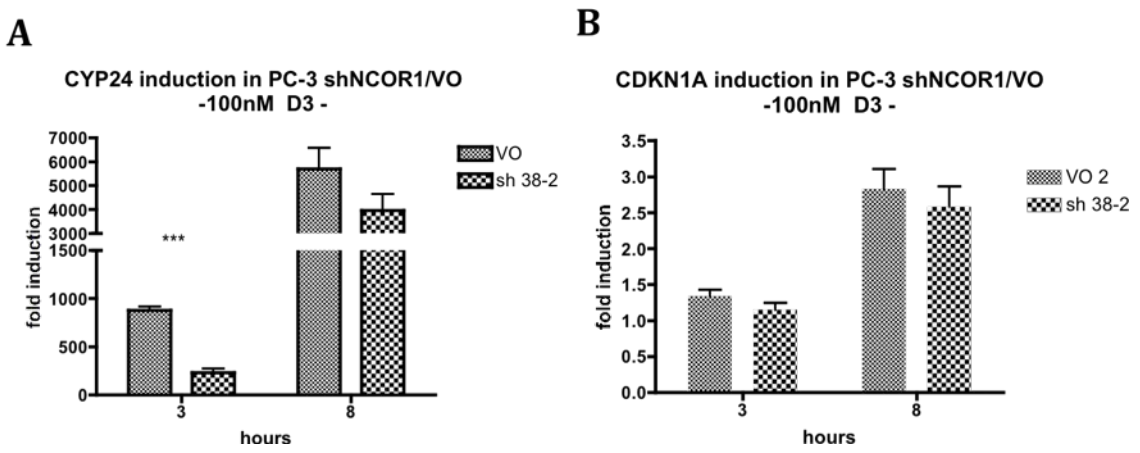

Fig 4.24 – *$1,25(OH)_2D_3$ action on CYP24 (A) and CDKN1A (B) mRNA accumulation. Whereas CDKN1A expression does not change in shNCOR1-PC-3 cells compared with PC-3-VO cells, CYP24 is less upregulated in NCOR1 knockdown cells. Total RNA was extracted form 6 well/plates and reverse-transcribed prior qRT-PCR. Student t-test was performed to find significant differences in the induction of the two genes in PC-3 transfected with shNCOR1 or VO, ***=p<0.01. Each graph is the average of three independent experiments +/- S.E.M..*

These data strongly indicate that NCOR1 is not only involved in a direct repression of target genes but also in a ligand-dependent transrepression of target genes. It has been shown that NCOR1 is involved in a ligand-dependent sumoylation of PPARγ that leads to recruitment of the corepressor complexes on the promoter of target genes and transcriptional inhibition [130]. It is unclear if NCOR1 either contributes

to the recruitment of corepressor complexes upon ligand treatment, or acts as a repressor for other repressor proteins, explaining why lower levels of NCOR1 lead to downregulation of some of the PPAR target genes.

4.1.11 – H3K9 acetylation at the TSS region of PPAR target genes

NCOR1 complexes with several HDACs modulating the acetylation status of histones and non-histone proteins. Histone 3 lysine 9 acetylation (H3K9Ac) is a widely used marked for active promoter regions that positively regulate transcription; the TSS region of two PPAR target genes, *CDKN1A* and *TGFBRAP1* were analysed to check whether 0.5 μM of either bezafibrate, SAHA or the combined treatment were able to promote H3K9 acetylation in PC-3 cells.

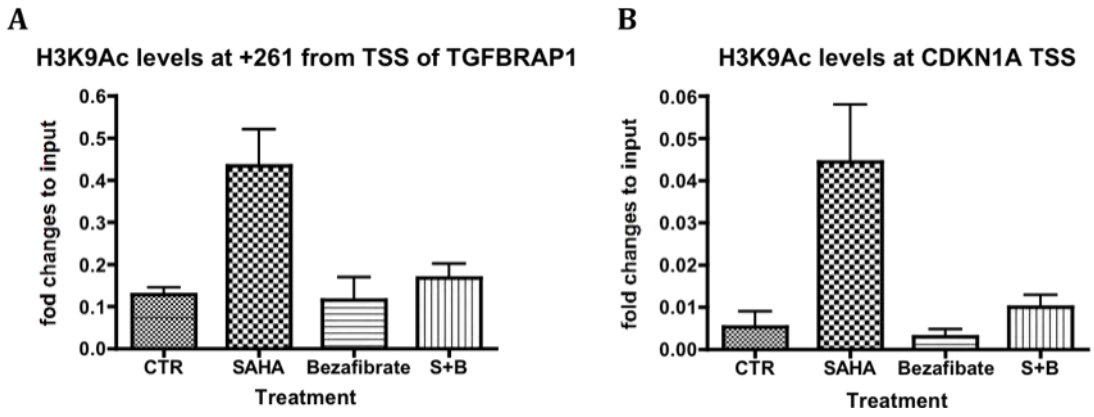

Fig 4.25 – *X-ChIP showing the acetylation levels of lysine 9 in the histone H3 (H3K9Ac) in TGFBRAP1 (A) and CDKN1A (B). Mid-exponential PC-3 cells were treated for 3 hours with 0.5 μM of either SAHA, bezafibrate or both. Cells were cross-linked, chromatin extracted and immunoprecipitated with H3K9Ac antibody; DNA was isolated and used for qRT-PCR (Sybr Green) with primers for the indicated regions of the TGFBRAP1 and CDKN1A genes. Data shown are mean of two biological replicated +/- S.E.M.. Fold changes were calculated comparing the H3K9Ac samples with the corresponding inputs.*

As shown in **Fig 4.25**, SAHA induced acetylation of H3K9 at the TSS region of both *CDKN1A* and *TGFBRAP1* as expected by the activity of a histone deacetylases inhibitor; interestingly bezafibrate not only didn't induce any acetylation at the TSS but cleared part of the acetylation on CDKN1A promoting a repressive chromatin environment. There is an interesting similarity in the two datasets suggesting that the epigenetic modification at their promoter region might me commonly regulated by the combined treatment.

To investigate better the involvement of NCOR1 in the epigenetic regulation of *CDKN1A* and *TGFBRAP1* and to confirm whether this would reflect the mRNA data, NCOR1 was knocked down in PC-3 cells with a siRNA approach and ChIP analysis after 3 hours of 0.5 μM bezafibrate treatment was undertaken.

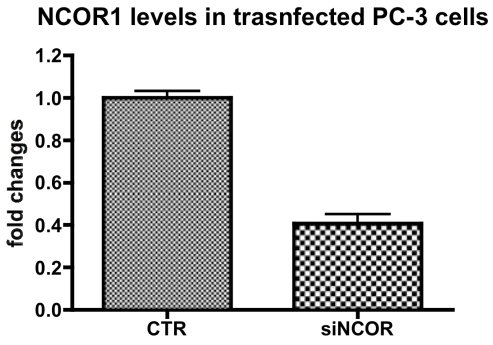

Fig 4.26 – *Knock down of NCOR via siRNA compared to scramble siRNA (as in [202]). Mid exponentially growing PC-3 cells were trasnfectd with 50 ng of siRNA or scrambled vector and incubated over-nigh at 37ºC; the following morning cells were harvested, total RNA was extracted and reverse transcribed prior to Q-RT-PCR analysis. Data shown are the mean of a biological duplicate +/- S.E.M..*

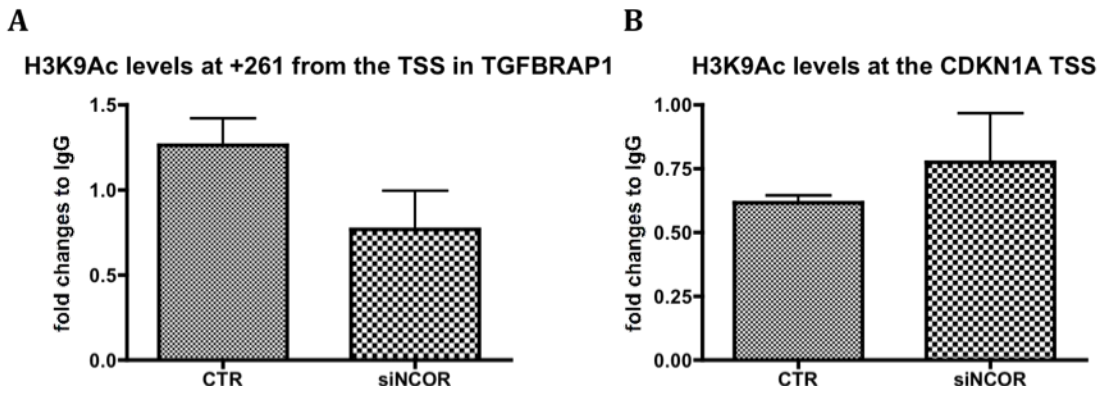

Fig 4.27 – *X-ChIP showing the acetylation levels of lysine 9 in the histone H3 (H3K9Ac) in TGFBRAP1 (A) and CDKN1A (B). Mid-exponential PC-3 cells were transfected with siNCOR or scramble siRNA (as in [202]) and incubated over-night; the media was changed the following morning and cells were treated for 3 hours with 0.5 μM of bezafibrate. Cells were cross-linked, chromatin extracted and immunoprecipitated with H3K9Ac antibody; DNA was isolated and used for qRT-PCR (Sybr Green) with primers for the indicated regions of the TGFBRAP1 and CDKN1A genes. Data shown are mean of two biological replicated +/- S.E.M.. Fold changes were calculated comparing the H3K9Ac samples with the corresponding IgGs.*

The results show that H3K9 acetylation at the TGFBRAP1 +261 region (chosen because the TSS region is rich in GC and no reliable primers were available) is reduced by lower levels of NCOR1 while H3K9 acetylation at the TSS of CDKN1A is increased. These results are consistent with the mRNA data from shNCOR1-PC-3 cells where after treatment with bezafibrate the expression of *TGBRAP1* and *CDKN1A* was, respectively, downregulated and upregulated. This suggests that NCOR1 epigenetically modulates the ligand-responsiveness of PPAR target genes through two different mechanisms: an active ligand-independent repression on *CDKN1A* and a ligand-dependent trans-activation on *TGFBRAP1*.

4.2 – Ncor1 AND Ncor2/Smrt KNOCKOUT AND KNOCK DOWN IN THE MOUSE PROSTATE

The importance of NCOR1 in prostate cancer was previously demonstrated, and indeed, a lower levels of this protein leads to increased sensitivity towards nuclear receptor ligands and de-repression of PPAR target genes. Another group demonstrated the key role of Ncor1 and Ncor2/Smrt in development creating deficient mice that died at embryonic day (E) 14.5 and 15.5, respectively; among the lethal heart defects, mutant mice showed abnormalities in neuronal and thymocyte development, as well as impaired erythropoiesis [139, 216].

These studies demonstrated that several organs are affected by the activity of both Ncor11 and Ncor1/Smrt and, in addition in prostate malignant and non malignant cells. Therefore we decided to study the role of Ncor1 and Ncor2/Smrt in prostate development by creating prostate-specific knock out and knock down mice for both corepressors.

4.2.1 – Knock out strategy for Ncor1 and Ncor2/Smrt in the mouse prostate

The initial approach aimed to design a reliable strategy to create a targeting construct that efficiently and selectively knocked out Ncor1 and Ncor2/Smrt in the mouse prostate. The Cre-LoxP system developed by Brian Sauer [217] has been widely used and exploits the ability of the Cre enzyme to recognize two specific sequences, LoxP sites, in the genome, bridge them together and exciding the sequence [218].

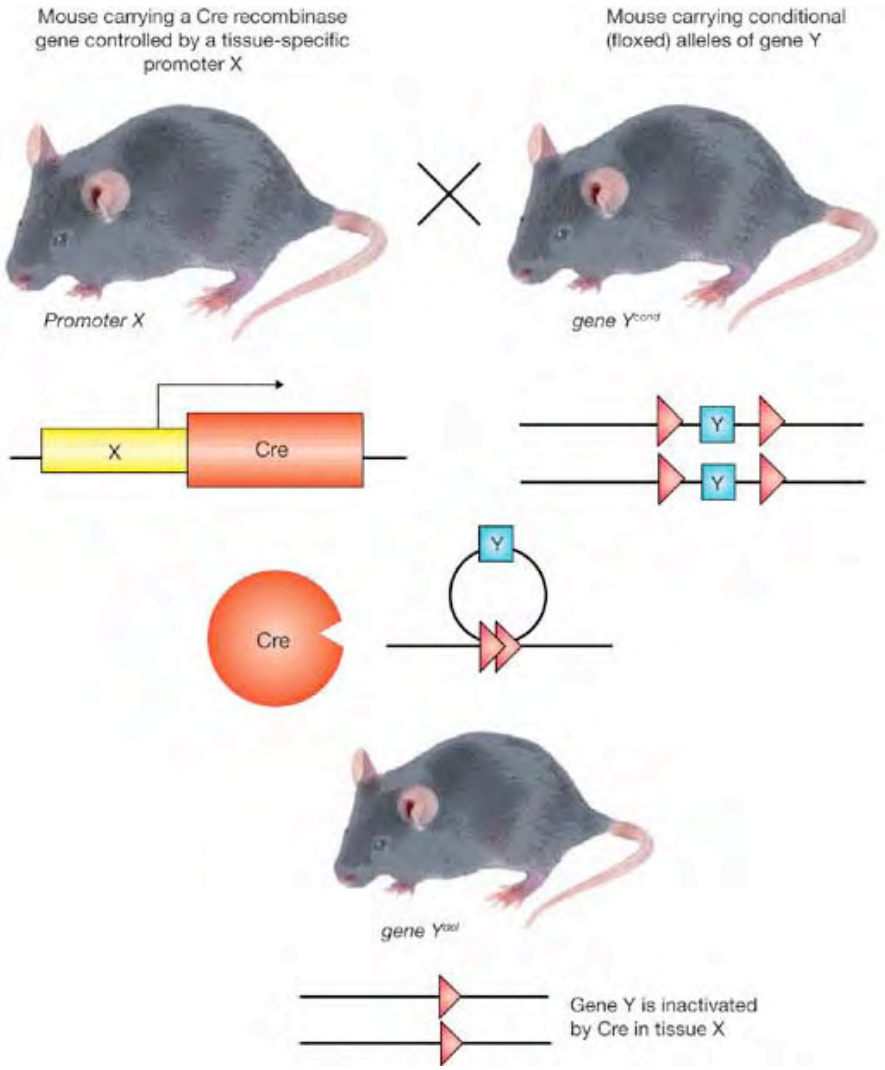

Fig 4.28 – *Schematic representation of the Cre-Lox system: the Cre gene is driven by a general or cell type/tissue specific promoter while the floxed allele contains the sequence, mainly critical exons, of interested flanked by two LoxP sites (red triangles). The Cre enzyme recognizes the LoxP sequences and promotes the excision of the target sequence leaving a single LoxP site on the genome (image taken from [218]).*

Moreover, to create a prostate-specific knock out, the Cre enzyme must be driven by a promoter active only in the mouse prostate; to do this we relied on the modified rat probasin, ARR_2PB, promoter. This promoter has been shown to have high prostate specificity and it has been successfully used in the past anytime there was the need of a prostate-specific activity [219].

The promoter is less than 500 base pairs long, it contains two androgen responsive regions that include a total of four androgen responsive elements, followed by the first 28 base pairs of the rat probasin gene.

RAT PROBASIN PROMOTER – ARR2PB

-286 -> +28 sequence

TAGTCATCATGTTTAAACATCTACCATTCCAGTTAAGAAAATATGATAGCATCTTGTTCTTAGTCTTTTTCTTAATAGGGACATAAAGCCCACAAATA
AAAATATGCCTGAAGAATGGGACAGGCATTGGGCATTGTCCATGCCTAGTAAAGTACTCCAAGAACCTATTTGTATACTAGATGACACAATGTCAA
TGTCTGTGTACAACTGCCAACTGGGATGCAAGACACTGCCCATGCCAATCATCCTGAAAAGCAGCTATAAAAAGCAGGAAGCTACTCTGCACCT
TGTCAGTGAGGTCCAGATACCTACAG

ARE1 -236 -> -223
ATCTTGTTCTTAGT
ARE2 -140 -> -117
GTAAAGTACTCCAAGAACCTATTT

ARR -244 -> -196
ATGATAGCATCTTGTTCTTAGTCTTTTTCTTAATAGGGACATAAAGCCCACAAATAAAAATATGCCTGAAGAATGGGACAGGCATTGGGCATTGTC
CATGCCTAGTAAAGTACTCCAAGAACCTATTTGTATACTAGATGACACAATG

(ARR)-286PB
ATGATAGCATCTTGTTCTTAGTCTTTTTCTTAATAGGGACATAAAGCCCACAAATAAAAATATGCCTGAAGAATGGGACAGGCATTGGGCATTG
TCCATGCCTAGTAAAGTACTCCAAGAACCTATTTGTATACTAGATGACACAATGTAGTCATCATGTTTAAACATCTACCATTCCAGTTAAGAAA
AATGATAGCATCTTGTTCTTAGTCTTTTTCTTAATAGGGACATAAAGCCCACAAATAAAAATATGCCTGAAGAATGGGACAGGCATTGGGCAT
TGTCCATGCCTAGTAAAGTACTCCAAGAACCTATTTGTATACTAGATGACACAATGTCAATGTCTGTGTACAACTGCCAACTGGGATGCAAGA
CACTGCCCATGCCAATCATCCTGAAAAGCAGCTATAAAAAGCAGGAAGCTACTCTGCACCTTGTCAGTGAGGTCCAGATACCTACAG

Fig 4.29 – *Representation of the ARR$_2$PB prostate-specific promoter. The promoter is divided into two androgen responsive regions (red) each one containing two androgen responsive elements (ARE1, ARE2 – blue), the two androgen responsive regions are separated by a linker region of 42 nt present in the original probasin promoter sequence (black) and the promoter ends with the first 28 nt or the rat probasin promoter (green).*

The presence of this promoter upstream the Cre gene would assure that the enzyme will be specifically expressed only in the prostate lobes (ventral, lateral and dorsal) and epithelium; tissues that do not express Cre will be unaffected.

The same promoter fragment will be inserted into the pDoner vector to drive the expression of the shRNAs for knock-down Ncor1 and Ncor2/Smrt selectively in prostatic tissues. The promoter will be driven by a tetracycline sensitive silencer

that, in absence of antibiotic, will repress the ARR_2PB promoter and no hairpins will be transcribed. Upon tetracycline treatment the silencer is inhibited and the ARR2PB promoter will be able to drive the expression of the hairpins that will knock down Ncor1 and Ncor2/Smrt.

4.2.2 – Selection of the homology regions for Ncor1 and Ncor2/Smrt

The homology region represents the fragment of DNA that will be modified to include critical exons flanked by LoxP sites and Neo-resistance cassette. For the purposes of this thesis we will use the same homology regions as described for the conventional Ncor1 and Ncor2/Smrt knock out [139, 216]; this should guarantee that the targeted gene is not able to produce any functional protein upon Cre-mediated recombination.

4.2.2.1 – Ncor1

For Ncor1 a 8.5 kb region spanning exon 7 to exon 11 was chosen with the aim of knocking out the critical exons 7 and 8. This would induce a frameshift mutation if the resulting mRNA were translated.

4.2.2.2 – Ncor2/Smrt

The homology region chosen for Ncor2/Smrt is 10 kb long, from exon 23 to exon 33, including then the critical exons 26, 27, 28, 29 and 30 that will be flanked by LoxP sites..

4.2.3 – Cloning the homology regions for Ncor1 and Ncor2/Smrt

The first step to obtain a targeting construct was to clone the homology region. All primers, reagents and protocols are listed in Materials and Methods.

The isolation of the homology region implies a PCR reaction and the purification of the bands from an agarose gel. The first attempts to amplify the region from genomic DNA from G4 [220] and TS3 ES cells (Shimizu and Schrewe, unpublished) were unsuccessful because no PCR product was amplified (data not shown). Therefore two different BACs were ordered, one for Ncor1 and one for Ncor2/Smrt, in order to increase the specificity of the reaction and enrich the template with the fragments containing the homology region.

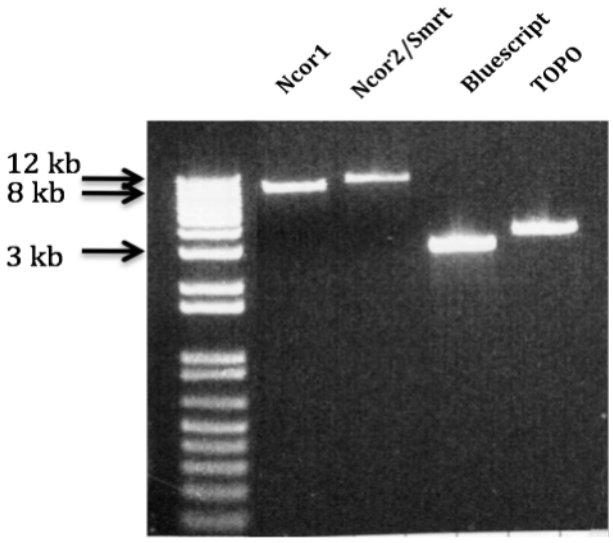

Fig 4.30 – *PCR amplification of the Ncor1 (8.5 kb) and Ncor2/Smrt (10 kb) homology region, included in the gel also the empty Bluescript and TOPO vector used in the cloning process.*

The desired fragments were successfully amplified from BAC DNA with the Phusion kit (see Materials and Methods) as seen in **Fig 4.30** ; the 8.5 (Ncor1) and 10 kb

(Ncor2/Smrt) bands were then purified and stored, ready to be ligated into the vector.

4.2.4 – Ligation of the homology regions into vectors

Two different vectors were used to clone the homology regions, BluescriptSK and pCR-BluntII-TOPO for Ncor1 and Ncor2/Smrt respectively.

However, the original pCR-BluntII-TOPO vector contains a PvuI restriction site in the sequence; looking that the homology region contains already a PvuI site designed to accommodate a LoxP site, the presence of both of them would generate two separate fragments instead of just opening the vector upon digestion. To overcome this the pCR-BluntII-TOPO vector was digested with PvuI, blunt ended and re-ligated in order to obtain a pCR-BluntII-TOPO without a PvuI site. To check that the vector didn't contain the restriction site anymore, a single and double digestion was performed with PvuI and EcoRI ± PvuI or ScaI. As shown in **Fig 4.31** the digestion with EcoRI, alone or in combination with PvuI or ScaI, linearized the vector while a supercoiled undigested vector was obtained digesting with PvuI in demonstration that the vector PvuI site was destroyed.

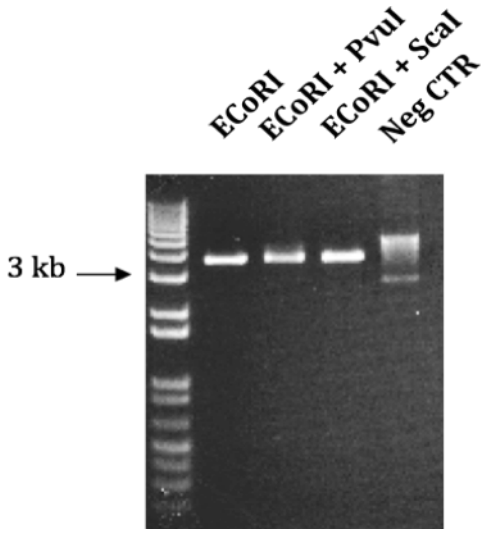

Fig 4.31 - *Digestion control of the pCR-BluntII-TOPO vector whitout a PvuI site. The modified vector contains only one EcoRI site, and the combined digestion with the PvuI and ScaI enzymes will linearize the vector instead of giving multiple fragments.*

Initially the ligation was unsuccessful due to the size of the fragment, the presence of sticky ends was needed then in both fragment and vector. New primers (Ncor1 XhoI Rev and Ncor1 Sac1 For for Ncor1 - Ncor2 EcorI Rev and Ncor2 EcoRI For for Ncor2. Sequences listed in **Table 3.2** of Matherials and Methods) were used to amplify the homology region from the BACs.; the Ncor1 fragment was then digested with XhoI and SacI and the Ncor2 fragment with EcoRI. The BluescriptSK vector was digested with SacI and XhoI and the pCR-BluntII-TOPO was digested with EcoRI in order to create complementary ends to the amplified homology regions and ligation was performed. A control digestion was made to check the presence of the right insert as shown in **Fig 4.32**.

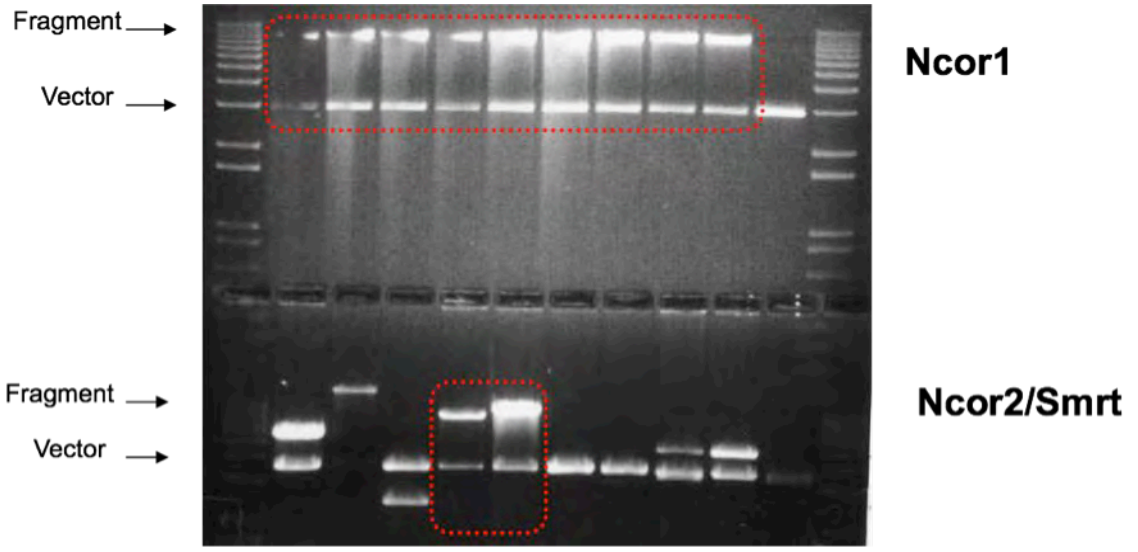

Fig 4.32 – *Digestion of the new samples ligated with Ncor1 and Ncor2/Smrt clones. Highlighted in red are the positive samples for Ncor1, 3 kb vector, 8.5 kb homology region (TOP) and Ncor2/Smrt, 3 kb vector, 10 kb homology region (BOTTOM).*

4.2.5 – Insertion of the first loxP site in the homology regions into into BluescriptSK and pCR-BluntII-TOPO vectors

The Cre-LoxP system requires the presence of two LoxP sites for a functional recombination. One LoxP site was cloned in the NcoI site in intron between exons 8 and 9 of the Ncor1 gene and the PvuI site in intron between exons 25 and 26 of the Ncor2/Smrt gene. The presence of the insert was confirmed with PCR screening for both targeting constructs using flanking primers as in **Fig 4.33**.

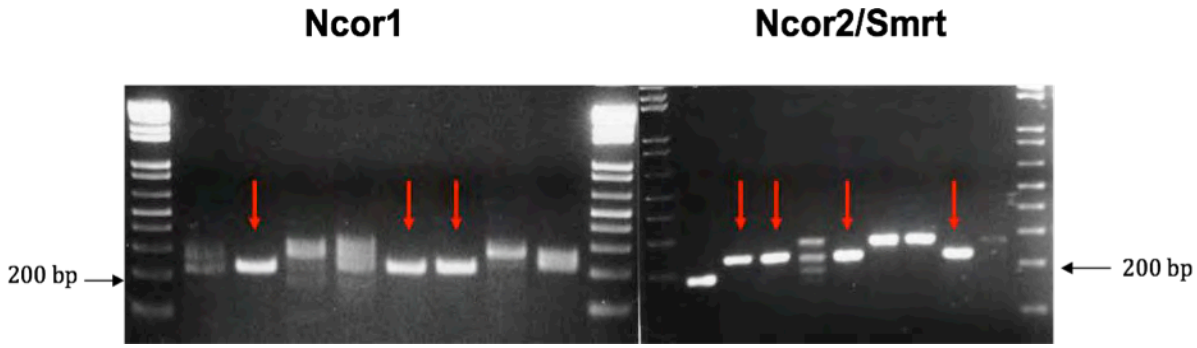

Fig 4.33 – *PCR analysis of the LoxP sites inserted in the Ncor1 (LEFT) and Ncor2/Smrt (RIGHT). Primers were flanking the insertion site and are listed in Table 3.3. Red arrows indicate positive clones at ~220 bp.*

4.2.6 – Isolation of the neo cassette and ligation into BluescriptSK and pCR-BluntII-TOPO vectors

The Neo-resistance cassette was originally part of the PL451 vector [221] containing a LoxP site and a neomycin selection cassette flanked by two FRT sites. Using the FLP-recombinase enzyme that excides the sequences included between the two FRT sites, the neo cassette can be removed with a mechanism similar to the Cre-Lox system. The fragment was isolated using EcoRV and NotI restriction enzymes, purified from agarose gel and Kleanow treated (to blunt the NotI restriction site). The pBluescript II SK-Ncor1 vector was digested with SnabI (blunt ends) and the pCR-BluntII-TOPO-Ncor2/Smrt vector with ScaI (blunt ends) and the blunted neo cassette was then ligated in these sites.

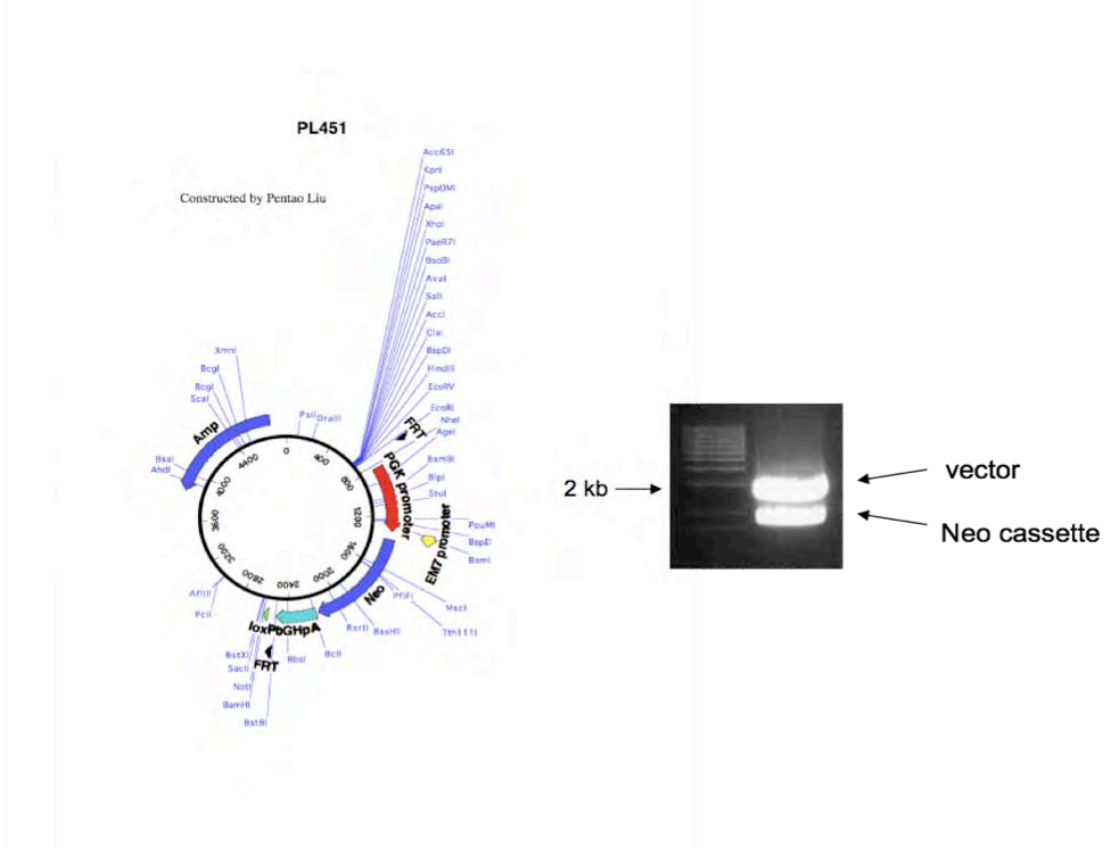

Fig 4.34 – *Scheme of the PL415 vector (LEFT) from which the neo-cassette was isolated and gel of the digestion with EcorV and NotI (RIGHT) showing the backbone of the vector and the neo cassette. The cassette was then isolated, purified and ligated into the Ncor1 and Ncor2/Smrt vectors.*

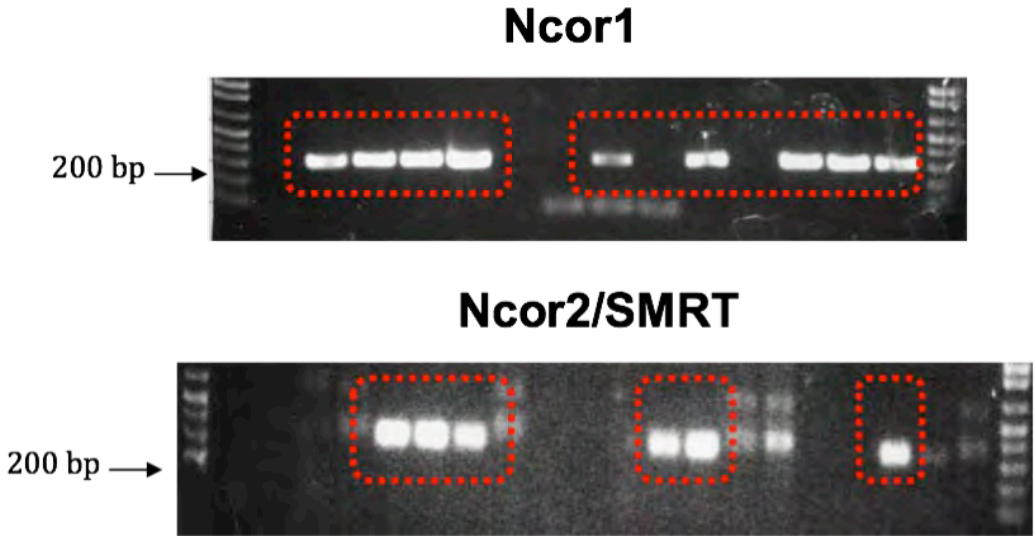

Fig 4.35 – *PCR screening for the Neo-cassette. Highlighted in the dotted red boxes are the positive clones.*

The presence of the neo-cassette was demonstrated via PCR analysis with the following combination of primers: Ncor1 SnaBI Rev and Neo 5' Rev for Ncor1, and Ncor2 ScaI For and Neo 5' For for Ncor2 (sequences listed in **Table 3.5**). Two reverse primers were used to screen the Ncor1 construct because the neo cassette in the Ncor1 construct has opposite orientation than the one in the Ncor2/Smrt construct. As shown in **Fig 4.35** the presence of the neo cassette was confirmed in several clones.

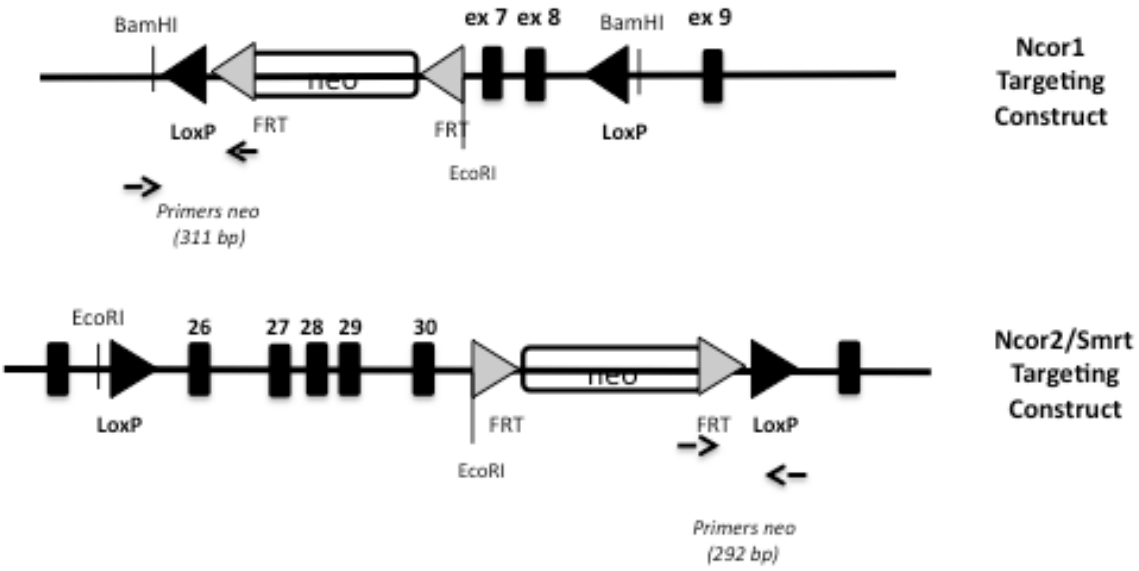

Fig 4.36 – *Schematic representation of the Ncor1 and Ncor2/Smrt construct containing the neo-cassette. Indicated is also the opposite orientation of the neo cassettes and the LoxP sites..*

4.2.7 – Digestions control and sequencing of candidate clones

Samples were checked for the presence of the right inserts via restriction enzyme digestion and then sequenced. Previously identified clones were digested with

BamH1 (Ncor1) and EcoRI (Ncor2/Smrt) to check the fragments lengths; as expected, the pBluescript II SK-Ncor1 vector gave three fragments of 6.7, 4.7 and 1.8 kb and the digested pCR-BluntII-TOPO-Ncor2/Smrt gave three bands at 3.4, 4.2 and 5.7 kb.

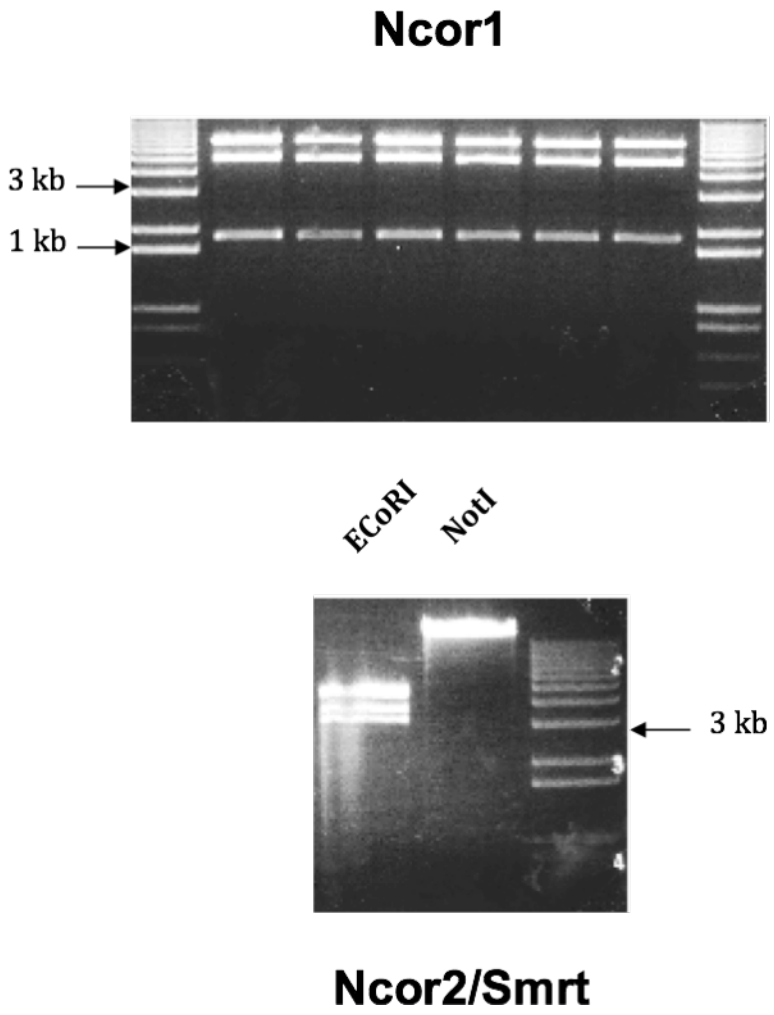

Fig 4.37 – *Digestion control for Ncor1 and Ncor2/Smrt clones. All the clones for Ncor1 (TOP) are positive with the right pattern; Ncor2/Smrt (BOTTOM) is correctly fragmented with EcoRI and linearized with NotI digestion.*

The positive samples were then sent to MWG (www.mwg.com) for sequencing and the results indicated the correct presence, in both vector, of the right constructs.

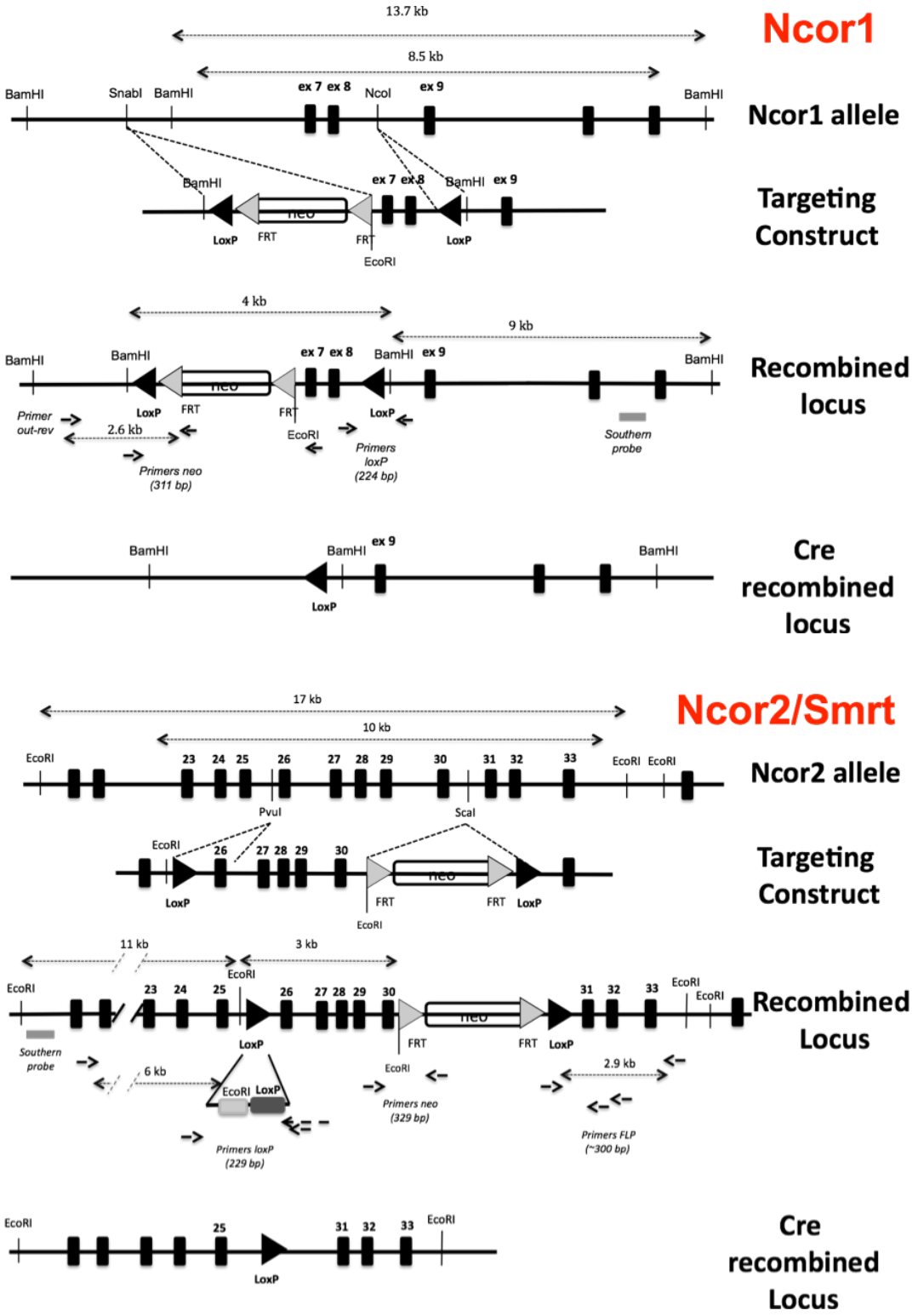

Fig 4.38 – *Schematic representation of the final constructs for Ncor1 (TOP) and Ncor2/Smrt (BOTTOM). For both genes are indicated the sites where the LoxP sites were inserted (NcoI for Ncor1 and PvuI for Ncor2/Smrt) and where the neo-cassettes*

were ligated (SnaBI for Ncor1 and ScaI for Ncor2/Smrt). The Ncor1 and Ncor2/Smrt wild type alleles are shown at the top of each image with indicated exon numbers and restriction sites. The targeting constructs containing loxP sites and neo cassettes is shown below the wild type alleles. In case recombination happens, the resulting floxed allele is here represented by the recombined locus. Lastly, upon action of the Cre enzyme the targeted exons will be excided and the Cre recombined locus will contain only one loxP site. Primers shown are listed in Materials and Methods.

4.2.9 – Electroporation of ES cells and G418 selection

After that positive clones were confirmed 10^7 G4 [220] embryonic stem cells were electroporated with 25 μg of construct, the cells plated on four 6 cm dishes and after 48-72 hours media was changed to selection medium, ES media plus 350 μg/ml of G418.

After 7-8 days of selection, approximately 200 single colonies were picked and expanded in 96 well plates to perform further screenings.

Fig 4.39 – *Example of a colony plate. Colonies were picked with a p10 tip under the microscope paying attention to isolate single colonies. Yellow wells contain cells that used all the nutrients and oxygen lowering the pH, hence, a shift in the color of the media. Red wells are instead empty due to manual error and the pH of the media remains unaltered.*

4.2.10 – Colony screening to identify positive clones via PCR and Southern blotting

In order to find which positive clones that contained the floxed allele (allele with the LoxP sites), the clones were screened via PCR and Southern blotting.

4.2.10.1 – PCR screening of the candidate clones

The first screening was PCR based amplifying a 2.6 kb fragment at the 5' of the homology region for Ncor1. Primers used were Ncor1 out Rev (outside of the homology region) and neo poly-A For (on the poly-A sequence of the neo cassette). Primer sequences are listed in **Table 3.6**.

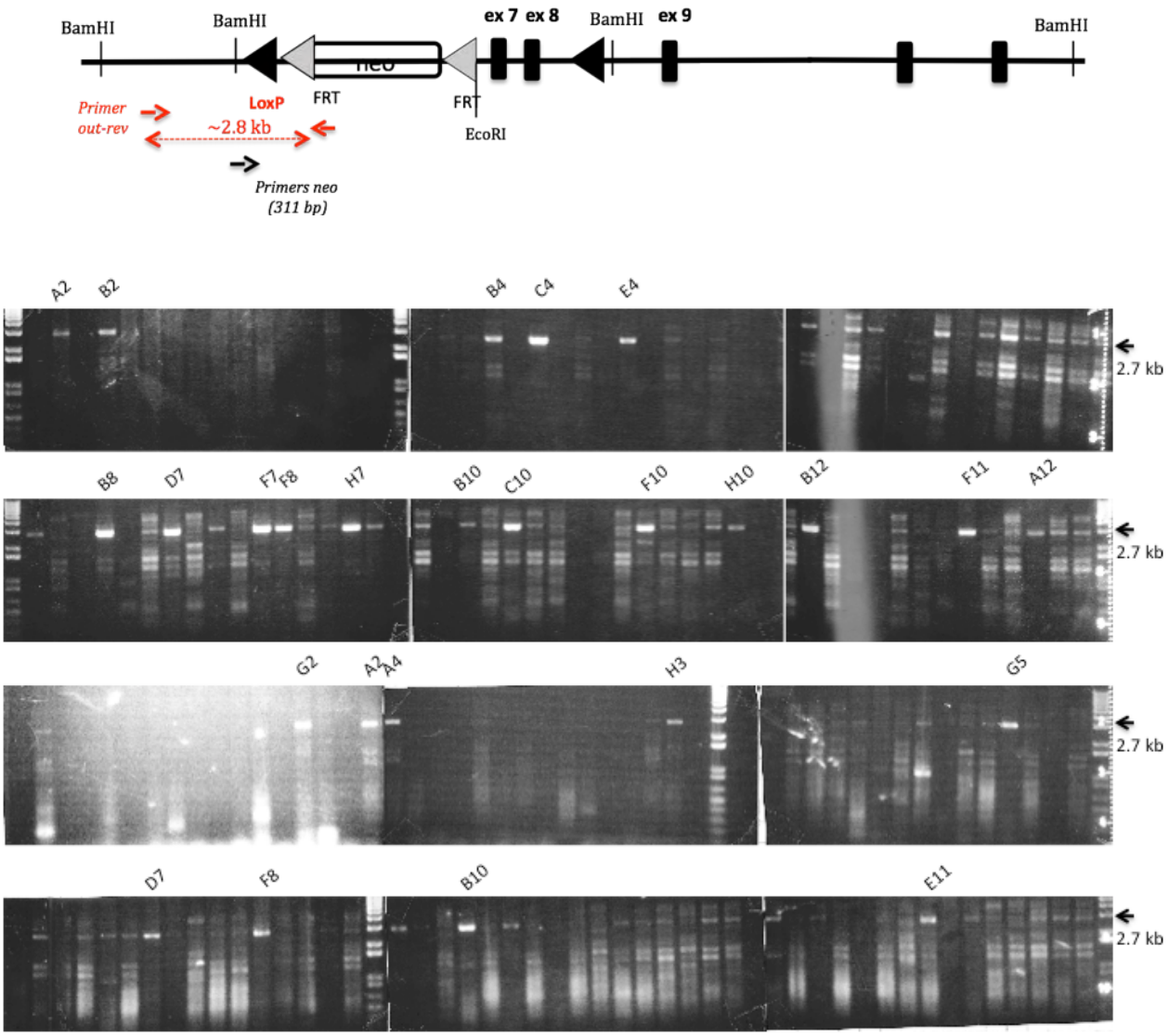

Fig 4.40 – *Schematic representation of the region amplified in the PCR screening for the Ncor1 colonies (TOP). The clones highlighted were then further screened (see below) to confirm the presence of the Neo-cassette.*

The PCR screening for the Ncor2/Smrt clones aimed to amplify a 3 kb fragment at the 3' of the homology region for Ncor2/Smrt. Primers used were Ncor2 out Rev (outside of the homology region) and neo poly-A For (on the poly-A sequence of the neo cassette). Primer sequences are listed in **Table 3.6**.

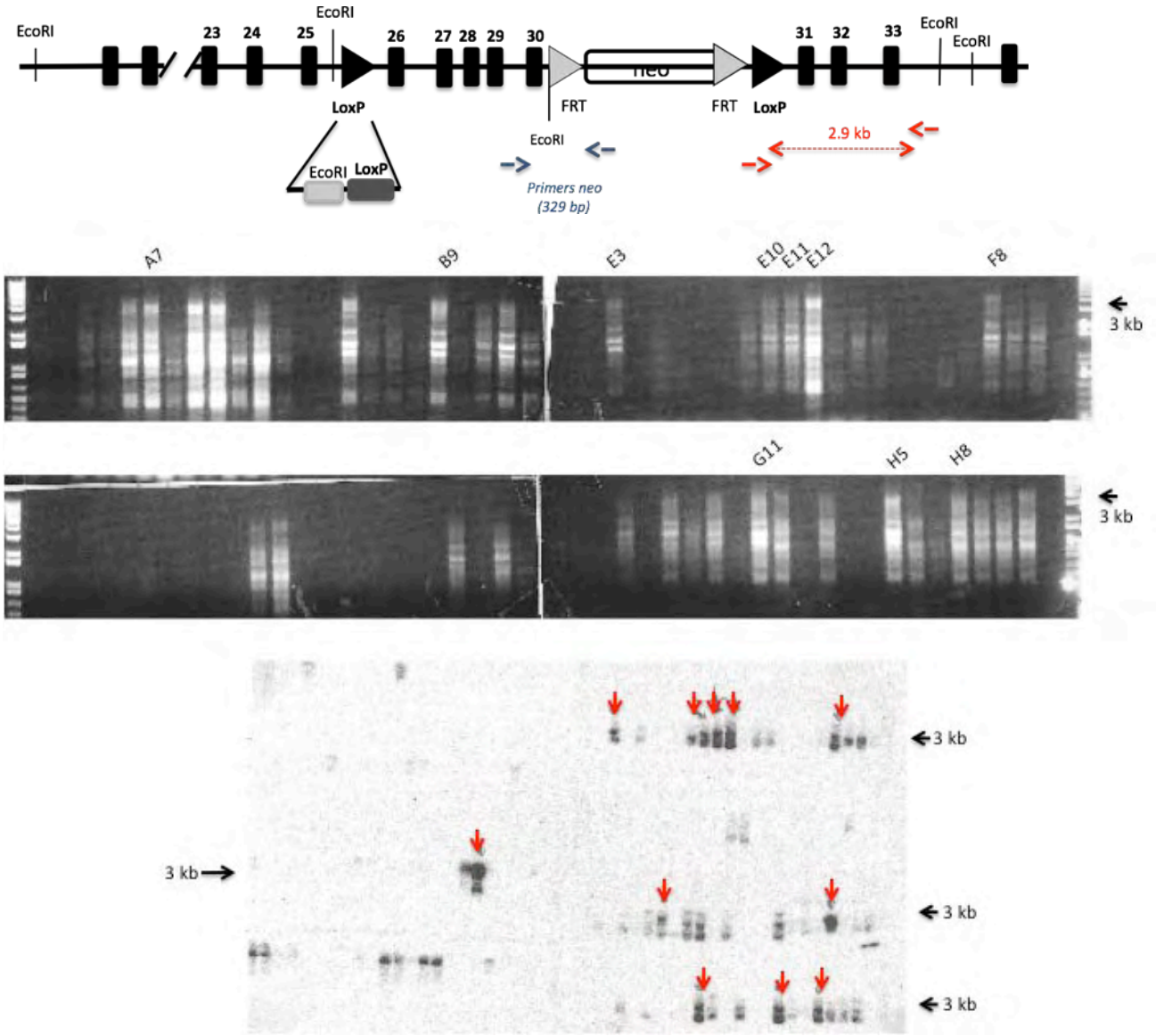

Fig 4.41 – *Schematic representation of the PCR screening for the Neo-cassette in the Ncor2/Smrt clones (TOP). A 2.9 kb region was amplified (MIDDLE) and to better localize the positive clones a southern blotting was performed (BOTTOM) using the samples ran in the gels as template. The probe was the 3' primer (Ncor2 out Rev – Table 3.6) used for the PCR. Red arrows indicate the positive clones used for further analysis.*

To confirm further the positive clones previously identified primers spanning the 5'

(Ncor1) and 3' (Ncor2/Smrt) end of the Neo resistance cassette were used; the

amplification of the 3 kb fragment would also confirm the presence one of the two LoxP sites needed for a correct Cre-Lox recombination.

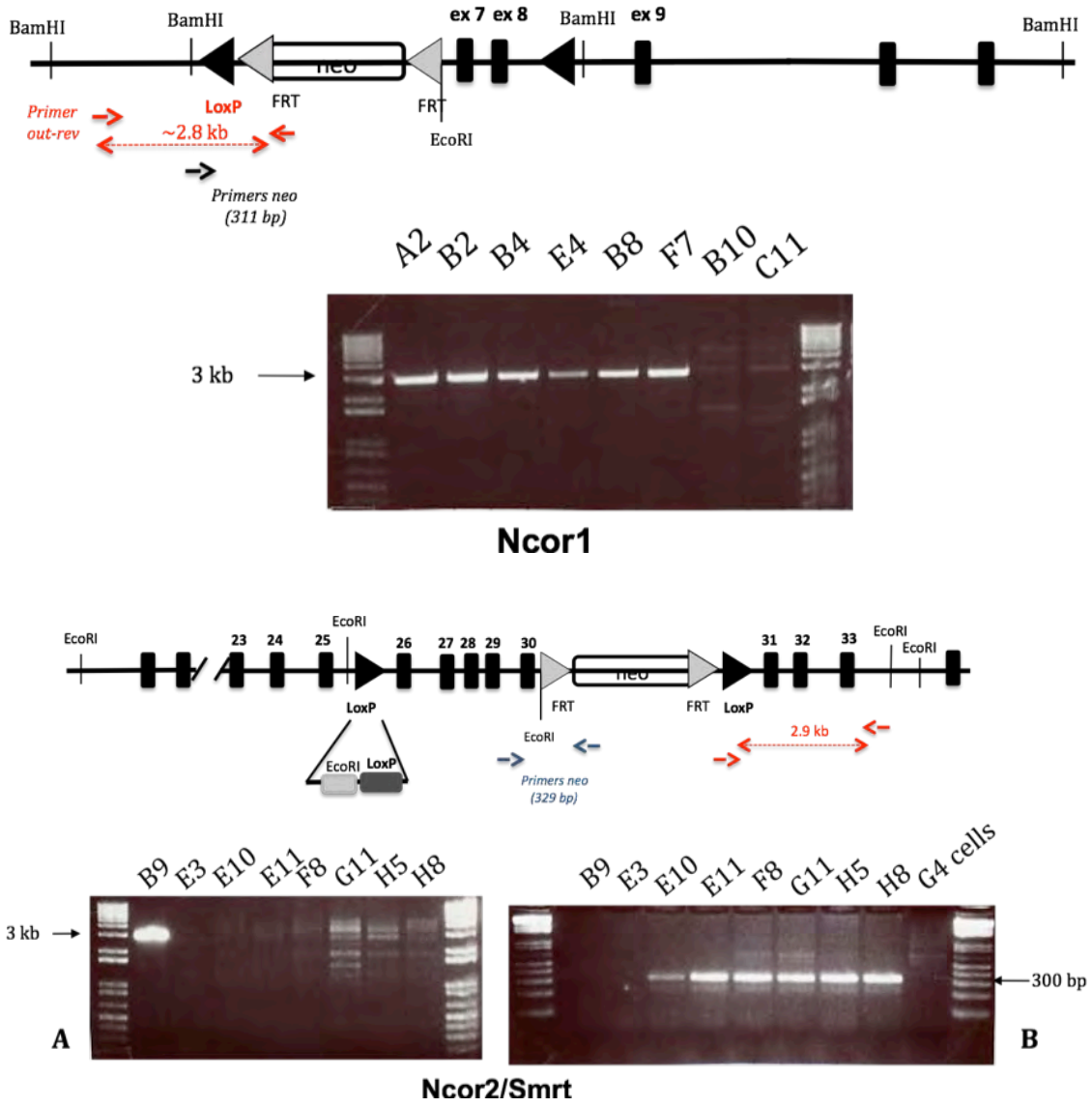

Fig 4.42 – *PCR screening for the Neo-cassette in Ncor1 clones (TOP) A2, B2, B4, E4, B8, F7, B10, C11 and Ncor2/Smrt (BOTTOM) clones B9, E3, E10, E11, F8, G11, H5, H8. I performed two different PCRs for Ncor2/Smrt, A-B, to confirm the results obtained in A.*

Next, second LoxP was checked expecting a ~220 bp fragment for the floxed allele plus a ~180 bp for the wild type allele.

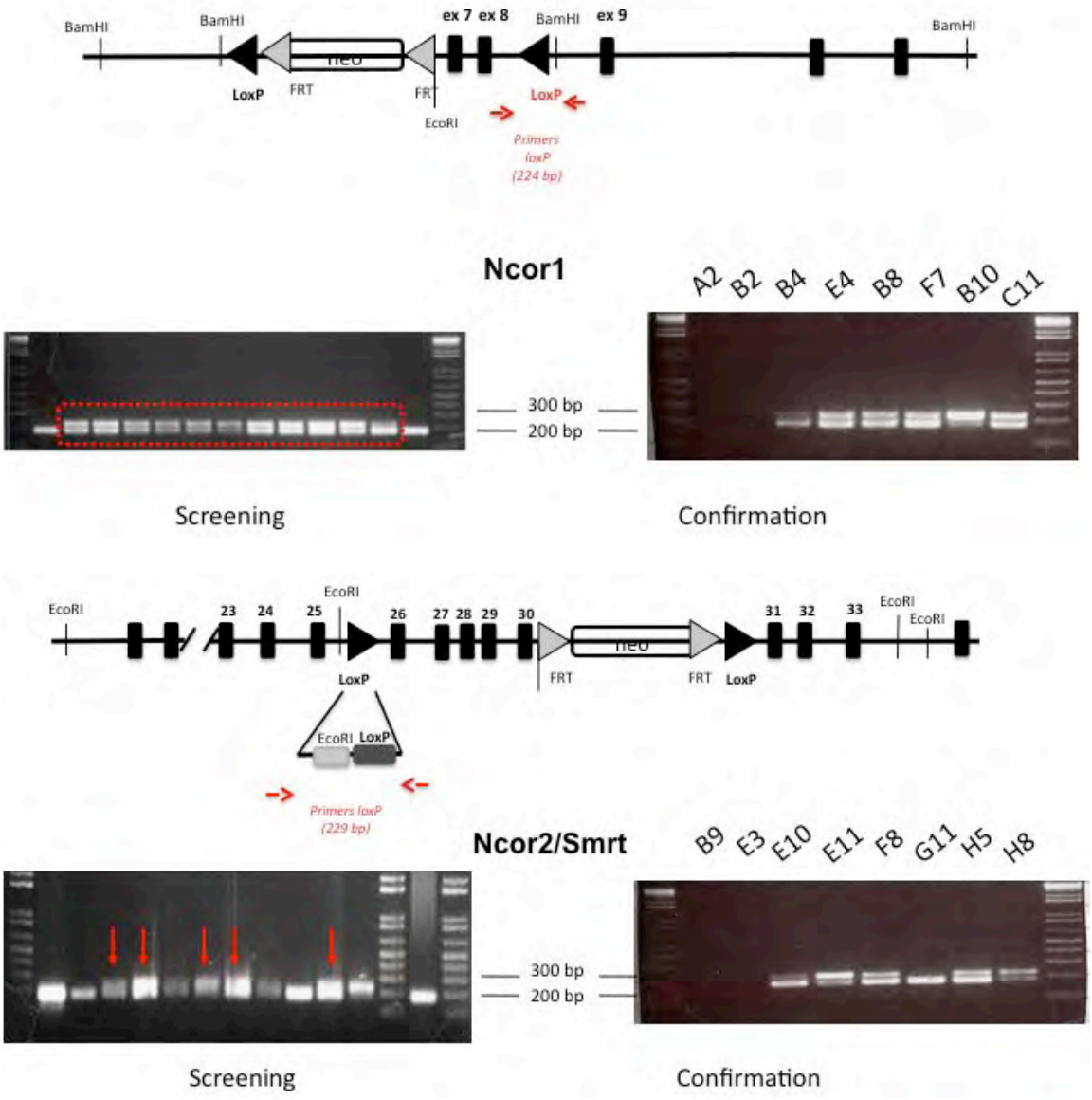

Fig 4.43 – *PCR analysis to confirm the screening results for the presence of the LoxP sites in the electroporated ES cells. It was also confirmed that the loxP sites in the Ncor1 and Ncor2/Smrt clones have opposite orientation.*

To confirm further the presence of the second LoxP site in the intron between exon 25 and 26 in the Ncor2/Smrt clones, a nested PCR was performed amplifying first a

6 kb fragment containing the LoxP site at the 3' end and then, for the next PCR, a 3' primer was designed with the last 2 nucleotides crossing the 3' boundary of the LoxP site. This was enough to confer specificity to the reaction and, as shown by the gel below, the negative clone in lane 6 was the only one not amplified as well as the wild type band was not amplified.

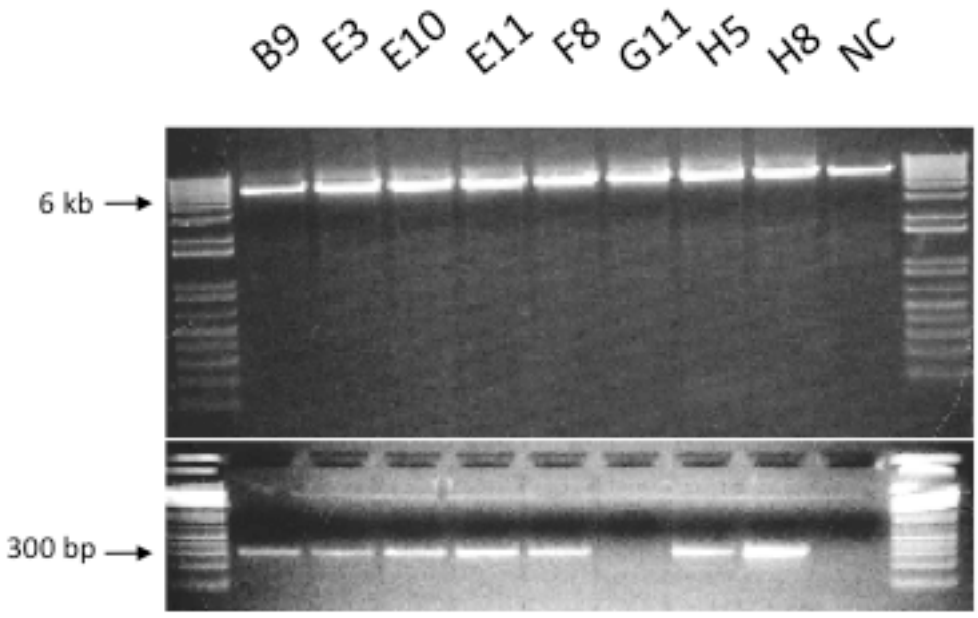

Fig 4.44 – *PCR screening of the LoxP site in the Ncor2/Smrt samples. On top the first 6 kb PCR, the bands were purified and used as a template for the second PCR showed at the bottom. For the first 6 kb PCR primers used were Ncor2 LoxP out FW and Ncor2 LoxP RW2 and for the nested PCR the primers used were Ncor2 PvuI For and Ncor2 LoxP RW2 (sequences listed in Tab 3.6).*

4.2.10.2 – Southern blotting screening of the candidate clones

In order to screen the opposite region of the construct Southern probes specific for our genes were designed.

The probe was designed to detect a 9 and 13.7 kb band for Ncor1 and Ncor2/Smrt, respectively. As is possible to see from the images below, Ncor1 clones presents equimolar bands floxed and non-floxed allele at the correct size while Ncor2/Smrt clones show the right wild type band and a ~14 kb fragment for the floxed allele.

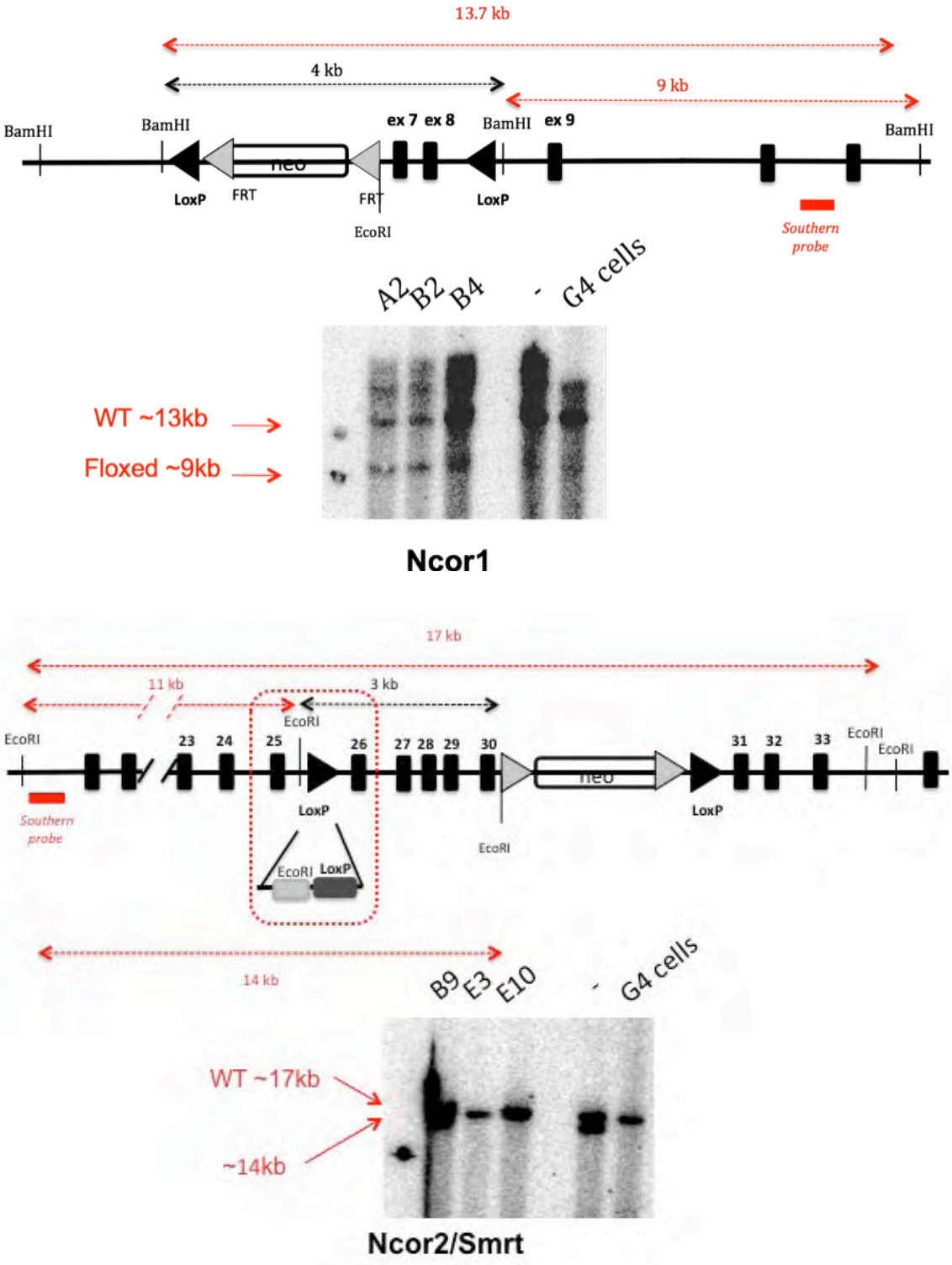

Fig 4.45 – *Southern blotting for Ncor1 (TOP) and Ncor2/Smrt (BOTTOM). Ncor1 clones show correctly the floxed allele, Ncor2/Smrt clones present instead a 14 kb fragment instead of the predicted 11 kb.*

To understand weather the presence of a 14 kb fragment was caused by a non-functional EcoRI site flanking the LoxP site, a 6 kb fragment that included the LoxP site was amplified and sequenced the PCR product; the results showed that the LoxP site is intact but when the probe was sequenced the sequence obtained did not match the original probe sequence explaining why the initial screening didn't work.

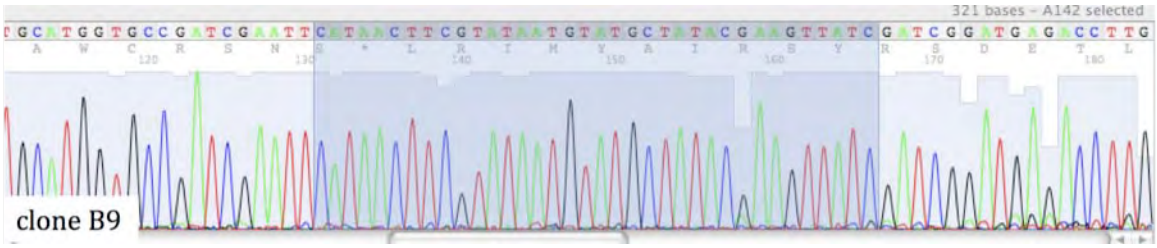

Fig 4.46 – *Sequence of the LoxP site for the B9 clone of Ncor2/Smrt. Highlighted in blue is the LoxP sequence, containing the EcoRI site.*

However, the positive and selective results from the PCR in **Fig 4.44** already confirmed the presence of the LoxP site in this region.

The presence of the correct neo cassette was also analysed via Southern blotting and, as shown in **Fig 4.47** B9, E11 and F8 for Ncor2/Smrt as well as B4 for Ncor1 were positive.

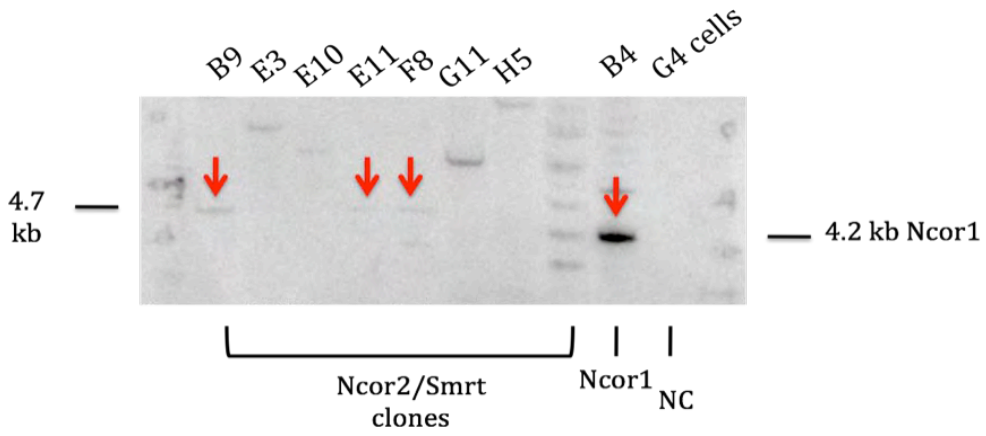

Fig 4.47 – *Southern blotting for Neo-cassette in Nco2/Smrt and Ncor1 clones digested with EcoRI. The predicted size was 4.7 kb for Ncor2/Smrt and 4.2 kb for Ncor1. DNA from G4 cells, as expected, was negative.*

The final clones chosen were B9 for Ncor2/Smrt and B4 for Ncor1 and they currently used at the Roswell Park Cancer Institute (Buffalo, NY, USA) for blastocyst injection in order to generate conditional knock-out mice.

4.2.11 – Knock down strategy via shRNA of Ncor1 and Ncor2/Smrt

Obtaining a knock out animal will allow working with a clean system with no residual activity of the target protein; however, there is no temporal control on the activity of the Cre enzyme that will be transcribed only when the mice reach puberty and the ARR_2PB promoter will be activated by the circulating hormones. To gain the temporal control over the knock down we sought to create an inducible system where the prostate-specific promoter is controlled by a tetracycline-regulated inhibitor, hence, treatment with Doxycycline will block the expression of the inhibitor allowing the short hairpin RNA to be transcribed.

The vector was created at the Department of Molecular Genetics at the Max Planck Institute for Molecular Genetics in Berlin (Germany); the final version contains a

Bluescript backbone, CMV promoter, eGFP reporter, ampicillin resistance and one insulator to avoid interferences on the promoter activity. The Doner vector can recombine with the ROSA26 locus (ES cell containing the ROSA26 locus were created at the Department of Developmental Genetics at the Max Plank Institute for Molecular Genetics in Berlin, Germany) that contains a tetracycline sensitive silencer. In the absence of tetracycline the silencer represses the activity of the ARR_2PB promoter while upon tetracycline treatment the activity of the silencer is inhibited, allowing the activation of the promoter. This gives the temporal control over the production of the shRNAs, hence over the knockdown, that would not be possible to achieve in the knockout system.

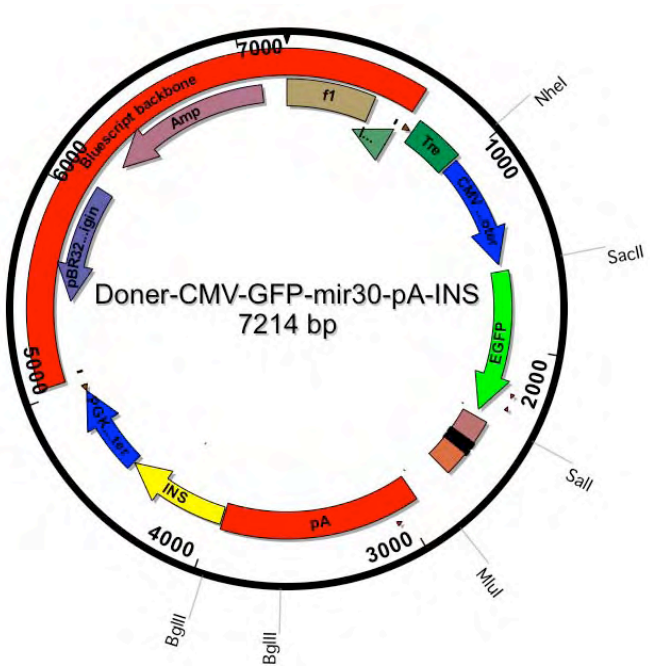

Fig 4.48 *– Map of the pDoner vector that will be used to create the prostate specific knock down of Ncor1 and Ncor2/Smrt. The CMV promoter will be substituted with the ARR_2PB promoter and the hairpins inserted in the mir30 site.*

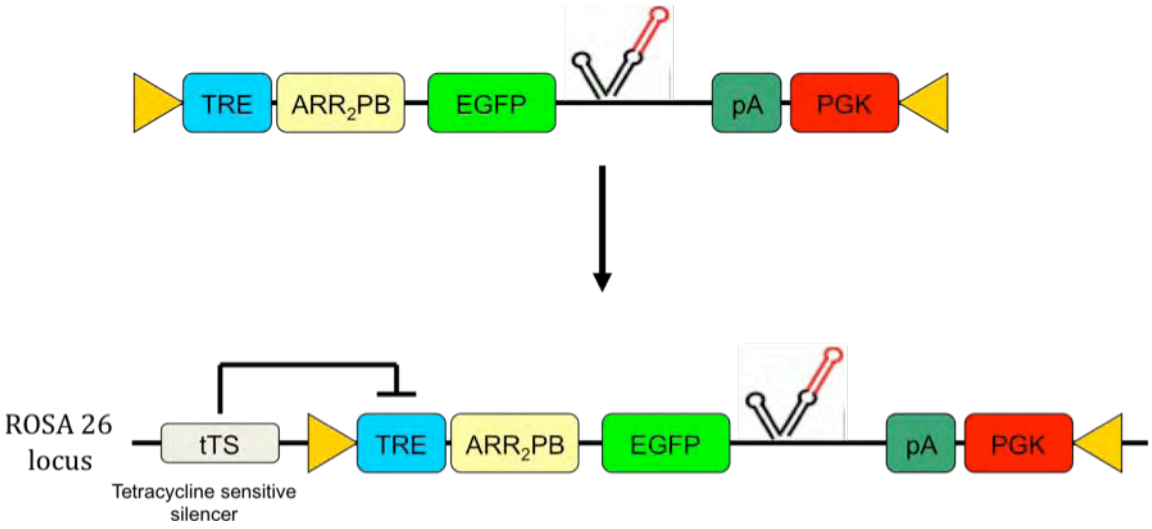

Fig 4.49 – *Scheme of the mechanism of action of the Doner vector inserted in the ROSA26 locus. In absence of tetracycline the silencer represses the activity of the ARR2PB promoter, blocking the production of the shRNAs. The presence of tetracycline inhibits the activity of the silencer, allowing the activation of the promoter and transcription of the shRNAs, hence, the knockdown of the target genes.*

4.2.12 – Design shRNA for Ncor1-Ncor2/Smrt

The first step in the creation of a knock down system was to design reliable hairpins that could efficiently target Ncor1 and Ncor2/Smrt; to do this the online siRNA design tool form Invitrogen (http://www.invitrogen.com) was used, three hairpins for gene were designed targeting respectively exons 11, 27 and 37 in Ncor1 and 8, 32 and 42 in Ncor2/Smrt. Sequences are available in Materials and Methods.

4.2.13 – Cloning, ligation and sequencing of the clones

The hairpins were cloned into the vector obtained with the original kit following the manufacturer's instructions (see Materials and Methods); digestion control was made from minipreps and samples were sent to sequencing to confirm the presence of the right hairpin.

(at the moment of writing this thesis the sequencing data are stored at the Max Planck Institute for Molecular Genetics, Berlin, Germany)

4.2.15 – Cloning of the promoter and ligation into the pDoner vector

In order to create a prostate-specific knock down the original a CMV promoter had to be exchanged with the ARR_2PB.

An 800 bp region containing the AAR_2PB promoter was amplified from genomic DNA coming form AAR_2PB-Cre mice (Roswell Park Cancer Institute, Buffalo, NY, USA), the product shown in **Fig 4.50** was isolated and ligated in the pCRII-TOPO vector for further cloning.

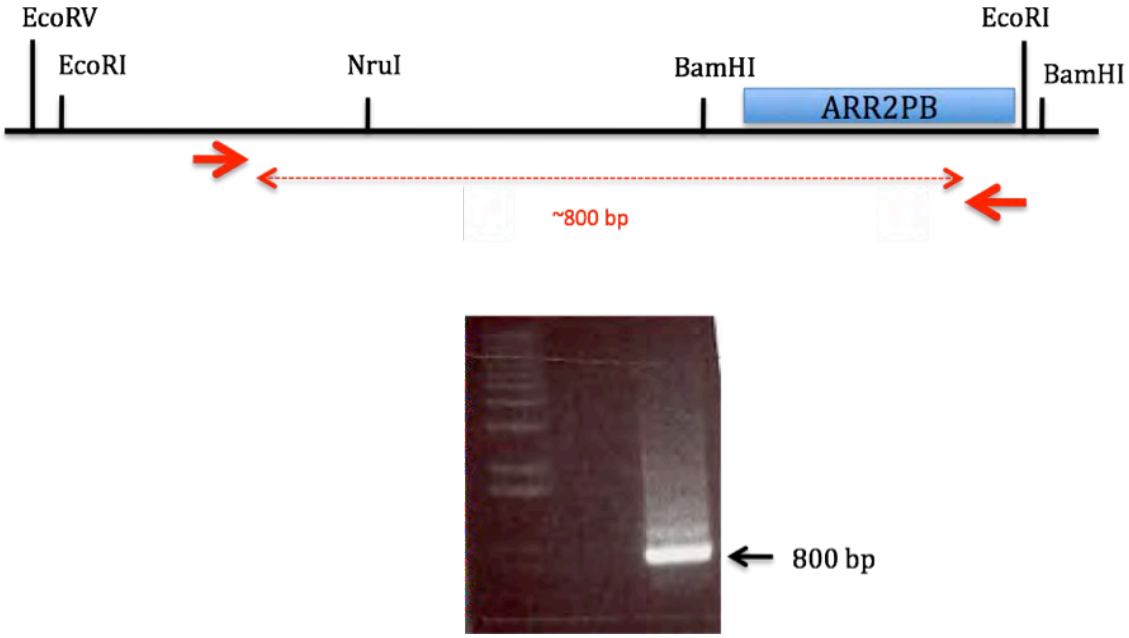

Fig 4.50 – *PCR amplification of the ARR2PB promoter from two samples with MIR13 FW and GFP RW primers. The bands were purified prior being digested with BamHI and blunt ended.*

After that DNA was isolated from bacteria a first PCR-based screening was performed to check which clones were positive. To do that primers outside the cloning region of the pCRII-TOPO vector were used and minipreps were digested with EcoRI the positive clones to confirm the presence of the promoter. As shown in **Fig 4.51** the right construct was present in two of the clones

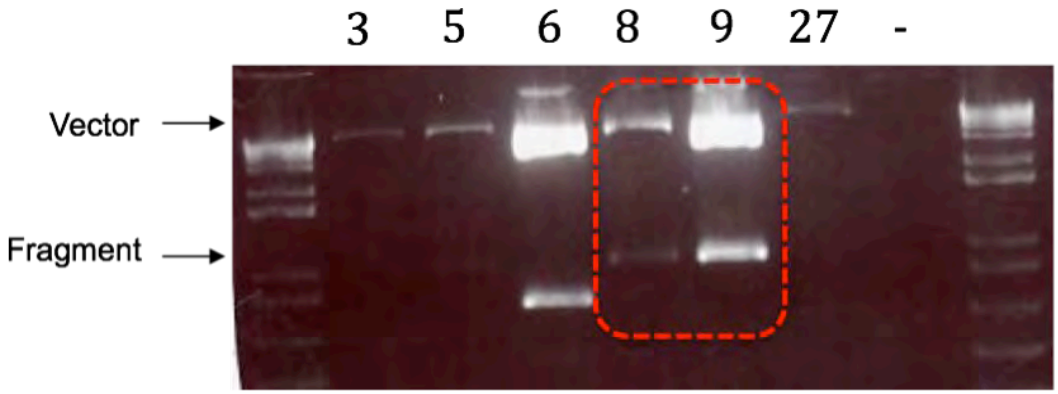

Fig 4.51 – *Digestion control of the pCRII-TOPO vector containing the ARR_2PB promoter. Digestion of the clones 8 and 9 gave the right fragment length, those clones were then sent to sequencing to confirm the presence of the promoter.*

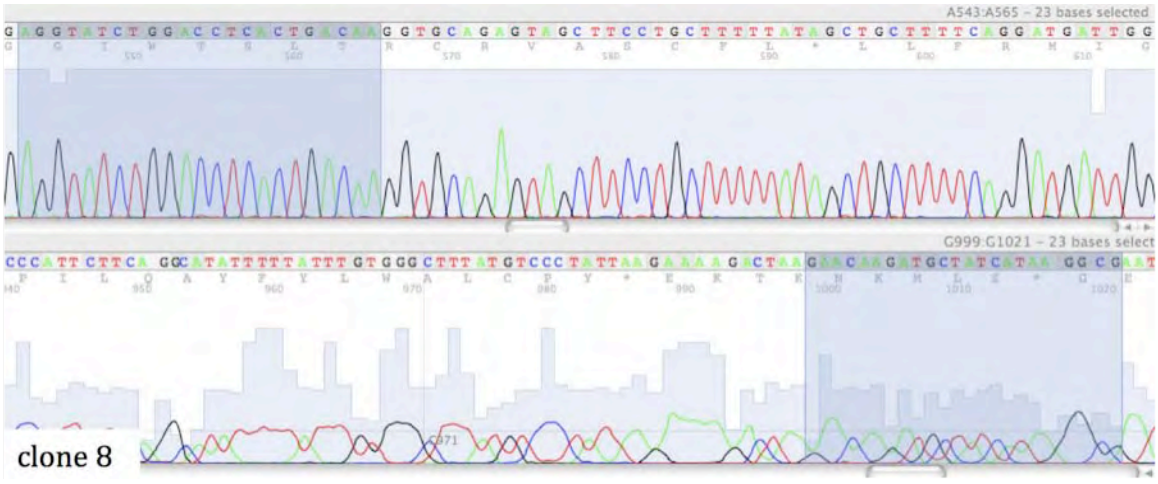

Fig 4.52 – *Sequencing results for the clone number 8 that resulted to be the only one with the promoter in the right orientation. Highlighted in blue the beginning and the end of the sequenced promoter region.*

In the meanwhile the original CMV promoter was excised with NheI and SacII and the vector blunt ended before ligating the ARR_2PB promoted into the pDoner vector. At the time of writing this thesis we are confirming the presence of the appropriate promoter into the vector.

4.3 – SYSTEMS BIOLOGY APPROACH TO MODEL CDKN1A TRASCTIPTIONAL INITIATION

4.3.1 – *CDKN1A* time course upon $1,25(OH)_2D_3$ treatment

4.3.1.1 – Background

The cyclin-dependent kinase inhibitor 1A (*CDKN1A*, encodes $p21^{(waf1/cip1)}$) gene is located on human chromosome 6 in position p21.2 [222]; CDKN1A blocks cell cycle progression at G1 binding to, and inhibiting the activity of cyclin-CDK2 or -CDK4 complexes, which is required for the phosphorylation of RB and the consequent release and activation of E2f-dependent gene expression; nonetheless, it is involved in the firing of replication origins and DNA synthesis (reviewed in [223]). The expression of this gene is tightly controlled for example by the tumor suppressor protein p53, through which this protein mediates the p53-dependent cell cycle G1 phase arrest in response to a variety of stress stimuli [222]. However, activation of CDKN1A in a p53-independent fashion has also been reported. CDKN1A does not only control cell cycle but also apoptosis; this can be accomplished in two different ways: 1) an active cell cycle is required to sense these agents and trigger apoptosis and the cytostatic effect of CDKN1A with the consequent inhibition of apoptosis, however, is counteracted by several mechanisms (i.e. downregulation of its expression) and 2) post-translational

modifications of CDKN1A such as its phosphorylation (which affects protein stability or cytoplasmic localization of CDKN1A) and its cleavage by caspase 3 also account for the differential effects on cell cycle arrest versus apoptosis [223]. Moreover, CDKN1A has a significant role in modulating DNA repair processes. First, by inhibiting cell cycle progression, p21 allows DNA repair to proceed while inhibiting apoptosis. Secondly, CDKN1A can compete for PCNA binding with several PCNA-reliant proteins that are directly involved in DNA repair processes [223].

Upon treatment, $1,25(OH)_2D_3$ binds to VDR and activates responsive elements in the CDKN1A promoter leading to transcription. $1,25(OH)_2D_3$ stimulation exerts profound anti-proliferative effect on non-malignant prostate cells RWPE-1 and G1 cell cycle arrest suggesting the involvement of the CDKN1A pathway. CDKN1A is also a Vitamin D Receptor target gene, ChIP analysis demonstrated indeed that the promoter region of CDKN1A contains three VDREs as well as p53 responsive elements [224, 225].

The micro-RNA miR106-B is a newly-identified transcript present in the intronic region of the MCM7 gene and able to promote *CDKN1A* degradation [226]. Recently, miR-106B was shown to be involved in multiple myeloma [227] and in chronic lymphocytic leukemia, the latter via association, and downregulation, of the E3-ubiquitinge ligase *Itch* with the net result of upregulating p73 and p53, favouring apoptosis [228]. To date, there are no publications showing the role of miR-106B in prostate cancer and preliminary results from our lab show that not only it's a regulator of *CDKN1A* transcription and degradation and correlates with its expression in tumor samples (personal communication, data not shown).

4.3.1.2 – Background data

Starting from the hypothesis that *CDKN1A* is involved in the antiproliferative effect of $1,25(OH)_2D_3$, a time course experiment over 24 hours was undertaken in RWPE-1 cells treated with 100 nM of $1,25(OH)_2D_3$. RNA was extracted and random hexamers were used to reverse transcribe the samples. *CDKN1A* induction was quantified with qRT-PCR TaqMan as described in Materials and Methods, each time point had a time zero matching control and the time points were the followings (in hours): 0.00, 0.16, 0.25, 0.32, 0.50, 0.66, 0.75, 0.82, 1.00, 1.16, 1.32, 1.50, 1.66, 1.82, 2.00, 3.00, 4.00, 5.00, 6.00, 8.00, 10.00, 12.00, 16.00, 18.00, 19.00, 20.00, 21.00, 22.00, 23.00 and 24.00.

The graph in **Fig 4.53** shows *CDKN1A* mRNA accumulation upon 100 nM $VitD_3$ treatment. The presence of ~10 minutes time points within the first hour offers an interesting and precise insight on the possible mechanism of transcription initiation in response to $1,25(OH)_2D_3$.

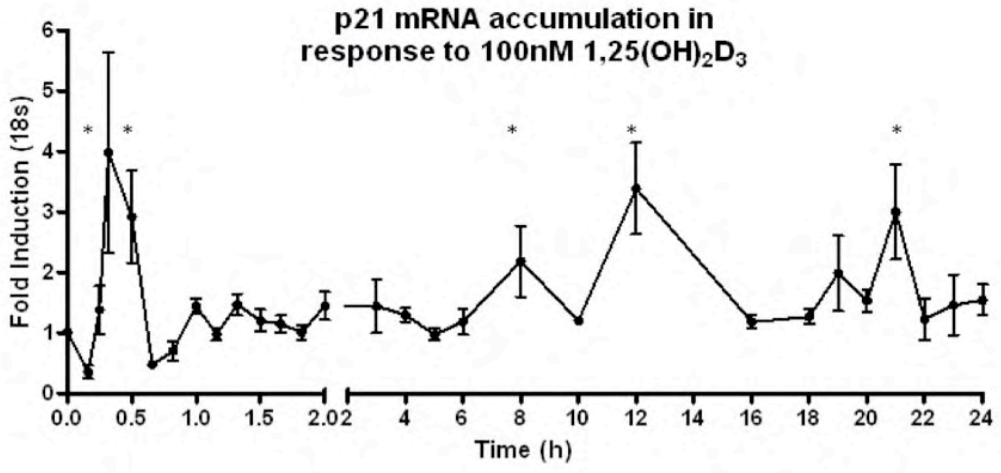

***Fig 4.53** – Time course for p21 mRNA accumulation upon $VitD_3$ treatment (James Thorne, University of Birmingham, Birmingham, UK). Mid-exponential RWPE-1 cells were treated with 100 nM $1,25(OH)_2D_3$, total RNA was extracted and reverse transcribed prior qRT-PCR. Student-t test was used to confirm time points significantly differentially expressed from the corresponding time zero control, *=p<0.01. Each data point is the mean of at least three biological replicates +/- S.E.M..*

The overall impression of the time course is that mRNA production and degradation follow a periodical pattern, reflected by peaks at 30 min, 8, 12 and 21 hours. The initial upregulation of *CDKN1A* at ~30 minutes just after an initial down-regulation of the mRNA levels and, very interestingly, the quick synthesis of mRNA was followed by an equally quick degradation of the detected mRNA. Taking in consideration the average time required by the RNA polymerase II to synthesize an RNA molecule (up to 3.6 kb/min [229]) and the length of the initial transcript (~ 6 kb), it's possible to estimate that it takes less than 2 minutes to synthesize one molecule of mRNA. Another variable that must also be considered is that random hexamers and not Oligo-dTs were used to reverse transcribe the RNA. This means that not only fully mature mRNA was synthesized but also non processed RNA molecules were used as template to produce cDNA. The time needed for the $1,25(OH)_2D_3$-VDR bound complex to enrich the promoter region and sequestrate the Pol-II in order to start transcription is relative quick and it's possible to assume that this happens in order of seconds. These data could easily sustain the idea that the initial peak could be caused by a quick stimulation mediated by the $1,25(OH)_2D_3$-VDR complex.

However, all the above data still do not explain the rapid degradation that occurs straight after 30 minutes peak. Physiological mRNA decay does not explain this case because it occurs too quickly. Ivanovska and colleagues demonstrated that the micro RNA miR-106B directly targets *CDKN1A* in two regions and that its silencing plays a key role in miR-106b-induced cell cycle phenotypes [230]. Time course experiments measuring miR-106b induction upon 100 nM $VitD_3$ treatment was made to confirm at the following

time points (in hours): 0.00, 0.16, 0.25, 0.32, 0.50, 0.66, 0.75, 0.82, 1.00, 1.16, 1.32, 1.50, 1.66, 1.82, 2.00, 3.00, 4.00, 5.00, 6.00, 8.00, 10.00, 12.00, 16.00, 18.00, 19.00, 20.00, 21.00, 22.00, 23.00 and 24.00. The results shown in **Fig 4.54**, illustrate that the expression pattern of miR-106B strictly resembles *CDKN1A* time course. The initial peak at ~30 mins is still present with a rapid induction followed by an equally quick degradation, as already observed for *CDKN1A*; also, magnitude and amplitude of the peaks at 12 and 22 hours match the peaks detected for CDKN1A.

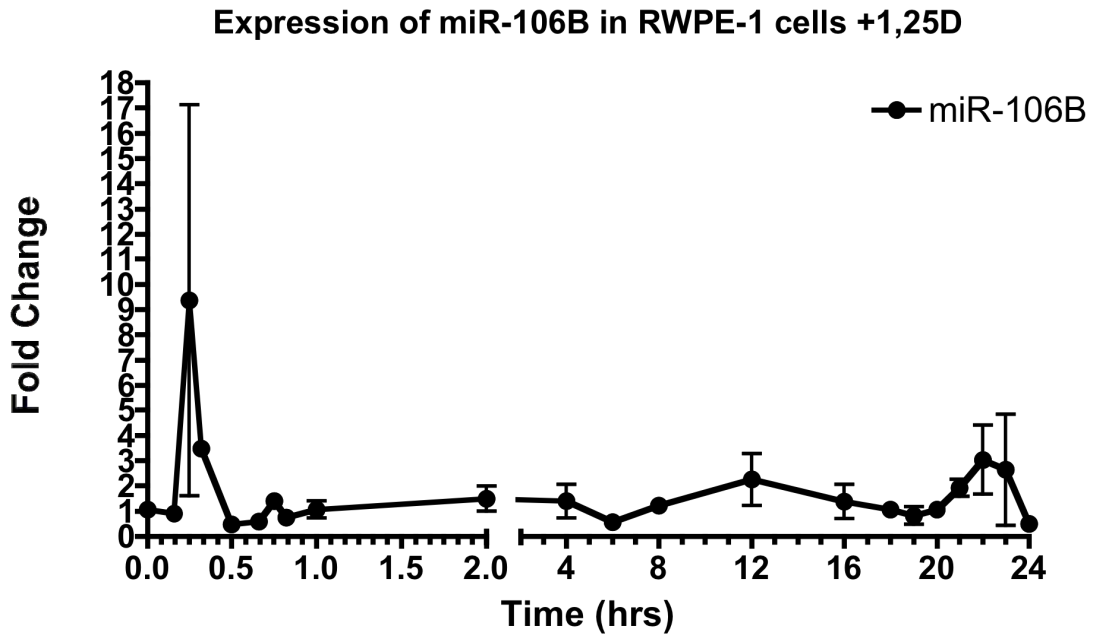

Fig 4.54 *– miR-106B time course in response to 1,25(OH)$_2$D$_3$ (Orla Maguire, Roswell Park Cancer Institute, Buffalo, NY, USA). Mid-exponential RWPE-1 cells were treated with 100 nM 1,25(OH)$_2$D$_3$, total RNA was extracted and miRNA specific reverse transcription was performed prior qRT-PCR. Data shown are the mean of at least three biological replicates.*

These results suggest a role for miR-106B in *CDKN1A* degradation indicating that the steep peak of *CDKN1A* could be due to the simultaneous production of the micro-RNA that then promotes *CDKN1A* degradation. For this to be true two conditions are required:

1) VDR and Pol-II must act similarly on the two promoters and 2) the production rate of *CDKN1A* and miR-106B must be similar.

To test the first hypothesis ChIP experiments for the phosphorylated form of the RNA Polymerase II on the *CDKN1A* promoter were performed at the following time points (in hours) upon 100nM of $VitD_3$ treatment: 0, 0.25, 0.5, 0.75, 1, 2, 4, 6, 12 and 24.

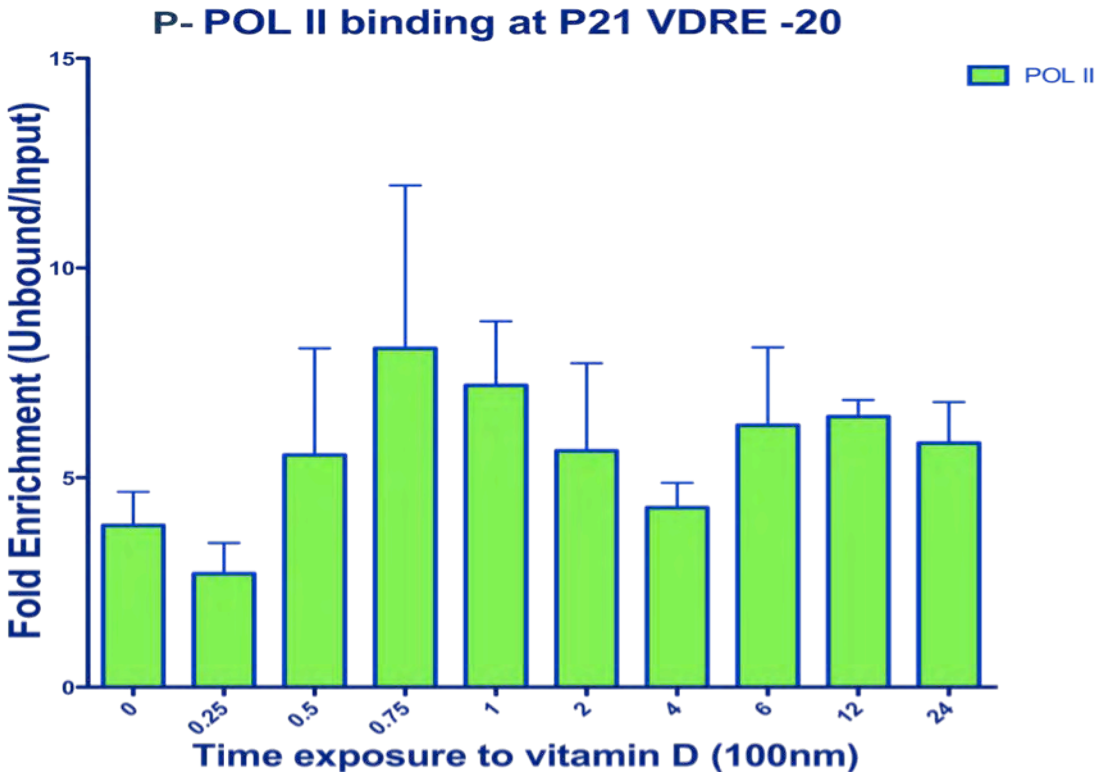

Fig 4.55 *– Phospho-PolII binding at the TSS of p21 (Craig Doig, University of Birmingham, Birmingham, UK). Mid-exponential RWPE-1 cells were treated with 100 nM 1,25(OH)$_2$D$_3$, chromatin was immunoprecipitated with anti-phosho PolII antibody and qRT-PCR was performed with primers covering the TSS region of the CDKN1A gene. Data shown are the mean of at least two biological replicate +/- S.E.M.. The bars indicate the amount of p-polII bound to the TSS of CDKN1A relative to the input (non-immunoprecipitated sample). An initial amount of phospho polymerase II is present at the transcription start site, if it moves into the gene regions, this would explain the lower amount of the enzyme found at 15 min (0.25); after the polymerase moves into the gene body, new enzyme is recruited at the TSS and it's detected at 45 min (0.75).*

4.3.1.3 – Model assumption

The interesting pattern shown in **Fig 4.55** indicates a quick decrease of the initial amount of phospho-PolII at the TSS consistent of the concept that the enzyme moves out of the TSS downstream into the gene. Subsequently new polymerases are cyclically recruited at the transcription start site and this is demonstrated by the oscillatory pattern with peaks at 45 minutes and 6 hours. The decrease in the enzyme's concentration after 15 minutes could be consistent with the idea of a poised polymerase [231, 232]. Stalling at the TSS is detected at the time-zero but not after 15 minute; if this was true the quick induction of both miR-106B and *CDKN1A* would be easily explained, and the delay for the formation of the VDR-CoActivators-pre-initiation-PolII complex can be ignored.

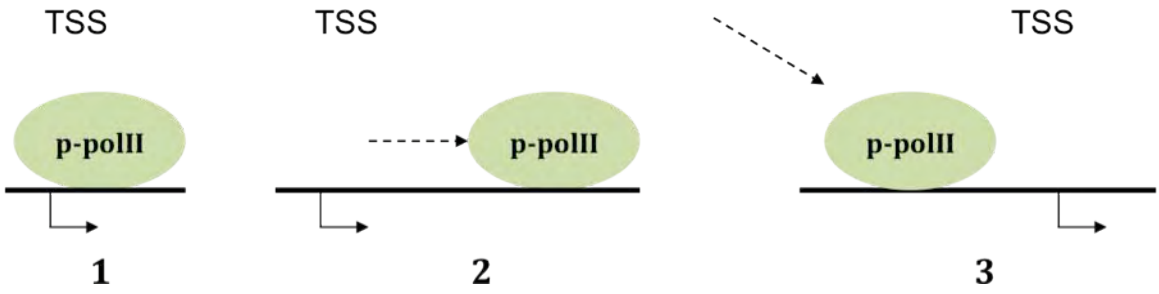

Fig 4.56 – *Schematic representation of the activity of the poised phospho polymerase on the promoter region. The polymerase stops at the TSS waiting for a stimulus (1) to then move into the gene (2) while new polymerase is recruited (3).*

4.3.1.4 - Poised Polymerase II, initial hypothesis

The mechanism of degradation of miR-106B remains theoretical since there are no experimental data indicating in what manner, or how quickly, the mature miRNAs are degraded; the miRNA could be either re-used after the target sequence is degraded or cleaved with the targeted transcript.

To explain the production rate of *CDKN1A* and miR-106B it must be mentioned that the miR-106B, miR-93, and miR-25 belong to a cluster of intronic miRNAs hosted in the MCM7 gene, which is a DNA helicase [226]. The whole cluster is transcribed in presence of the right conditions; generally the first transcript is processed, in order, through the Drosha and Dicer enzymes and complexed with RISC to exert its silencing potential [233, 234]. These reactions require time and, as only the mature form of miR-106B was detected by PCR, it can be assumed that either 1) poised polymerase was present on the TSS of the miRNA cluster and 2) the whole process requires less than 30 minutes. The length of the transcript has also to be kept in consideration; the pre-miRNA initial transcript is a few kilobases long, *CDKN1A* transcript is around 6 kb and with a PolII moving at the maximum speed of 3.6 kb/min it would require no more than 2 or 3 minutes to produce one RNA molecule that then has to be processed. To confirm this, ongoing experiments aim to quantify the basal number of *CDKN1A* and miR-106b molecules in RWPE-1 cells in order to understand which magnitude the fold changes refer to. For example, four fold induction with 10 initial molecules of either *CDKN1A* or miR-106B would indicate that 40 mature RNA molecules were detected; if instead the initial number of molecules was 200 it would means that the production rate would be 20 times higher!

4.3.2 – CDKN1A model of transcriptional initiation

4.3.2.1 – Model description

The model can be schematically described as in Fig 4.57: here the complex VDR/D3 promotes the activation of the poised phospho-PolII that sits on the promoter region of CDKN1A (pPolII/CDKN1A) and miR-106B (pPolII/miR106B) (or the gene MCM7 that contains the cluster with miR-106B); both species are quickly accumulated and the phospo-PolII can cycle (or be recruited "de-novo") and promote the transcription of new CDKN1A and miR-106B. Moreover, miR-106B accumulation also promotes the degradation of CDKN1A and it is degraded by independent mechanism.

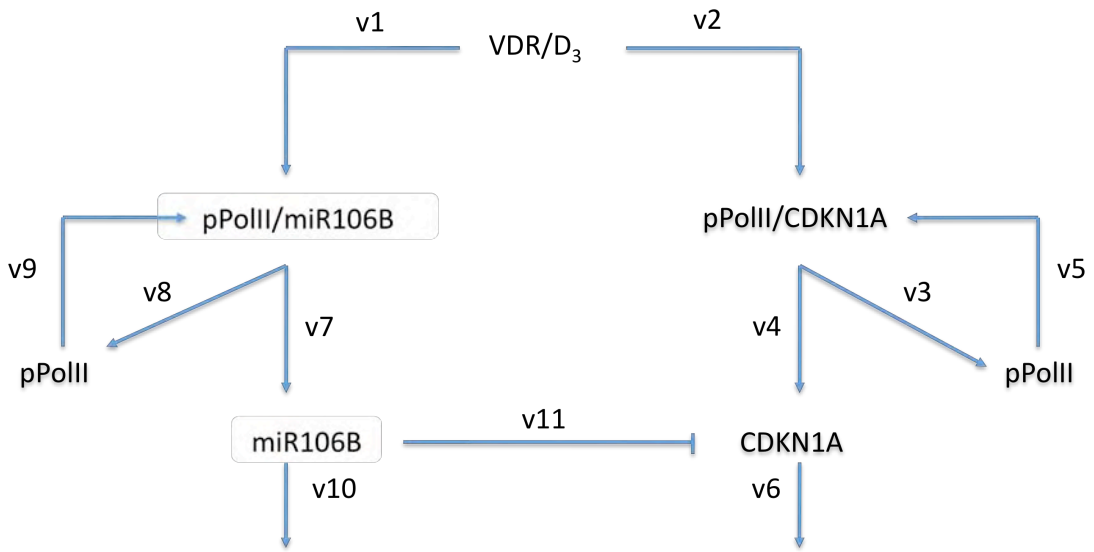

Fig 4.57 *– Model describing the transcriptional regulation of CDKN1A and miR-106B. Briefly: the complex VDR/D3 activates at the same moment the transcription of CDKN1A and miR-106B via phospho-PolII, after the initial transcription of the two molecules miR-106B mediates CDKN1A degradation, altough both are still degraded also by independent mechanisms*

All the parameters implemented in the model above were empirically derived testing their validity inside of the ODE model. Several values were tested before choosing those listed in **Fig 4.58**.

$d[VDR/D_3]/dt = - v1 - v2$
$d[pPolII/miR106B]/dt = v1 + v9 - v7 - v8$
$d[pPolII/CDKN1A]/dt = v2 + v5 - v3 - v4$
$d[miR106B]/dt = v7 - v10 - v11$
$d[CDKN1A]/dt = v4 - v6 - v11$

v1	$= k1[VDR/D_3]$	k1	= 0.1
v2	$= k2[VDR/D_3]$	k2	= 0.1
v3	= k3[pPolII/CDKN1A]	k3	= 0.005
v4	= k4[pPolII/CDKN1A]	k4	= 0.1
v5	= k5[pPolII]	k5	= 0.25
v6	= k6[CDKN1A]	k6	= 0.1
v7	= k7[pPolII/miR106B]	k7	= 0.1
v8	= k8[pPolII/miR106B]	k8	= 0.005
v9	= k9[pPolII]	k9	= 0.25
v10	= k10[miR106B]	k10	= 0.1
v11	= k11[miR106B]	k11	= 4

Fig 4.58 *– Differential equations describing the model described above. Different parameter were tested in order to find the values that better fitted the model; listed are the differential equations (as d[x]/dt) with the respective reactions and parameters.*

Applying the functions described above to miR-106B and *CDKN1A* mRNA accumulation gave an interesting insight on the transcriptional initiation and mRNA degradation.

The initial hypothesis, translated into time constraints and differential equations, hypothesized the presence of a poised polymerase in *CDKN1A* promoter; this allows a rapid production of the mRNA but at the same moment miR-106B production occurs at the same rate. The time constraints used assume that the production of both species is dependent of phospho-pol II activity with a higher production rate in the first 30 minutes

(~1800 seconds). After this time the degradation of *CDKN1A* is dependent on the presence of miR-106B that is then degraded by an independent pathway.

For modeling, the focus was on the first 45 minutes of the time courses because of the frequency of time points chosen and because of the mechanistic events on the promoter region of *CDKN1A* that allow such an early peak to happen. All the constants were adjusted to reflect as much as possible the biological real values and the initial hypothesis.

The ODE model demonstrates that the kinetics of *CDKN1A* closely reflect that of miR-106b due to similar activity of the phospho-PolII on the respective promoter regions. To better isolate the temporal effect of p-PolII and miR-106B on the *CDKN1A* mRNA, time constraints were used and an algorithm was created where questioned: *if* within the first 30 minutes (1800 sec) the production of miR-106B and *CDKN1A* depends on p-PolII and *if* after 30 minutes (>1800 sec) the miR-106B molecules are bound to *CDKN1A* mRNA leading to its rapid degradation *then* what would happen? The results show that this series of events can explain the quick peak in *CDKN1A* mRNA induction and the subsequent steep degradation before going back to steady state. P-PolII is possibly poised on the TSS region and, upon stimulation, quickly moves to transcribe the gene showing a quick down-regulation just before new p-PolII are recruited.

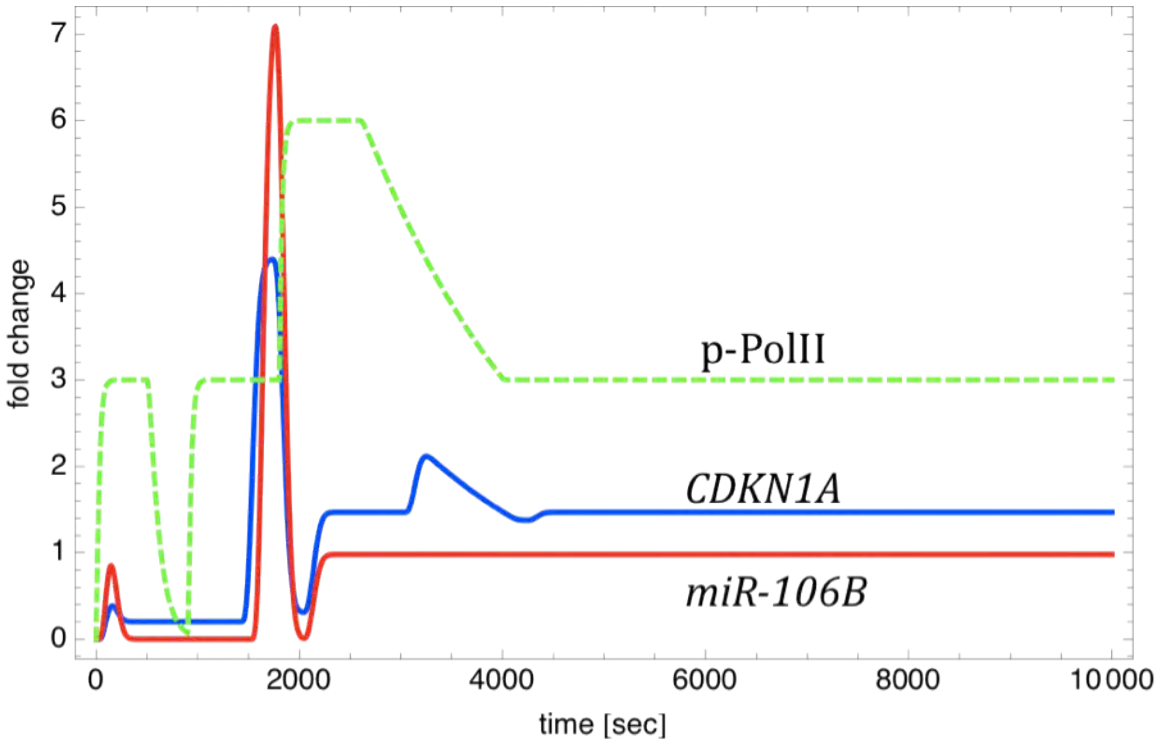

Fig 4.59 – *Simulation run for all the species: miR106b (red), CDKN1A (blue) and phospho-polII (green dashed). The initial downregulation of pPol-II is the one responsible for the induction of CDKN1A and miR-106B and the first part of the steep peak at 1800 sec (30 min); while their concentration increases miR-106B from 1800 sec onwards quickly controls CDKN1A degradation leading to down regulation present in the second part of the steep peak. After that all the species return to steady state.*

However, the limitations of this model reside on the fact that ODE can describe accurately the dynamic events in a system composed by a high number of molecules. This implies that two molecules have almost always a high probability to collide, or interact, due to their high number. In a few cells system, or in a single cell system, this is unlikely because, even if there might be a high number of transcription factors or enzymes, the number of responsive elements, or genes (e.g. *CDKN1A*) is limited and the probability that they "find" or "are found" by the respective counterparts must be taken into consideration. Furthermore these limitations are increased due to compartmentalization, and protein-protein interactions that may limit co-factor

availability. Beside the limitation that this model presents, it was anyway possible to confirmed the mechanistic events that can occur on the promoter region of *CDKN1A* and miR-106B, suggesting the regulatory role of the micro-RNA in *CDKN1A* mRNA accumulation and the dual action of VDR and $1,25(OH)_2D_3$ on those two genes.

To address these limitations an alternative modeling approach was used. A stochastic model was applied that had been built by Katja Rybakova, a fellow ESR in the NucSys network, (Free University of Amsterdam, Amsterdam, The Netherlands) to demonstrate the validity of the previous assumptions (poised polymerase and miR-106B controlling *CDKN1A* degradation). The simulation of the model was ran for 1000 cells and the population average for each time point was taken (reflecting what is measured in wet lab experiments).

The model relies on few general assumptions:

1. The polymerase is the present (poised) on the promoter of both *CDKN1A* and mir106B at t=0, start of the experiment (from the experimental data)

2. The average time in which the promoters is active is 5 min and the average number of polymerases that leave during that time is 3

3. Promoter(s) average reactivation time is 40 min, average time to elongate and process the mRNA and miR-106B is 15 min, the average degradation time of both is also 15 min (times taken to match the data observation)

4. The promoter reactivation, elongation and degradation times all have gamma-distributed waiting times (i.e. very reproducible times, that create delays between

the promoter activation events, elongation start and finish and mRNA production and destruction) – because they are all multiple-step processes. This also explains why stochastic rather than ODE framework is required.

As the actual mechanism of the miR-106B degradation is unclear three different simulations were ran:

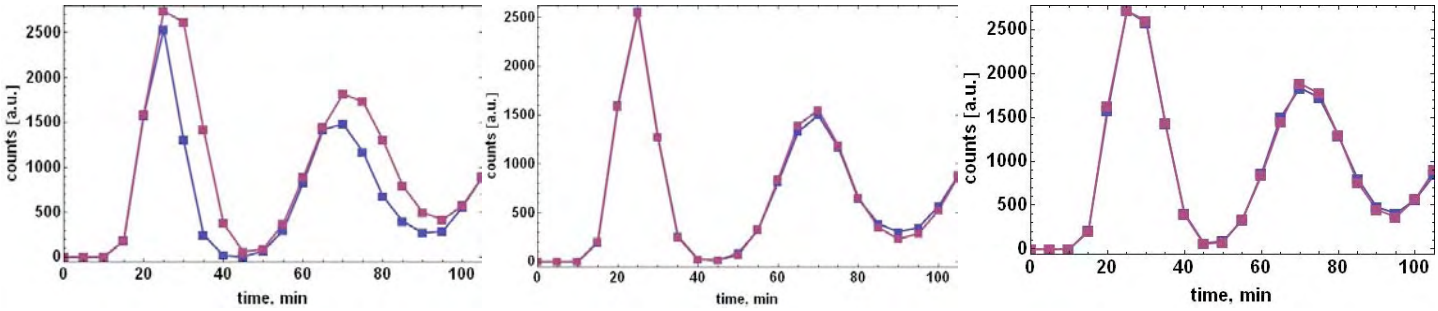

Fig 4.60 – *Three different simulations of the activity of CDKN1A (violet) miR-106B (blue). In the left panel miR-106B is degraded quicker than CDKN1A because it's degraded by an independent mechanism; the center and right panels produce the same kinetic for both miR-106B and CDKN1A. Time and concentration are indicated on the x and y axes, respectively.*

In the first model miR-106B enhances the degradation of *CDKN1A* mRNA but it's own degradation goes via independent mechanism; in the second model miR-106B enhances the degradation of *CDKN1A* mRNA which also leads to its own degradation; in the third model there is no interaction between the mRNA and mir-106B, but because the deg kinetics are similar the observed effect is the same. All the models gave very similar results, however, the hypothesis of miR-106B being responsible for the steep degradation of *CDKN1A* could be discriminated by inhibiting miR-106B via siRNA and repeating the first hour of the *CDKN1A* time course previously described. These experiments are in progress.

Neither of the models was used to simulate the behaviour of the system in case of siRNA against any of the species. This is a further step that will confirm the role of each component in the network and those data will be particularly interesting based on the fact that the VDR transcriptome, including *CDKN1A* transcription, is de-regulated in cancer. The results will also suggested a series of follow up wet-lab experiments to confirm and/or elucidate better the mechanisms through which $1,25(OH)_2D_3$ mediates gene transcription.

5 – CONCLUSIONS AND FUTURE STUDIES

5.1 – Project summary

Multiple lines of evidence support the idea that the NR transcriptome is disrupted in prostate malignancies by altered nuclear co-repressors expression leading to epigenetic silencing. This leads to a general loss of responsiveness towards NR ligands, hence, promoting survival of prostate cancer cells even upon agonist treatment. The use of the HDAC inhibitor SAHA in combination with NR ligands led to significant, but selective, increased antiproliferative effect. It was also demonstrated that elevated NCOR1 levels contributed to the skewed NR network, by creating a stably transfected shNCOR1-PC-3 cell line. This system had an increased, although selective, sensitivity towards NR ligands (EPA, ETYA, bezafibrate, ATRA) at the transcriptional (by modulation of the expression of NR target genes) and phenotypical (by increased anti-proliferative effect of NR agonists) level. The specificity of NCOR1 action in the epigenome was elucidated with ChIP experiments showing that the TSS regions of two different PPARα and -γ target genes (CDKN1A and TGFBRAP1) were differentially affected by the knockdown of NCOR1. H3K9Ac increased at the *CDKN1A* TSS and reduced in *TGFBRAP1* upon bezafibrate treatment. A systems biology approach was also used to generate a model of NR activation with which to quantitate the mechanistic events at the *CDKN1A* TSS region, suggesting that the early transcriptional events are regulated not only by epigenetic events and NR binding but also by miRNA activity.

Finally, as *in vivo* experiments by other groups have demonstrated the lethality of Ncor1 and Ncor2/Smrt knockouts, to date no group has demonstrated the role of those two corepressors in prostate development. As part of the project for this thesis, prostate-specific knockout constructs were prepared and mice are currently being bred at the Roswell Park Cancer Institute in Buffalo, NY (USA).

5.2 – Mechanism of action of the combined treatment NR ligands and SAHA

As a general mechanism of action, ligand-bound NRs change the conformation of the AF2 chain. This displaces corepressor and HDAC-containing complexes in favour of coactivator complexes. The presence of coactivator complexes leads to a more permissive chromatin conformation due to the presence of HAT proteins that in turn enables access to the basal transcription machinery. This physiological equilibrium between activation and repression can be modulated by administration of lipophilic NR agonist molecules thereby activating transcription of target genes and promoting downstream phenotypical effects. Banwell et. al. demonstrated that the NR function is epigenetically corrupted in breast cancer cells with a loss of responsiveness to $1,25(OH)_2D_3$; administration of the histone deacetylases inhibitors TSA restored VDR antiproliferative ability [190, 235]. A similar lesion was shown in prostate cancer cells where NCOR2/SMRT suppresses VDR responsiveness and result in $1,25(OH)_2D_3$ insensitivity [62]. Proliferation studies showed that the addition of an HDAC inhibitor (TSA or NaB) in combination with $1,25(OH)_2D_3$ significantly potentiated the inhibition of aggressive, $1,25(OH)_2D_3$-resistant prostate cancer cell lines, PC-3 and DU-145 [211]. Furthermore, it was

shown that the anti-proliferative $1,25(OH)_2D_3$-target gene GADD45α, was silenced in prostate cancer cell lines and primary cultures, and the addition of TSA with $1,25(OH)_2D_3$ enabled its re-expression [62]. The current study investigated to what extent there was a greater loss of NR responsiveness in PC-3 cells towards a panel NR ligands (ETYA, EPA, bezafibrate, RA, T3). Interestingly whilst the combined treatment of $1,25(OH)_2D_3$ and TSA enhanced VDR activity, co-treatment with the hydroxamic acid-based HDACi SAHA neither enhanced VDR proliferation nor gene regulation, although it had super-additive antiproliferative effect if combined with the other NR agonists, notably towards PPARs.

SAHA targets classes I, II and IV, but not the NAD^+-dependent class III enzymes. This selectivity is due to the presence of a zinc atom at the bottom of the binding pocket of class I, II and IV HDACs that is recognised by the hydroxamic group of SAHA. It inhibits partially purified HDAC1 and HDAC3, and causes accumulation of acetylated H2A, H2B, H3 and H4. However, a number of non-histone proteins such as YY1, MyoD, p53, GATA1, Rb, Tubulin and HSP90 [236] are also targeted. SAHA has a very good safety profile, it is FDA-approved and currently used in clinical trials for leukemia, myelodysplastic syndromes and renal cancer [236].

Bezafibrate is also an FDA-approved drug with a good safety profile mainly used for its antilipidemic action; its effects have been widely studied in patients with coronary diseases and diabetes. Recent trials also demonstrated its action on acute myeloid leukemia and CLL cell lines [101, 102]. Its action is mediated through binding PPARα and -γ inducing release of the corepressor complexes and promoting transcription of the target genes. Bezafibrate-bound PPARs, as well as other ligand-

bound NR, change the conformation of the AF2 domain recruiting coactivators and releasing corepressor complexes. However, several holo-NR undergoes post-translational modifications such as phosphorylation, acetylation or sumoylation. To date, there have been no studies on the acetylation of PPARα or -γ, however, SIRT1 (HDAC class III) was shown to repress PPARγ by docking with both NCOR and NCOR2/SMRT [237]. It is noteworthy to remember that SAHA does not to inhibit the SIRT enzymes, therefore suggesting that this enzyme in prostate might not play a strong repressive role on PPARγ.

Previously, it was shown that, compared with wild-type ERα, glutamine or arginine substitutions at ERα acetylation sites enhanced estrogen dependent activity of ERα suggesting that ERα acetylation by p300 normally suppresses ligand sensitivity. However, ERα acetylation appears to augment unliganded, basal constitutive activity as TSA and NaB stimulated unliganded ERα activity and this induction was abolished in cells with acetylation-deficient ERα mutants [238]. Similarly, acetylation-deficient AR mutants hindered the activation of the AR in the absence of ligand, but the hormone-dependent transactivation was also abolished, implying that acetylation of the AR by p300 is essential for full effective AR signalling [239]. Compared with wild-type AR in the presence of dihydrotestosterone, alanine substitutions at AR acetylation sites (630 or 632/633) showed a 10-fold increased binding of NCOR1 [240]. Thus, acetylation of the critical AR lysine residues appears to prevent the recruitment of corepressors and activate both unliganded and liganded AR signalling. There are several studies demonstrating that NCOR1 is not involved only in ligand-independent repression of target genes. An example is the

ligand dependent transrepression of PPAR target genes was shown by Pascual et al. where a ligand-dependent SUMOylation of the PPARγ ligand-binding domain, targets PPARγ to NCOR1/HDAC3 complexes on inflammatory gene promoters. This prevents recruitment of the ubiquitylation/19S proteosome machinery and the signal-dependent removal of corepressor complexes required for gene activation. As a result, NCOR1 complexes are not cleared from the promoter and target genes are maintained in a repressed state [130].

If a post translational acetylation of PPARα and -γ prevented NCOR1 binding, treatment with SAHA may preserve the acetylation status of the receptor in favour of an active receptor. This could also suggest that in the pool of PPARs inside of the cell, only a certain number of them are bound to NCORs/HDACs, hence, silencing transcription, while a percentage are active [241]. Treatment with SAHA would increase the amount of PPARs available (reducing the number of those complexed with NCORs/HDACs) and the co-treatment with bezafibrate would then additively enhance the activity of PPARs and the activation of their target genes. However, further studies on the acetylation of PPARα and -γ are necessary to support this hypothesis.

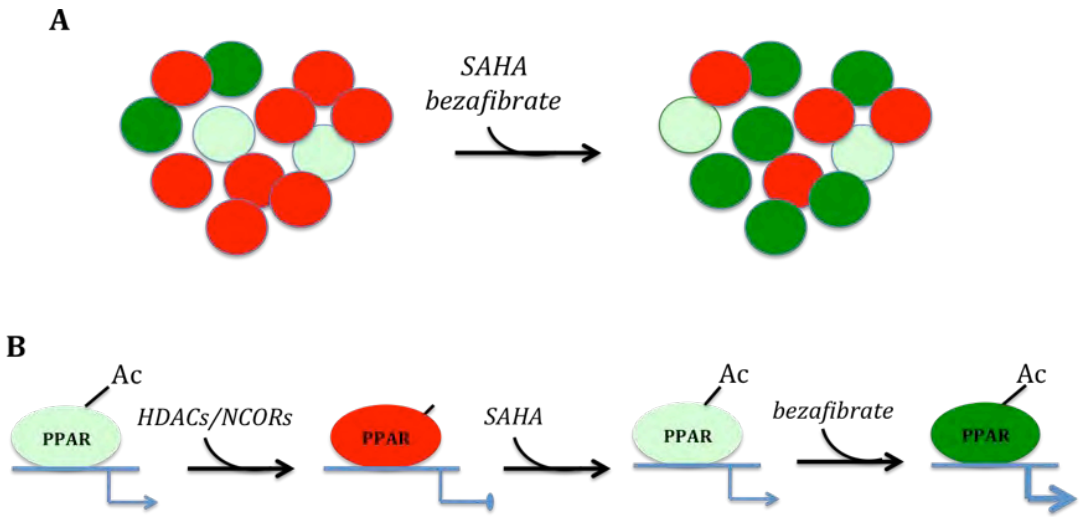

Fig. 5.1 – *Representation of the proposed additive mechanism of action of SAHA and bezafibrate in PC-3. (A) A pool of PPARs is acetylated due to the interaction with elevated levels of NCOR1 and HDAC3 that promote de-acetylation of the receptor. Treatment with SAHA and bezafibrate restores acetylation levels and promotes ligand-dependent receptor activation. (B) Interaction of NCORs/HDACs complexes with PPAR deacetylates the receptor, SAHA restores the acetylation levels and bezafibrate additively activates PPAR. Red circles indicates repressed receptor, light green circles indicates acetylated and physiologically active receptors (e.g. by endogenous ligand) and dark green circles indicate receptors additively activated by bezafibrate.*

Interestingly, knocking down NCOR1 in PC-3 cells via siRNA, modulated the acetylation of H3K9 at the TSS region and closely reflects the mRNA levels of both *CDKN1A* and *TGFBRAP1* being upregulated and downregulated, respectively, upon bezafibrate treatment either with SAHA or in shNCOR1 background. This suggests that NCOR1 negatively regulates the transcription of *CDKN1A* and at the same time mediates independent regulation of *TGFBRAP1*.

For both CDKN1A and TGFBRAP1 TSS regions, SAHA efficiently promoted H3K9 acetylation while bezafibrate alone was not able to promote accumulate H3K9Ac; the combined treatment did not have any additive effect and the acetylation levels were comparable to those of bezafibrate alone. These data suggest that bezafibrate

actually reduces the acetylation marks in opposition to SAHA's activity although sustaining *CDKN1A* transcription and repressing *TGFBRAP1* mRNA accumulation.

Another interesting NCOR1-dependent mechanism of action has been described in pituitary cells where T3 decreased transcription, increasing histone acetylation, of a reporter gene controlled by the TSHα promoter (-840 to +1). T3 promotes acetylation of H3K9 and H3K18 and release of HDAC3, TBL-1 and NCOR1-NCOR2/SMRT from the TSHα promoter. ChIP analyses of a positively regulated target gene showed increased histone acetylation and corepressor complex release with T3 treatment. Microarray analyses suggested a subset of negatively regulated genes in response to increased histone acetylation. These findings demonstrated the role of NCOR1/HDAC3 complex in negative regulation of TSHα gene expression and show that similar complexes and overlapping epigenetic modifications can participate in both negative and positive transcriptional regulation [242]. Similarly, $1.25\alpha(OH)_2D_3$ treatment in MCF7 cells was shown to recruit VDR, the transcription factor WSTF and HDACs to the 1α(OH)ase promoter leading to reduced levels of H3K14Ac at the TSS and transcriptional silencing [243].

These studies suggest that ligand-dependent transrepression is actually a common, although selective, event shared between several NRs. However, it is still unclear why only certain genes are targeted and if this is a phenomena specific for a certain time points and/or corepressor complexes. The NR network is integrated at multiple levels with feed-back and feed-forward signalling loops that modulate in time the transcription of target genes. Time course analysis with SAHA and bezafibrate demonstrated a dynamic regulation of mRNA accumulation that can

either up- or down-regulate the same gene at different time points (e.g. *PTGS2*); although this modulation can be influenced by epigenetic modification at different regions, the cohort of complexes and TF interacting with *PTGS2* promoter can also vary through time, therefore, leading to different transcriptional responses. Further time-resolved ChIP analysis could elucidate better the epigenetic mechanism behind the cyclical regulation of PPARα and -γ target genes.

Ellis et al. investigated the correlation between TSA treatment with histone modification and transcriptional activation/repression of target genes. They analysed *CDKN1A* and *SRC* promoters, being a positively and negatively regulated by TSA, respectively. A panel of histone acetylated residues such as H3K9, H3K14, H4K5, H4K8, H4K12 and H4K16 were analysed upon a time course experiment in two different cell lines treated with 1 μM of TSA, although this is a very high concentration when TSA IC_{50} is approximately 20nM. The results consistently showed increased acetylation at the TSS region of all the genes irrespectively from the mRNA regulation data [244].

These observations indicate that the additive effect of SAHA and bezafibrate on the PPAR target genes is not caused only by modification of the chromatin environment but could also be mediated by the acetylation state of non-histone protein (e.g. PPAR, Rb or p53) while bezafibrate promoted transrepression of *TFBRAP1* was already demonstrated by the reduced acetylation pattern of *TGFBRAP1* TSS in siNCOR1 treated PC-3 cells. Although NCOR1 regulate transcriptional plasticity over both target choice and periodicity, further time course studies could elucidate better the acetylation at the TSS at promoter regions of PPAR target genes while 3C

experiments [245] could indicate possible distal spatial control over transcription. However, the novel finding is that NCOR1 blocks both up and down regulated critical factors targetable with epigenetic therapy.

5.3 – Corepressor functions in prostate development

In vivo experiments demonstrated that both Ncor1 and Ncor2/Smrt knockout are lethal. Ncor1$^{-/-}$ mice die at ED 15.5 because of severe anemia and secondary edema [138], while Ncor2/Smrt$^{-/-}$ embryos die at ED 16.5 because of heart defects and defects in CNS development [139]. Ncor1 is also a key regulator in neural stem cells differentiation as Ncor1-disrupted mice displayed impaired self-renewal and spontaneous differentiation in astroglia-like cells [137]. Other studies highlighted that 3T3-L1 cells with reduced levels of either NCOR1 or NCOR2/SMRT, had increased expression of adiponectin, perilipin, and C/EBPα and adipogenic markers, upon PPARγ agonist treatment; these cells exhibited increased expression of adipocyte-specific genes and increased production of lipid droplets, as compared with control cells [136]. NCOR1 and NCOR2/SMRT are negative regulators of transcription induced by the β-catenin-TCF4 complex [246]; this is activated by the WNT signalling that can modulate epithelial cell proliferation during prostate morphogenesis.

AR, ERα and RAR are regulated by both NCOR1 and NCOR2/SMRT; Ar is fundamental for correct prostate development, as mice with dysfunctional Ar do not develop prostate, and tightly controls the expression of Nkx3.1 that is detectable

two days before the appearance of prostatic buds. ERα attenuates the androgenic effect in the developing gland while RAR cross talks with ERα during prostate development regulating fertility and gland morphology (described in the Introduction).

Therefore, it is possible to predict that prostate specific knock out of Ncor1 and Ncor2/Smrt will interfere with the pathways of Ar, Er and Rar modifying the expression of downstream target genes. High estradiol levels lead to branching inhibition but action of the Er is also antagonized by Rar signalling; over-activation of the Ar signalling could cause hyper-proliferation of the prostate or irregular growth of the stroma and epithelia causing morphological and functional disfunctions. The β-catenin-Tcf4 complex will be also hyper-activated due to the lack Ncor1 and Ncor2/Smrt possibly leading to epithelial hyperplasia and bigger prostate. However, the phenotype obtained could be different between the two knock outs as the classical knock outs of Ncor1 and Ncor2/Smrt caused different phenotypical outputs.

5.4 – Mechanistic modeling of CDKN1A transcriptional regulation

A realistic approach for understanding biological network is the “bottom up” approach, where experimental data collected are used to and implemented into models to make predictions regarding the behavior of a certain network. Those predictions can then be confirmed with new wet-lab experiments appositely designed to validate and support the *in silico* findings.

The ODE model predicted that *CDKN1A* and miR-106B are commonly regulated by p-PolII while miR-106B controls degradation of *CDKN1A* before that the system goes back to a steady state. Limitations of ODE models are principally that they won't describe the accurately the events inside a few cell population. A stochastic model can overcome this and capture the dynamics of molecular systems within a few molecular species – i.e. transcriptional initiation from a single gene. This approach has been successfully used to describe the cycling of PPARδ to a response element within the promoter of the PDK4 gene regulatory region [247] and, applied to *CDKN1A* transcriptional events, closely reflect mRNA and ChIP data. Although this model has to be refined further, it strongly suggests that the timing of *CDKN1A* transcriptional activation and subsequent mRNA accumulation can be dependent upon miR-106B action that not only is involved in the steep degradation at 30 minutes but also controls the timing of mRNA accumulation.

However, it is important to run both stochastic and ODE models simulating the knock down of the species involved in order to precisely confirm the initial hypothesis. As wet-lab validations, knock down of MCM7 (the gene containing the mir106-B cluster) and miR-106B, and cycloheximide experiments could support the modeling results and confirm the direct effect of ligand-bound VDR on *CDKN1A* transcriptional. Nonetheless, the results obtained so far suggest that the predicted double mechanism of action of miR-106B can be extended to other miRNA target genes to describe their cyclical activation by NR ligands and their function in PCa. NCOR1 and NCOR2/SMRT also play a repressive role in *CDKN1A* mRNA

accumulation and implementing those data in the model could also help predicting the transcriptional events in Ncor1 and Ncor2/Smrt knock out animals.

5.5 – Future directions

The prostate specific knockout mice are currently being bred at the Roswell Park Cancer Institute in Buffalo, NY (USA) to better understand the dynamic contribution of Ncor1 and Ncor2/Smrt in prostate development is necessary to monitor the expression of those two genes from embryonic (or from when the first prostate is detectable) to adult prostate. To date no such data are available even if several transcripts have been observed from bud induction to prostate gland formation such as Bmps, Hoxa and Wnt (reviewed in [17]). Once the knock out in the mice is confirmed, it will be possible to analyse the expression of key genes (*Nkx3.1, Hoxa13, Hoxd13*) as well as it will be insightful to analyse the Shh, Wnt and Bmp pathways. The TGF signalling, already involved in the Bmp pathway, is also modulated by TGFBRAP1 (PPAR target and regulated by Ncor1) binding to TGFβ receptors that was reported to relate to tumorigenesis [248, 249]. Moreover, the NR network will probably be affected by the lack of Ncor1 and Ncor2/Smrt and the expression of downstream targets of AR, ERα and RAR will be measured. Immunohistochemical analysis of Ncor1$^{-/-}$ and Ncor2/Smrt$^{-/-}$ prostates will be undertaken to understand the histological and morphological consequences of the knockouts. To profile genome-wide the transcriptome of Ncor1$^{-/-}$ and Ncor2/Smrt$^{-/-}$ prostates it will be worthwhile to undertake a microarray analysis comparing WT

animals with the knock outs and the two knock outs with each other; this will help identify cohort of genes that will be uniquely or commonly regulated by Ncor1 and Ncor2/Smrt. There will also be the possibility to cross these mice with either Pten$^{-/-}$ or TRAMP prostate cancer models to understand the combinatorial role or Ncor1 and Ncor2/Smrt with other key regulators in a PCa background. It would be also interesting to test in these mice whether sensitivity of the growing tumour towards NR ligands (i.e. bezafibrate) is increased or decreased by the lack of Ncor1 and Ncor2/Smrt. A further step in the understanding the combinatorial role between Ncor1 and Ncor2/Smrt would be to cross the two single knock outs to create mice lacking both corepressors in the prostate; however, it is important initially to evaluate the consequences of the single knock out before undertaking this experiments.

Saramaki et al. demonstrated the cyclical looping VDR-mediated at in three different regions of the CDKN1A promoter that correlate with mRNA accumulation [250]. Similarly, in breast cancer cell lines, the ERα has been shown to initiate interchromosomal contacts that generate specific and parallel transcription and co-ordination of mRNA accumulation patterns [251]. Applying this concept to the PPAR target genes could help understanding better the mechanism of action of the PPAR transcriptome in prostate malignancies. Also, to profile more precisely the epigenetic modification induced by bezafibrate in prostate cancer cells, a Native ChIP (N-ChIP) approach [252] would be more suitable than a X-ChIP approach; this would allow to capture with a better resolution and sensitivity the periodicity of histone modifications in prostate cancer cells.

Finally the integration of those data in a stochastic model of the epigenetic modulation PPAR-mediated in prostate cancer cells could help to formulate patients predictions on the effect of bezafibrate (already FDA approved) on prostate cancer. This model could be also be expanded to other NRs and it would also be interesting to compare the prediction of the model made for a malignant system with those obtained from a model designed for a non-malignant system; this approach, together with the identification of markers dictating ligand insensitivity (i.e. corepressors), could help predict the sensitivity of patients to NR therapy, hence, reducing the risk for the patient to develop a more aggressive disease (i.e. in AR antagonist treated patients) and designing more personal and efficient treatments.

JOURNAL PUBLICATIONS RELATED TO THIS THESIS

Abedin SA, Thorne J, **Battaglia S**, Maguire O, Hornung LB, Doherty AP, Mills IG, Campbell MJ (2009). Elevated NCOR1 disrupts a network of dietary-sensing nuclear receptors in bladder cancer cells. Carcinogenesis Mar;30(3):449-56. (impact factor 5.4)

Battaglia S, Thorne J, Hornung L B, Doig CL, Liu S, Sucheston LE, Bianchi A, Khanim F, Gommersall LM, Coulter HSC, Rhaka S, Giddings, I. Cooper C, McCabe, CJ, Bunce CM, & Campbell MJ (2009). Elevated NCOR1 disrupts PPAR signaling in prostate cancer and forms a targetable epigenetic lesion. (Submitted to Oncogene)

Thorne JL, Maguire O, Doig CL, **Battaglia S**, O'Neill LP Turner BM, McCabe CJ & Campbell MJ (2009) Histone modifications and miRNA expression combine to determine CDKN1A (encodes p21(waf1/cip1)) transcriptional periodicity and cell fate decisions (Submitted to Molecular Cell)

Battaglia S, Maguire O & Campbell MJ (2009). Transcription factor co-repressors in cancer biology; disruption and targeting. (Submitted to Carcinogenesis)

CONFERENCE PROCEEDINGS

- **International Conference of System Biology**; Sweden, Goteborg, Aug 2008; poster: "*NCoR Activity in the Prostate System*"
- **Keystone Meeting: Nuclear Receptor Steroids**; Canada, Whistler March 2008; poster: "*NCoR activity in the prostate system"*.
- **Diet and Cancer meeting**; England, Nottingham, June 2007; poster: "*Epigenetic corruption of fatty acid and bile acid signalling in prostate malignancies*" (poster prize)
- **Chromatin meeting**; England, Nottingham, May 2007; poster: *"Chromatin remodeling and nuclear receptors activity in prostate cancer"*
- **FEBS advanced course on system biology**; Austria, Gosau, March 2007; poster: *"Activity of the Vitamin D receptor during the cell cycle"*
- **International Conference on Differentiation Therapy and Innovative Therapeutics in Oncology**; France, Paris (Versaille), November 2006; oral presentation "*An epigenetic lesion attenuates signalling via nuclear receptors in prostate cancer"*

COURSES:

October 2007

- "*Advanced speaking and lecturing skills for international staff*", University of Birmingham, Birmingham, UK

September 2007

- "*Mechanism of gene expression*", University of Kuopio, Kuopio, Finland; held by Prof. Carsten Calberg.

June 2007

- "*Mouse embryonic stem cell culture training course*", Max Planck Institute for Molecular Genetics, Berlin, Germany; held by Dr Heiner Screwe.
- "*Presentation skills*", University of Birmingham, Birmingham, UK.

October 2006

- "*Customer Training for GeneSpring Workshops, Intermediate Level* (Microarray analysis)", University of Birmingham, Birmingham, UK.

UNIVERSITY LECTURES:

(University of Birmingham, Birmingham, UK)

- *Getting published*
- *How to make the most of your research with business*
- *Multiplex fluorescent bead-based assay*
- *Stem Cells: the basics, the hype and the reality*
- *What should I expect to achieve my PhD?*
- *Neuroimmunopharmacology - Prozac, Ecstasy & Amphetamines: using psychotropic drugs to beat cancer*
- *In situ hybridization: from theory to practice*
- *Immunohistochemestry: from theory to practice*
- *Monitoring microcirculation using intravital microscopy*

REFERENCES:

1. McNeal, J.E., *The prostate gland: morphology and pathobiology.* Monogr. Urol, 1983. **4**: p. 3-37.
2. Timms, B.G., *Prostate development: a historical perspective.* Differentiation, 2008. **76**(6): p. 565-77.
3. Shannon, J.M. and G.R. Cunha, *Autoradiographic localization of androgen binding in the developing mouse prostate.* Prostate, 1983. **4**(4): p. 367-73.
4. Takeda, H., T. Mizuno, and I. Lasnitzki, *Autoradiographic studies of androgen-binding sites in the rat urogenital sinus and postnatal prostate.* J Endocrinol, 1985. **104**(1): p. 87-92.
5. Takeda, H. and C. Chang, *Immunohistochemical and in-situ hybridization analysis of androgen receptor expression during the development of the mouse prostate gland.* J Endocrinol, 1991. **129**(1): p. 83-9.
6. Wang, Y., et al., *Cell differentiation lineage in the prostate.* Differentiation, 2001. **68**(4-5): p. 270-279.
7. Hayward, S.W., G.R. Cunha, and R. Dahiya, *Normal development and carcinogenesis of the prostate. A unifying hypothesis.* Ann N Y Acad Sci, 1996. **784**: p. 50-62.
8. Marker, P.C., et al., *Hormonal, cellular, and molecular control of prostatic development.* Dev Biol, 2003. **253**(2): p. 165-74.
9. Prins, G.S. and L. Birch, *The developmental pattern of androgen receptor expression in rat prostate lobes is altered after neonatal exposure to estrogen.* Endocrinology, 1995. **136**(3): p. 1303-14.
10. Hayward, S.W., et al., *Epithelial development in the rat ventral prostate, anterior prostate and seminal vesicle.* Acta Anat (Basel), 1996. **155**(2): p. 81-93.
11. Collins, A.T., et al., *Identification and isolation of human prostate epithelial stem cells based on alpha(2)beta(1)-integrin expression.* J Cell Sci, 2001. **114**(Pt 21): p. 3865-72.
12. Magi-Galluzzi, C. and M. Loda, *Molecular events in the early phases of prostate carcinogenesis.* Eur Urol, 1996. **30**(2): p. 167-76.
13. Aumuller, G., *Morphologic and endocrine aspects of prostatic function.* Prostate, 1983. **4**(2): p. 195-214.
14. Gakunga, P., et al., *Hyaluronan is a prerequisite for ductal branching morphogenesis.* Development, 1997. **124**(20): p. 3987-97.
15. Wilhelm, D. and P. Koopman, *The makings of maleness: towards an integrated view of male sexual development.* Nat Rev Genet, 2006. **7**(8): p. 620-31.
16. Schneider, A., et al., *Targeted disruption of the Nkx3.1 gene in mice results in morphogenetic defects of minor salivary glands: parallels to glandular duct morphogenesis in prostate.* Mech Dev, 2000. **95**(1-2): p. 163-74.
17. Prins, G.S. and O. Putz, *Molecular signaling pathways that regulate prostate gland development.* Differentiation, 2008. **76**(6): p. 641-59.
18. Greenberg, N.M., et al., *Prostate cancer in a transgenic mouse.* Proc Natl Acad Sci U S A, 1995. **92**(8): p. 3439-43.

19. Wang, X.D., et al., *Notch1-expressing cells are indispensable for prostatic branching morphogenesis during development and re-growth following castration and androgen replacement.* J Biol Chem, 2004. **279**(23): p. 24733-44.
20. Bierie, B., et al., *Activation of beta-catenin in prostate epithelium induces hyperplasias and squamous transdifferentiation.* Oncogene, 2003. **22**(25): p. 3875-87.
21. Yang, A., et al., *p63, a p53 homolog at 3q27-29, encodes multiple products with transactivating, death-inducing, and dominant-negative activities.* Mol Cell, 1998. **2**(3): p. 305-16.
22. Signoretti, S., et al., *p63 is a prostate basal cell marker and is required for prostate development.* Am J Pathol, 2000. **157**(6): p. 1769-75.
23. Brown, T.R., et al., *Deletion of the steroid-binding domain of the human androgen receptor gene in one family with complete androgen insensitivity syndrome: evidence for further genetic heterogeneity in this syndrome.* Proc Natl Acad Sci U S A, 1988. **85**(21): p. 8151-5.
24. Charest, N.J., et al., *A frameshift mutation destabilizes androgen receptor messenger RNA in the Tfm mouse.* Mol Endocrinol, 1991. **5**(4): p. 573-81.
25. Takeda, H., I. Lasnitzki, and T. Mizuno, *Analysis of prostatic bud induction by brief androgen treatment in the fetal rat urogenital sinus.* J Endocrinol, 1986. **110**(3): p. 467-70.
26. Cohen, R.N., et al., *The nuclear corepressors recognize distinct nuclear receptor complexes.* Mol Endocrinol, 2000. **14**(6): p. 900-14.
27. Chen, J.D. and R.M. Evans, *A transcriptional co-repressor that interacts with nuclear hormone receptors.* Nature, 1995. **377**(6548): p. 454-7.
28. Gloyna, R.E., P.K. Siiteri, and J.D. Wilson, *Dihydrotestosterone in prostatic hypertrophy. II. The formation and content of dihydrotestosterone in the hypertrophic canine prostate and the effect of dihydrotestosterone on prostate growth in the dog.* J Clin Invest, 1970. **49**(9): p. 1746-53.
29. Quigley, C.A., et al., *Androgen receptor defects: historical, clinical, and molecular perspectives.* Endocr Rev, 1995. **16**(3): p. 271-321.
30. Bardin, C.W., et al., *Androgen metabolism and mechanism of action in male pseudohermaphroditism: a study of testicular feminization.* Recent Prog Horm Res, 1973. **29**: p. 65-109.
31. Brown, T.J., M. Sharma, and N.J. MacLusky, *Localization and measurement of occupied androgen receptors in thaw-mounted rat and human prostate tissue sections by in vitro autoradiography.* Steroids, 1995. **60**(2): p. 239-47.
32. Lipschutz, J.H., B.A. Foster, and G.R. Cunha, *Differentiation of rat neonatal ventral prostates grown in a serum-free organ culture system.* Prostate, 1997. **32**(1): p. 35-42.
33. Hsieh, C.L., et al., *A luciferase transgenic mouse model: visualization of prostate development and its androgen responsiveness in live animals.* J Mol Endocrinol, 2005. **35**(2): p. 293-304.
34. Lubahn, D.B., et al., *Alteration of reproductive function but not prenatal sexual development after insertional disruption of the mouse estrogen receptor gene.* Proc Natl Acad Sci U S A, 1993. **90**(23): p. 11162-6.

35. Eddy, E.M., et al., *Targeted disruption of the estrogen receptor gene in male mice causes alteration of spermatogenesis and infertility.* Endocrinology, 1996. **137**(11): p. 4796-805.
36. Huang, L., et al., *The role of Fgf10 signaling in branching morphogenesis and gene expression of the rat prostate gland: lobe-specific suppression by neonatal estrogens.* Dev Biol, 2005. **278**(2): p. 396-414.
37. Timms, B.G., S.L. Petersen, and F.S. vom Saal, *Prostate gland growth during development is stimulated in both male and female rat fetuses by intrauterine proximity to female fetuses.* J Urol, 1999. **161**(5): p. 1694-701.
38. Prins, G.S., *Neonatal estrogen exposure induces lobe-specific alterations in adult rat prostate androgen receptor expression.* Endocrinology, 1992. **130**(4): p. 2401-12.
39. McDowell, E.M., K.P. Keenan, and M. Huang, *Restoration of mucociliary tracheal epithelium following deprivation of vitamin A. A quantitative morphologic study.* Virchows Arch B Cell Pathol Incl Mol Pathol, 1984. **45**(2): p. 221-40.
40. De Luca, L.M., *Retinoids and their receptors in differentiation, embryogenesis, and neoplasia.* FASEB J, 1991. **5**(14): p. 2924-33.
41. Aboseif, S.R., et al., *Effect of retinoic acid on prostatic development.* Prostate, 1997. **31**(3): p. 161-7.
42. Prins, G.S., et al., *Retinoic acid receptors and retinoids are up-regulated in the developing and adult rat prostate by neonatal estrogen exposure.* Endocrinology, 2002. **143**(9): p. 3628-40.
43. Collins, A.T. and N.J. Maitland, *Prostate cancer stem cells.* Eur J Cancer, 2006. **42**(9): p. 1213-8.
44. Kasper, S., *Exploring the origins of the normal prostate and prostate cancer stem cell.* Stem Cell Rev, 2008. **4**(3): p. 193-201.
45. Fargeas, C.A., et al., *Identification of novel Prominin-1/CD133 splice variants with alternative C-termini and their expression in epididymis and testis.* J Cell Sci, 2004. **117**(Pt 18): p. 4301-11.
46. Richardson, G.D., et al., *CD133, a novel marker for human prostatic epithelial stem cells.* J Cell Sci, 2004. **117**(Pt 16): p. 3539-45.
47. Shepherd, C.J., et al., *Expression profiling of CD133+ and CD133- epithelial cells from human prostate.* Prostate, 2008. **68**(9): p. 1007-24.
48. Collins, A.T., et al., *Prospective identification of tumorigenic prostate cancer stem cells.* Cancer Res., 2005. **65**(23): p. 10946-10951.
49. Feinberg, A.P., R. Ohlsson, and S. Henikoff, *The epigenetic progenitor origin of human cancer.* Nat Rev Genet, 2006. **7**(1): p. 21-33.
50. Sell, S., *Stem cell origin of cancer and differentiation therapy.* Crit Rev Oncol Hematol, 2004. **51**(1): p. 1-28.
51. Parkin, D.M., et al., *Global cancer statistics, 2002.* CA Cancer J Clin, 2005. **55**(2): p. 74-108.
52. Tomlins, S.A., M.A. Rubin, and A.M. Chinnaiyan, *Integrative biology of prostate cancer progression.* Annu Rev Pathol, 2006. **1**: p. 243-71.

53. Gleason, D.F. and G.T. Mellinger, *Prediction of prognosis for prostatic adenocarcinoma by combined histological grading and clinical staging.* J Urol, 1974. **111**(1): p. 58-64.
54. Steck, P.A., et al., *Identification of a candidate tumour suppressor gene, MMAC1, at chromosome 10q23.3 that is mutated in multiple advanced cancers.* Nat Genet, 1997. **15**(4): p. 356-62.
55. Li, J., et al., *PTEN, a putative protein tyrosine phosphatase gene mutated in human brain, breast, and prostate cancer.* Science, 1997. **275**(5308): p. 1943-7.
56. Chen, H., et al., *NKX-3.1 interacts with prostate-derived Ets factor and regulates the activity of the PSA promoter.* Cancer Res, 2002. **62**(2): p. 338-40.
57. Magee, J.A., S.A. Abdulkadir, and J. Milbrandt, *Haploinsufficiency at the Nkx3.1 locus. A paradigm for stochastic, dosage-sensitive gene regulation during tumor initiation.* Cancer Cell, 2003. **3**(3): p. 273-283.
58. Mostaghel, E.A., et al., *Intraprostatic androgens and androgen-regulated gene expression persist after testosterone suppression: therapeutic implications for castration-resistant prostate cancer.* Cancer Res, 2007. **67**(10): p. 5033-41.
59. Kokontis, J.M., N. Hay, and S. Liao, *Progression of LNCaP prostate tumor cells during androgen deprivation: hormone-independent growth, repression of proliferation by androgen, and role for p27Kip1 in androgen-induced cell cycle arrest.* Mol Endocrinol, 1998. **12**(7): p. 941-53.
60. McPhaul, M.J., *Mechanisms of prostate cancer progression to androgen independence.* Best Pract Res Clin Endocrinol Metab, 2008. **22**(2): p. 373-88.
61. Slattery, M.L., *Vitamin D receptor gene (VDR) associations with cancer.* Nutr Rev, 2007. **65**(8 Pt 2): p. S102-4.
62. Khanim, F.L., et al., *Altered SMRT levels disrupt vitamin D(3) receptor signalling in prostate cancer cells.* Oncogene, 2004. **23**(40): p. 6712-6725.
63. Abedin, S.A., et al., *Epigenetic corruption of VDR signalling in malignancy.* Anticancer Res, 2006. **26**(4A): p. 2557-66.
64. Richter, F., et al., *Retinoid and androgen regulation of cell growth, epidermal growth factor and retinoic acid receptors in normal and carcinoma rat prostate cells.* Mol Cell Endocrinol, 1999. **153**(1-2): p. 29-38.
65. Jeronimo, C., et al., *Quantitative RARbeta2 hypermethylation: a promising prostate cancer marker.* Clin Cancer Res, 2004. **10**(12 Pt 1): p. 4010-4.
66. Campbell, M.J., et al., *Expression of retinoic acid receptor-beta sensitizes prostate cancer cells to growth inhibition mediated by combinations of retinoids and a 19-nor hexafluoride vitamin D3 analog.* Endocrinology, 1998. **139**(4): p. 1972-1980.
67. Segawa, Y., et al., *Expression of peroxisome proliferator-activated receptor (PPAR) in human prostate cancer.* Prostate, 2002. **51**(2): p. 108-16.
68. Campbell, M.J., C. Carlberg, and H.P. Koeffler, *A Role for the PPARgamma in Cancer Therapy.* PPAR Res, 2008. **2008**: p. 314974.
69. Bernard, D., et al., *Myc confers androgen-independent prostate cancer cell growth.* J Clin Invest, 2003. **112**(11): p. 1724-31.
70. Taipale, J. and P.A. Beachy, *The Hedgehog and Wnt signalling pathways in cancer.* Nature, 2001. **411**(6835): p. 349-54.

71. Karhadkar, S.S., et al., *Hedgehog signalling in prostate regeneration, neoplasia and metastasis.* Nature, 2004. **431**(7009): p. 707-12.
72. Rhodes, D.R., et al., *Meta-analysis of microarrays: interstudy validation of gene expression profiles reveals pathway dysregulation in prostate cancer.* Cancer Res, 2002. **62**(15): p. 4427-33.
73. Klezovitch, O., et al., *Hepsin promotes prostate cancer progression and metastasis.* Cancer Cell, 2004. **6**(2): p. 185-95.
74. Bracken, A.P., et al., *EZH2 is downstream of the pRB-E2F pathway, essential for proliferation and amplified in cancer.* EMBO J., 2003. **22**(20): p. 5323-5335.
75. Dreyer, C., et al., *Control of the peroxisomal beta-oxidation pathway by a novel family of nuclear hormone receptors.* Cell, 1992. **68**(5): p. 879-87.
76. *A unified nomenclature system for the nuclear receptor superfamily.* Cell, 1999. **97**(2): p. 161-3.
77. Michalik, L., B. Desvergne, and W. Wahli, *Peroxisome-proliferator-activated receptors and cancers: complex stories.* Nat.Rev.Cancer, 2004. **4**(1): p. 61-70.
78. Kersten, S. and W. Wahli, *Peroxisome proliferator activated receptor agonists.* EXS, 2000. **89**: p. 141-51.
79. Braissant, O., et al., *Differential expression of peroxisome proliferator-activated receptors (PPARs): tissue distribution of PPAR-alpha, -beta, and -gamma in the adult rat.* Endocrinology, 1996. **137**(1): p. 354-66.
80. Berger, J. and D.E. Moller, *The mechanisms of action of PPARs.* Annu Rev Med, 2002. **53**: p. 409-35.
81. Issemann, I. and S. Green, *Activation of a member of the steroid hormone receptor superfamily by peroxisome proliferators.* Nature, 1990. **347**(6294): p. 645-50.
82. Sher, T., et al., *cDNA cloning, chromosomal mapping, and functional characterization of the human peroxisome proliferator activated receptor.* Biochemistry, 1993. **32**(21): p. 5598-604.
83. Jones, P.S., et al., *Chromosomal localisation, inducibility, tissue-specific expression and strain differences in three murine peroxisome-proliferator-activated-receptor genes.* Eur J Biochem, 1995. **233**(1): p. 219-26.
84. Yeldandi, A.V., M.S. Rao, and J.K. Reddy, *Hydrogen peroxide generation in peroxisome proliferator-induced oncogenesis.* Mutat Res, 2000. **448**(2): p. 159-77.
85. Fajas, L., et al., *The organization, promoter analysis, and expression of the human PPARgamma gene.* J Biol Chem, 1997. **272**(30): p. 18779-89.
86. Girnun, G.D., et al., *APC-dependent suppression of colon carcinogenesis by PPARgamma.* Proc Natl Acad Sci U S A, 2002. **99**(21): p. 13771-6.
87. Clay, C.E., et al., *Early de novo gene expression is required for 15-deoxy-Delta 12,14-prostaglandin J2-induced apoptosis in breast cancer cells.* J Biol Chem, 2001. **276**(50): p. 47131-5.
88. Chen, G.G., et al., *Apoptosis induced by activation of peroxisome-proliferator activated receptor-gamma is associated with Bcl-2 and NF-kappaB in human colon cancer.* Life Sci, 2002. **70**(22): p. 2631-46.

89. Patel, L., et al., *Tumor suppressor and anti-inflammatory actions of PPARgamma agonists are mediated via upregulation of PTEN.* Curr Biol, 2001. **11**(10): p. 764-8.
90. Lim, H., et al., *Cyclo-oxygenase-2-derived prostacyclin mediates embryo implantation in the mouse via PPARdelta.* Genes Dev, 1999. **13**(12): p. 1561-74.
91. He, T.C., et al., *PPARdelta is an APC-regulated target of nonsteroidal anti-inflammatory drugs.* Cell, 1999. **99**(3): p. 335-45.
92. Barak, Y., et al., *Effects of peroxisome proliferator-activated receptor delta on placentation, adiposity, and colorectal cancer.* Proc Natl Acad Sci U S A, 2002. **99**(1): p. 303-8.
93. Di-Poi, N., et al., *Antiapoptotic role of PPARbeta in keratinocytes via transcriptional control of the Akt1 signaling pathway.* Mol Cell, 2002. **10**(4): p. 721-33.
94. Tenenbaum, A., et al., *Bezafibrate for the secondary prevention of myocardial infarction in patients with metabolic syndrome.* Arch Intern Med, 2005. **165**(10): p. 1154-60.
95. Peters, J.M., et al., *Bezafibrate is a dual ligand for PPARalpha and PPARbeta: studies using null mice.* Biochim Biophys Acta, 2003. **1632**(1-3): p. 80-9.
96. Cabrero, A., et al., *Bezafibrate reduces mRNA levels of adipocyte markers and increases fatty acid oxidation in primary culture of adipocytes.* Diabetes, 2001. **50**(8): p. 1883-90.
97. Goldenberg, I., M. Benderly, and U. Goldbourt, *Update on the use of fibrates: focus on bezafibrate.* Vasc Health Risk Manag, 2008. **4**(1): p. 131-41.
98. Fernandes-Santos, C., et al., *Pan-PPAR agonist beneficial effects in overweight mice fed a high-fat high-sucrose diet.* Nutrition, 2009.
99. Nakajima, T., et al., *Bezafibrate at clinically relevant doses decreases serum/liver triglycerides via down-regulation of sterol regulatory element-binding protein-1c in mice: a novel peroxisome proliferator-activated receptor alpha-independent mechanism.* Mol Pharmacol, 2009. **75**(4): p. 782-92.
100. Strakova, N., et al., *Peroxisome proliferator-activated receptors (PPAR) agonists affect cell viability, apoptosis and expression of cell cycle related proteins in cell lines of glial brain tumors.* Neoplasma, 2005. **52**(2): p. 126-36.
101. Hayden, R.E., et al., *Treatment of primary CLL cells with bezafibrate and medroxyprogesterone acetate induces apoptosis and represses the pro-proliferative signal of CD40-ligand, in part through increased 15dDelta12,14,PGJ2.* Leukemia, 2009. **23**(2): p. 292-304.
102. Tiziani, S., et al., *Metabolomic profiling of drug responses in acute myeloid leukaemia cell lines.* PLoS ONE, 2009. **4**(1): p. e4251.
103. Kohno, H., et al., *Suppression of colitis-related mouse colon carcinogenesis by a COX-2 inhibitor and PPAR ligands.* BMC Cancer, 2005. **5**: p. 46.
104. Ogawa, Y., et al., *Follow-up CT findings of tamoxifen-induced non-alcoholic steatohepatitis (NASH) of breast cancer patients treated with bezafibrate.* Oncol Rep, 2003. **10**(5): p. 1473-8.
105. McKenna, N.J., R.B. Lanz, and B.W. O'Malley, *Nuclear receptor coregulators: cellular and molecular biology.* Endocr Rev, 1999. **20**(3): p. 321-44.

106. Cunliffe, V.T., *Eloquent silence: developmental functions of Class I histone deacetylases.* Curr Opin Genet Dev, 2008.
107. Kurokawa, R., et al., *Polarity-specific activities of retinoic acid receptors determined by a co-repressor.* Nature, 1995. **377**(6548): p. 451-4.
108. Stacey, M.W., et al., *Nuclear receptor co-repressor gene localizes to 17p11.2, a frequently deleted band in malignant disorders.* Genes Chromosomes Cancer, 1999. **25**(2): p. 191-3.
109. Park, E.J., et al., *SMRTe, a silencing mediator for retinoid and thyroid hormone receptors-extended isoform that is more related to the nuclear receptor corepressor.* Proc Natl Acad Sci U S A, 1999. **96**(7): p. 3519-24.
110. Aasland, R., A.F. Stewart, and T. Gibson, *The SANT domain: a putative DNA-binding domain in the SWI-SNF and ADA complexes, the transcriptional co-repressor N-CoR and TFIIIB.* Trends Biochem Sci, 1996. **21**(3): p. 87-8.
111. Zhang, J., et al., *The N-CoR-HDAC3 nuclear receptor corepressor complex inhibits the JNK pathway through the integral subunit GPS2.* Mol Cell, 2002. **9**(3): p. 611-23.
112. Humphrey, G.W., et al., *Stable histone deacetylase complexes distinguished by the presence of SANT domain proteins CoREST/kiaa0071 and Mta-L1.* J Biol Chem, 2001. **276**(9): p. 6817-24.
113. Andres, M.E., et al., *CoREST: a functional corepressor required for regulation of neural-specific gene expression.* Proc Natl Acad Sci U S A, 1999. **96**(17): p. 9873-8.
114. Codina, A., et al., *Structural insights into the interaction and activation of histone deacetylase 3 by nuclear receptor corepressors.* Proc Natl Acad Sci U S A, 2005. **102**(17): p. 6009-14.
115. Horlein, A.J., et al., *Ligand-independent repression by the thyroid hormone receptor mediated by a nuclear receptor co-repressor.* Nature, 1995. **377**(6548): p. 397-404.
116. Ordentlich, P., et al., *Unique forms of human and mouse nuclear receptor corepressor SMRT.* Proc Natl Acad Sci U S A, 1999. **96**(6): p. 2639-44.
117. Privalsky, M.L., *The role of corepressors in transcriptional regulation by nuclear hormone receptors.* Annu.Rev.Physiol, 2004. **66**: p. 315-360.
118. Yoon, H.G., et al., *Purification and functional characterization of the human N-CoR complex: the roles of HDAC3, TBL1 and TBLR1.* EMBO J., 2003. **22**(6): p. 1336-1346.
119. Guenther, M.G., et al., *A core SMRT corepressor complex containing HDAC3 and TBL1, a WD40-repeat protein linked to deafness.* Genes Dev, 2000. **14**(9): p. 1048-57.
120. Li, H., et al., *Characterization of receptor interaction and transcriptional repression by the corepressor SMRT.* Mol Endocrinol, 1997. **11**(13): p. 2025-37.
121. Perissi, V. and M.G. Rosenfeld, *Controlling nuclear receptors: the circular logic of cofactor cycles.* Nat Rev Mol Cell Biol, 2005. **6**(7): p. 542-54.
122. Xu, H.E., et al., *Structural basis for antagonist-mediated recruitment of nuclear co-repressors by PPARalpha.* Nature, 2002. **415**(6873): p. 813-817.
123. Perissi, V., et al., *Molecular determinants of nuclear receptor-corepressor interaction.* Genes Dev., 1999. **13**(24): p. 3198-3208.

124. Goodson, M.L., B.A. Jonas, and M.L. Privalsky, *Alternative mRNA splicing of SMRT creates functional diversity by generating corepressor isoforms with different affinities for different nuclear receptors.* J.Biol.Chem., 2005.
125. Faist, F., et al., *Alternative splicing determines the interaction of SMRT isoforms with nuclear receptor-DNA complexes.* Biosci Rep, 2008.
126. Jonas, B.A., et al., *Response of SMRT (silencing mediator of retinoic acid and thyroid hormone receptor) and N-CoR (nuclear receptor corepressor) corepressors to mitogen-activated protein kinase kinase kinase cascades is determined by alternative mRNA splicing.* Mol Endocrinol, 2007. **21**(8): p. 1924-39.
127. Cohen, R.N., et al., *The specificity of interactions between nuclear hormone receptors and corepressors is mediated by distinct amino acid sequences within the interacting domains.* Mol.Endocrinol., 2001. **15**(7): p. 1049-1061.
128. Webb, P., et al., *The nuclear receptor corepressor (N-CoR) contains three isoleucine motifs (I/LXXII) that serve as receptor interaction domains (IDs).* Mol Endocrinol, 2000. **14**(12): p. 1976-85.
129. Hu, X. and M.A. Lazar, *The CoRNR motif controls the recruitment of corepressors by nuclear hormone receptors.* Nature, 1999. **402**(6757): p. 93-96.
130. Pascual, G., et al., *A SUMOylation-dependent pathway mediates transrepression of inflammatory response genes by PPAR-gamma.* Nature, 2005. **437**(7059): p. 759-763.
131. Prokhortchouk, A., et al., *The p120 catenin partner Kaiso is a DNA methylation-dependent transcriptional repressor.* Genes Dev, 2001. **15**(13): p. 1613-8.
132. Yoon, H.G., et al., *N-CoR mediates DNA methylation-dependent repression through a methyl CpG binding protein Kaiso.* Mol.Cell, 2003. **12**(3): p. 723-734.
133. Gao, Z., et al., *Coactivators and corepressors of NF-kappaB in IkappaB alpha gene promoter.* J Biol Chem, 2005. **280**(22): p. 21091-8.
134. Metivier, R., et al., *Estrogen receptor-alpha directs ordered, cyclical, and combinatorial recruitment of cofactors on a natural target promoter.* Cell, 2003. **115**(6): p. 751-763.
135. Fernandez-Majada, V., et al., *Aberrant cytoplasmic localization of N-CoR in colorectal tumors.* Cell Cycle, 2007. **6**(14): p. 1748-52.
136. Yu, C., et al., *The nuclear receptor corepressors NCoR and SMRT decrease PPARgamma transcriptional activity and repress 3T3-L1 adipogenesis.* J.Biol.Chem., 2005.
137. Hermanson, O., K. Jepsen, and M.G. Rosenfeld, *N-CoR controls differentiation of neural stem cells into astrocytes.* Nature, 2002. **419**(6910): p. 934-939.
138. Jepsen, K., et al., *Combinatorial roles of the nuclear receptor corepressor in transcription and development.* Cell, 2000. **102**(6): p. 753-63.
139. Jepsen, K., et al., *SMRT-mediated repression of an H3K27 demethylase in progression from neural stem cell to neuron.* Nature, 2007. **450**(7168): p. 415-9.
140. Nishio, H. and M.J. Walsh, *CCAAT displacement protein/cut homolog recruits G9a histone lysine methyltransferase to repress transcription.* Proc.Natl.Acad.Sci.U.S.A, 2004. **101**(31): p. 11257-11262.

141. Duan, Z., et al., *Gfi1 coordinates epigenetic repression of p21Cip/WAF1 by recruitment of histone lysine methyltransferase G9a and histone deacetylase 1.* Mol Cell Biol, 2005. **25**(23): p. 10338-51.
142. Jepsen, K., et al., *Cooperative regulation in development by SMRT and FOXP1.* Genes Dev, 2008. **22**(6): p. 740-5.
143. Hodgson, M.C., et al., *The androgen receptor recruits nuclear receptor corepressor (N-CoR) in the presence of mifepristone via its amino and carboxy terminii revealing a novel molecular mechanism for androgen receptor antagonists.* J.Biol.Chem., 2004.
144. Cheng, S., et al., *Inhibition of the dihydrotestosterone-activated androgen receptor by nuclear receptor corepressor.* Mol.Endocrinol., 2002. **16**(7): p. 1492-1501.
145. Chong, J.A., et al., *REST: a mammalian silencer protein that restricts sodium channel gene expression to neurons.* Cell, 1995. **80**(6): p. 949-57.
146. Ding, Z., L.L. Gillespie, and G.D. Paterno, *Human MI-ER1 alpha and beta function as transcriptional repressors by recruitment of histone deacetylase 1 to their conserved ELM2 domain.* Mol Cell Biol, 2003. **23**(1): p. 250-8.
147. Hakimi, M.A., et al., *A core-BRAF35 complex containing histone deacetylase mediates repression of neuronal-specific genes.* Proc Natl Acad Sci U S A, 2002. **99**(11): p. 7420-5.
148. Shi, Y., et al., *Histone demethylation mediated by the nuclear amine oxidase homolog LSD1.* Cell, 2004. **119**(7): p. 941-53.
149. Metzger, E., et al., *LSD1 demethylates repressive histone marks to promote androgen-receptor-dependent transcription.* Nature, 2005. **437**(7057): p. 436-9.
150. Lee, M.G., et al., *An essential role for CoREST in nucleosomal histone 3 lysine 4 demethylation.* Nature, 2005. **437**(7057): p. 432-5.
151. Collins, C., et al., *Positional cloning of ZNF217 and NABC1: genes amplified at 20q13.2 and overexpressed in breast carcinoma.* Proc Natl Acad Sci U S A, 1998. **95**(15): p. 8703-8.
152. Thillainadesan, G., et al., *Genome analysis identifies the p15ink4b tumor suppressor as a direct target of the ZNF217/CoREST complex.* Mol Cell Biol, 2008. **28**(19): p. 6066-77.
153. Almeida, L.O., et al., *Mutational analysis of genes p14ARF, p15INK4b, p16INK4a, and PTEN in human nervous system tumors.* Genet Mol Res, 2008. **7**(2): p. 451-9.
154. Noda, H., et al., *Promoter hypermethylation of tumor-related genes in sporadic colorectal cancer in young patients.* J Exp Clin Cancer Res, 2007. **26**(4): p. 521-6.
155. Rosu-Myles, M. and L. Wolff, *p15Ink4b: dual function in myelopoiesis and inactivation in myeloid disease.* Blood Cells Mol Dis, 2008. **40**(3): p. 406-9.
156. Zhu, Q., et al., *Lysine-specific demethylase 1 (LSD1) Is required for the transcriptional repression of the telomerase reverse transcriptase (hTERT) gene.* PLoS ONE, 2008. **3**(1): p. e1446.
157. Nan, X., et al., *DNA methylation specifies chromosomal localization of MeCP2.* Mol Cell Biol, 1996. **16**(1): p. 414-21.

158. Meehan, R.R., J.D. Lewis, and A.P. Bird, *Characterization of MeCP2, a vertebrate DNA binding protein with affinity for methylated DNA.* Nucleic Acids Res, 1992. **20**(19): p. 5085-92.
159. Lunyak, V.V., et al., *Corepressor-dependent silencing of chromosomal regions encoding neuronal genes.* Science, 2002. **298**(5599): p. 1747-1752.
160. Nagase, T., et al., *Prediction of the coding sequences of unidentified human genes. XX. The complete sequences of 100 new cDNA clones from brain which code for large proteins in vitro.* DNA Res, 2001. **8**(2): p. 85-95.
161. Fernandes, I., et al., *Ligand-dependent nuclear receptor corepressor LCoR functions by histone deacetylase-dependent and -independent mechanisms.* Mol Cell, 2003. **11**(1): p. 139-50.
162. Baek, S.H., et al., *Exchange of N-CoR corepressor and Tip60 coactivator complexes links gene expression by NF-kappaB and beta-amyloid precursor protein.* Cell, 2002. **110**(1): p. 55-67.
163. Pepe, G.J. and E.D. Albrecht, *Actions of placental and fetal adrenal steroid hormones in primate pregnancy.* Endocr Rev, 1995. **16**(5): p. 608-48.
164. Katsanis, N., et al., *Localisation of receptor interacting protein 140 (RIP140) within 100 kb of D21S13 on 21q11, a gene-poor region of the human genome.* Hum Genet, 1998. **102**(2): p. 221-3.
165. Cavailles, V., et al., *Nuclear factor RIP140 modulates transcriptional activation by the estrogen receptor.* Embo J, 1995. **14**(15): p. 3741-51.
166. Castet, A., et al., *Multiple domains of the Receptor-Interacting Protein 140 contribute to transcription inhibition.* Nucleic Acids Res, 2004. **32**(6): p. 1957-66.
167. Heery, D.M., et al., *A signature motif in transcriptional co-activators mediates binding to nuclear receptors.* Nature, 1997. **387**(6634): p. 733-6.
168. Treuter, E., et al., *A regulatory role for RIP140 in nuclear receptor activation.* Mol Endocrinol, 1998. **12**(6): p. 864-81.
169. Augereau, P., et al., *The nuclear receptor transcriptional coregulator RIP140.* Nucl Recept Signal, 2006. **4**: p. e024.
170. Wei, L.N., et al., *Receptor-interacting protein 140 directly recruits histone deacetylases for gene silencing.* J Biol Chem, 2000. **275**(52): p. 40782-7.
171. Chinnadurai, G., *CtBP, an unconventional transcriptional corepressor in development and oncogenesis.* Mol Cell, 2002. **9**(2): p. 213-24.
172. Shi, Y., et al., *Sharp, an inducible cofactor that integrates nuclear receptor repression and activation.* Genes Dev, 2001. **15**(9): p. 1140-51.
173. Hatchell, E.C., et al., *SLIRP, a small SRA binding protein, is a nuclear receptor corepressor.* Mol Cell, 2006. **22**(5): p. 657-68.
174. Allfrey, V.G., R. Faulkner, and A.E. Mirsky, *Acetylation and Methylation of Histones and Their Possible Role in the Regulation of Rna Synthesis.* Proc Natl Acad Sci U S A, 1964. **51**: p. 786-94.
175. Brownell, J.E., et al., *Tetrahymena histone acetyltransferase A: a homolog to yeast Gcn5p linking histone acetylation to gene activation.* Cell, 1996. **84**(6): p. 843-51.
176. Taunton, J., C.A. Hassig, and S.L. Schreiber, *A mammalian histone deacetylase related to the yeast transcriptional regulator Rpd3p.* Science, 1996. **272**(5260): p. 408-11.

177. Verdin, E., *Histone Deacetylases - Transcriptional Regulation and Other Cellular Functions.* Humana Press, 2006.
178. Grandori, C., et al., *The Myc/Max/Mad network and the transcriptional control of cell behavior.* Annu Rev Cell Dev Biol, 2000. **16**: p. 653-99.
179. Laherty, C.D., et al., *SAP30, a component of the mSin3 corepressor complex involved in N-CoR-mediated repression by specific transcription factors.* Mol.Cell, 1998. **2**(1): p. 33-42.
180. Zhang, Y., et al., *SAP30, a novel protein conserved between human and yeast, is a component of a histone deacetylase complex.* Mol Cell, 1998. **1**(7): p. 1021-31.
181. Verdin, E., F. Dequiedt, and H.G. Kasler, *Class II histone deacetylases: versatile regulators.* Trends Genet, 2003. **19**(5): p. 286-93.
182. Fischle, W., et al., *Enzymatic activity associated with class II HDACs is dependent on a multiprotein complex containing HDAC3 and SMRT/N-CoR.* Mol.Cell, 2002. **9**(1): p. 45-57.
183. Kawaguchi, Y., et al., *The deacetylase HDAC6 regulates aggresome formation and cell viability in response to misfolded protein stress.* Cell, 2003. **115**(6): p. 727-38.
184. Tran, P.B. and R.J. Miller, *Aggregates in neurodegenerative disease: crowds and power?* Trends Neurosci, 1999. **22**(5): p. 194-7.
185. Gartenberg, M.R., *The Sir proteins of Saccharomyces cerevisiae: mediators of transcriptional silencing and much more.* Curr Opin Microbiol, 2000. **3**(2): p. 132-7.
186. Frye, R.A., *Characterization of five human cDNAs with homology to the yeast SIR2 gene: Sir2-like proteins (sirtuins) metabolize NAD and may have protein ADP-ribosyltransferase activity.* Biochem Biophys Res Commun, 1999. **260**(1): p. 273-9.
187. North, B.J., et al., *The human Sir2 ortholog, SIRT2, is an NAD+-dependent tubulin deacetylase.* Mol Cell, 2003. **11**(2): p. 437-44.
188. Bruggeman, F.J. and H.V. Westerhoff, *The nature of systems biology.* Trends Microbiol, 2007. **15**(1): p. 45-50.
189. Hornberg, J.J., et al., *Cancer: a Systems Biology disease.* Biosystems, 2006. **83**(2-3): p. 81-90.
190. Banwell, C.M., et al., *Altered nuclear receptor corepressor expression attenuates vitamin d receptor signaling in breast cancer cells.* Clin.Cancer Res., 2006. **12**(7): p. 2004-2013.
191. Wishart, D., *ClustanGraphics: Interactive Graphics for Cluster Analysis.* Computing Science and Statistics, 1997. **29**: p. 48-51.
192. Laird, P.W., et al., *Simplified mammalian DNA isolation procedure.* Nucleic Acids Res, 1991. **19**(15): p. 4293.
193. Ramirez-Solis, R., A.C. Davis, and A. Bradley, *Gene targeting in embryonic stem cells.* Methods Enzymol, 1993. **225**: p. 855-78.
194. Rashid, S.F., et al., *1alpha,25-dihydroxyvitamin D(3) displays divergent growth effects in both normal and malignant cells.* Steroids, 2001. **66**(3-5): p. 433-440.
195. Kim, J.Y., Y.L. Son, and Y.C. Lee, *Involvement of SMRT Corepressor in Transcriptional Repression by the Vitamin D Receptor.* Mol Endocrinol, 2008.

196. Ting, H.J., et al., *Increased expression of corepressors in aggressive androgen-independent prostate cancer cells results in loss of 1alpha,25-dihydroxyvitamin D3 responsiveness.* Mol Cancer Res, 2007. **5**(9): p. 967-80.
197. Annicotte, J.S., et al., *Peroxisome proliferator-activated receptor gamma regulates E-cadherin expression and inhibits growth and invasion of prostate cancer.* Mol Cell Biol, 2006. **26**(20): p. 7561-74.
198. Chang, T.H. and E. Szabo, *Enhanced growth inhibition by combination differentiation therapy with ligands of peroxisome proliferator-activated receptor-gamma and inhibitors of histone deacetylase in adenocarcinoma of the lung.* Clin.Cancer Res., 2002. **8**(4): p. 1206-1212.
199. McDonald, D., et al., *Nucleoplasmic beta-actin exists in a dynamic equilibrium between low-mobility polymeric species and rapidly diffusing populations.* J Cell Biol, 2006. **172**(4): p. 541-52.
200. Dundr, M., et al., *Actin-dependent intranuclear repositioning of an active gene locus in vivo.* J Cell Biol, 2007. **179**(6): p. 1095-103.
201. Ou, H., et al., *Effect of nuclear actin on endothelial nitric oxide synthase expression.* Arterioscler Thromb Vasc Biol, 2005. **25**(12): p. 2509-14.
202. Abedin, S.A., et al., *Elevated NCOR1 disrupts a network of dietary-sensing nuclear receptors in bladder cancer cells.* Carcinogenesis, 2009.
203. Lal, A., et al., *A public database for gene expression in human cancers.* Cancer Res., 1999. **59**(21): p. 5403-5407.
204. Zandbergen, F., et al., *The G0/G1 switch gene 2 is a novel PPAR target gene.* Biochem.J., 2005. **392**(Pt 2): p. 313-324.
205. Matilainen, M., et al., *Regulation of multiple insulin-like growth factor binding protein genes by 1alpha,25-dihydroxyvitamin D3.* Nucleic Acids Res., 2005. **33**(17): p. 5521-5532.
206. Towsend, K., et al., *Identification of VDR-responsive gene signatures in breast cancer cells.* Oncology, 2006. **71**(1-2): p. 111-123.
207. Degenhardt, T., et al., *The insulin-like growth factor binding protein 1 gene is a primary target of peroxisome proliferator-activated receptors.* J.Biol.Chem., 2006.
208. Chene, G., et al., *n-3 and n-6 polyunsaturated fatty acids induce the expression of COX-2 via PPARgamma activation in human keratinocyte HaCaT cells.* Biochim Biophys Acta, 2007. **1771**(5): p. 576-89.
209. Janabi, N., *Selective inhibition of cyclooxygenase-2 expression by 15-deoxy-Delta(12,14)(12,14)-prostaglandin J(2) in activated human astrocytes, but not in human brain macrophages.* J Immunol, 2002. **168**(9): p. 4747-55.
210. Khanim, F.L., et al., *Altered SMRT levels disrupt vitamin D3 receptor signalling in prostate cancer cells.* Oncogene, 2004. **23**(40): p. 6712-25.
211. Rashid, S.F., et al., *Synergistic growth inhibition of prostate cancer cells by 1 alpha,25 Dihydroxyvitamin D(3) and its 19-nor-hexafluoride analogs in combination with either sodium butyrate or trichostatin A.* Oncogene, 2001. **20**(15): p. 1860-1872.
212. Rhodes, D.R., et al., *Oncomine 3.0: genes, pathways, and networks in a collection of 18,000 cancer gene expression profiles.* Neoplasia, 2007. **9**(2): p. 166-80.

213. Debruyne, P., S. Vermeulen, and M. Mareel, *The role of the E-cadherin/catenin complex in gastrointestinal cancer.* Acta Gastroenterol.Belg., 1999. **62**(4): p. 393-402.
214. Morin, P.J., *beta-catenin signaling and cancer.* Bioessays, 1999. **21**(12): p. 1021-1030.
215. Lang, S.H., et al., *Prostate epithelial cell lines form spheroids with evidence of glandular differentiation in three-dimensional Matrigel cultures.* Br.J.Cancer, 2001. **85**(4): p. 590-599.
216. Jepsen, K., et al., *Combinatorial roles of the nuclear receptor corepressor in transcription and development.* Cell, 2000. **102**(6): p. 753-763.
217. Sauer, B., *Manipulation of transgenes by site-specific recombination: use of Cre recombinase.* Methods Enzymol, 1993. **225**: p. 890-900.
218. Rosenthal, N. and S. Brown, *The mouse ascending: perspectives for human-disease models.* Nat Cell Biol, 2007. **9**(9): p. 993-9.
219. Wu, X., et al., *Generation of a prostate epithelial cell-specific Cre transgenic mouse model for tissue-specific gene ablation.* Mech Dev, 2001. **101**(1-2): p. 61-9.
220. George, S.H., et al., *Developmental and adult phenotyping directly from mutant embryonic stem cells.* Proc Natl Acad Sci U S A, 2007. **104**(11): p. 4455-60.
221. Liu, P., N.A. Jenkins, and N.G. Copeland, *A highly efficient recombineering-based method for generating conditional knockout mutations.* Genome Res, 2003. **13**(3): p. 476-84.
222. El-Deiry, W.S., et al., *WAF1, a potential mediator of p53 tumor suppression.* Cell, 1993. **75**(4): p. 817-825.
223. Abbas, T. and A. Dutta, *p21 in cancer: intricate networks and multiple activities.* Nat Rev Cancer, 2009. **9**(6): p. 400-14.
224. Saramaki, A., et al., *Regulation of the human p21(waf1/cip1) gene promoter via multiple binding sites for p53 and the vitamin D3 receptor.* Nucleic Acids Res., 2006. **34**(2): p. 543-554.
225. Friedman, S.L., et al., *Resistance to p53-mediated growth arrest and apoptosis in Hep 3B hepatoma cells.* Oncogene, 1997. **15**(1): p. 63-70.
226. Petrocca, F., et al., *E2F1-regulated microRNAs impair TGFbeta-dependent cell-cycle arrest and apoptosis in gastric cancer.* Cancer Cell, 2008. **13**(3): p. 272-86.
227. Pichiorri, F., et al., *MicroRNAs regulate critical genes associated with multiple myeloma pathogenesis.* Proc Natl Acad Sci U S A, 2008. **105**(35): p. 12885-90.
228. Sampath, D., et al., *Specific activation of microRNA106b enables the p73 apoptotic response in chronic lymphocytic leukemia by targeting the ubiquitin ligase Itch for degradation.* Blood, 2009. **113**(16): p. 3744-53.
229. Darzacq, X., et al., *In vivo dynamics of RNA polymerase II transcription.* Nat Struct Mol Biol, 2007. **14**(9): p. 796-806.
230. Ivanovska, I., et al., *MicroRNAs in the miR-106b family regulate p21/CDKN1A and promote cell cycle progression.* Mol Cell Biol, 2008. **28**(7): p. 2167-74.
231. Margaritis, T. and F.C. Holstege, *Poised RNA polymerase II gives pause for thought.* Cell, 2008. **133**(4): p. 581-4.
232. Muse, G.W., et al., *RNA polymerase is poised for activation across the genome.* Nat Genet, 2007. **39**(12): p. 1507-11.

233. Tijsterman, M. and R.H. Plasterk, *Dicers at RISC; the mechanism of RNAi.* Cell, 2004. **117**(1): p. 1-3.
234. Wiemer, E.A., *The role of microRNAs in cancer: no small matter.* Eur J Cancer, 2007. **43**(10): p. 1529-44.
235. Banwell, C.M., et al., *Targeting 1alpha,25-dihydroxyvitamin D3 antiproliferative insensitivity in breast cancer cells by co-treatment with histone deacetylation inhibitors.* J.Steroid Biochem.Mol.Biol., 2004. **89-90**(1-5): p. 245-249.
236. Marks, P.A. and R. Breslow, *Dimethyl sulfoxide to vorinostat: development of this histone deacetylase inhibitor as an anticancer drug.* Nat Biotechnol, 2007. **25**(1): p. 84-90.
237. Picard, F., et al., *Sirt1 promotes fat mobilization in white adipocytes by repressing PPAR-gamma.* Nature, 2004. **429**(6993): p. 771-6.
238. Wang, C., et al., *Direct acetylation of the estrogen receptor alpha hinge region by p300 regulates transactivation and hormone sensitivity.* J Biol Chem, 2001. **276**(21): p. 18375-83.
239. Fu, M., et al., *p300 and p300/cAMP-response element-binding protein-associated factor acetylate the androgen receptor at sites governing hormone-dependent transactivation.* J Biol Chem, 2000. **275**(27): p. 20853-60.
240. Tilley, W.D., et al., *Mutations in the androgen receptor gene are associated with progression of human prostate cancer to androgen independence.* Clin Cancer Res, 1996. **2**(2): p. 277-85.
241. Molnar, F., M. Matilainen, and C. Carlberg, *Structural determinants of the agonist-independent association of human peroxisome proliferator-activated receptors with coactivators.* J Biol Chem, 2005. **280**(28): p. 26543-56.
242. Wang, D., et al., *Negative regulation of TSHalpha target gene by thyroid hormone involves histone acetylation and corepressor complex dissociation.* Mol Endocrinol, 2009. **23**(5): p. 600-9.
243. Kato, S., et al., *Ligand-induced transrepressive function of VDR requires a chromatin remodeling complex, WINAC.* J Steroid Biochem Mol Biol, 2007. **103**(3-5): p. 372-80.
244. Ellis, D.J., Z.K. Lawman, and K. Bonham, *Histone acetylation is not an accurate predictor of gene expression following treatment with histone deacetylase inhibitors.* Biochem Biophys Res Commun, 2008. **367**(3): p. 656-62.
245. Simonis, M., J. Kooren, and W. de Laat, *An evaluation of 3C-based methods to capture DNA interactions.* Nat Methods, 2007. **4**(11): p. 895-901.
246. Song, L.N. and E.P. Gelmann, *Silencing mediator for retinoid and thyroid hormone receptor and nuclear receptor corepressor attenuate transcriptional activation by the beta-catenin-TCF4 complex.* J Biol Chem, 2008. **283**(38): p. 25988-99.
247. Degenhardt, T., et al., *Population-level transcription cycles derived from stochastic timing of single-cell transcription.* Cell, 2009. **in press**.
248. Charng, M.J., et al., *A novel protein distinguishes between quiescent and activated forms of the type I transforming growth factor beta receptor.* J Biol Chem, 1998. **273**(16): p. 9365-8.
249. Wurthner, J.U., et al., *Transforming growth factor-beta receptor-associated protein 1 is a Smad4 chaperone.* J Biol Chem, 2001. **276**(22): p. 19495-502.

250. Saramaki, A., et al., *Cyclical chromatin looping and transcription factor association on the regulatory regions of the p21 (CDKN1A) gene in response to 1alpha,25-dihydroxyvitamin D3.* J Biol Chem, 2009. **284**(12): p. 8073-82.
251. Hu, Q., et al., *Enhancing nuclear receptor-induced transcription requires nuclear motor and LSD1-dependent gene networking in interchromatin granules.* Proc Natl Acad Sci U S A, 2008. **105**(49): p. 19199-204.
252. O'Neill, L.P. and B.M. Turner, *Immunoprecipitation of native chromatin: NChIP*. Methods, 2003. **31**(1): p. 76-82.